



HAL
open science

Characterization of de novo metastatic prostate cancer : an ancillary study of the PEACE-1 phase 3 clinical trial

Cédric Pobel

► **To cite this version:**

Cédric Pobel. Characterization of de novo metastatic prostate cancer : an ancillary study of the PEACE-1 phase 3 clinical trial. *Cancer*. Université Paris-Saclay, 2024. English. NNT : 2024UP-ASL118 . tel-04879135

HAL Id: tel-04879135

<https://theses.hal.science/tel-04879135v1>

Submitted on 10 Jan 2025

HAL is a multi-disciplinary open access archive for the deposit and dissemination of scientific research documents, whether they are published or not. The documents may come from teaching and research institutions in France or abroad, or from public or private research centers.

L'archive ouverte pluridisciplinaire **HAL**, est destinée au dépôt et à la diffusion de documents scientifiques de niveau recherche, publiés ou non, émanant des établissements d'enseignement et de recherche français ou étrangers, des laboratoires publics ou privés.

Characterization of *de novo* metastatic prostate cancer: an ancillary study of the PEACE-1 phase 3 clinical trial

Caractérisation des cancers de la prostate métastatiques *de novo* : une étude ancillaire de l'essai clinique de phase 3 PEACE1

Thèse de doctorat de l'université Paris-Saclay

École doctorale n° 582, Cancérologie : Biologie, Médecine, Santé (CBMS)

Spécialité de doctorat : Sciences du cancer

Graduate School : Life Science and Health. Référent : Faculté de Médecine

Thèse préparée dans l'unité de recherche **Prédicteurs moléculaires et nouvelles cibles en oncologie (Université Paris-Saclay, INSERM, Institut Gustave Roussy)** sous la direction du **Pr Yohann LORIOT, PUPH** et la co-direction du **Pr Christophe MASSARD, PUPH**.

Thèse soutenue à Paris-Saclay, le 10 décembre 2024, par

Cédric POBEL

Composition du Jury

Membres du jury avec voix délibérative

Eva COMPERAT

Professeur, Sorbonne Université
(hôpital Tenon)/ Medical university of
Vienna

Présidente & Rapporteur

Alexandra MASSON-LECOMTE

Professeur, Université de Paris (hôpital
Saint-Louis)

Rapporteur & Examinatrice

Geraldine PIGNOT

Docteur, Institut Paoli-Calmettes à
Marseille

Examinatrice

Bertrand TOMBAL

Professeur, Université catholique de
Louvain (Clinique Universitaire St Luc
à Bruxelles)

Examineur

Titre : Caractérisation des cancers de la prostate métastatiques de novo : une étude ancillaire de l'essai clinique de phase 3 PEACE1.

Mots clés : Cancer de la prostate, pronostic, biomarqueurs, médecine translationnelle, multi-omique, cancer neuroendocrine

Résumé :

Introduction

Le cancer de la prostate *de novo* métastatique sensible à la castration représente 5 à 10% des cancers de la prostate au diagnostic mais est responsable de 50% des décès liés aux cancers de la prostate tous stades confondus. Dans cette étude ancillaire de l'essai PEACE-1, notre hypothèse était que les variants agressifs ou neuroendocrines peuvent être détectés dès le diagnostic.

Matériels et méthodes

Nous avons rapatrié de façon centralisée les prélèvements en paraffine des biopsies au diagnostic des patients inclus dans PEACE1 (NCT01957436) pour réaliser des analyses d'immunohistochimie (IHC), de séquençage de nouvelle génération (NGS) et de transcriptomique.

Résultats

Parmi les 1172 patients avec un cancer de la prostate *de novo* métastatique sensible à la castration, 595 avait du matériel centralisé et rapatrié. En IHC, l'expression d'au

moins un marqueur neuroendocrine (parmi la synaptophysine, CD56 ou la chromogranine A) était retrouvée pour 26,2% des patients et était indépendamment associée à une survie globale diminuée (HR=1.53, CI95%[1.14-2.06], p=0.005). Aucun biomarqueur ne pouvait prédire le bénéfice de l'abiraterone. L'altération d'au moins deux gènes parmi *TP53*, *PTEN* et/ou *RBI* était indépendamment associée à un mauvais pronostic (HR=2.63, CI95%[1.10-6.30], p=0.03). En transcriptomique, nous avons trouvé une sous-expression de la voie du récepteur aux androgènes et une sur-expression de la voie E2F et G2M chez les patients non-répondeurs. Une expression élevée de la signature neuroendocrine et basse de la signature du récepteur aux androgènes était associée à un moins bon pronostic.

Conclusion

Au total, nous montrons à un niveau multiomique que des caractéristiques neuroendocrines sont présentes au diagnostic chez les patients avec un cancer de la prostate *de novo* métastatique sensible à la castration, et que celles-ci sont associées à un mauvais pronostic.

Title: Characterization of *de novo* metastatic prostate cancer: an ancillary study of the PEACE-1 phase 3 clinical trial.

Keywords: prostatic neoplasms, prognosis, biomarkers, translational medicine, multiomics, neuroendocrine cell

Abstract:

Introduction

De novo metastatic castration sensitive prostate cancer (dnmCSPC) represents 5–10% of PC diagnoses but causes 50% of PC-related deaths. In this ancillary study of the PEACE1 trial, we hypothesized that aggressive or neuroendocrine-like variants could be detected at diagnosis.

Materials and methods

We centrally retrieved paraffin-embedded biopsies at diagnosis from PEACE1 (NCT01957436) trial patients for immunochemistry (IHC), next generation sequencing (NGS) and transcriptomic analyses.

Results

From the 1172 dnmCSPC patients randomized in PEACE-1, 595 had a paraffin-embedded sample collected and centrally reviewed. In IHC, at least one

neuroendocrine marker (among synaptophysin, CD56 or chromogranin A) was expressed in 26.2% of patients and was independently associated with a shorter overall survival (HR=1.53, CI95%[1.14-2.06], p=0.005). No biomarker predicted the benefit of abiraterone. The alteration of at least 2 genes among *TP53*, *PTEN* and/or *RBI* was independently associated with worse prognosis (HR=2.63, CI95%[1.10-6.30], p=0.03). At a gene expression level, we found an AR pathway under-expression with an E2F and G2M pathway over-expression in non-responder patients. A high neuroendocrine signature and a low androgen receptor signature expression was associated with worse outcomes.

Conclusion

Altogether, we show at a multiple omics level that NE features are present at diagnosis in dnmCSPC and are associated with worse prognosis.

Résumé substantiel

Introduction :

Le cancer de la prostate *de novo* métastatique sensible à la castration représente 5 à 10% des cancers de la prostate au diagnostic mais est responsable de 50% des décès liés aux cancers de la prostate tous stades confondus. Les mécanismes d'agressivité et de résistance aux traitements ont été principalement rapportés au stade plus avancé de cancer la prostate métastatique résistant à la castration mais peu au stade *de novo* métastatique sensible à la castration. Dans cette étude ancillaire de l'essai PEACE-1, notre hypothèse était que des variants agressifs ou neuroendocrines peuvent être détectés dès le diagnostic.

Matériels et méthodes :

Nous avons rapatrié de façon centralisée les prélèvements en paraffine des biopsies au diagnostic des patients inclus dans PEACE1 (NCT01957436) pour réaliser des analyses phénotypiques, génomiques et transcriptomiques. En immunohistochimie (IHC), dix marqueurs ont été utilisés : Récepteur aux androgènes, NKX3.1, ERG, synaptophysine, chromogranine A, CD56, p53, Rb1, Ki67 et PTEN. Le séquençage de nouvelle génération (NGS) a été réalisé avec les panels Cancer Core Europe (CCE) et OncoDeep (410 et 638 gènes respectivement). Les analyses de transcriptomique ont été réalisées avec la technique d'hybridation de l'ARN nanoString nCounter® en utilisant le panel tumor signaling 360™ et un panel sur mesure de signatures neuroendocrines et d'activation du récepteur aux androgènes.

Résultats :

Parmi les 1172 patients avec un cancer de la prostate *de novo* métastatique sensible à la castration, 595 avait du matériel centralisé et rapatrié. Les analyses IHC étaient contributives pour 394 patients, les analyses génomiques pour 180 patients and les analyses transcriptomiques pour 194 patients. En IHC, l'expression d'au moins un marqueur neuroendocrine (parmi la synaptophysine, CD56 ou la chromogranine A) était retrouvée pour 26,2% des patients et était indépendamment associée à une survie globale diminuée (HR=1.53, CI95% [1.14-2.06], p=0.005). La signature neuroendocrine en NGS avec l'altération d'au moins deux gènes parmi *TP53*, *PTEN* et/ou *RB1* chez 7,6% des patients était indépendamment associée à un mauvais pronostic (HR=2.63, CI95% [1.10-6.30], p=0.03). En transcriptomique, une expression élevée de la signature neuroendocrine et basse de la signature du récepteur aux androgènes était associée à un moins bon pronostic. Chez les patients non répondeurs, nous avons trouvé une sous-expression de la voie du récepteur aux androgènes et une sur-expression de la voie E2F et G2M. Des gènes associés au cancer de la prostate neuroendocrine (NEPC) tels que *EZH2* et *AURKA* étaient également sur-exprimés. Les tumeurs avec des marqueurs neuroendocrines positifs en IHC avaient une surexpression des voies E2F, G2M et MYC avec une sous-expression de la voie du récepteur aux androgènes. Des gènes NEPC étaient sur-exprimés avec *PROX1*, *DLL3*, *DNMT1*, *KDM1A*, *SEZ6* et *TOP2A*. Les tumeurs avec une signature neuroendocrine en NGS avaient également une sur-expression des voies E2F, G2M, MYC et une sous-expression de la voie du récepteur aux androgènes. Des gènes NEPC étaient également sur-exprimés dans ce groupe avec *SOX2*, *DLL3*, *PROX1*, *TOP2A*, *DNMT1*. Aucun biomarqueur phénotypique ou transcriptomique ne pouvait prédire le bénéfice de l'abiraterone. L'expression des marqueurs neuroendocrines en IHC était hétérogène dans la tumeur avec des zones positives et négatives. La plupart de ces tumeurs était classées comme adénocarcinome pur par le compte-rendu diagnostique initial local car ces marqueurs ne sont pas réalisés systématiquement en pratique courante.

Conclusion :

Au total, nous montrons à un niveau multiomique que des caractéristiques neuroendocrines sont présentes au diagnostic chez les patients avec un cancer de la prostate *de novo* métastatique sensible à la castration, et que celles-ci sont associées à un mauvais pronostic. Cette sous-population de clones agressifs présents dès le diagnostic parmi la population majoritaire d'adénocarcinome pourrait être ciblée en première ligne en association aux thérapeutiques standards. Certains gènes et voies neuroendocrines surexprimés dans cette cohorte sont déjà ciblés par des traitements en cours de développement au stade plus avancé de cancer la prostate métastatique résistant à la castration.

Table of contents

1. INTRODUCTION.....	9
A. EPIDEMIOLOGY	9
B. BIOLOGY OF PROSTATE CANCER	11
I. HISTOLOGICAL DEFINITION	11
II. ONCOGENIC PATHWAYS	12
III. DNA REPAIR DEFICIENCY	14
IV. TUMOR PROLIFERATION AND CELL CYCLE REGULATION	15
V. EPIGENETIC	16
VI. EPITHELIAL MESENCHYMAL TRANSITION	17
VII. TUMOR MICROENVIRONMENT	18
VIII. PROGNOSTIC FACTORS: NEUROENDOCRINE AND AGGRESSIVE VARIANTS.....	20
IX. GENOMIC LANDSCAPE ACCORDING TO DIFFERENT STAGES	22
C. TREATMENT LANDSCAPE IN METASTATIC PROSTATE CANCER.....	24
I. ANDROGEN DEPRIVATION THERAPY	24
II. CHEMOTHERAPY	24
III. AR PATHWAY INHIBITORS.....	24
IV. CHEMOTHERAPY AND HORMONOTHERAPY COMBINATION	24
V. PARP INHIBITORS	24
VI. RADIONUCLIDE TREATMENT.....	25
VII. DENOSUMAB	25
VIII. THERAPEUTIC PERSPECTIVES	25
D. MECHANISMS OF RESISTANCE TO TREATMENT	27
I. ANDROGEN DEPRIVATION THERAPY	27
II. DOCETAXEL	30
III. ANDROGEN RECEPTOR PATHWAY INHIBITORS	31
IV. CABAZITAXEL	32
V. PARP INHIBITORS	32
VI. RESISTANCE TO PSMA-LUTETIUM	33
E. HYPOTHESIS	33
F. OBJECTIVES	34
2. MATERIALS AND METHODS	34
A. STUDY DESIGN.....	34
B. ENDPOINTS	34
I. CO-PRIMARY ENDPOINTS	34
II. SECONDARY ENDPOINTS.....	35
III. EXPLORATORY ENDPOINTS	35

C. SAMPLE SIZE	35
D. SAMPLES PREPARATION	36
I. WP1: PHENOTYPE ANALYSIS	36
II. WP2: GENOMIC ANALYSIS	37
III. WP3: TRANSCRIPTOMIC ANALYSES	37
E. STATISTICAL ANALYSES	40
I. GENERALITIES	40
II. STATISTICAL CONVENTIONS AND MISSING DATA	40
III. BASELINE CHARACTERISTICS	40
IV. BIOMARKERS	41
V. ANALYSIS OF CO-PRIMARY ENDPOINTS	42
VI. ANALYSIS OF SECONDARY ENDPOINT	43
VII. STATISTICAL SOFTWARE	43
<u>3. RESULTS</u>	<u>44</u>
A. DESCRIPTIVE ANALYSES	44
I. OVERALL COHORT	44
II. PHENOTYPIC ANALYSIS COHORT	48
III. GENOMIC ANALYSIS COHORT	50
IV. TRANSCRIPTOMIC ANALYSIS COHORT	56
B. PROGNOSTIC ANALYSIS	57
I. PHENOTYPIC ANALYSIS COHORT	57
II. GENOMIC ANALYSIS COHORT	62
III. TRANSCRIPTOMIC ANALYSIS COHORT	65
C. PREDICTIVE ANALYSIS	75
I. PHENOTYPIC ANALYSIS COHORT	75
II. GENOMIC ANALYSIS COHORT	76
III. TRANSCRIPTOMIC ANALYSIS COHORT	76
D. CORRELATION WITH PSA RESPONSE AT 8 MONTHS	76
I. PHENOTYPIC ANALYSIS COHORT	77
II. GENOMIC ANALYSIS COHORT	79
III. TRANSCRIPTOMIC ANALYSIS COHORT	79
E. CORRELATION WITH TUMORAL BURDEN	81
I. PHENOTYPIC ANALYSIS COHORT	81
II. GENOMIC ANALYSIS COHORT	83
III. TRANSCRIPTOMIC ANALYSIS COHORT	83
F. CORRELATION BETWEEN IHC AND NGS	86
G. PHENOTYPIC HETEROGENEITY	88
H. COMPARISON WITH LOCAL PATHOLOGIST REPORTS	90
<u>4. DISCUSSION</u>	<u>91</u>
<u>5. PERSPECTIVES</u>	<u>95</u>
<u>6. REFERENCES</u>	<u>98</u>

Abbreviations

ABCB1	ATP-binding cassette sub-family B member 1
ADT	Androgen deprivation therapy
APC	Adenomatous polyposis coli protein
AR	Androgen receptor
ARPI	Androgen receptor pathway inhibitors
ASCL1	Achaete-scute homolog 1
ATM	Ataxia–telangiectasia mutated
AUC	Area Under Curve
AURKA	Aurora kinase A
BCL2	B-cell lymphoma 2
BET	Bromodomain and extra-terminal
BRCA	BRCA1/2 Breast CAncer gene
BRD	Bromodomain-containing
CBP	CREB-binding protein
CDK	Cyclin dependent kinase
CDKN1B	Cyclin-dependent kinase inhibitor 1B
CEACAM5	Carcinoembryonic antigen-related cell adhesion molecule 5
CHD1	Chromodomain helicase DNA-binding protein 1
CI	Confidence interval
CNV	Copy number variation
COX-2	COX-2 cyclooxygenase-2
CSNK2A1	Casein kinase 2A.1
DHEA	Dehydroepiandrosterone
DHT	Dihydrotestosterone
DLL3	Delta-like protein 3
DNA-PKcs	DNA-dependent protein kinase catalytic subunit
DNMTs	DNA methylation by DNA methyltransferases
EGFR	Epithelial growth factor receptor
EMT	Epithelial-mesenchymal transition
ERG	ETS-related gene
ERK	Extracellular signal-regulated kinases
ETS	E-26 transformation-specific
EZH2	Enhancer of zeste homolog 2
FDR	False discovery rate
FGFR	Fibroblast growth factor receptor
FLT-3	Fms-like tyrosine kinase 3 receptor
FOXA1	Forkhead box A1
FOXC2	Forkhead box protein C2
GDF15	Growth differentiation factor 15
GSEA	Gene Set Enrichment Analysis

GSVA	Gene Set Variance Analysis
HATs	Histone acetyl transferases
HDACs	Histone deacetylases
HGF	Hepatocyte growth factor
HIF-1 α	Hypoxia inducible factor 1 alpha
HOXB13	Homeobox B13
HR	Hazard ratio
IHC	Immunohistochemistry
IKK	I κ B kinase complex
IL	Interleukine
INSM1	Insulinoma-associated protein 1
ISUP	International Society of Urological Pathology
JAK-STAT	Janus kinase/signal transducer and activator of transcription
KIFC1	Kinesin family member C1
LSD1	Lysine-specific demethylase 1
MAPK	Mitogen-activated protein kinase
mCSPC	Metastatic castration-sensitive prostate cancer
mCRPC	Metastatic castration-resistant prostate cancer
MDM2	Mouse double minute 2 homolog
MMP	Matrix metalloproteinases
MRP1	Multidrug resistance protein 1
mTOR	Mammalian target of rapamycin
NE	Neuroendocrine
NEPC	Neuroendocrine prostate cancer
NEmk	At least one neuroendocrine marker positive among synaptophysin, CD56 or chromogranin A
NHEJ	Non-homologous end-joining
NOTCH	Neurogenic locus notch homolog protein
ORA	Over-Representation Analysis
OS	Overall survival
P-gp	P-glycoprotein
PARG	Poly(ADP-ribose) glycohydrolase
PARP1	Poly(ADP-ribose) polymerase 1
PCWG2	Prostate Cancer Working Group 2
PDGFR	Platelet-derived growth factor receptor
PFS	Progression free survival
PH	Proportional hazards
PI3K	Phosphoinositide 3-kinase
POU3F2/BRN2	POU domain, class 3, transcription factor 2
PSA	Prostate-specific antigen
PTEN	Phosphatase and TENsin homolog
RAF	Rapidly accelerated fibrosarcoma

RANKL	Nuclear factor κ B ligand
Ras	Rat sarcoma virus
Rb1	Retinoblastoma
RNF43	E3 ubiquitin protein ligase
rPFS	Radiographic progression-free survival
RTKs	Receptor tyrosine kinases
SLCO1B3	Solute carrier organic anion transporter family member 1B3
SLFN11	Schlafen 11
SMADS	Mothers against decapentaplegic homologue
SCLC	Small cells lung cancer
SNV	Single nucleotide variant
SOX2	SRY-Box transcription factor 2
SPOP	Speckle-type pox virus and zinc finger (POZ) protein
SRC	Steroid receptor coactivators
TCGA	The Cancer Genome Atlas
TET2	Tet methylcytosine dioxygenase 2
TGF- β	Transforming growth factor β
TNF- α	Tumor necrosis factor alpha
TSalt	Loss of at least two tumor suppressor genes among TP53, PTEN or RB1
VEGFR	Vascular endothelial growth factor receptor
ZEB	Zinc-finger E-box-binding

1. Introduction

a. Epidemiology

Worldwide, prostate cancer accounted for 1.4 million new cases and 375 000 deaths in 2020. The highest incidences were recorded in Northern and Western Europe, the Caribbean, Australia/New Zealand, North and South America, and Southern Africa¹ (figure 1 & 2). Within the European Union, prostate cancer is the most frequently occurring cancer in men (23.2%) and the third cause of cancer death (9.9%), after lung and colorectal cancers².

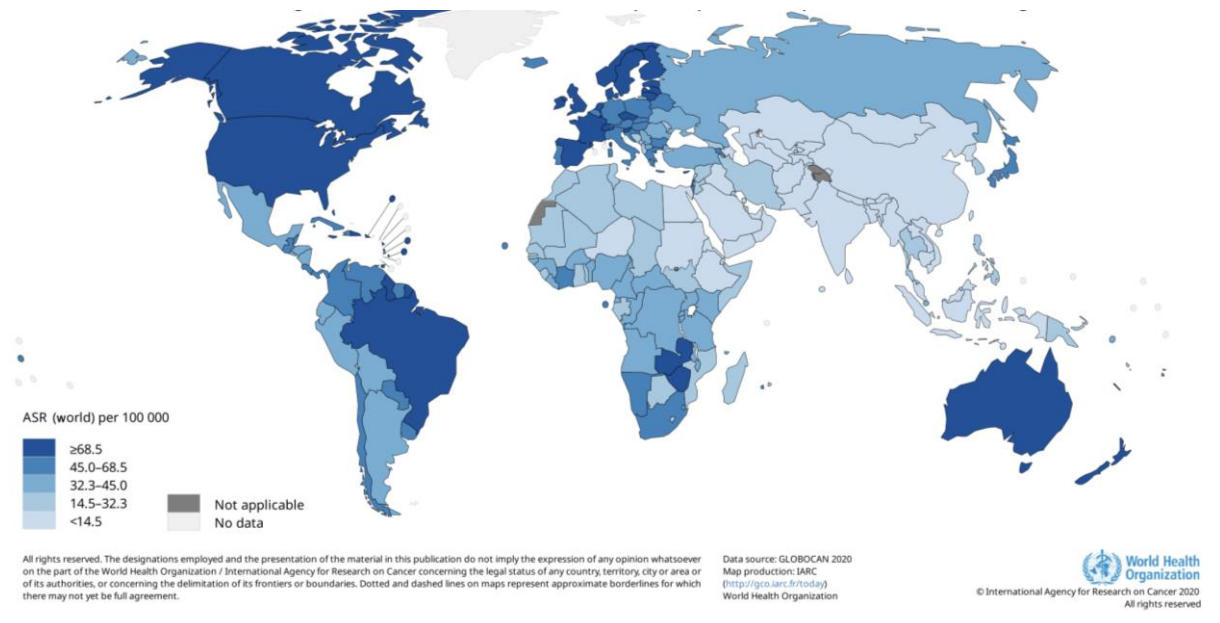


Figure 1: Estimated age-standardized incidence rates (world) in 2020, prostate, males, all ages¹.

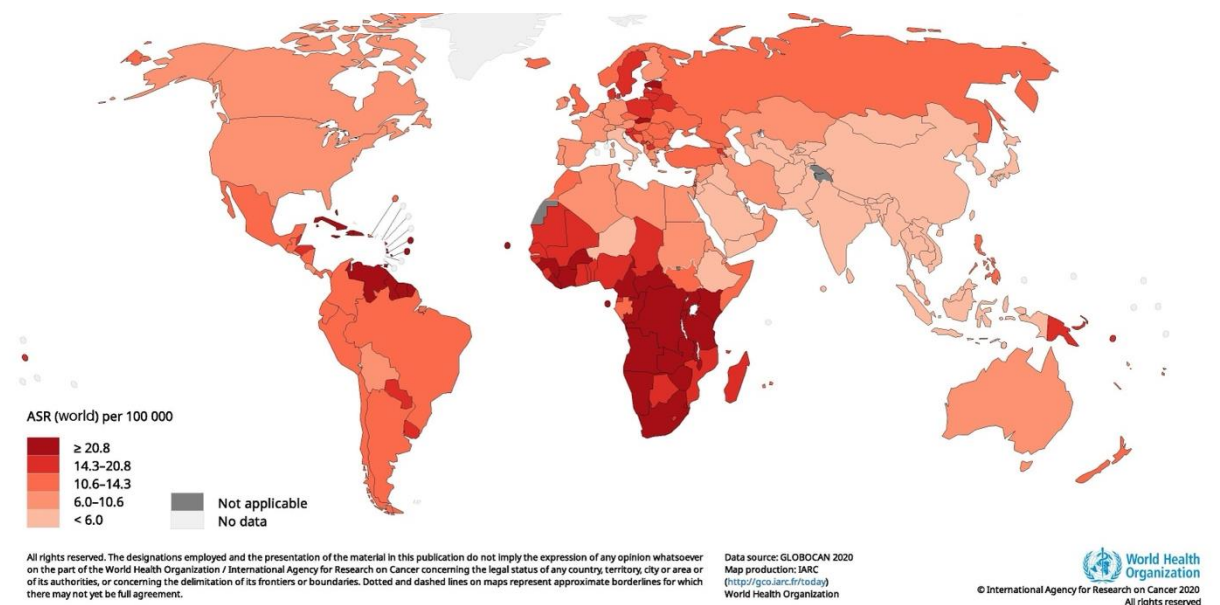


Figure 2: Estimated age-standardized mortality rates (world) in 2020, prostate, males, all ages¹.

Commonly established risk factors include age, family history, germinal variants (mostly *BRCA2* or *HOXB13*), metabolic syndrome/obesity and toxic like chlordecone. An increased incidence and mortality in African origin population has been reported. However, the role of ethnicity as a risk factor is unclear, given that race is a social construct. Reason of these findings could be more linked to genetics associated with ancestry/geographic origin, environmental factors, or social determinants of health^{1,3}.

In developed countries, *de novo* metastatic prostate represents 5 to 10% of total prostate cancer diagnoses but are causing almost 50% of prostate cancer-related deaths. This epidemiologic characteristic probably reflects their higher aggressiveness compared to localized prostate cancer secondarily evolving to metastatic relapse⁴. The incidence of *de novo* metastatic castration sensitive prostate cancer (mCSPC) has dramatically declined since the 1990's thanks to prostate-specific antigen (PSA) screening. However, this trend has come to halt, which is potentially related to a reduction of screening due to its debated effect on mortality (figure 3)⁵. This stagnation could also be linked to the fact that some of this mCSPC exhibit aggressive features leading to a rapid metastatic evolution, even before any prostate-related urinary symptom emerges.

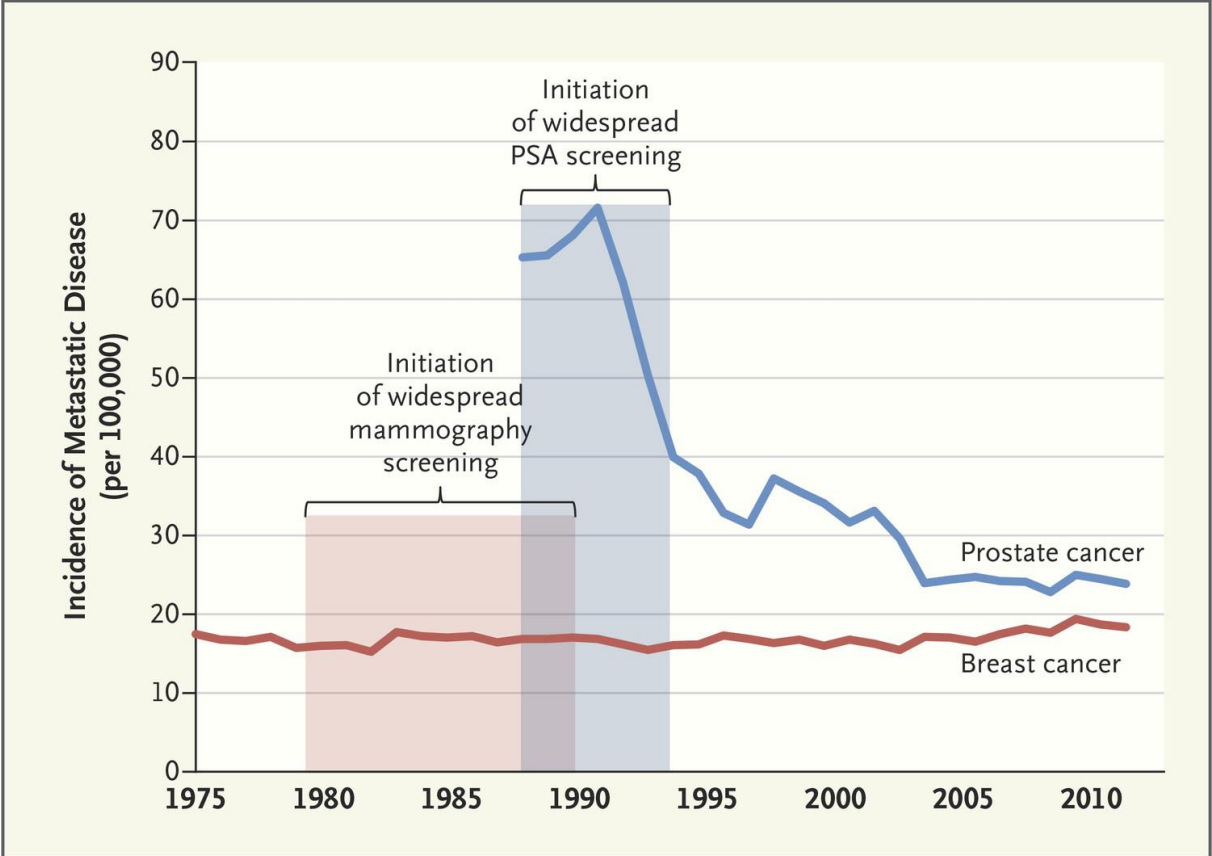


Figure 3: Incidence of cancers harboring metastasis at initial diagnosis⁵.

b. Biology of prostate cancer

i. Histological definition

Most of prostate cancers are adenocarcinoma. The diagnostic is largely based on morphology. The 2015 modified Gleason grading schematic diagram according to the International Society of Urological Pathology (ISUP) is a strong prognostic factor at early stage (figure 4). The other rare acinar adenocarcinomas are atrophic, pseudohyperplastic, microcystic, foamy, mucinous (colloid), signet ring-like cells, pleomorphic giant cells, and sarcomatoids. The later three have a worse prognosis.

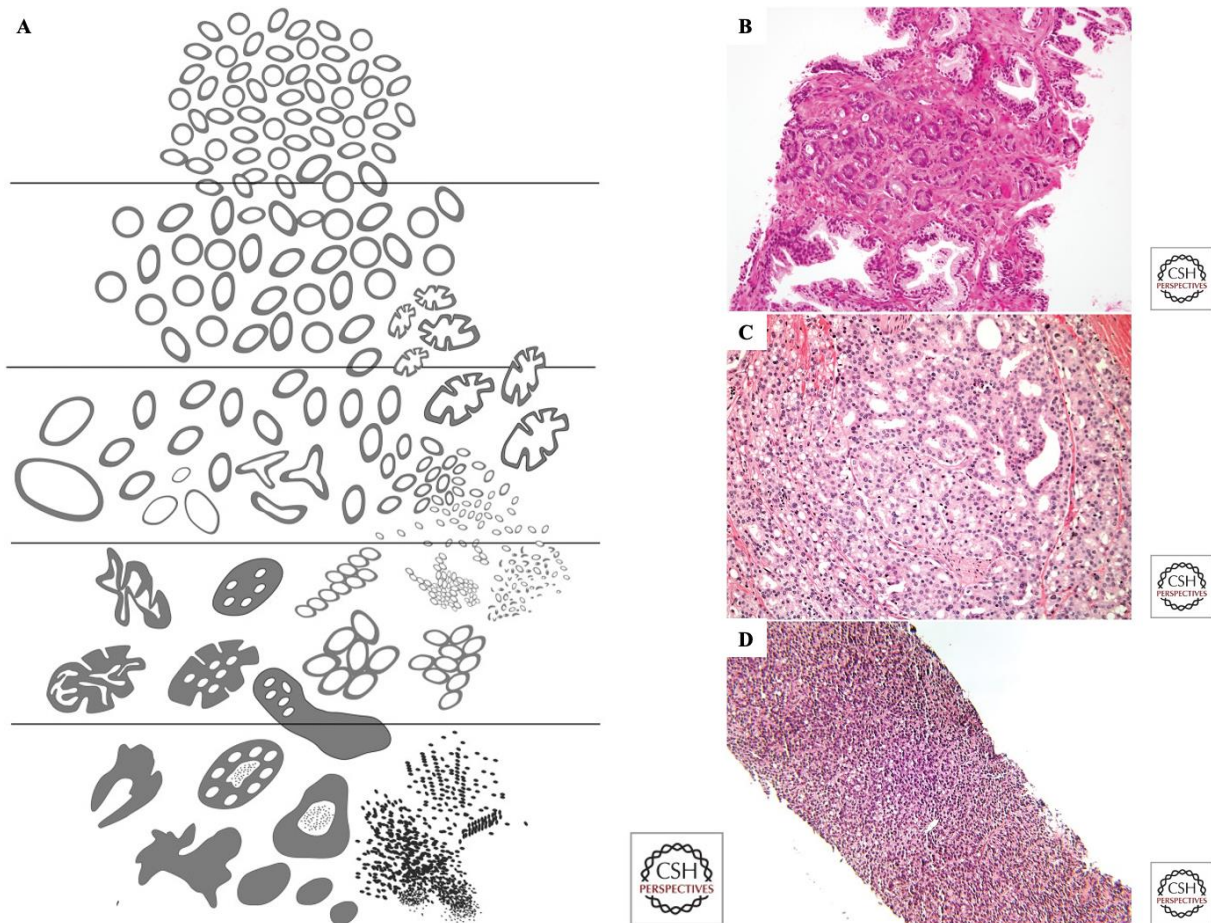


Figure 4: Prostate cancer adenocarcinoma histology and ISUP⁶.

A: Prostate cancer grades. 2015 modified Gleason grading schematic diagram according to the International Society of Urological Pathology (ISUP). Grade patterns 1 (*top*) through 5 (*bottom*)

B: Adenocarcinoma of the prostate, Gleason grade 3 + 3 = score of 6 (grade group 1), with single, separate, well-formed glands in needle core biopsy from prostate.

C: Adenocarcinoma of the prostate, Gleason grade 4 + 4 = score of 8 (grade group 4), with cribriform and fused glands in needle core biopsy from prostate.

D: Adenocarcinoma of the prostate, Gleason grade 5 + 5 = score of 10 (grade group 5), with solid sheet-like growth in needle core biopsy from prostate.

Non-acinar carcinoma comprises ductal adenocarcinoma, urothelial carcinoma, squamous neoplasms, basal cell carcinoma, and neuroendocrine (NE) tumors. Pure ductal (1% of prostate cancer) and mixed ductal acinar carcinomas (5% of prostate cancer) exhibit a worse prognosis. Squamous and basal cell carcinomas are rare. NE carcinomas are more common, and their diagnosis is based on morphology, helped if needed by NE markers (synaptophysin, chromogranin and/or CD56). Adenocarcinoma with NE differentiation, small-cell NE carcinoma, and large-cell NE carcinoma have been described. The first type is the most frequent, especially in later stage of prostate cancer due to treatment pressure. Pure small-cell NE carcinoma is rare and aggressive. Large cell-NE carcinoma is extremely rare⁶.

More recently, deep phenotypic characterization of metastatic castration-resistant prostate cancer (mCRPC) metastases revealed 5 phenotypes (e.g. tumor with mixed features expressing both androgen receptor (AR) as well as NE markers) and showed strong association of phenotypes and clinical outcomes. These phenotypes are AR-high tumors, AR-low tumors, amphicrine tumors composed of cells expressing AR and NE genes, double-negative tumors, and tumors with small cell without AR activity. Although, this phenomenon is mainly observed in patients developing resistance to castration^{7,8}. Several biological phenomena have been described underlying these histological characteristics.

ii. Oncogenic pathways

Here we focused on major pathways well-established in prostate cancer tumorigenesis which are summarized in figure 5.

AR

AR activation is the major oncogenic pathway in prostate cancer. Testosterone is produced by testis (90%) and adrenal glands (10%) with a minor autocrine secretion by tumor cells. After passing from blood flow to cytoplasm, testosterone is transformed in dihydrotestosterone (DHT) by the 5-alpha reductase enzyme. Then, DHT activates the AR ligand binding domain. AR is a nuclear receptor and acts as a transcription factor which binds to DNA by its N-terminal domain, triggering cellular growth and PSA production⁹. The AR axis has several crosstalk with other pathways described below.

Co-factors are known for their role in AR regulation. Forkhead box A1 (FOXA1) is a transcription factor known as a “pioneer factor” interacting with AR transcription activity. High FOXA1 expression is associated with an AR over expression¹⁰. Speckle-type pox virus and zinc finger (POZ) protein (SPOP) are a substrate adaptor of cullin 3-based E3 ligase. Wild type *SPOP* is a tumor suppressor degrading AR via ubiquitination. Therefore, mutational *SPOP* is linked to AR activation¹¹. Steroid receptor coactivators (SRC) are capable of acetyltransferase activity which promotes AR-induced transcription⁹.

ERG (ETS-related gene) is a transcription factor and a member of the E-26 transformation-specific (ETS) family. One of them, the *TMPRSS2-ERG* fusion is a common event in prostate cancer. In this case the promoter region of *TMPRSS2*, which contains elements sensitive to androgen, fused to the coding region of *ERG*. This event leads to the overexpression of *ERG* and its effect on gene activation triggering loss of E-cadherin - a marker of Epithelial-mesenchymal transition (EMT) - cell mobility and invasion. Crosstalk with AR has also been described¹².

NKX3.1 is a homeobox gene known as a tumor suppressor because its loss is associated with cancer progression. *NKX3.1* colocalized with AR gene in the genome. Collaboration between *NKX3.1*, AR and *Foxa1* modulate genes expression. *NKX3.1* could also be involved in epithelial cell growth, cell differentiation, and stem cell maintenance^{13,14}.

PI3K/AKT/mTOR

This pathway is frequently involved in prostate cancer (30-50%) by either inactivation of Phosphatase and TENsin homolog (*PTEN*), activation of phosphoinositide 3-kinase (*PI3K*) or *AKT* activation. Various receptor tyrosine kinases (RTKs) could trigger this pathway. After activation, PI3K will phosphorylate PIP2 leading to PIP3. The later will activate all the downstream proteins such as AKT and Mammalian target of rapamycin (mTOR). AR activation and thereby transcriptional activity is linked to this pathway by molecular interactions and crosstalk with Akt¹⁵.

Wnt/beta-cathenine

Prostate cancer cells could exhibit embryonic signaling pathways that are silenced in differentiated cells. Wnt proteins activate the transmembrane Frizzled receptors therefore reducing the formation of cytoplasmic β -catenin complexes leading to a higher level of free β -catenin and its translocation to the nucleus. Adenomatous polyposis coli protein (APC) loss of function decreases the β -catenin complexes degradation which also leads to an over activation of this pathway. These series of events result in the activation of transcriptional factors such as C-myc or CREB-binding protein (CBP)-p300¹⁶.

Nf-kb

When RTK are activated by ligands like tumor necrosis factor alpha (TNF- α) or interleukin (IL)-1, the Nf-kb canonical pathway led to phosphorylation of I κ B inhibitor proteins through I κ B kinase complex (IKK) made of IKK α , IKK β and the scaffolding protein NEMO. I κ B ubiquitination and further degradation by the proteasome is then triggered, resulting in the NF- κ B dimers releasing and translocation into the nucleus. When these NF- κ B proteins such as p50 and p65 are activated, they form homo- or heterodimeric structures which are a transcriptional factor and will bind to κ B enhancer sites along the DNA. Its activation leads to a deregulation of IL-6 expression. AR independent tumorigenesis has been found to be linked to NF- κ B activation at a protein and transcriptomic level *in vitro* because AR is one the NF- κ B target genes. TNF- α , a proinflammatory cytokine which induces NF- κ B and downstream target genes, is highly expressed in prostate cancer. Crosstalk between NF- κ B and p53 has also been described. Activation of NF- κ B in apoptosis is associated with a hyperactivation of p53, making the balance of their activities therefore crucial for cell fate decision¹⁶.

JAK-STAT

Inducers such as IL-6 will trigger the Janus kinase/signal transducer and activator of transcription (JAK-STAT) pathway by binding to the membrane receptor JAK, which in turn phosphorylate STAT proteins leading to gene regulation. Among them STAT3 is an antiapoptotic, proangiogenic and cell growth inducer¹⁶.

MAPKinase

Many different RTK like EGFR (epithelial growth factor receptor), c-Kit, PDGFR (Platelet-derived growth factor receptor), VEGFR (vascular endothelial growth factor receptor), FGFR (fibroblast growth factor receptor) and FLT-3 (Fms-like tyrosine kinase 3 receptor) can trigger the rat sarcoma virus (Ras)-GTP complex which then activates the rapidly accelerated fibrosarcoma (RAF) kinase, and therefore the extracellular signal-regulated kinases (ERK)

pathway, which in turn phosphorylates the MEK kinase and, subsequently, phosphorylates and activates the next pathway component Mitogen-activated protein kinase (MAPK)/ERK. Downstream targets of the MAPKs include the two transcription factors c-Jun and c-Fos, but also p53. This cascade led to cell proliferation, differentiation, and morphogenesis. In prostate cancer, its activation is mostly due to alterations on RTKs cited above¹⁶.

TGF-β/SMAD signaling

When the transforming growth factor-β (TGF-β) binds to its receptor, mothers against decapentaplegic homologue (SMADS) intracellular proteins are recruited and transduce the signal into the nucleus to regulate gene expression. This overexpression leads to cell growth, adhesion, migration, cell differentiation, embryonic development, and apoptosis regulation. TGF-β is produced by CD4⁺ T cells and regulatory T cells suggesting an effect on immune tumor evasion¹⁶.

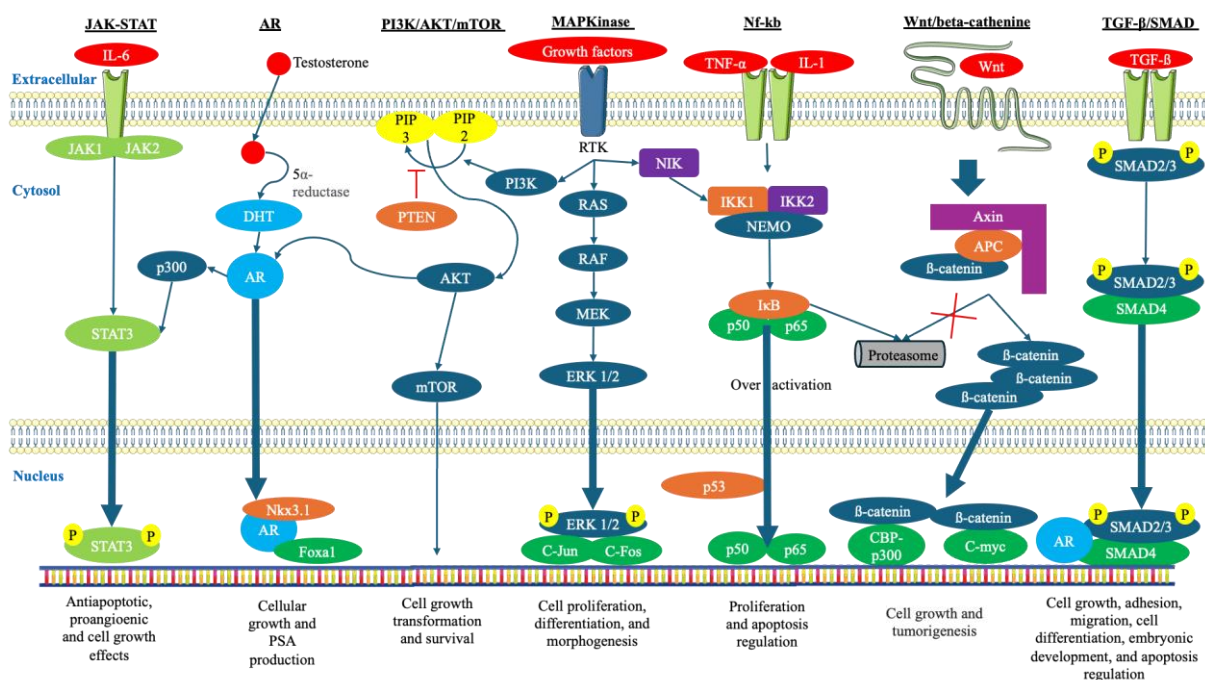


Figure 5: Summary of major oncogenic pathways in prostate cancer.

AKT: serine/threonine kinase, APC: Adenomatous polyposis coli, AR: androgen receptor, CBP: CREB-binding protein, DHT: Dihydrotestosterone, FOXA1: Forkhead box A1, IKK: IκB kinase, IL-1: Interleukin 1, IL-6: Interleukin 6, JAK: Janus kinase, mTOR: Mammalian target of rapamycin, PI3K : phosphoinositide 3-kinase, PIP2: Phosphatidylinositol (4,5) bisphosphate, PIP3: Phosphatidylinositol (3,4,5) trisphosphate, PTEN: Phosphatase and TENSin homolog, SMAD: mothers against decapentaplegic homologue, STAT: Signal transducer and activator of transcription, TGF-β: transforming growth factor-β, TNF-α: Tumor necrosis factor alpha.

iii. DNA repair deficiency

BRCA 1 and 2 are involved in double strand break repair by homologous recombination. Single strand break repair is another major mechanism of DNA repair in which Poly(ADP-ribose) polymerase 1 (PARP1) plays a key role. Based on this knowledge, inhibitors of PARP lead to cell apoptosis by synthetic lethality in tumor with homologous recombination defect. Other common DNA repair defects include proteins such as Ataxia–telangiectasia mutated (ATM), which senses DNA damage and activates homologous recombination, RAD51

involved in homologous recombination as well and MLH1, MSH2, MSH6 or PMS2 for mismatch repair pathway. In a crosstalk, AR regulates DNA-dependent protein kinase catalytic subunit (DNA-PKcs) which play a role in double strand break repair by non-homologous end joining (figure 6)¹⁷. Cyclin dependent kinase (CDK)12 form a heterodimeric complex with its activating partner, cyclin K. These kinases prevent genomic instability through the regulation of DNA damage response genes. Therefore, biallelic loss of CDK12 could be immunogenic and increase response to immune checkpoint inhibitors¹⁸.

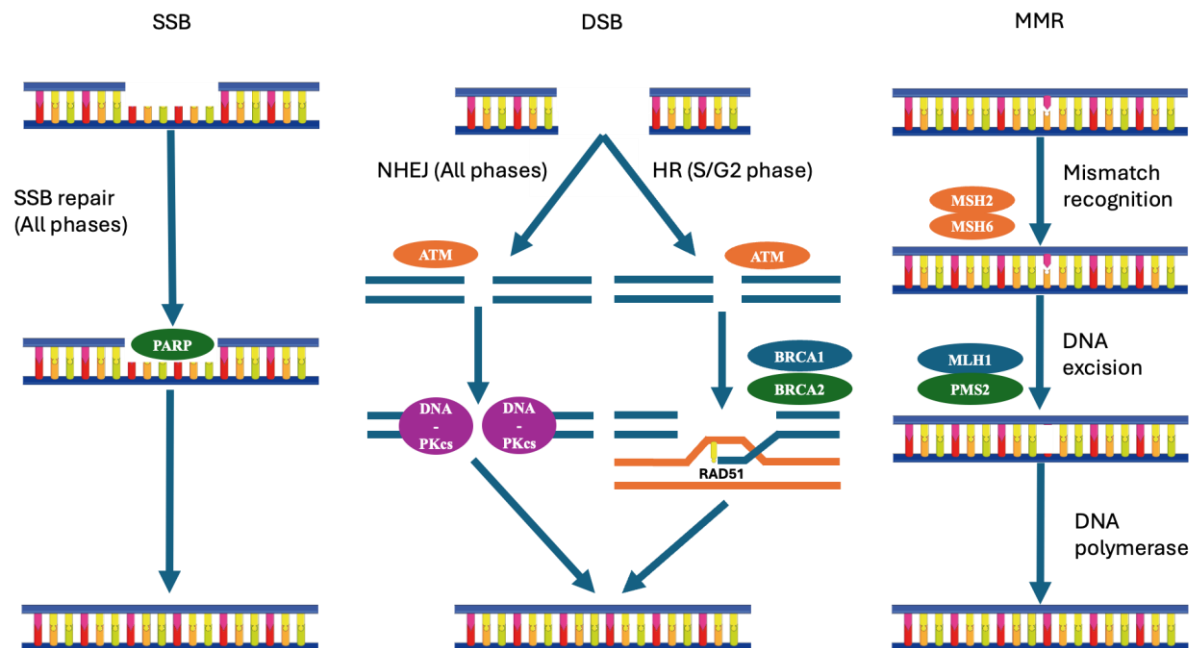


Figure 6: Main DNA repair pathways involved in prostate cancer.

ATM: ataxia–telangiectasia mutated, BRCA: Breast Cancer, DNA-PKcs: DNA-dependent protein kinase catalytic subunit, DSB: double strand break, HR: homologous recombination, MMR: mismatch repair, NHEJ: non-homologous end joining SSB: single strand break.

iv. Tumor proliferation and cell cycle regulation

The transcription factor p53 was initially considered as pro-oncogenic in the 1970's but its role as a tumor suppressor is now established. Under cellular stress, p53 will trigger gene expression leading to cell cycle arrest, DNA repair and metabolic adaptation, or could trigger apoptosis in case of irreversible damage. Mouse double minute 2 homolog (MDM2) also downregulates p53 activation by ubiquitination and is upregulated by p53 itself in a feedback loop during the absence of cellular stress. The p53 pivotal role in cell fate in case of cellular damage make it an essential surrogate and probably explains why *TP53* loss of function is the most frequent alterations found in cancer¹⁹.

Retinoblastoma (Rb1) is involved in cell cycle arrest. When activated by hypophosphorylation, Rb1 binds to gene promoters leading to the suppression of cell cycle inducers like E2F. *RBI* loss could lead to unregulated AR activity and dysregulated cell cycle via E2F, ultimately inducing cell proliferation²⁰.

PI3K/AKT/mTOR and MAPKinase pathways intervene in the process of AR transcription of genes promoting the G1 to S phase transition. In this process AR promote cyclin D1 which in turn activates CDK4 and CDK6 thereby leading to cell proliferation. The cyclin D-CDK4/6 complex also inactivates the retinoblastoma Rb1 tumor suppressor protein strengthening this proliferative effect²¹

v. Epigenetic

DNA modification

Several gene expression regulations such as increased DNA methylation by DNA methyltransferases (DNMTs) and decreased activity of DNA methylase like tet methylcytosine dioxygenase 2 (TET2) were described in prostate cancer. In mCRPC, promoter methylation silences tumor suppressor genes or others such as *AR*, adhesion genes like (*CD44*, chromodomain helicase DNA-binding protein 1 (*CHD1*)), cell cycle genes (*CCND2*, *Cyclin-dependent kinase inhibitor 1B (CDKN1B)*) or apoptotic genes (*B-cell lymphoma 2 (BCL2)*)²².

Histone modification

AR pathway activation leads to histone acetylation needed for all the active transcription ensuing. Histone acetylation at lysine residues is promoting AR target genes expression. This phenomenon is controlled by histone acetyl transferases (HATs) and histone deacetylases (HDACs). Bromodomain-containing (BRD) proteins are part of the bromodomain and extra-terminal (BET) family of chromatin readers and recognize mono-acetylated histones leading to chromatin remodeling, and finally transcription. HAT domain and bromodomain of the p300 and CBP proteins interact with transcription factors. In prostate cancer, p300 and CBP are highly homologous and frequently upregulated. Enhancer of zeste homolog 2 (EZH2) silences transcription through trimethylation of histones and is over-expressed in prostate cancer. Additionally, in mCRPC, EZH2 is a coactivator of transcription factors such as the AR (figure 7). Lysine-specific demethylase 1 (LSD1), or KDM1A, is a histone demethylase which regulate AR transcriptional activity via H3K4 demethylation. LSD1 can also demethylate and therefore activate FOXA1 leading to the recruitment of AR-dependent enhancers²².

Micro RNAs

More recently, micro RNAs or miRNAs has been described as small endogenous non-coding RNAs (18–25 nucleotides) inhibiting protein synthesis by cleaving or blocking the transcription of mRNAs. These miRNAs are circulating in blood and therefore could be biomarkers of interest. Depending on which mRNA is targeted, and thereby the corresponding protein expression, several oncogenic pathways could be regulated leading to either tumorigenesis or cancer suppression. For example, miR-21 has been reported to promote tumor invasiveness and associated with mCRPC when miR-34a is a tumor suppressor by inducing cell-cycle arrest, senescence and apoptosis²³.

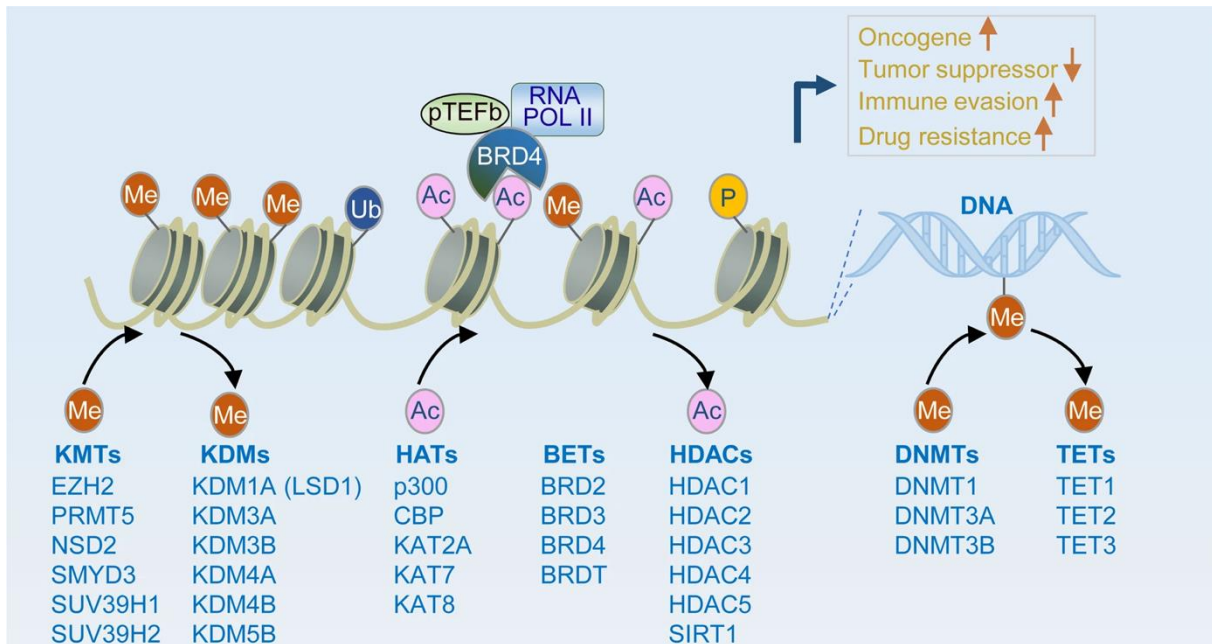


Figure 7: Schematic of epigenetic regulation in prostate cancer through histone modification (such as acetylation, methylation, phosphorylation, and ubiquitination) or DNA modifications (such as methylation) leading to upregulation of oncogenes or reduction of tumor suppression genes²⁴.

BET: Bromodomain and extra-terminal, BRD: Bromodomain-containing, DNMTs: DNA methyltransferases, HDACs: Histone deacetylases, HATs: Histone acetyl transferases bromodomain and extra-terminal, KDM: Histone lysine demethylase, TETs: Ten-eleven translocation proteins.

vi. Epithelial mesenchymal transition

All this transcription regulation could lead to the well-known process of transition from adherent epithelial-like cells to a more aggressive mesenchymal-like phenotype with motility capacity allowing metastatic spreading. A reverse process, from mesenchymal to epithelial phenotype, could also be involved for tumor progression. The transcription factors SNAIL, TWIST, and zinc-finger E-box-binding (ZEB) regulate gene expression leading to the epithelial phenotype repression and the mesenchymal phenotype activation. Some pathways mentioned above promote EMT including TGF- β /SMAD, Wnt/beta-catenine, NOTCH, hedgehog, and growth factors. More recently, Forkhead box protein C2 (FOXC2) has been identified as an EMT regulating transcription factor. Other above-mentioned factors such FOXA1 and ERG play a role in the EMT. Epigenetic mechanisms might be involved as well (figure 8)²⁵.

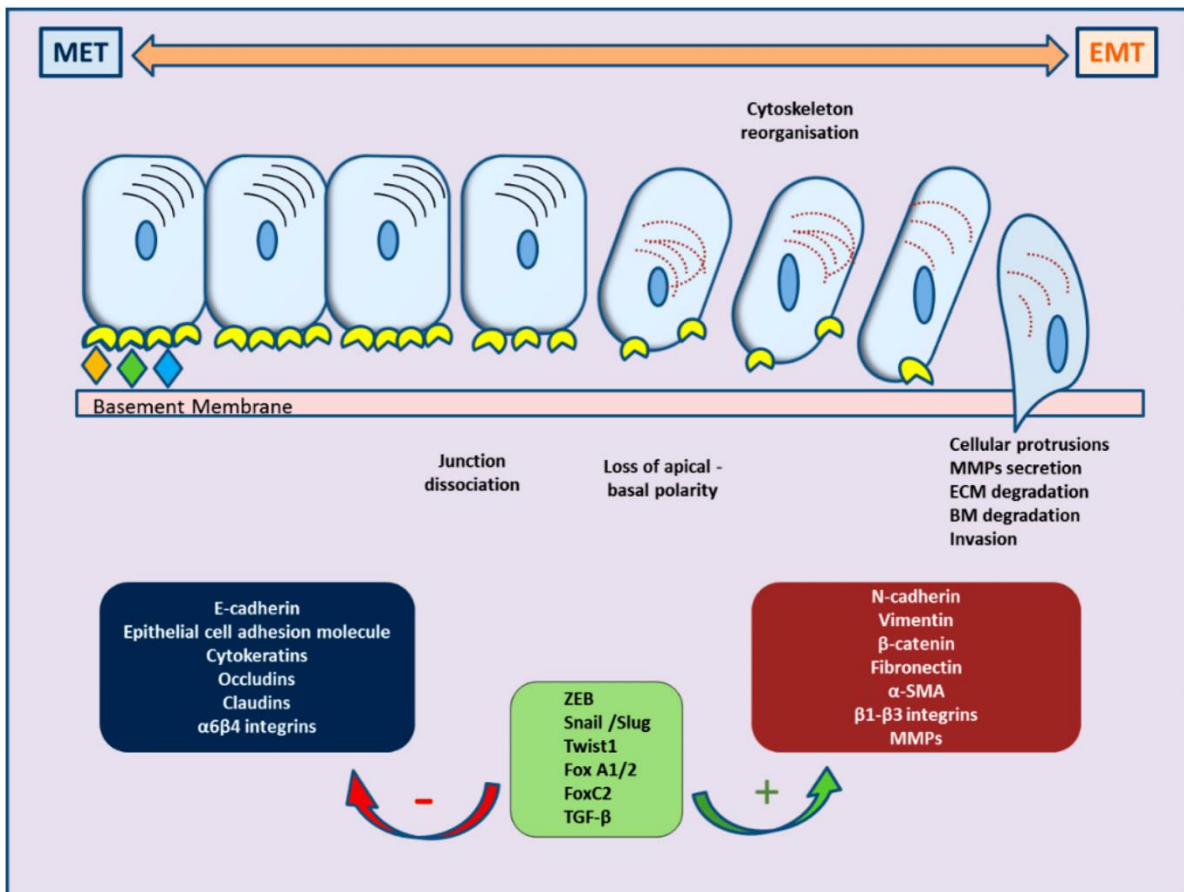


Figure 8: Cellular changes and main molecular events during epithelial–mesenchymal transition and the reverse mesenchymal–epithelial transition²⁵.

α-SMA: Alpha Smooth Muscle Actin, BM: Basal membrane, ECM: Extra cellular matrix, TGF-β: transforming growth factor beta, MMPs: metalloproteinases, ZEB: zinc-finger E-box-binding.

vii. Tumor microenvironment

In connection with all these pathways end tumor cells transformation, the tumor microenvironment plays a key role in prostatic epithelial cells transformation to cancer progression via chemokines, cytokines, or other enzymes. Cancer associated fibroblast is a major actor in this process by secreting TGF-β, IL-6, growth differentiation factor 15 (GDF15), FGF, hepatocyte growth factor (HGF), hypoxia inducible factor 1 alpha (HIF-1α), and VEGF. These factors promote angiogenesis and extra cellular matrix alteration after fibroblast activation by tumoral cells and ultimately stimulate cancer progression. Inflammatory cells CD3+ T-cells, CD20+ B-cells, macrophages, natural killer cells, mast cells, and macrophages produce oncogenic cytokines and chemokines like TNF, NFκB, IL-6, IL-8, and VEGF. Stroma remodeling by matrix metalloproteinases (MMP) acting on collagens, fibronectins, and laminin has been described in prostate cancer. Cancer stem cells expressing diverse markers including CD44, CD133, and ALDH are found in niches within the tumor microenvironment and could play a role in tumor progression. COX-2 cyclooxygenase-2 (COX-2) and PDGF secreted by prostate cancer cells, among other factors, also stimulate angiogenesis (figure 9)²⁶. All these mechanisms could transform prostate cancer cells into more aggressive clones.

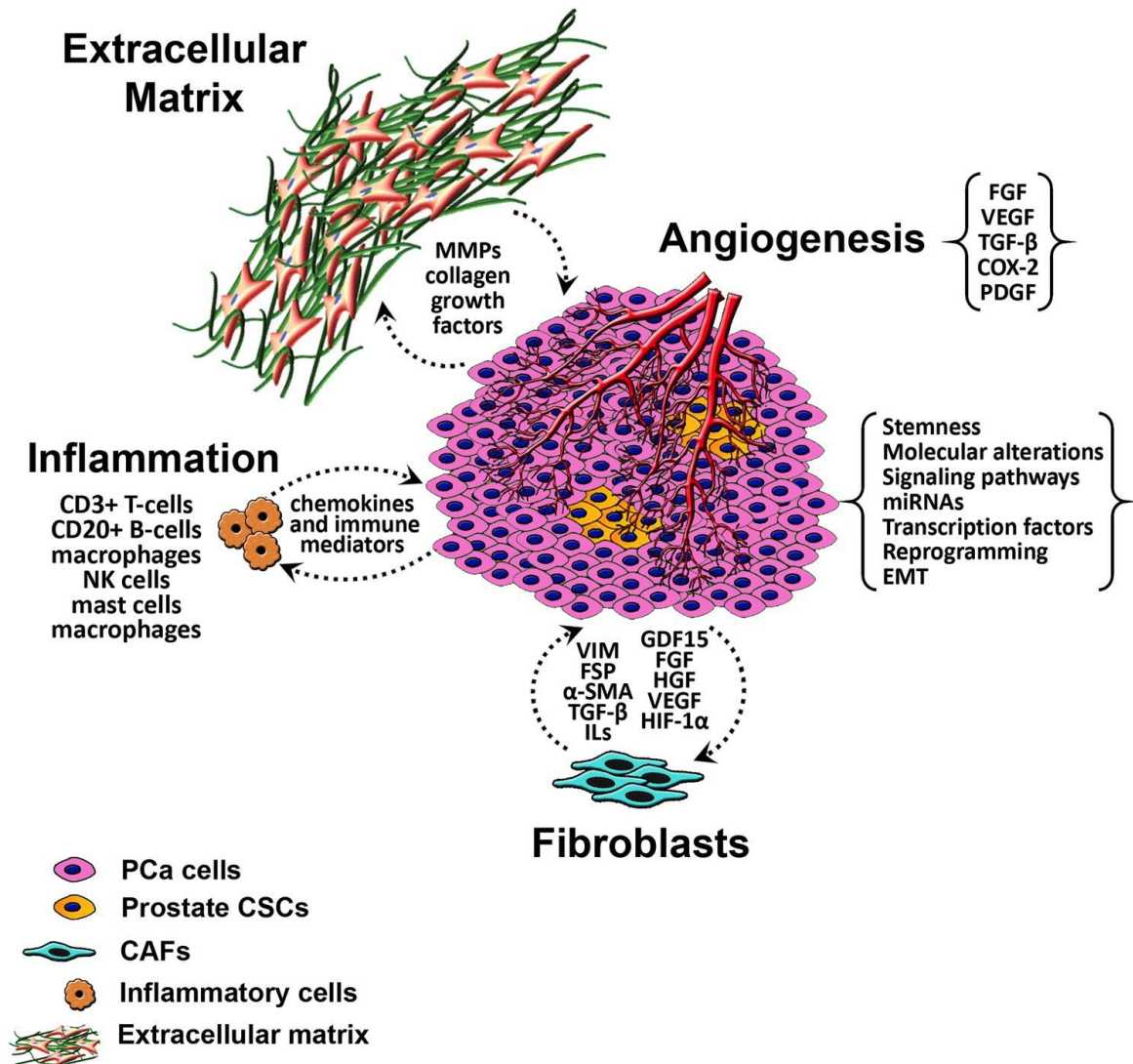


Figure 9: Schematic diagram of the tumor microenvironment in prostate cancer²⁶.

α -SMA: alpha smooth muscle actin, CAFs: cancer associated fibroblasts, CSCs: cancer stem cells, COX-2: cyclooxygenase-2, ECM: extracellular matrix, EMT: epithelial-to-mesenchymal transition, FGF: fibroblast growth factor, FSP: fibroblast specific protein, GDF15: growth differentiation factor 15, HGF: hepatocyte growth factor, ILs: interleukins, miRNAs: micro-RNAs, MMP: matrix metalloproteinases, NK cells: natural killer cells, PCa: prostate cancer, PDGF: platelet-derived endothelial cell growth factor, TGF- β : transforming growth factor beta, VEGF: vascular endothelial growth factor.

viii. Prognostic factors: neuroendocrine and aggressive variants

Localized prostate cancer

For over two decades now, the D'Amico classification based on clinical tumor size, PSA and Gleason score has been commonly used. This score predicting biochemical recurrence risk stratification is the cornerstone for localized treatment choice²⁷. No immunochemistry (IHC) marker is associated with prognosis for localized prostate cancer and NE markers expression assessment showed conflicting results²⁸.

DECIPHER is a transcriptomic score using a random forest algorithm based on the expression of 22 genes linked to androgen receptor signaling, cell proliferation, differentiation, motility, and immune modulation. Since 2013, it has shown clinical utility in localized prostate cancer to help treatment decision²⁹. An ancillary study of the STAMPEDE phase 3 trial abiraterone cohort showed an association between metastatic free survival and the DECIPHER score for patients with a high-risk localized prostate cancer. Interestingly, type 1 interferon signaling linked with increased tumor lymphocyte infiltration was also associated with worse outcomes.

mCRPC

NE transdifferentiation is more frequent than *de novo* NE prostate cancer (NEPC) and happen in up to 20-30% of mCRPC. These NE forms emerge under androgen treatment with different characteristics reflecting their AR-independent state with NE phenotypic markers, lineage plasticity and activation of alternative pathways for survival. Double negative tumors with loss of AR expression without NE markers probably represent an intermediate state. These two phenotypes could be grouped under the term of aggressive variants which has extensively been described these last 5 years. In clinical practice, these aggressive variants could be encountered in patients with a younger age at diagnosis, visceral rather than only bone metastasis, lytic rather than osteoblastic bone lesions and a relatively low PSA. In IHC, these NE or aggressive forms of prostate cancer are characterized by at least one NE marker positivity (i.e. chromogranin A, synaptophysin or CD56) and a certain level of AR expression loss (figure 10).

At a molecular level, loss of at least two tumor suppressor genes among *TP53*, *PTEN* or *RBI* (TSalt) has been profusely reported in this more aggressive subtype, by allowing lineage plasticity and prostate cancer cells reprogramming through epigenetic (via *EZH2*). *N-Myc*, a transcription factor essential for brain development, has also been found to be involved in AR independence and lineage determination through epigenetic reprogramming. Its amplification is almost systematically occurring with aurora kinase A (*AURKA*) amplification, which regulates mitotic division³⁰.

Regarding transcriptomic, a 70-gene NEPC classifier developed by Beltran et al. identified as NEPC more aggressive mCRPC. In 20% of cases, this score was elevated in adenocarcinomas, which could represent tumors in transition to NEPC or aggressive variant³¹. *CHD1* is a protein required for chromatin opening and thereby allowing transcription. Lineage plasticity happening under androgen deprivation therapy (ADT) is associated with *CHD1* loss by inducing a lineage-specific transcriptome in addition to the deregulation of AR signaling³². Other transcription factor has been reported to promote transition to NEPC such as SRY-Box transcription factor 2 (*SOX2*), Achaete-scute homolog 1 (*ASCL1*), POU domain, class 3, transcription factor 2 (*POU3F2/BRN2*)³⁰.

Surfactome also exhibits specific features such as delta-like protein 3 (DLL3) and carcinoembryonic antigen-related cell adhesion molecule 5 (CEACAM5) proteins over-expressed in NE tumor from several organs³³. All these biological mechanisms have been reported in mCRPC but *de novo* prostate cancer is poorly described with no aggressive variants identified yet.

mCSPC

As in localized prostate cancer with the D'Amico score, PSA has been reported to be prognostic in more advanced stages³⁴. In PEACE-1 in particular, PSA response at 8 months (i.e. < 0.2 ng/ml) was associated with a longer OS³⁵. NEPC harboring morphological features as mentioned above are rare at initial diagnostic with a frequency of 1 to 5% if accounting for pure and mixed with adenocarcinoma associated. These tumors are known to be more aggressive with a *de novo* metastatic presentation and a worse prognosis. In IHC synaptophysin/chromogranin A are positive with either AR/PSA/PSMA/ERG/NKX3.1 loss of expression and a higher ki67 index. Some tumors could express a range of NE IHC markers without classical morphological findings reflecting a more diverse phenotype or transdifferentiation ongoing from adenocarcinoma to NEPC. The prognosis of such intermediate tumors define by IHC remains unclear and understudied in mCSPC²⁸.

In the same ancillary study of STAMPEDE but focusing on the metastatic patients, the DECIPHER score had a prognostic value. Transcriptomic signature of *PTEN* or *TP53* loss was also associated with a worse prognosis. However, none of their transcriptomic signatures (AR-A, PAM50, PSC, and the DECIPHER) were predictive of abiraterone benefit on OS³⁶. The prognostic value of DECIPHER has also been reported in other phase 3 ancillary study with mCSPC patients such as CHAARTED (docetaxel) and TITAN (apalutamide)²⁹. All these data are calling for a more extensive investigation in *de novo* mCSPC of the prognostic factors already reported for mCRPC patients.

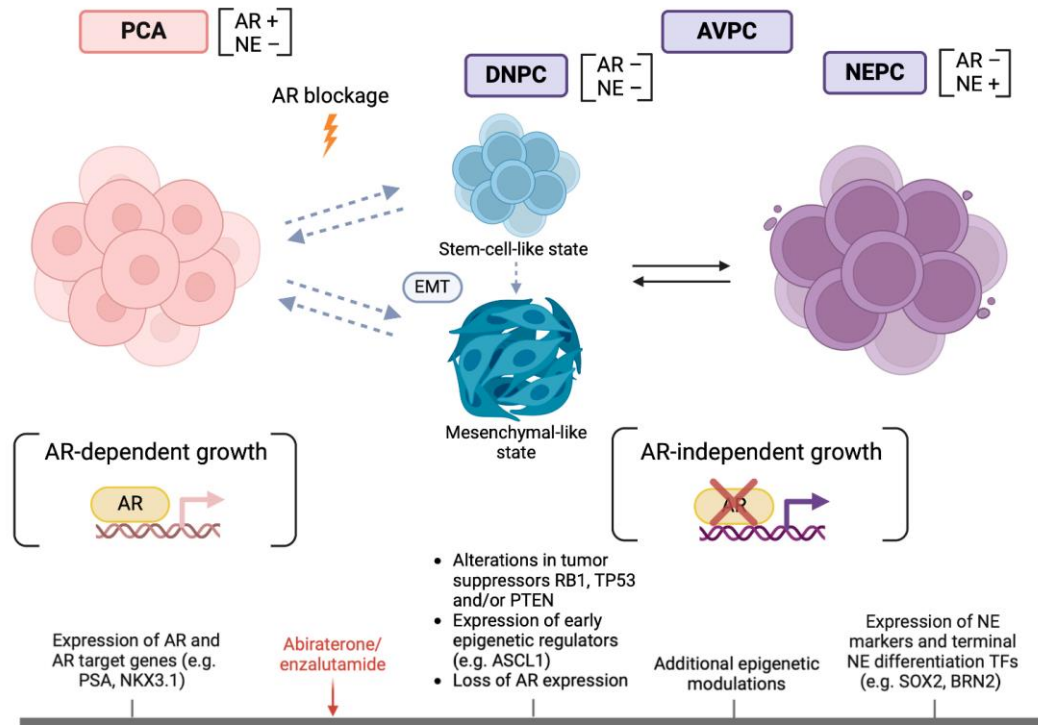


Figure 10: Molecular and phenotypic changes involved in transition to NEPC³⁰.

AR: Androgen receptor, ASCL1: Achaete-scute homolog 1, AVPC: Aggressive variant prostate cancer, BRN2 (POU3F2): POU domain class 3 transcription factor 2, DNPC/ Double negative prostate cancer, EMT: Epithelial-to-mesenchymal transition, NE: Neuroendocrine, NEPC: Neuroendocrine prostate cancer, PCA: Prostate adenocarcinoma, PTEN: Phosphatase and tensin homolog, SOX2: SRY-Box transcription factor 2, RB1: Retinoblastoma protein 1, TP53: Tumor protein 53.

ix. Genomic landscape according to different stages

Localized prostate cancer

In early stage, prostate cancer harbors less alterations. In one of The Cancer Genome Atlas (TCGA) cohort comprising 333 localized prostate cancer, alterations found by whole exome sequencing were mostly on E26 transformation-specific (*ETS*) family fusion (59.0%), *PTEN* (17.0%), *SPOP* (11.0%), *TP53* (8.0%), *CHD1* (7.0%), *ATM* (6.0%), *SPINK1* (6.0%), *KMT2C* (4.0%), *FOXA1* (4.0%), *BRCA2* (3.0%) and *KMT2D* (3.0%)³⁷.

mCRPC

Advanced prostate cancers are more genetically altered and mCRPC has been extensively studied in several cohorts. In one of the largest, the SU2C-PCF with 150 mCRPC, most frequent alterations in whole exome sequencing were *AR* (62.7%), *ETS* family fusion (56.7%), *TP53* (53.3%), *PTEN* (40.7%), *BRCA2* (13.3%), *KMT2C* (12.7%), *FOXA1* (12.0%), *ZBTB16* (10.0%), *RBI* (9.3%), *APC* (8.7%), *CHD1* (8.0%) and *SPOP* (8.0%)³⁸. In the MSK-Impact cohort of 164 patients with mCRPC, alterations found using the MSK-IMPACT assay were *AR* (52.0%), *TP53* (48.0.3%), *PTEN* (29.0%), *RBI* (18.0%), *APC* (15.0%), *FOXA1*

(12.0%), *KMT2C* (10.0%), *ATM* (11.0%), *CDK12* (11.0%), *BRCA2* (10.0%), *FANCA* (7.0%) and *KMT2D* (7.0%)³⁹. To note, most of AR alterations were amplifications.

De novo mCSPC

Compared to mCRPC, mCSPC harbored relatively less AR alterations due to their non-exposure to castration, with fewer data available in the literature. The 140 mCSPC patients of the MSK-Impact cohort had alterations in *TP53* (30.0%), *PTEN* (18.0%), *APC* (14.0%), *SPOP* (11.0%), *FOXA1* (10.0%), *KMT2C* (9.0%), *BRCA2* (7.0%), *RBI* (7.0%), *CDK12* (6.0%) and *CTNNB1* (6.0%)³⁹. In the 115 mCSPC patients of the STAMPEDE cohort, comprising 98% of *de novo*, most frequent alterations were *PTEN* (34.0%), *TP53* (33.0%), *ETS* family fusions (33.0%), *PIK3CA* (9.0%), *APC* (7.0%), *CTNNB1* (7.0%), *ATM* (6.0%), *CDK12* (6.0%), *KDM6A* (5.0%) and *SPOP* (4.0%)⁴⁰. *BRCA2* alterations were only found in 2.0% of patients⁴⁰. Table 1 summarized the frequency for each alteration according to the stages of the disease.

Table 1: frequency of genomic alterations according to stages of the disease in different cohorts.

Genomic alterations		Frequency (%)				
Pathway	Gene	Localized	mCNPC		mCRPC	
		TCGA ³⁷ (n=333)	MSK-IMPACT ³⁹ (n=140)	STAMPEDE ⁴⁰ (n=118)	MSK-IMPACT ³⁹ (n=164)	SU2C-PCF ³⁸ (n=150)
AR pathway	<i>AR</i>	0	4	0	52	63
	<i>FOXA1</i>	4	10	0	12	12
	<i>SPOP</i>	11	11	4	5	8
	ETS fusion	59	NA	33	NA	57
Lineage plasticity and neuroendocrine differentiation	<i>TP53</i>	8	18	33	29	53
	<i>RBI</i>	1	7	1	18	9
	<i>CHD1</i>	7	NA	0	NA	8
DNA damage repair	<i>BRCA2</i>	3	7	2	10	13
	<i>BRCA1</i>	0	1	0	2	1
	<i>ATM</i>	6	2	6	11	7
	<i>FANCA</i>	0	3	1	7	NA
	<i>CDK12</i>	2	6	6	11	5
	<i>MSH2</i>	0	2	2	3	2
	<i>MLH1</i>	0	1	0	1	1
PI3K-AKT-mTOR	<i>PTEN</i>	17	18	34	29	41
	<i>PIK3CA</i>	2	4	9	3	5
	<i>PIK3CB</i>	0	NA	3	NA	6
	<i>PIK3R1</i>	0	4	3	5	5
	<i>AKT1</i>	1	1	1	1	1
Wnt-β-catenin	<i>APC</i>	0	14	7	15	9
	<i>CTNNB1</i>	2	6	7	3	4
	<i>RNF43</i>	0	1	0	3	3

mCNPC: metastatic castration naïve prostate cancer, mCRPC: metastatic castration resistant prostate cancer

c. Treatment landscape in metastatic prostate cancer

Here we focused on systemic treatments approved in France (summarized in figure 11 & 12).

i. Androgen deprivation therapy

Castration is the cornerstone of prostate cancer treatment since the 1940's⁴¹. Surgical or biological castration with LHRH agonist/antagonist are used for biological relapse or metastatic disease, for life³.

ii. Chemotherapy

After a long period of time without any new efficient treatment discovery, docetaxel, a microtubule inhibitor, was the first chemotherapy with a benefit in OS approved mCRPC⁴² in 2004 and mCSPC⁴³ in 2015. Cabazitaxel, another taxane, was approved in 2010 after progression with docetaxel⁴⁴. However, responses to these cytotoxic treatments are rarely prolonged and they cause cumulative toxicity.

iii. AR pathway inhibitors

AR pathway inhibitors (ARPI) approval was a breakthrough for the management of prostate cancer because of their efficiency and relatively acceptable toxicity. Abiraterone, a CYP17A1 inhibitor blocking adrenal testosterone production, was the first approved in 2011 for mCRPC⁴⁵ and in 2017 for mCSPC⁴⁶. Enzalutamide, the first AR inhibitor ever developed, was available in 2012 for mCRPC⁴⁷ and 2019 for mCSPC⁴⁸. Others AR inhibitors followed mostly developed in the non-metastatic castration resistant setting such as apalutamide⁴⁹ and darolutamide⁵⁰ in 2019. Enzalutamide was also approved in this setting in 2018⁵¹. Apalutamide was available for mCSPC⁵² in 2019. Despite their long response for some patients, progression with resistance occurred inevitably, calling for more efficient therapeutic development.

iv. Chemotherapy and hormonotherapy combination

To overcome these resistances to chemotherapy and hormonotherapy, combination treatment has been recently assessed. In PEACE1 clinical trial published in 2022, castration with docetaxel and abiraterone showed a benefit in overall survival (OS) for patients with a high burden disease and a benefit in progression free survival (PFS) for low volume patients⁵³. ARASENS confirmed this gain in OS regardless of tumoral burden with another triplet treatment made of castration, docetaxel and darolutamide the same year⁵⁴.

v. PARP inhibitors

Targeted therapies have been developed as well to overcome resistance to standard treatment. The first approved PARP inhibitor in France was Olaparib in 2020 for mCRPC after ARPI only for patients harboring *BRCA1* or *BRCA2* alterations⁵⁵. Niraparib + abiraterone was also approved for the same alterations but in first line mCRPC⁵⁶ in 2023 and olaparib + abiraterone in first line mCRPC regardless of *BRCA* mutations the same year⁵⁷. More recently, talazoparib + enzalutamide has been approved in 2024 in the same setting⁵⁸. Response to these treatments for patients with *ATM* alterations or other DNA damage repair genes remains unclear⁵⁹.

vi. Radionuclide treatment

Other strategies to develop targeted therapies focused on radionuclide treatment. The first approved was radium 223, an alpha-emitter targeting bone in 2013 for patients with mCRPC and metastases limited to bones⁶⁰. More recently, ¹⁷⁷Lu-PSMA-617 was approved in 2021 for mCRPC expressing PSMA⁶¹.

vii. Denosumab

Denosumab is an antibody inhibiting the nuclear factor κ B ligand (RANKL) involved in osteoclast stimulation which leads to bone destruction. It was approved for mCRPC with bone metastases in 2011 to prevent skeletal related events⁶².

viii. Therapeutic perspectives

New hormonotherapy

ODM 208 is a CYP11A1 inhibitor blocking the production of all steroid hormones and precursors, upstream of the CYP17A1 targeted by abiraterone. It has shown promising signals of efficacy in mCRPC patients harboring an AR mutations after ARPI in early phase clinical trials⁶³.

Immunotherapy

Immune checkpoint inhibitors did not show any activity in prostate cancer. Combinations of immune checkpoint inhibitor are under investigation with docetaxel, enzalutamide or olaparib. CDK12 aberrations, as described above, could be associated with some response to immune checkpoint inhibitors but need further confirmation of efficacy. Patients with MSI high prostate cancer benefit from pembrolizumab for half of them and even if this treatment is not reimburse in France in this setting, these patients can be included in clinical trial²⁴.

PTEN/PI3K/AKT/mTOR pathway

Despite pre-clinical activity, no efficacy of Pi3k, Akt or mTOR inhibitors in prostate cancer has been demonstrated yet in a randomized trial. Some of them are currently under evaluation in combination with ARPI²⁴.

CDK4/6

Tumor hyperproliferation can be targeted by CDK4/6 inhibitors. Palbociclib, ribociclib and abemaciclib, already approved in hormonal positive breast cancer, are under investigation in mCRPC²⁴.

Epigenetic

Several agents targeting epigenetic mechanisms previously cited are currently in clinical development. Histone methylation is targeted by EZH2 inhibitors, histone acetylation by p300/CBP inhibitors, BRD proteins by BET inhibitors, histone acetylation deacetylation by HDAC inhibitors and DNA methylation by DNMT inhibitors. These therapies could also be used to treat NEPC prostate cancer²⁴.

Treatment targeting neuroendocrine differentiation

Yet, there is no treatment with strong proof of efficacy available for NEPC. Pure NEPC are usually treated with platin etoposide-based regimen by homology with NE small cells lung cancer (SCLC). Adenocarcinoma mixed with NE histology has no standard treatment either. Platine associated with etoposide, docetaxel or cabazitaxel showed an increased toxicity without clear benefit. Given the response to immune checkpoint inhibitors in SCLC, these therapies are under investigation for NEPC. AURKA inhibitor alisertib showed some response in NEPC patients. Other treatments targeting the surface proteins delta-like 3 (DLL3) and carcinoembryonic antigen-related cell adhesion molecule 5 (CEACAM5) are in clinical development including antibodies drug conjugates, chimeric antigen receptor T cells or bi-specific antibodies³³.

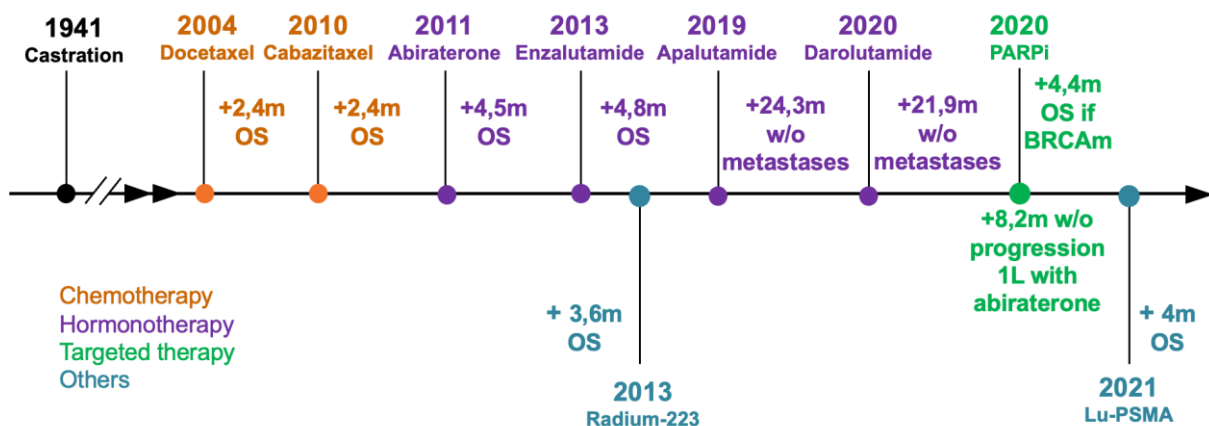


Figure 11: Systemic treatment evolution in prostate cancer with their respective dates of approval in France.

OS: overall survival

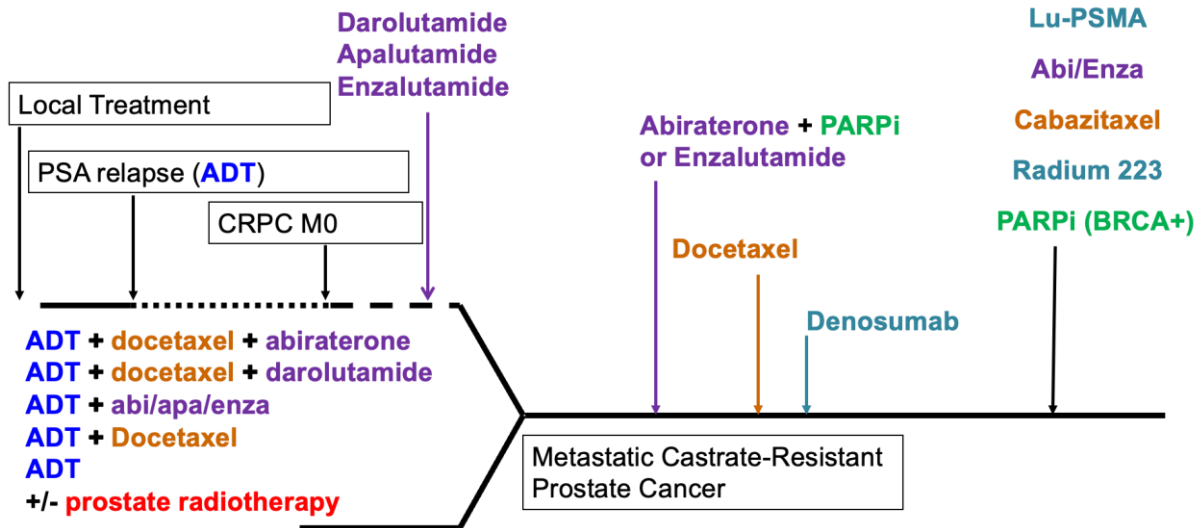


Figure 12: Systemic treatment option in prostate cancer according to disease stage. ADT: androgen deprivation therapy, CRPC: castration resistant prostate cancer, PARPi: Poly(ADP-ribose) polymerase (PARP) inhibitor, PSA: Prostate specific antigen.

d. Mechanisms of resistance to treatment

Several by-pass mechanisms for treatment resistance, linked to the biology outlined above, have been reported.

i. Androgen deprivation therapy

AR amplification and mutations/hypersensitivity pathway/promiscuous pathway

AR amplifications, leading to hypersensitivity to androgen, are found in 30-80% of mCRPC cell lines and 20% of mCRPC metastases. Mutations of the 5 α -reductase could induce higher levels of DHT. Several point mutations of the *AR* gene such as *T877A*, *L701H*, *V715M*, *W741C* have been described and lead to an increased *AR* activity with non-androgenic steroids stimulation or low level of androgen. Most of them concern the ligand binding domain⁶⁴.

Co-activators and co-repressors

Over 150 different molecules have been identified to either enhance (co-activators) or repress (co-repressors) transcriptional activity. Most of them are enzymes modulating other proteins in the complex, through phosphorylation, methylation, acetylation or ubiquitylation. Others are molecular chaperones, recruiters of transcriptional machinery and RNA splicing regulators. FKBP51 promotes androgen-stimulated transcriptional activity and growth. The androgen-independent IL-6 mediated *AR* activation in the presence of STAT3 is promoted by p300/CBP⁶⁴.

Aberrant activation (post-translational modification)/ outlaw pathway

Some pathways mentioned above are involved in resistance to ADT such as PI3K/AKT/mTOR and NF- κ B. Other growth factor pathways could participate by triggering tumor growth when IGF and KGF bind and activate AR in castrated states. IGF-1R, IL-6R, and EGFR growth receptor activate downstream pathways MAPK, PI3K/AKT/mTOR, and STAT signaling. The RTKs Her-2/neu, EGFR, and insulin-like growth factor 1 receptor (IGF-1R) stabilize the AR activity and promote androgen independence⁶⁴.

Altered steroidogenesis

Adrenal glands are an alternative source of androgens by producing dehydroepiandrosterone (DHEA) and its sulfated form DHEA-S which will be converted to androstenedione either in the prostate or adrenal gland by 3 β HSD, encoded by HSD3B. Androstenedione will be transformed in testosterone and after that in DHT by 17 β HSD3, AKR1C3 and steroid-5 α -reductase. When under ADT, androstenedione will convert in 5 α -dione before DHT, therefore bypassing testosterone. Apart from this pathway, steroidogenic enzymes like HSD3B1, HSD3B2, HSD17B3, AKR1C3, and SRD5A1 could be over-expressed leading to *de novo* production androgens (figure 13). Autocrine tumoral secretion of testosterone has also been described⁶⁴.

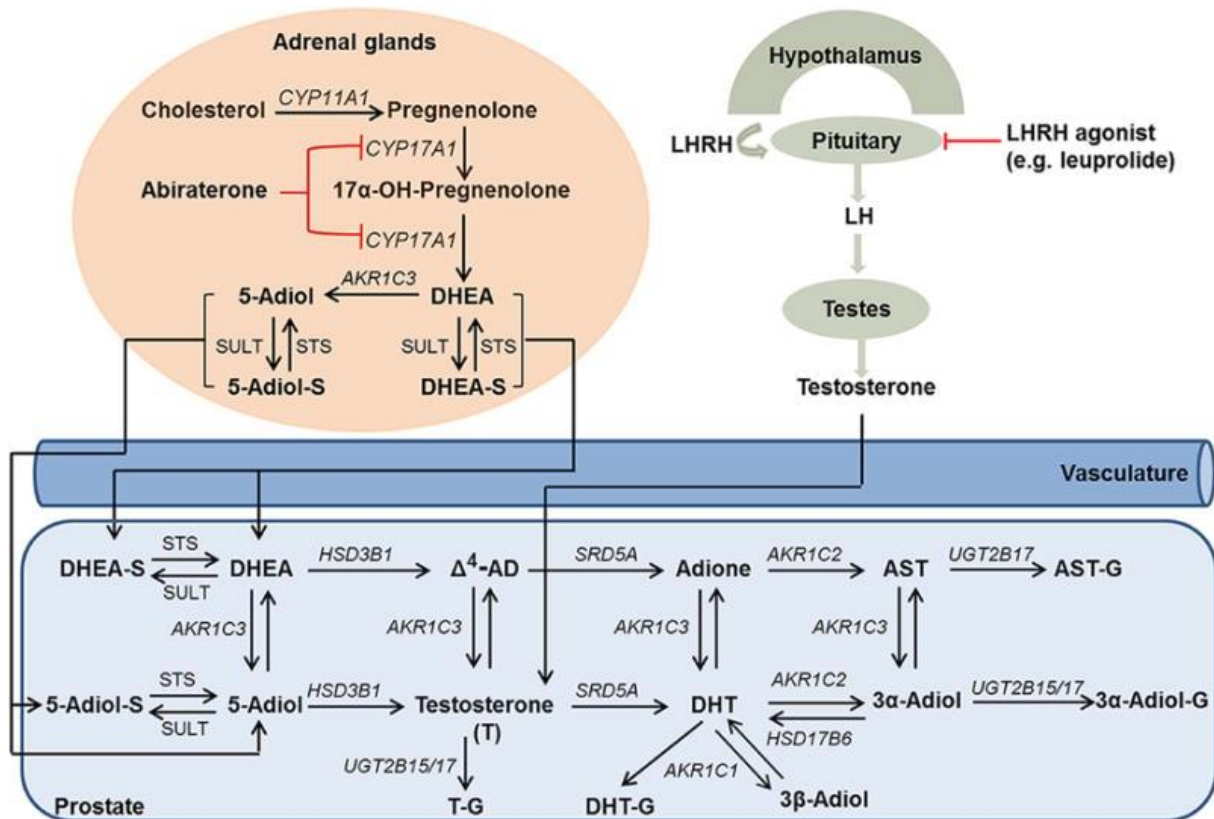


Figure 13: Androgen biosynthesis and metabolism in patients with prostate cancer⁶⁵.

3 α -Adiol, 5 α -androstane-3 α ,17 β -diol; 3 β -adiol, 5 α -androstane-3 β ,17 β -diol; 5-adiol, 5-androstene-3 β ,17 β -diol; Adione, 5 α -androstane-3,17-dione; Δ^4 -AD, Δ^4 -androstene-3,17-dione; AST, androsterone; DHEA, dehydroepiandrosterone; DHT, 5 α -dihydrotestosterone; -G, glucuronide; -S, sulfate. Enzymes are identified by their gene names which are in italics. *AKR1C1*, 20 α -hydroxysteroid dehydrogenase; *AKR1C2*, type 3 3 α -hydroxysteroid dehydrogenase; *AKR1C3*, type 5 17 β -hydroxysteroid dehydrogenase; *CYP11A1*, cytochrome P450 11A1; *CYP17A1*, cytochrome P450 17A1; *HSD3B1*, type 1 3 β -hydroxysteroid dehydrogenase; *HSD17B6*, type 6 17 β -hydroxysteroid dehydrogenase; *SRD5A*, 5 α -reductase; STS, sulfatase; SULT, sulfotransferase.

AR variants

These variants are constitutively active due to the C-terminal ligand binding domain loss. The most prominent are AR-V1, AR-V567 and AR-V7, the latter being the most extensively described. Another type is AR-V8 lacking a DNA-binding domain therefore remaining in the plasma membrane and only activating signaling pathways (figure 14)⁶⁴.

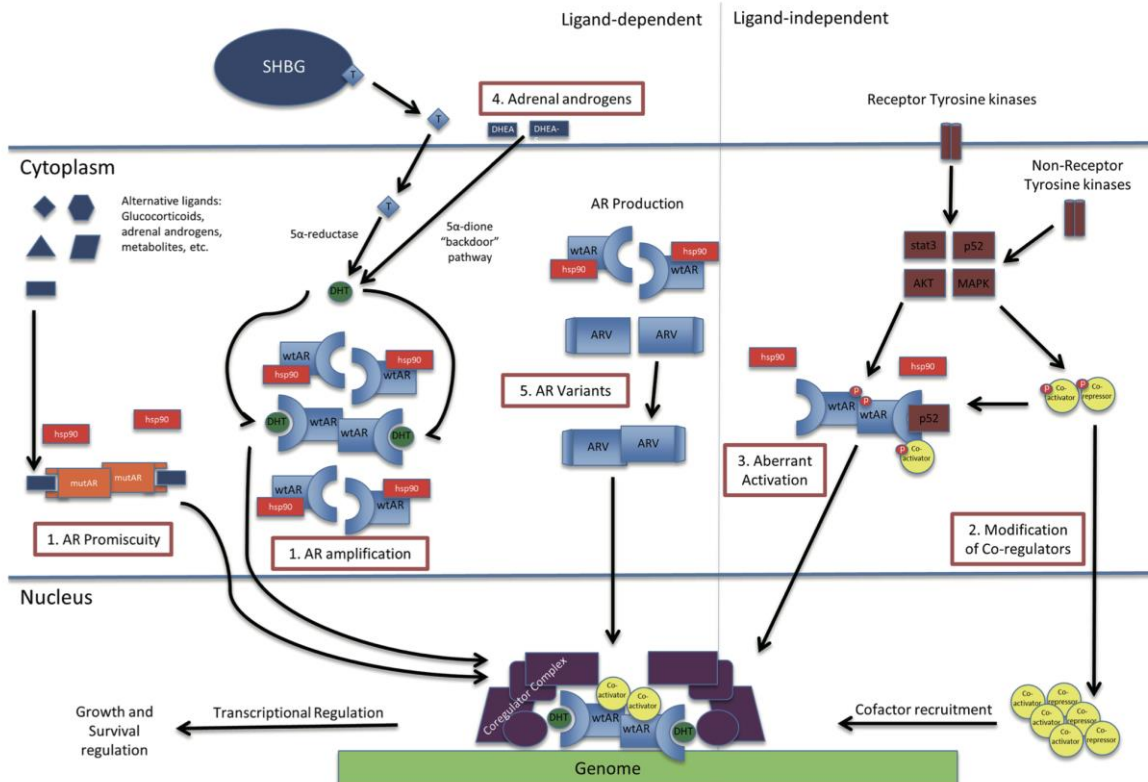


Figure 14: summary of androgen- dependent mechanisms of resistance leading from hormone-naïve to castration-resistance prostate cancer⁶⁴.

ARV: androgen receptor variant, DHT: dihydrotestosterone, mutAR: mutated androgen receptor, SHBG: sex hormone binding globulin, T: testosterone, wtAR: wild-type androgen receptor.

ii. Docetaxel

Multidrug transporters

The P-glycoprotein (P-gp) or ATP-binding cassette sub-family B member 1 (ABCB1) is an ABC protein encoded by the *MDR1* gene. It is an ATP dependent efflux pump which will decrease the intracellular concentration of docetaxel. This transmembrane protein is highly expressed in blood brain barrier. Other transporters suspected to play a minor role in docetaxel resistance are multidrug resistance protein 1 (MRP1) and solute carrier organic anion transporter family member 1B3 (SLCO1B3)⁶⁶.

Taxane resistance associated with alterations of the tubulin/microtubule system

Tubulin mutations involving class I β -tubulin, β III-tubulin (TUBB3 overexpression) or MAPT could affect docetaxel binding and therefore its antitumoral activity. Tubulin post-translational modifications, mainly in the C-terminal portion, have also been described or even reduction in tubulin content. Overexpression of ERG leads to docetaxel resistance by interaction with β -tubulin and alteration of microtubule dynamics⁶⁶.

Cancer stem cells

Prostate cancer cells surviving to docetaxel expressed the cancer stem cell markers CD44 and CD133, and ALDH. Cell lines resistant to docetaxel showed increased activity of NOTCH and Hedgehog pathways associated with cancer stem cells⁶⁶.

Centrosome clustering

Kinesins, motor proteins that hydrolyze ATP and move along microtubule filaments, play a role in cellular cargo transport and mitosis. They might be associated with resistance to docetaxel in solid tumors, including prostate cancer. KIF11 separates spindle poles during mitosis. KIF11 inhibitors showed anti-tumor activity against docetaxel resistant prostate cancer cell lines. Kinesin family member C1 (KIFC1) is a motor protein involved in centrosome clustering. KIFC1 was associated with a poor prognosis after docetaxel⁶⁶.

PI3K/AKT signaling

As described above, this pathway is upregulated in prostate cancer. Long-term ADT and docetaxel have been shown to enhance AKT expression. Additionally, preclinical data show that PI3K or AKT inhibitors could restore docetaxel sensitivity⁶⁶.

iii. Androgen receptor pathway inhibitors

Androgen receptor pathway

Patients with AR amplifications are at higher risk of progression when treated with ARPI. Similar effects are found for mutations of the ligand binding domain *F877L*, *H875Y*, *T878A* and *L702H*. Among them *H875Y* and *T878A* lead to AR promiscuity, allowing the AR pathway activation by estrogens and progesterone. *H875Y* and *L702H* can be stimulated by glucocorticoid binding. *L702H*, emerging under abiraterone treatment, induces AR activation by prednisone. These mutations are involved in both abiraterone and enzalutamide resistance, but increased role of *L702H* and *T878A* have been found in abiraterone and *F877L* via glucocorticoid in enzalutamide resistance. AR-V7 has also been widely described in resistance to ARPI⁶⁷.

Lineage plasticity

As mentioned above, multiple data showed that *TP53*, *PTEN* or *RBI* loss of function lead to a cellular plasticity and pluripotency, with NE differentiation, associated with ARPI resistance. Epigenetic reprogramming via overexpression of *EZH2* and *N-MYC* is leading to NE differentiation. Loss of *CHD1* is also *playing* a role in chromatin dysregulation and lineage plasticity. EMT dependent of the transcriptional factor *SNAIL* induces enzalutamide resistance by AR activity promotion. The TGF β pathway also activates EMT under enzalutamide via *SMAD2* and *FOXA1*⁶⁷.

DNA repair

Another mechanism of resistance to ARPI is linked to homologous recombination deficiency due to *BRCA1* and/or *BRCA2* alterations. *ATM* has a more indirect contribution. Other less established DNA damage repair genes of interest are *CHEK2*, *BRIP1*, *RAD51D*, *PALB2* and *FANCL*. *CDK12* have also been linked to enzalutamide resistance⁶⁷.

PI3K/AKT/mTOR pathway

PTEN loss, activation mutations of *PIK3CB* and *AKT1* or amplification of *PIK3CA* have been reported to emerge under enzalutamide. Other studies on circulating tumor cells found *MET* alterations with promiscuity functionality activating PI3K–AKT–mTOR, Ras–MAPK, JAK–STAT and Wnt– β -catenin pathways⁶⁷.

Wnt– β -catenin pathway

Under ARPI, this pathway could be activated by alterations of its own proteins cascade such as *CTNNB1* (β -catenin), *APC*, *RNF43* (E3 ubiquitin protein ligase). Estimations show that 11% of mCRPC progress under ARPI because of one of these 3 alterations. *WNT* mutations can also be involved⁶⁷.

Angiogenesis

β -catenin is also found in hypoxic tumors, which promotes the upregulation of HIF1 α . Therefore, a complex made of β -catenin, HIF1 α and AR will favor HIF1 α and AR crosstalk and influence androgen response elements. This crosstalk has been demonstrated *in vitro* by inhibition of HIF1 α and AR leading to downregulation of AR and HIF-mediated transcription, vascular endothelial growth factor expression and cell proliferation⁶⁷.

iv. Cabazitaxel

Fewer mechanisms of resistance have been established yet for cabazitaxel with scattered data available, mostly *in vitro*. As for docetaxel, P-gp/ABCB1 drug efflux play a role. Alterations in microtubule dynamicity because of higher expression of *TUBB3* encoding for class III β -tubulin have also been identified. Decreased BRCA1 activity and EMT activation could also be associated with cabazitaxel resistance⁶⁸. Other *in vitro* data showed an increased activity of ERK and PI3K/AKT signaling in cell lines under cabazitaxel treatment⁶⁹.

v. PARP inhibitors

Upregulation of drug efflux pumps

Once again, PARPi resistance could be linked to P-gp/ABCB1 overexpression *in vivo*⁵⁹.

Target-related mechanisms of resistance

PARP1 mutations impair PARPi affinity or preserve the enzyme activity even when bounded by PARPi. Some mutations impair the catalytic site or domains necessary for trapping PARP1 onto DNA. *In vitro* data show mutations of PARG, an enzyme removing PAR chains from target proteins, poly(ADP-ribose) glycohydrolase (PARG) cause resistance to PARPi⁵⁹.

Restoration of BRCA1/2 function

Reversion mutations or epigenetic alterations could induce the re-expression of a BRCA1 or BRCA2 wild-type protein or result in hyalomorphic variants. These reversion mutations have also been described after platinum-based regimen. They were not exclusively found in *BRCA1/2* but have also been identified in other homologous recombination-related genes such as *RAD51C*, *RAD51D* and *PALB2*⁵⁹.

BRCA-independent restoration of homologous recombination

Another way to restore homologous recombination is the emergence of compensatory mutations resulting in re-wiring DNA repair. Loss of the axis 53BP1–RIF1–REV7–shieldin involved in non-homologous end-joining (NHEJ) bypass the effects of BRCA1 loss on homologous recombination and genomic instability, but not BRCA2 loss. Loss of ERCC6L2, an accessory NHEJ factor active upstream, also restore DNA end-resection, resulting in partial restoration of homologous recombination and resistance to PARP inhibitors in BRCA1-deficient cells. Overexpression of TIRR134, TRIP13 and miRNA-622 promote homologous recombination and suppress NHEJ leading to an impaired sensitivity of BRCA1-deficient cells to PARP inhibitors⁵⁹.

Restoration of fork stability

MRE11 is a nuclease necessary to resolve stalled replication forks. When BRCA is deficient, uncontrolled resection of stalled forks leads to genomic instability. Depletion of the MLL3/4 complex protein PTIP or the nucleosome remodeling factor CHD4 inhibits MRE11 recruitment, leading to fork protection and decreased sensitivity to PARPi in BRCA1/2-deficient cells. SMARCA1, a chromatin remodeling complex, also promotes the MRE11-dependent degradation of nascent DNA in BRCA1/2-deficient cells. As with the loss of PTIP, its depletion induces resistance to PARPi. RADX also plays a role in replication fork protection. When depleted, BRCA2-deficient cells restore fork protection avoiding the cytotoxic effects of PARPi. Loss of *SLFN11* (Schlafen 11) allowed cells to start the S phase in case of replicative stress by inhibiting prolonged G1/S phase pause. Consequently, PARPi activities in BRCA1/2-proficient and BRCA2-deficient cells is decreased⁵⁹.

vi. Resistance to PSMA-lutetium

In vitro and *in vivo* data show that resistance to PSMA-lutetium is due to deregulation of DNA damage/replication stress response with alterations of *ATM*, *ATR*, *CSNK2A1* (Casein kinase 2A.1). *TP53* loss of function also induces less response to PSMA-lutetium. Other pathways like androgen receptor PI3K/AKT and MYC signaling seem to be involved⁷⁰. Up to now, data from patients samples are lacking to explain resistance to PSMA-lutetium.

e. Hypothesis

Our hypothesis is that aggressive variants containing a certain proportion of NE or NE-like cells could be detected at diagnosis and explain why some patients do not respond well to the treatment received in PEACE1. We also expect to find previously described alterations in tumor suppressor genes *TP53*, *PTEN* and *RBI*, DNA repair mechanism particularly *BRCA2*, as well as PI3K and Wnt pathway activation.

f. Objectives

All these biological mechanisms and biomarkers have been widely assessed in mCRPC but less in *de novo* mCSPC. In this form of prostate cancer with a worse prognosis, mechanisms of aggressivity linked to AR bypass or NEPC differentiation could be detected as an early event at diagnosis. For these reasons, we aimed to analyze the samples of patients treated in this setting who were included in this phase 3 clinical trial. Our objectives were to identify biomarkers present in prostate cancer cells pre-treatment to predict patient outcomes and decipher the genomic landscape of *de novo* mCSPC.

2. Materials and methods

a. Study design

PEACE-1 (Eudract 2012-00142-35; NCT 01957436) is a European academic randomized factorial design phase III trial evaluating the efficacy of AA+ prednisone and of local radiotherapy on top of standard of care (ADT +/-docetaxel) in patients with mCSPC conducted within the European PEACE consortium. The co-primary endpoints of this study are OS and radiographic progression-free survival (rPFS). The study has completed the accrual in December 2018.

Overall, 1173 patients (920 in France) have been prospectively enrolled, and their clinical data collected in this trial. The distribution of patients in the treatment arms is described in the table below:

Arm	Arm A (SOC alone) N=296	Arm B (SOC+AA+prednisone) N=292	Arm C (SOC+local RT) N=293	Arm D (SOC+AA+local RT+ prednisone) N=292
SOC				
ADT	118	115	116	114
ADT + docetaxel	178	177	177	178

Since the PRTK-K translational research program was nationally funded, only French patients in the "PEACE-1" study were eligible. Among the French patients, 745 have consented for ancillary studies. Study design has been implemented to collect both blood samples and archival tumor tissue, that have been stored at Unicancer tumor biobank Centre Léon BERARD, to conduct DNA and phenotype analysis of tumor blocks and cell-free DNA analysis. The initial protocol was reviewed and first approved on July 10, 2013, by the French Independent Ethics Committee (Comité de Protection des Personnes Ile de France VII). The protocol complied with the ethical principles of the Declaration of Helsinki and was approved by Institutional Review Boards at each study site. A pre-specified statistical analysis plan was approved by the PEACE-1 steering committee.

b. Endpoints

i. Co-primary endpoints

For each studied biomarker, we have analyzed:

- the association between the biomarker and the outcomes (*prognostic value*);

- the existence of an interaction between the biomarker and the treatment (AA) on the outcomes (*predictive value*).

Here, the term "biomarker" refers to a molecular alteration (e.g. genetic mutation) or a phenotypic alteration (from IHC data). The outcomes assessed were the co-primary endpoints of the PEACE1 study, i.e. the radiographic Progression-Free Survival (rPFS) and the Overall Survival (OS).

OS was defined as the time from randomization to the time of death from any cause. rPFS was defined as the time from randomization to radiographic progression or death. Radiographic progression was defined according to an adapted version of Prostate Cancer Working Group 2 (PCWG2) criteria (either a RECIST progression in case of measurable lesions or the appearance of at least 2 new lesions on bone scan)⁷¹. In contrast to PCWG2 criteria, a second bone scan is not mandatory to confirm radiographic progression. The date of radiographic progression was the date of progression as per the above definition.

It should be noted that a patient can enter the post-CRPC follow-up if progressive disease has been established by a PSA rise only, without radiographic progressive disease. In this scenario, imaging monitoring continued every 6 months and radiographic progression may be established later. For patients alive without radiographic progression at the time of analysis, data were censored at the date of last follow-up.

ii. Secondary endpoints

The secondary endpoints aim to decipher the frequency of DNA alterations and pathways dysregulations in *de novo* mCSPC from PEACE-1, using genomic and transcriptomic data.

iii. Exploratory endpoints

For each study biomarker (from IHC data or molecular genetic mutations), we studied the association between the biomarker and the PSA response at 8 months, disease burden. The PSA response at 8 months was defined as a PSA level ≤ 0.2 ng/ml or a PSA level >0.2 ng/ml measured 8 months after the initiation of ADT. Disease burden was classified as high or low according to the CHAARTED study criteria⁴³ i.e. high volume defined as the presence of visceral metastases or at least four bone lesions with one beyond the vertebral bodies and pelvis.

c. Sample size

In 2020 when the translational study was designed, among the 745 French patients who consented to the assessment of biomarkers, 291 progressions/deaths (rPFS events) and 222 deaths (OS events) had occurred. At this time, we supposed that under a pessimistic scenario where 30% of the samples would not be recovered from the centers or where some biological analyses would be inconclusive, it would remain at least 200/155 events to analyze the prognostic value of biomarkers on rPFS /OS. Moreover, at this moment we were not aware of the prevalence or the prognostic effect of the biomarkers. Hence, several scenarios of simulation were performed to ensure the power of the study.

Statistical justification for the study of the prognostic value of the biomarkers:

Considering that at least 200 rPFS events would have been available, the table below summarizes the power of the study to identify prognostic biomarkers depending on the prevalence and the prognostic effect of the studied biomarker (Hazard Ratio: HR) and the number of biomarkers to be tested (thus the alpha level).

Prevalence of the molecular alteration	Power of the study for a true HR=2 and a two-sided alpha=0.05*	Power of the study for a true HR=1.5 and a two-sided alpha=0.05	Power of the study for a true HR=2 and a two-sided alpha=0.005	Power of the study for a true HR=1.5 and a two-sided alpha=0.005
10%	0.961	0.494	0.821	0.195
20%	0.994	0.682	0.956	0.354
30%	0.998	0.761	0.979	0.446
40%	0.999	0.798	0.985	0.495
50%	0.999	0.815	0.986	0.520

*Power of the study to reject the null hypothesis that the Hazard Ratio (HR) equals 1, if the true HR=2, at a two-sided 0.05 significance level in a Cox regression model. Calculations were computed using the function `powerCT.default0` from the `powerSurvEpi` library in the R software version 4.0.2.

Statistical justification for the study of the predictive value of the biomarkers:

Studying the predictive value of a biomarker comes to studying whether there was a statistical interaction between the biomarker and the treatment. If there was a statistical interaction, the Hazard Ratio of the treatment effect (here $HR_{\text{Abiraterone Acetate}}$) in the subgroup of patients with the molecular alteration (e.g. biomarker positive) was statistically different from the $HR_{\text{Abiraterone Acetate}}$ in the subgroup of patients without the molecular alteration (biomarker negative). If we study a binary biomarker (biomarker positive vs negative) with 0.5 prevalence and assuming an exponential survival, then the observed number of 200 rPFS events provided approximately 80% of power to detect a treatment-by-biomarker interaction when the ratio of the HR for the effect of Abiraterone Acetate on rPFS in the biomarker-positive group to the HR in the biomarker-negative group is equal to 2.2 (or 0.45) at a two-sided 5% significance level⁷².

d. Samples preparation

i. WP1: Phenotype analysis

Pathology quality control processes were the same than those used for WP1. For IHC assays, 10x 4 μm -thick slides were prepared. IHC staining was performed on serial 3 μm formalin-fixed paraffin embedded tumor tissue. Ten slides were necessary to assess 10 markers and thereby identify key phenotypes of prostate cancer (AR [Cell signaling, clone D6F11], NKX3.1 [Bio SB/Diagomics, clone P356], ERG [Biocare Medical, clone 9FY], synaptophysin [Dako, clone DAK-SYNAPTO], Chromogranin A [Dako, clone DAK-A3], CD56 [Roche, MRQ-42], p53 [Dako, clone DO-7], Rb1 [Leica, clone 13A10], Ki67 [Dako, clone MIB-1]) and PTEN[Zytomed (Diagomics), clone A2b1]. Tissue samples were processed according to conventional procedures; histological quality controls were made before IHC. Immunostaining was performed using automated stainers (Ventana Benchmark Ultra). All HES and AR slides were digitalized and stored for further pathomic analyses.

ii. WP2: Genomic analysis

Pathology quality control and DNA extraction

A semiquantitative analysis of the quality of the tumor tissue block was performed on a hematoxylin, eosin and safran (HES)-stained serial section of the tumor by team 4. The tissue quality was scored (score 1–2 = poor, 3–4 = moderate, 5–6 = good) on the basis of the sum of the tissue vitality (1 = poor, 2 = moderate, 3 = good) and tumor percentage (0 = <5%, 1 = 5%–20%, 2 = 20%–49%, 3 = ≥50%). Samples were excluded when the total tissue quality score is 2 or less, or when the tumor percentage <10% for targeted exome sequencing. We performed a microdissection with three 10µm FFPE tissue pieces to obtain sufficient nucleic acid material. DNA isolation was performed using The QIAGEN AllPrep DNA/RNA FFPE Kit. DNA was quantified with the Quant-iT high-sensitivity PicoGreen double-stranded DNA Assay Kit (Invitrogen). The Illumina FFPE QC kit was used for DNA quality control tests according to the manufacturer's protocol.

Targeted Exome Analysis

Our strategy was to avoid whole exome sequencing and rather to focus on a cancer gene panel to give a deeper coverage and increase the robustness of the data. It was based on Cancer Core Europe (CCE) and OncoDeep testing for tumor profiling, which analyses a large panel of cancer-related biomarkers (410 and 638 genes respectively) for assessment of single nucleotide variant (SNV) and copy number variation (CNV) including critical genes in prostate cancer, e.g. AR, DNA repair genes, PI3K pathway and cell signaling (*RBI*, *TP53*). In addition, this panel makes it possible to measure tumor mutation burden and microsatellite instability. Sample preparation was conducted by following the laboratory process and manufacturer protocols. Sequencing was performed on a sequencer (Illumina) at Gustave Roussy Institute.

iii. WP3: transcriptomic analyses

After completion of WP1 and WP2, we used remaining white slides with a tumor percentage ≥ 30% and a minimum of 2 slides for transcriptomic analyses. The nanoString nCounter® RNA hybridization assay is the only technology available for transcriptomic analyses on this type of scattered material. We used the nanoString nCounter® platform and the tumor signaling 360™ panel with an additional nCounter flex panel of 50 genes for mitochondrial metabolism, AR activation and NEPC differentiation signature as detailed in table 2 and derived from previous publications³¹. RNA extraction was performed by spotting on the corresponding HES slide and FFPE scraping of tumor zone on white slides followed by a Maxwell® RSC RNA FFPE method. This material was centrifugated at 120000 rpm for 20 seconds. Mineral oil was added in every sample (300µl) and heated at 80°C for 2 minutes. A lysis master mix was added in each sample (250µl) and centrifugated for 20 seconds at 10000 rpm. We heated them for one hour at 56°C and another hour at 80°C. After 15 minutes at room temperature and centrifugation at 10000 rpm for 2 minutes, RNA was extracted using the RSC RNA FFPE method of the Maxwell® RSC Instrument. Dosages were made with the Qubit™ Assays. Samples were stored at -20°C before further analyses.

Samples were concentrated using speed vac when the concentration was too low and diluted when concentration was too high to obtain a similar RNA quantity of 10 ng for all samples. All samples were plated in 96 wells plates with two universal human reference RNA samples as positive controls (Agilent, P/N: 740000) and two H₂O samples as negative controls.

Amplification was performed on all samples using the Low RNA Input Kit before hybridization with the nCounter[®] Analysis System from nanoString^{MC}. We added 4µl of the 10X RT Primer Mix in each sample. We added the RT Master Mix by combining the components 10x RT Enzyme Mix and 10x RT Primer Mix (0,5µL per samples for each). Samples were then put in a thermal cycler with a heated lid for the following steps: primer anneal at 25°C for 10 minutes, first strand cDNA synthesis at 42°C for 60 minutes, enzyme inactivation at 85°C for 5 minutes and finally hold at 4°C.

We then performed the Multiplexed target enrichment protocol. We added the Amplification Master Mix by combining 1,5µL of 5X dT Amp Master Mix, 1µL of Low Input Primers (500 nM per primer) and 1µL of Additional Low Input Primers for Panel Plus Targets for each sample. We then performed 10 cycles of amplification in the thermal cycler with the following steps: one cycle of initial Denaturation at 95°C for 10 minutes, 10 cycles of successive denaturation at 95°C for 15 seconds and annealing at 60°C for 4 minutes and finally hold at 4°C. Before proceeding to the hybridization step, we denatured the dsDNA in the samples to make it more accessible to the nCounter[®] probes by incubating the enriched samples for 2 minutes at 95°C and then cooling them on ice for at least 2 minutes.

For hybridization, we prepared a Hybridization Master Mix by adding 70 µL of Hybridization Buffer to the Reporter CodeSet tube and added 8 µL in each sample. We added RNase-free water to bring the total volume of each assay to 16 µL and then 2 µL of Capture ProbeSet to each tube. We heated the tubes with the thermal cycler at 65°C for 16 hours and kept them at 4°C after that. We then proceeded the samples with the nCounter Prep Station following the manufacturer instructions.

Table 2: List of genes included in the transcriptomic signatures with mitochondrial metabolism and signatures adapted from Beltran et al for NEPC and AR³¹.

NEPC signature ³¹	RNA level for NEPC signature (CRPC-NE vs CRPC-Adeno) ³¹	AR signature ³¹	RNA level for AR signature (CRPC-AR high vs CRPC-AR low) ³¹	Mitochondrial metabolism signature	RNA level for mitochondrial metabolism signature
<i>ASXL3</i>	Over-expressed	<i>ABCC4</i>	Over-expressed	<i>ACAT1</i>	Over-expressed
<i>AURKA</i>	Over-expressed	<i>ACSL3</i>	Over-expressed	<i>ACAT2</i>	Over-expressed
<i>BRINP1</i>	Over-expressed	<i>ADAM7</i>	Over-expressed	<i>BDH1</i>	Over-expressed
<i>CCND1</i>	Under-expressed	<i>AR</i>	Over-expressed	<i>OXCT1</i>	Over-expressed
<i>CREBBP</i>	Under-expressed	<i>FOLH1</i>	Over-expressed	<i>OXCT2</i>	Over-expressed
<i>DICER1</i>	Under-expressed	<i>GNMT</i>	Over-expressed		
<i>DNMT1</i>	Over-expressed	<i>HERC3</i>	Under-expressed		
<i>EZH2</i>	Over-expressed	<i>KLK2</i>	Over-expressed		
<i>FOXP1</i>	Under-expressed	<i>KLK3</i>	Over-expressed		
<i>GATA2</i>	Under-expressed	<i>MANIA1</i>	Under-expressed		
<i>HOXB13</i>	Under-expressed	<i>NKX3-1</i>	Over-expressed		
<i>JAKMIP2</i>	Over-expressed	<i>PMEPA1</i>	Over-expressed		
<i>KCNB2</i>	Over-expressed	<i>TMPRSS2</i>	Over-expressed		
<i>KCND2</i>	Over-expressed	<i>ZBTB10</i>	Over-expressed		
<i>KIAA0408</i>	Over-expressed				
<i>KLK3</i>	Under-expressed				
<i>KLK4</i>	Under-expressed				
<i>LMAN1L</i>	Under-expressed				
<i>LRRC16B</i>	Over-expressed				
<i>MAP10</i>	Over-expressed				
<i>MAPKAPK3</i>	Under-expressed				
<i>MMP2</i>	Under-expressed				
<i>MYCN</i>	Over-expressed				
<i>MYH9</i>	Under-expressed				
<i>NKX3-1</i>	Under-expressed				
<i>NRSN1</i>	Over-expressed				
<i>NUP93</i>	Under-expressed				
<i>OPHN1</i>	Under-expressed				
<i>PAX8</i>	Under-expressed				
<i>PCSK1</i>	Over-expressed				
<i>PIEZO1</i>	Under-expressed				
<i>PROX1</i>	Over-expressed				
<i>PSCA</i>	Under-expressed				
<i>RAB27B</i>	Under-expressed				
<i>RB1</i>	Under-expressed				
<i>RBBP6</i>	Under-expressed				
<i>RGS7</i>	Over-expressed				
<i>RIPK2</i>	Under-expressed				
<i>SCG3</i>	Over-expressed				
<i>SEC11C</i>	Over-expressed				
<i>SEZ6</i>	Over-expressed				
<i>SLC44A4</i>	Under-expressed				
<i>SOGA3</i>	Over-expressed				
<i>SPDEF</i>	Under-expressed				
<i>ST8SIA3</i>	Over-expressed				
<i>SVOP</i>	Over-expressed				
<i>SYT11</i>	Over-expressed				
<i>TC2N</i>	Under-expressed				
<i>TRIM33</i>	Under-expressed				
<i>TRIM9</i>	Over-expressed				
<i>UPK2</i>	Under-expressed				

e. Statistical analyses

i. Generalities

All analyses were performed following the intention-to-treat principle, i.e. analyzed as randomized.

Quantitative variables were described in terms of median, interquartile range, minimum, and maximum or mean and standard deviation. Histograms were also provided to describe the distribution of quantitative variables from immunohistochemistry analyses. Qualitative variables were described in terms of number and proportion. Barplots were presented for categorical variables from immunohistochemistry analyses.

Univariate association between clinical factors and categorical biomarkers from IHC analyses were evaluated using Chi-squared tests or Fisher tests, if necessary.

Survival curves were estimated using Kaplan-Meier methods and compared with the log-rank test. The proportional hazards (PH) assumption over time in the Cox PH model were tested using Schoenfeld's residuals and if appropriate by introducing a time-dependent interaction with the marker. The type-I error rate alpha was fixed to 0.05 (two-sided).

ii. Statistical conventions and missing data

For IHC biomarkers missing values handling, multiple imputations were planned to compute regression models on a complete data set. The R package "mice" was used to execute the multiple imputation.

Three variables were identified as potentially linked to phenotype data missingness: the time between the biopsy and the start of the biological analysis (in months), the tumor cell percentage on tissue samples and the number of tissue samples collected. They were placed in an imputation model. The clinical factors used to adjust the regression models were also placed in the imputation model. In case of missing values for these variables, a first imputation step was performed using the mean for a continuous variable and a logistic regression for a binary variable. The Nelson-Aalen estimators (cumulative hazard rate) and the survival status were placed in the imputation model as predictors as it is suggested to provide better imputation results using the R package mice. The estimates from 10 repeated complete data analyses were pooled into a single set of estimates and standard errors. If a biomarker had more than 30% of missing values, it was imputed and was not used in the regression models.

iii. Baseline characteristics

Baseline characteristics of patients were described according to:

- demographical characteristics (age, sex, ECOG performance status)
- initial tumor characteristics (TNM classification, disease extent, disease burden, Gleason score)
- treatment during PEACE-1 study (i.e. abiraterone, radiotherapy, docetaxel)
- duration between initial diagnosis and randomization in PEACE-1 study
- biopsy materials characteristics (number of blocks, type of material and tumor percentage).

iv. Biomarkers

i. WP1: Genomic analysis

Only alterations classified as pathogenic or likely pathogenic were considered for analyses. Bioinformatics analyses was performed by the Gustave Roussy bioinformatics platform (Dr Etienne Rouleau) according to local workflow and standard pipeline. Manual review of copy number calls for selected oncogenes and tumor suppressors was performed, accounting for tumor content. Only SNV with a variant allele frequency $\geq 10\%$ were considered. Deletion threshold was $\times 0.5$ and $\times 6$ for amplification.

ii. WP2: Phenotype analysis

A semi-quantitative score (H-score) considered the staining intensity, and we established the percentage of stained cells for each marker (Dr Cedric Pobel) with a double lecture from a pathologist (Pr Jean-Yves Scoazec). Some of the markers analyses results were expressed in categories, in percentage or in terms of H-score. The latter was dichotomized according to clinical reference thresholds. Percentages values of ki67 was normalized using a log transformation.

NE markers (Synaptophysin, CD56 and chromogranin A) were considered as negative if the H-scores of Synaptophysin, CD56 and chromogranin A are all equal to 0, or positive if at least one H-score is strictly positive. When the H-score(s) of non-missing value(s) was (were) equal to 0 and there was (were) at least one missing H-score value, NE markers were considered as missing.

AR score and AR marking were used to create two new characterizations for this biomarker. The first had three categories: negative (score negative), weak (score positive and marking weak or marking weak heterogeneous) and positive (score positive and marking nuclear or marking cytoplasmic or marking nuclear and cytoplasmic). The second characterization had two categories about the AR marking: AR cytoplasmic (marking the cytoplasm and the nucleus or marking the cytoplasm alone) and AR nuclear (marking the nucleus weak heterogeneous or marking weak).

Five different categories of phenotypes according to current phenotypes classification were investigated grouping NE markers and AR markers: AR-high luminal tumors, AR-low luminal tumors, amphicrine tumors composed of cells co-expressing AR and NE genes, double-negative tumors (i.e., AR- / NE markers-), and tumors with small cell without AR activity (NEPC).

These phenotype categories were defined in detail as:

- AR-high luminal tumors with a strong AR activity: AR score was positive, AR marking was nuclear and NE markers were all negative
- AR-low luminal tumors with a weak AR activity: AR score was positive with a marking either cytoplasmic and nuclear, weak, or weak heterogeneous, and the NE markers were all negative
- Amphicrine tumors: AR score was positive, regardless to the AR marking type (nuclear, nuclear and cytoplasmic, cytoplasmic, weak heterogeneous or weak) and at least one of the NE markers was positive
- Double negative tumors: AR score was negative, and all the NE markers were negative
- NEPC: AR score was negative and at least one of the NE markers was positive.

iii. WP3: transcriptomic analyses

Gene count data were processed through the pipeline of the nsolver software for quality control and normalization. Samples with quality control (QC) flag for RNA content under or above 2 standard deviations were excluded. After normalization on negative control samples (H₂O), samples with mRNA content normalization factor under 0.1 or above 10 were excluded. Genes that had less than 5 counts for any of the compared condition levels were discarded. Differential expression analyses were performed using the DESeq2⁷³ package v1.44.0. GSEA (Gene Set Enrichment Analysis) and ORA (Over-Representation Analysis) were performed using the clusterProfiler⁷⁴ v4.12.0 and DOSE⁷⁵ v3.30.0 R packages, using multiple term databases in their latest version (MSigDb v7.1, WikiPathways, KEGG, Reactome, DisGenet, DiseaseOntology, GeneOntology, NCG). GSVA (Gene Set Variance Analysis) were performed using the GSVA⁷⁶ package v1.52.3, using the same term banks as for GSEA/ORA. Association of GSVA scores with clinical annotations were assessed with a Kruskal-Wallis test. Samples unsupervised clustering was performed using the skmeans⁷⁷ v0.2-17, for 2 to 9 putative classes. All p-values from any statistical test performed were FDR-adjusted using the Benjamini-Hochberg method⁷⁸. NEPC, AR and metabolism scores were calculated for each study participant as a z-score value from normalized RNA count for each gene. We used the negative z-score (z-score x (-1)) for under-expressed gene and the positive z-score for over-expressed genes (table 2).

v. Analysis of co-primary endpoints

i. General model

To evaluate the prognostic effect of a biomarker, multivariable Cox PH regression models were used to estimate the hazard ratio (HR) and the associated 95% confidence interval (CI). To evaluate the predictive effect of a biomarker, an interaction between the biomarker and the abiraterone was added and a Wald test for the interaction performed. At first, we considered each biomarker one by one. Later, we tried grouping them according to the category of phenotype they belong to, and we considered each phenotype one by one.

We adjusted the Cox regression analysis for radiotherapy and docetaxel to be taken into account for the study design and disentangle the effect of AA from the effect of the other treatments received. The randomization stratification criteria (ECOG 0 vs 1-2, type of castration and disease burden high vs low), as well as two known prognostic factors: the Gleason score <7 vs ≥7 and the age in categories (<60 years; ≥60-69 years; ≥70 years) was also used to adjust the Cox regression models.

We used the linear predictor of the final multivariable model as prognostic score for each patient. We used tertiles of the prognostic score to define different prognostic classes. Forest plots and survival curves were generated.

ii. Prognostic signature

Univariate analysis

The prognostic role of each biomarker was first assessed via a biomarker-specific Cox model containing the main effect of the biomarker. An unadjusted and an adjusted analysis for the clinicopathological factors as outlined above was performed. The HR for the main effect of each biomarker provided a measure of its prognostic value and the associated Wald test a

measure of its statistical significance. HRs were presented together with their 95% confidence intervals (CIs) and P-values.

Multivariable analysis

The prognostic role of biomarkers was assessed via a multivariable Cox model with adjustments for clinicopathological factors as described above.

iii. Predictive signature

Univariate analysis

The predictive role of each biomarker was first assessed via a biomarker-specific Cox model containing the main effect of the biomarker, the main effect of the treatment and the interaction between the treatment and the biomarker. An unadjusted and an adjusted analysis for the clinicopathological factors as outlined above was performed. The HR for the interaction between the treatment and the biomarker provided a measure of its predictive value and the associated Wald test a measure of its statistical significance. HRs were presented together with their 95% CIs and P-values. We represented by means of a forest plot the obtained estimated HRs and 95% CIs by biomarker value.

Multivariable analysis

The predictive role of biomarkers was assessed via a multivariable Cox model containing the main effect of the treatment, the main effect of some of the biomarkers and the interaction between treatment and some of the biomarkers, with adjustments for clinical factors as described above.

vi. Analysis of secondary endpoint

The frequency of DNA alterations and transcriptomic pathways was compared with localized PC and mCRPC tumors using public genomic databases. Similarly, but using only the data from PEACE1, the frequency of DNA alterations and transcriptomic pathways was compared between patients depending of PSA at 8 months ≥ 0.02 ng/ml or not and high volume vs low volume.

vii. Statistical software

The statistical analysis was carried out using R version 4.4.0 software at Gustave Roussy Institute (Biostatistics and Epidemiology Office).

3. Results

a. Descriptive analyses

i. Overall cohort

Of the 1172 patients full trial population randomized in PEACE-1 (NCT01957436), 745 patients from France consented to this ancillary study. Paraffin-embedded samples were collected for 595 patients (80%) and centrally reviewed. Phenotypic analyses were contributive for 394 patients, genomic for 180 and transcriptomic for 194. In total, 133 patients among the 595 (22.4%) had no contributive analyses (figure 15). The distribution of the patient characteristics was similar between the full trial, phenotypic, genomic and transcriptomic cohorts (table 3).

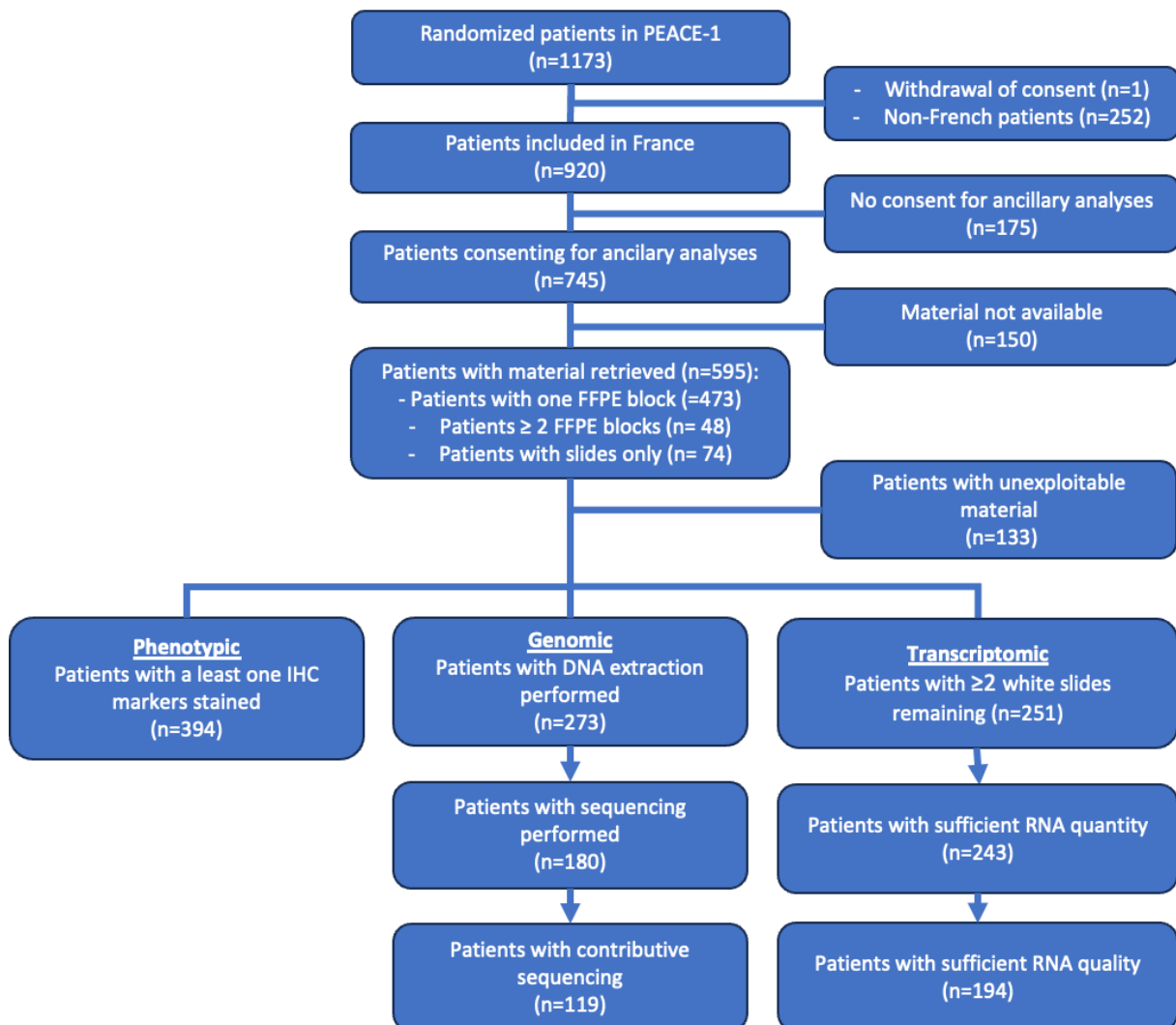


Figure 15: flowchart. HES: Hematoxylin eosine safran, IHC: immunochemistry.

Table 3: Description of population at baseline.

n (%)	Full trial (n=1172)	IHC (n=394)	NGS (n=119)	Transcriptomic (n=194)
<u>Treatment arm</u>				
Arm A	296 (25.3)	101 (25.6)	32 (26.9)	51 (26.3)
Arm B	292 (24.9)	97 (24.6)	31 (26.1)	42 (21.6)
Arm C	293 (25.0)	100 (25.4)	25 (21.0)	54 (27.8)
Arm D	291 (24.8)	96 (24.4)	31 (26.1)	47 (24.2)
<u>Age</u>				
<60	271 (23.1)	87 (22.1)	24 (20.2)	47 (24.2)
60-70	431 (36.8)	133 (33.8)	43 (36.1)	67 (34.5)
>70	470 (40.1)	174 (44.2)	52 (43.7)	80 (41.2)
<u>Performance status</u>				
0	824 (70.3)	259 (65.7)	73 (61.3)	132 (68.0)
1-2	348 (29.7)	135 (34.3)	46 (38.7)	62 (32.0)
<u>Gleason score</u>				
<8	278 (24.2)	100 (25.9)	22 (18.8)	41 (21.6)
≥8	870 (75.8)	286 (74.1)	95 (81.2)	149 (78.4)
Missing data	24	8	2	4
<u>T stage</u>				
T1	46 (4.0)	19 (4.9)	5 (4.2)	8 (4.2)
T2	203 (17.8)	74 (19.0)	21 (17.8)	31 (16.3)
T3	597 (52.2)	216 (55.4)	64 (54.2)	107 (56.3)
T4	198 (17.3)	57 (14.6)	20 (16.9)	33 (17.4)
Tx	99 (8.7)	24 (6.2)	8 (6.8)	11 (5.8)
Missing data	29	4	1	4
<u>N stage</u>				
N-	361 (31.7)	114 (29.5)	35 (29.9)	51 (26.8)
N+	632 (55.5)	210 (54.3)	62 (53.0)	108 (56.8)
Nx	146 (12.8)	63 (16.3)	20 (17.1)	31 (16.3)
Missing data	33	7	2	4
<u>Disease extent</u>				
Bone metastasis	947 (80.8)	312 (79.2)	97 (81.5)	139 (71.6)
Lymph node only	99 (8.4)	37 (9.4)	14 (11.8)	22 (11.3)
Visceral metastasis	126 (10.8)	45 (11.4)	8 (6.7)	33 (17.0)
<u>Disease burden</u>				
High	667 (56.9)	221 (56.1)	66 (55.5)	112 (57.7)
Low	505 (43.1)	173 (43.9)	53 (44.5)	82 (42.3)
<u>Type of castration</u>				
LHRH agonist	784 (66.9)	239 (60.7)	75 (63.0)	115 (59.3)
LHRH antagonist	384 (32.8)	154 (39.1)	44 (37.0)	78 (40.2)
Surgical castration	4 (0.3)	1 (0.3)	0	1 (0.5)

Among the 595 patients with material retrieved, 65 had IHC and NGS data without transcriptomic, and 178 had IHC without any NGS or transcriptomic, 36 had IHC and NGS without transcriptomic, 115 had IHC and transcriptomic without NGS and 18 NGS without any IHC or transcriptomic. Most of the biopsies at baseline were prostate cores for 185 patients (86.9%), transurethral resection of the prostate for 51 (8.6%), bone metastases for 10 (1.7%), lymph nodes for 8 (1.3%), prostatectomies for 2 (0.3%), liver metastases for 2 (0.3%) and lung metastases for 1 (0.2%). Other biopsies were less frequent (table 4).

Table 4: Description of tumoral materials retrieved.

	IHC & NGS & transcriptomic (n=65)	IHC & NGS but no transcriptomic (n=36)	IHC & transcriptomic but no NGS (n=115)	IHC but no NGS or transcriptomic (n=178)	No IHC or transcriptomic but NGS (n=18)	Transcriptomic but no IHC or NGS (n=14)	Not contributive (n=169)	All patients with material retrieved (n=595)
Delay between biopsy and analysis (years)								
<i>Min / Max</i>	3.9 / 8.4	4.1 / 9.1	3.9 / 8.8	3.8 / 9.0	4.0 / 8.4	5.3 / 8.5	3.9 / 9.0	3.8 / 9.1
<i>Med [IQR]</i>	5.3 [4.9;6.2]	6.4 [5.3;7.5]	5.9 [5.1;7.1]	6.4 [5.2;7.4]	5.5 [5.0;6.5]	6.2 [5.7;7.0]	6.2 [5.2;7.2]	6.1 [5.2;7.1]
<i>Mean (std)</i>	5.6 (1.1)	6.4 (1.4)	6.1 (1.2)	6.3 (1.3)	5.8 (1.2)	6.4 (0.9)	6.2 (1.3)	6.2 (1.3)
<i>n (Unknown)</i>	64 (1)	35 (1)	115 (0)	178 (0)	18 (0)	14 (0)	167 (2)	591 (4)
Type of biopsy								
<i>Bone marrow</i>	1 (1.5)	0 (0)	0 (0)	0 (0)	0 (0)	0 (0)	0 (0)	1 (0.2)
<i>Bone metastasis</i>	3 (4.6)	1 (2.8)	1 (0.9)	4 (2.2)	0 (0)	0 (0)	1 (0.6)	10 (1.7)
<i>Liver metastasis</i>	0 (0)	0 (0)	1 (0.9)	0 (0)	0 (0)	0 (0)	1 (0.6)	2 (0.3)
<i>Lung metastasis</i>	0 (0)	0 (0)	1 (0.9)	0 (0)	0 (0)	0 (0)	0 (0)	1 (0.2)
<i>Lymph node</i>	1 (1.5)	1 (2.8)	1 (0.9)	2 (1.1)	0 (0)	0 (0)	3 (1.8)	8 (1.3)
<i>Prostate biopsy</i>	40 (61.5)	26 (72.2)	103 (89.6)	163 (91.6)	16 (88.9)	11 (78.6)	158 (93.5)	517 (86.9)
<i>Prostatectomy</i>	0 (0)	0 (0)	0 (0)	2 (1.1)	0 (0)	0 (0)	0 (0)	2 (0.3)
<i>TURP</i>	20 (30.8)	7 (19.4)	8 (7.0)	7 (3.9)	2 (11.1)	3 (21.4)	6 (3.6)	53 (8.9)
<i>TURBT</i>	0 (0)	1 (2.8)	0 (0)	0 (0)	0 (0)	0 (0)	0 (0)	1 (0.2)
<i>Unknown</i>	0	0	0	0	0	0	0	0
Number of paraffin blocks retrieved								
<i>Min / Max</i>	1.0 / 7.0	1.0 / 2.0	0 / 6.0	0 / 6.0	1.0 / 1.0	0 / 3.0	0 / 2.0	0 / 7.0
<i>Med [IQR]</i>	1.0 [1.0;1.0]	1.0 [1.0;2.0]	1.0 [1.0;1.0]	1.0 [1.0;1.0]	1.0 [1.0;1.0]	0 [0;0]	1.0 [1.0;1.0]	1.0 [1.0;1.0]
<i>Mean (std)</i>	1.1 (0.8)	1.4 (0.5)	1.0 (0.6)	1.1 (0.7)	1.0 (0)	0.2 (0.8)	0.8 (0.5)	1.0 (0.6)
<i>n (Unknown)</i>	65 (0)	36 (0)	115 (0)	178 (0)	18 (0)	14 (0)	169 (0)	595 (0)
Tumoral percentage								
<i>Min / Max</i>	30.0 / 80.0	10.0 / 80.0	10.0 / 80.0	0 / 80.0	10.0 / 60.0	30.0 / 70.0	0 / 70.0	0 / 80.0
<i>Med [IQR]</i>	50.0 [40.0;60.0]	50.0 [20.0;52.5]	50.0 [30.0;50.0]	20.0 [10.0;40.0]	50.0 [22.5;50.0]	40.0 [30.0;50.0]	30.0 [10.0;50.0]	30.0 [20.0;50.0]
<i>Mean (std)</i>	48.9 (14.0)	44.4 (21.8)	45.1 (14.2)	25.4 (18.8)	40.6 (17.0)	43.6 (13.4)	28.7 (20.3)	35.4 (20.1)
<i>n (Unknown)</i>	65 (0)	36 (0)	115 (0)	177 (1)	18 (0)	14 (0)	112 (57)	537 (58)
Number of tissu slides retrieved								
<i>Min / Max</i>	0 / 0	0 / 20.0	0 / 20.0	0 / 50.0	0 / 0	10.0 / 39.0	0 / 22.0	0 / 50.0
<i>Med [IQR]</i>	0 [0;0]	0 [0;10.0]	0 [0;0]	0 [0;0]	0 [0;0]	20.0 [11.8;20.0]	0 [0;10.0]	0 [0;0]
<i>Mean (std)</i>	0 (0)	4.4 (5.8)	2.3 (6.2)	3.2 (7.4)	0 (0)	18.4 (7.5)	4.4 (7.5)	3.5 (7.2)
<i>n (Unknown)</i>	52 (13)	25 (11)	80 (35)	130 (48)	14 (4)	14 (0)	141 (28)	456 (139)

IHC: immunochemistry, NGS: next generation sequencing, TURBT: transurethral removal of bladder tumor, TURP: transurethral resection of the prostate.

ii. Phenotypic analysis cohort

Among the 394 patients with a contributive IHC, only 60 (10.1%) had an interpretable PTEN marker due to technical difficulties. Therefore, PTEN was excluded from analyses. AR negative tumor was found for 8 patients (2.1%), synaptophysin positive for 72 (18.8%), CD56 positive for 41 (11.2%), chromogranin A positive for 102 (73.8%). At least one NEPC marker among these 3 (NEmk) was positive in 102 patients (26.2%). Other detailed marker results are summarized in table 5 and illustrated in figure 16. Phenotypes were AR luminal high for 150 patients (38.1%), AR luminal weak for 97 (24.6%), amphicrine for 95 (24.1%), double negative for 3 (0.8%) and NEPC for 5 (1.3%).

Table 5: Description of IHC markers.

n (%)	IHC completed (n=394)
AR	
AR cytoplasmic & nuclear	110 (29.1)
AR negative	8 (2.1)
AR nuclear	221 (58.5)
AR weak	39 (10.3)
Unknown	16
Synaptophysin	
Negative	310 (81.1)
Positive	72 (18.8)
Unknown	12
CD56	
Negative	325 (88.8)
Positive	41 (11.2)
Unknown	28
Chromogranin A	
Negative	287 (26.2)
Positive	102 (73.8)
Unknown	5
NEmk	
Positive	102 (26.2)
Negative	287 (73.8)
Unknown	23
PTEN	
PTEN > 10	12 (20.0)
PTEN ≤ 10	48 (80.0)
Unknown	334
p53	
p53 positive or null	137 (37.2)
p53 wild type	231 (62.8)
Unknown	26
Rb1	
Negative	85 (24.0)
Positive	269 (76.0)
Unknown	40
ERG	
Negative	221 (63.7)
Positive	126 (36.3)
Positive control unstained	23
Unknown	24
NKX3.1	
NKX3.1 < 300	192 (54.2)
NKX3.1 = 300	162 (45.8)
Unknown	40

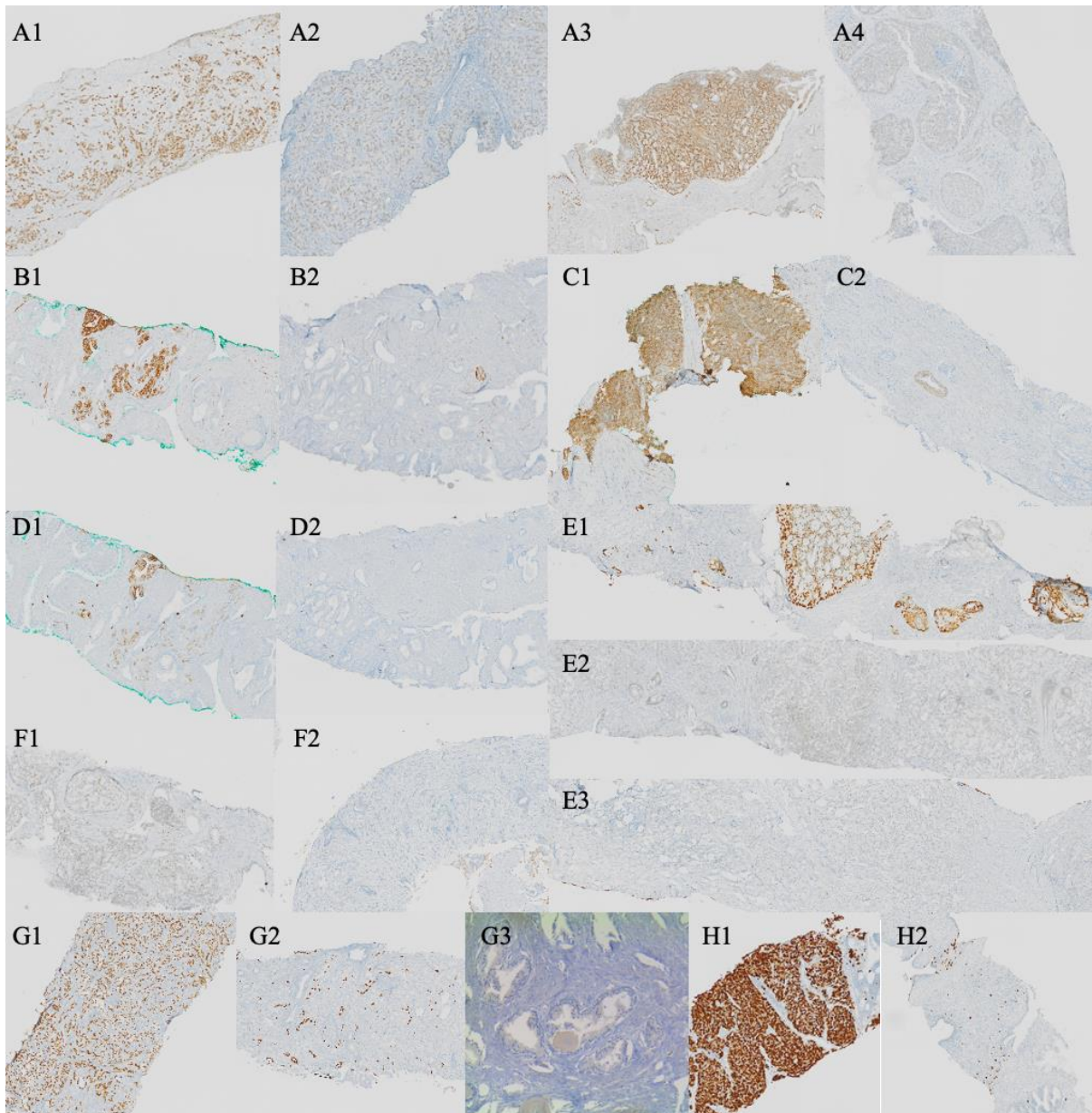


Figure 16: IHC expression.

A1: AR positive, A2: AR weak, A3: AR positive cytoplasmic and nuclear, A4: AR negative

B1: Synaptophysin positive, B2: Synaptophysin negative,

C1: CD56 positive, C2: CD56 negative,

D1: Chromogranin positive, D2: Chromogranin negative,

E1: p53 positive, E2: p53 normal, E3: p53 null,

F1: Rb1 positive, F2: Rb1 negative,

G1: ERG positive, G2: ERG negative with border cell positive (positive control), G3: ERG negative with border cell negative (positive control negative),

H1: Ki67 high at 95%, H2: Ki67 low at 2%.

IHC quantitative variables distribution

H-score for NE markers were more frequently low under 50 but with some patients having a higher score (figure 17).

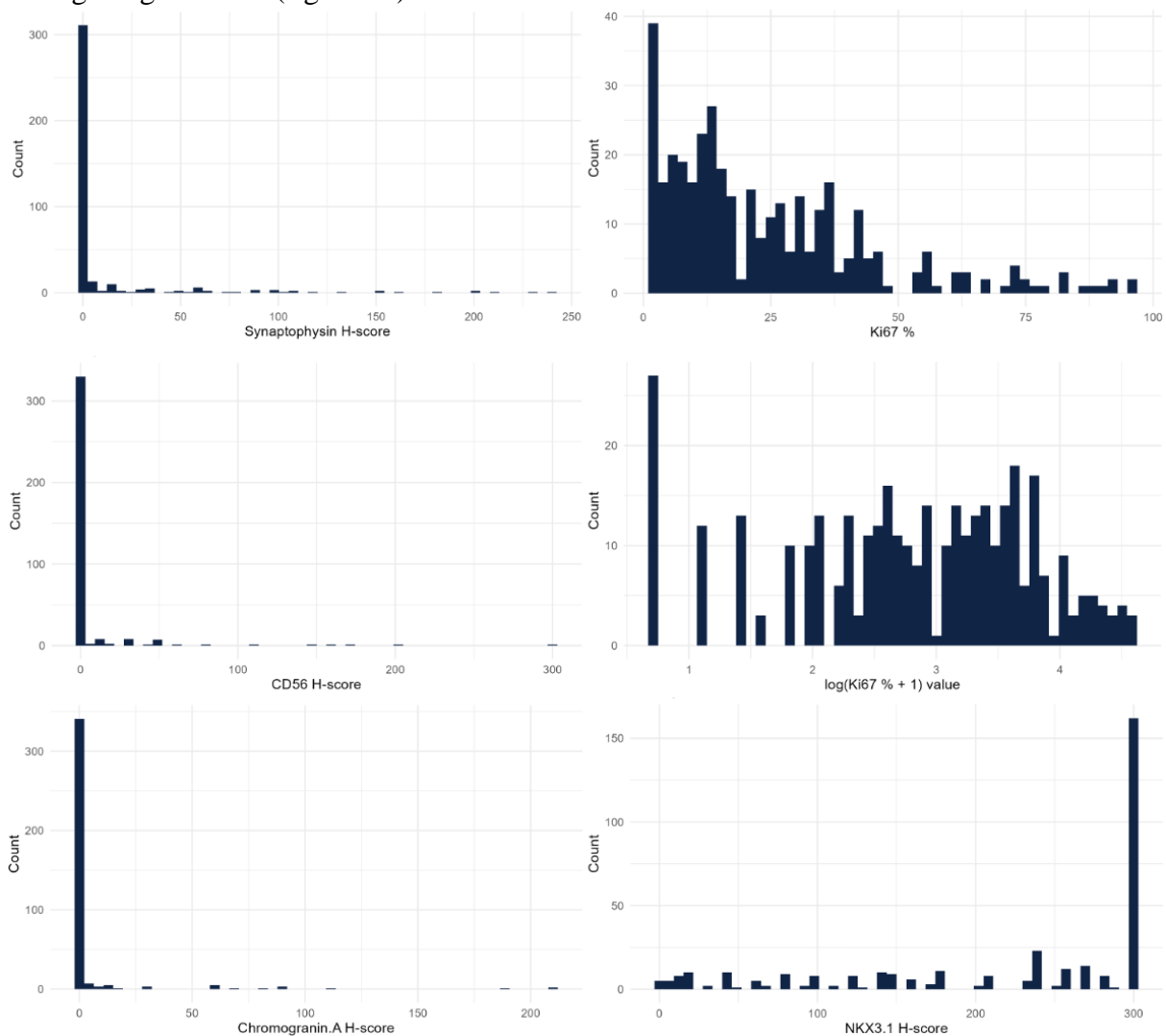


Figure 17: Distribution for synaptophysin, CD56, chromogranin A, Ki67, log(Ki67 +1) and NKX3.1.

iii. Genomic analysis cohort

In total, 273 patients had DNA extraction for sequencing. Among them, 180 had a sufficient quantity of DNA. Twenty patients were sequenced by the OncoDeep panel with 9 contributive and 160 patients were sequenced by the CCE panel with 110 contributive. At the end, sequencing was interpretable for 119 patients (i.e. 43.6% of 272 extracted and 66.1% of 180 sequenced, figure 15 flowchart). We found 183 single nucleotide variants (SNVs), 17 copy number variations (CNVs) with 15 deletion and 3 amplifications among these patients (table 6). Most frequent alterations involved *TP53*, *PTEN*, *CDK12*, *ATM*, *BRCA2*, *APC*, *SPOP*, *CREBBP*, *PIK3CA*, *MUTYH* and *RBI*. Only one patient had an *AR* mutation. (figure 17, table 7 & 8). All patients had a microsatellite stability (MSS) status.

Table 6: absolute number of alteration types.

	<i>n</i>	%
<i>SNV</i>	183	91.0
<i>CNV (deletion)</i>	15	7.5
<i>CNV (amplification)</i>	3	1.5

CNV: copy number variation, SNV: single nucleotide variants.

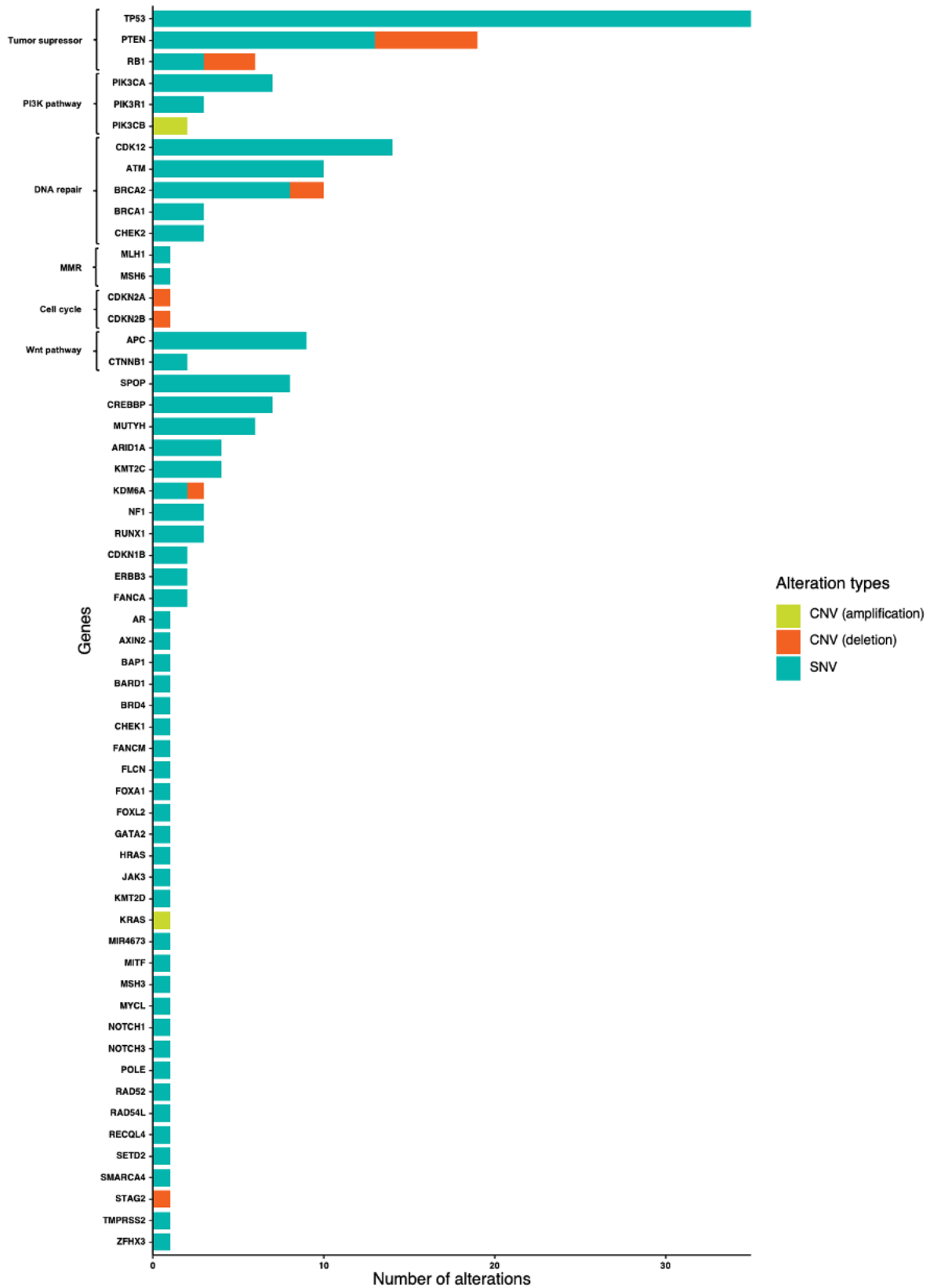


Figure 17: Box plot representing the absolute number of alterations and their types, grouped by pathway.

Table 7: absolute number of alterations.

	n alterations	%
<i>TP53</i>	35.0	17.4
<i>PTEN</i>	19.0	9.5
<i>CDK12</i>	14.0	7.0
<i>ATM</i>	10.0	5.0
<i>BRCA2</i>	10.0	5.0
<i>APC</i>	9.0	4.5
<i>SPOP</i>	8.0	4.0
<i>CREBBP</i>	7.0	3.5
<i>PIK3CA</i>	7.0	3.5
<i>MUTYH</i>	6.0	3.0
<i>RB1</i>	6.0	3.0
<i>ARID1A</i>	4.0	2.0
<i>KMT2C</i>	4.0	2.0
<i>BRCA1</i>	3.0	1.5
<i>CHEK2</i>	3.0	1.5
<i>KDM6A</i>	3.0	1.5
<i>NF1</i>	3.0	1.5
<i>PIK3R1</i>	3.0	1.5
<i>RUNX1</i>	3.0	1.5
<i>CDKN1B</i>	2.0	1.0
<i>CTNNB1</i>	2.0	1.0
<i>ERBB3</i>	2.0	1.0
<i>FANCA</i>	2.0	1.0
<i>PIK3CB</i>	2.0	1.0
<i>AR</i>	1.0	0.5
<i>AXIN2</i>	1.0	0.5
<i>BAP1</i>	1.0	0.5
<i>BARD1</i>	1.0	0.5
<i>BRD4</i>	1.0	0.5
<i>CDKN2A</i>	1.0	0.5
<i>CDKN2B</i>	1.0	0.5
<i>CHEK1</i>	1.0	0.5
<i>FANCM</i>	1.0	0.5
<i>FLCN</i>	1.0	0.5
<i>FOXA1</i>	1.0	0.5
<i>FOXL2</i>	1.0	0.5
<i>GATA2</i>	1.0	0.5
<i>HRAS</i>	1.0	0.5
<i>JAK3</i>	1.0	0.5
<i>KMT2D</i>	1.0	0.5
<i>KRAS</i>	1.0	0.5
<i>MIR4673</i>	1.0	0.5
<i>MITF</i>	1.0	0.5
<i>MLH1</i>	1.0	0.5
<i>MSH3</i>	1.0	0.5
<i>MSH6</i>	1.0	0.5
<i>MYCL</i>	1.0	0.5
<i>NOTCH1</i>	1.0	0.5
<i>NOTCH3</i>	1.0	0.5
<i>POLE</i>	1.0	0.5
<i>RAD52</i>	1.0	0.5
<i>RAD54L</i>	1.0	0.5
<i>RECQL4</i>	1.0	0.5
<i>SETD2</i>	1.0	0.5
<i>SMARCA4</i>	1.0	0.5
<i>STAG2</i>	1.0	0.5
<i>TMPRSS2</i>	1.0	0.5
<i>ZFHX3</i>	1.0	0.5

Table 8: number of patients for each alteration.

	n patients	%
<i>TP53</i>	35.00	21.88
<i>PTEN</i>	16.00	10.00
<i>CDK12</i>	11.00	6.88
<i>ATM</i>	10.00	6.25
<i>BRCA2</i>	9.00	5.62
<i>SPOP</i>	8.00	5.00
<i>CREBBP</i>	7.00	4.38
<i>APC</i>	6.00	3.75
<i>MUTYH</i>	6.00	3.75
<i>RB1</i>	6.00	3.75
<i>PIK3CA</i>	5.00	3.12
<i>KMT2C</i>	4.00	2.50
<i>ARID1A</i>	3.00	1.88
<i>BRCA1</i>	3.00	1.88
<i>CHEK2</i>	3.00	1.88
<i>KDM6A</i>	3.00	1.88
<i>NF1</i>	3.00	1.88
<i>PIK3R1</i>	3.00	1.88
<i>RUNX1</i>	3.00	1.88
<i>CDKN1B</i>	2.00	1.25
<i>CTNNB1</i>	2.00	1.25
<i>ERBB3</i>	2.00	1.25
<i>FANCA</i>	2.00	1.25
<i>PIK3CB</i>	2.00	1.25
<i>AR</i>	1.00	0.62
<i>AXIN2</i>	1.00	0.62
<i>BAP1</i>	1.00	0.62
<i>BARD1</i>	1.00	0.62
<i>BRD4</i>	1.00	0.62
<i>CDKN2A</i>	1.00	0.62
<i>CDKN2B</i>	1.00	0.62
<i>CHEK1</i>	1.00	0.62
<i>FANCM</i>	1.00	0.62
<i>FLCN</i>	1.00	0.62
<i>FOXA1</i>	1.00	0.62
<i>FOXL2</i>	1.00	0.62
<i>GATA2</i>	1.00	0.62
<i>HRAS</i>	1.00	0.62
<i>JAK3</i>	1.00	0.62
<i>KMT2D</i>	1.00	0.62
<i>KRAS</i>	1.00	0.62
<i>MIR4673</i>	1.00	0.62
<i>MITF</i>	1.00	0.62
<i>MLH1</i>	1.00	0.62
<i>MSH3</i>	1.00	0.62
<i>MSH6</i>	1.00	0.62
<i>MYCL</i>	1.00	0.62
<i>NOTCH1</i>	1.00	0.62
<i>NOTCH3</i>	1.00	0.62
<i>POLE</i>	1.00	0.62
<i>RAD52</i>	1.00	0.62
<i>RAD54L</i>	1.00	0.62
<i>RECQL4</i>	1.00	0.62
<i>SETD2</i>	1.00	0.62
<i>SMARCA4</i>	1.00	0.62
<i>STAG2</i>	1.00	0.62
<i>TMPRSS2</i>	1.00	0.62
<i>ZFHX3</i>	1.00	0.62

When looking at alterations per patients, no cluster was found to be visually associated with tumor burden (figure 18) nor PSA response at 8 months ≥ 0.2 ng/ml (figure 19).

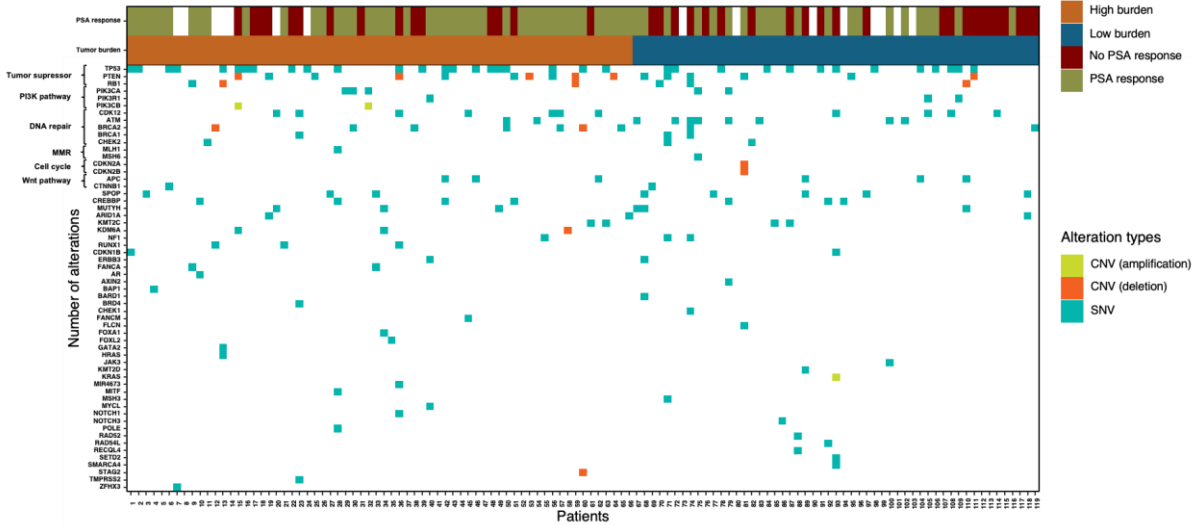


Figure 18: “heatmap” representing gene alterations and their type for each patient. Patients are grouped according to tumor burden high vs low.

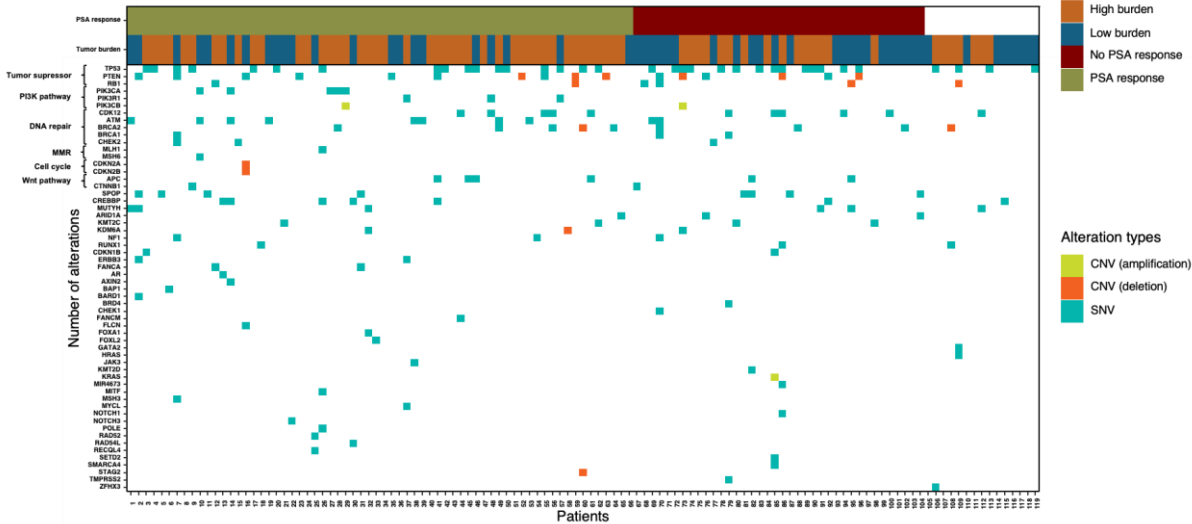


Figure 19: “heatmap” representing gene alterations and their type for each patient. Patients are grouped according to PSA response at 8 months ≥ 0.2 ng/ml vs < 0.2 ng/ml.

Correlation between genomic alterations

As shown in table 9 & 10, no correlation was found between each of the most frequent alterations even when compared with the TSalt (signature with at least 2 genes altered among *TP53*, *PTEN* and/or *RB1*) and DNA repair alterations (*BRCA1*, *BRCA2*, *ATM*, *CDK12* or *CHEK2*).

Table 9: Correlation using a Fisher's exact test for the most frequent alterations.

	<i>TP53</i>	<i>PTEN</i>	<i>CDK12</i>	<i>ATM</i>	<i>BRCA2</i>
<i>TP53</i>	-	0.556	0.729	0.721	1
<i>PTEN</i>	-	-	0.642	1	1
<i>CDK12</i>	-	-	-	0.596	0.596
<i>ATM</i>	-	-	-	-	0.166
<i>BRCA2</i>	-	-	-	-	-

Table 10: Correlation using a Fisher's exact test between the most frequent alterations and genomic classification.

	TSalt (≥ 2 genes altered among <i>TP53</i> , <i>PTEN</i> and/or <i>RBI</i>)	DNA repair alterations (<i>BRCA1</i> , <i>BRCA2</i> , <i>ATM</i> , <i>CDK12</i> and/or <i>CHEK2</i>)
<i>TP53</i>	-	0.818
<i>PTEN</i>	-	1
<i>CDK12</i>	0.195	-
<i>ATM</i>	0.559	-
<i>BRCA2</i>	0.520	-

iv. Transcriptomic analysis cohort

Among the 251 patients with sufficient material for RNA extraction, 194 (77.0%) had contributive samples after quantity and quality assessments. Sample characteristics are summarized in table 11.

Table 11: Sample characteristics for patients with contributive transcriptomic analysis.

	n (%)
Biopsy type	
<i>Bone marrow</i>	1 (0.5)
<i>Bone</i>	4 (2.1)
<i>Liver</i>	1 (0.5)
<i>Lung</i>	1 (0.5)
<i>Lymph node</i>	2 (1.0)
<i>Prostate biopsy</i>	154 (79.4)
<i>TURP</i>	31 (16.0)
Tumor percentage	
<i>Min / Max</i>	30.0 / 80.0
<i>Med [IQR]</i>	50.0 [30.0;60.0]
<i>Mean (std)</i>	46.2 (14.0)
<i>N (NA)</i>	194 (0)
White slide thickness (μm)	
3	170 (87.6)
4	16 (8.2)
10	8 (4.1)
White slide number	
<i>Min / Max</i>	2.0 / 38.0
<i>Med [IQR]</i>	4.0 [3.0;4.0]
<i>Mean (std)</i>	4.9 (4.2)
<i>N (NA)</i>	194 (0)
White slide temperature conservation	
-20°C	170 (87.6)
4°C	24 (12.4)

TURP: Transurethral resection of the prostate.

b. Prognostic analysis

i. Phenotypic analysis cohort

AR luminal high patients had a longer median rPFS of 3.4 years and AR luminal low a median of 2.6 years. Amphicrine patients had a slightly shorter median rPFS of 2.0 years. NEPC phenotype had a worse rPFS with a median of 0.7 years but with only 5 patients. Double negative patients seemed to have a longer rPFS but with only 3 patients in this subgroup (figure 20).

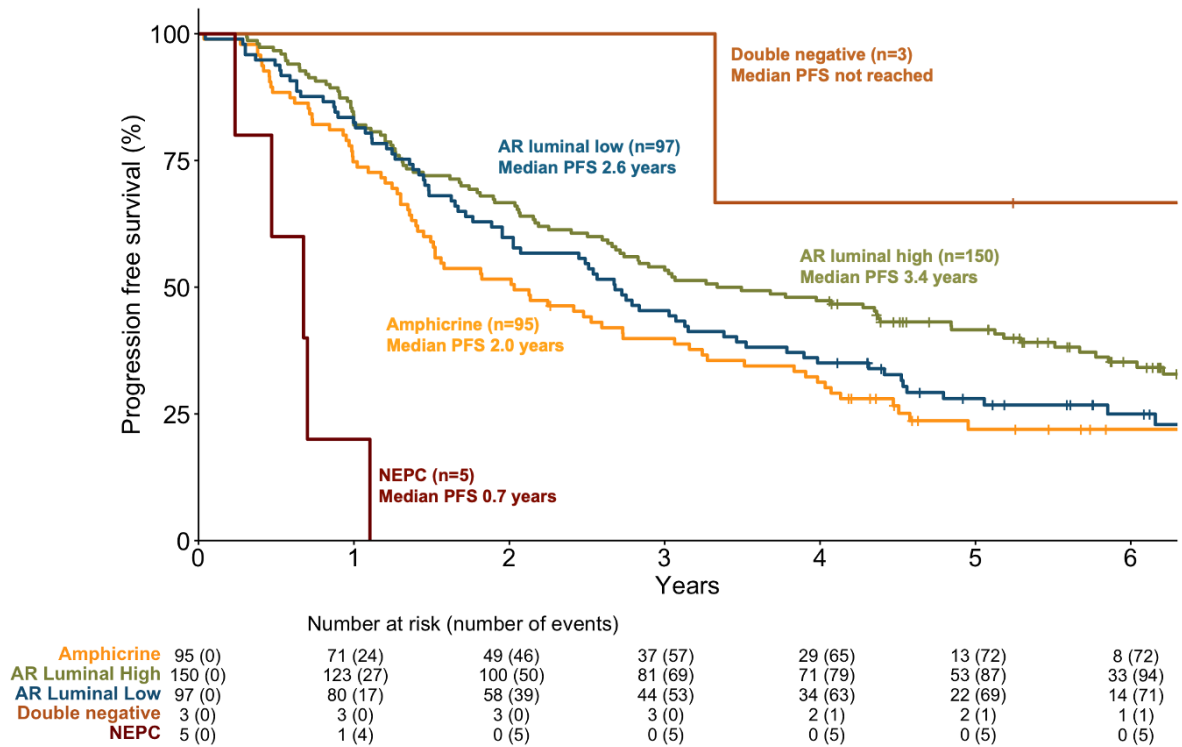


Figure 20: rPFS according to the 5 phenotypes.

Regarding prognosis, AR luminal high and AR luminal low had a median OS of 5.7 and 4.8 years respectively. Amphicrine patients had a median OS of 4.0 years slightly shorter compared to luminal patients. NEPC phenotype had also the worse OS with a median of 1.1 years and double negative patients seemed to have a longer OS with a median of 5.5 but the interpretation is limited by the number of patients (figure 21). Adjusted cox model with imputation for rPFS and OS analyses for the phenotypes with enough patients are resumed in table 12 & 13.

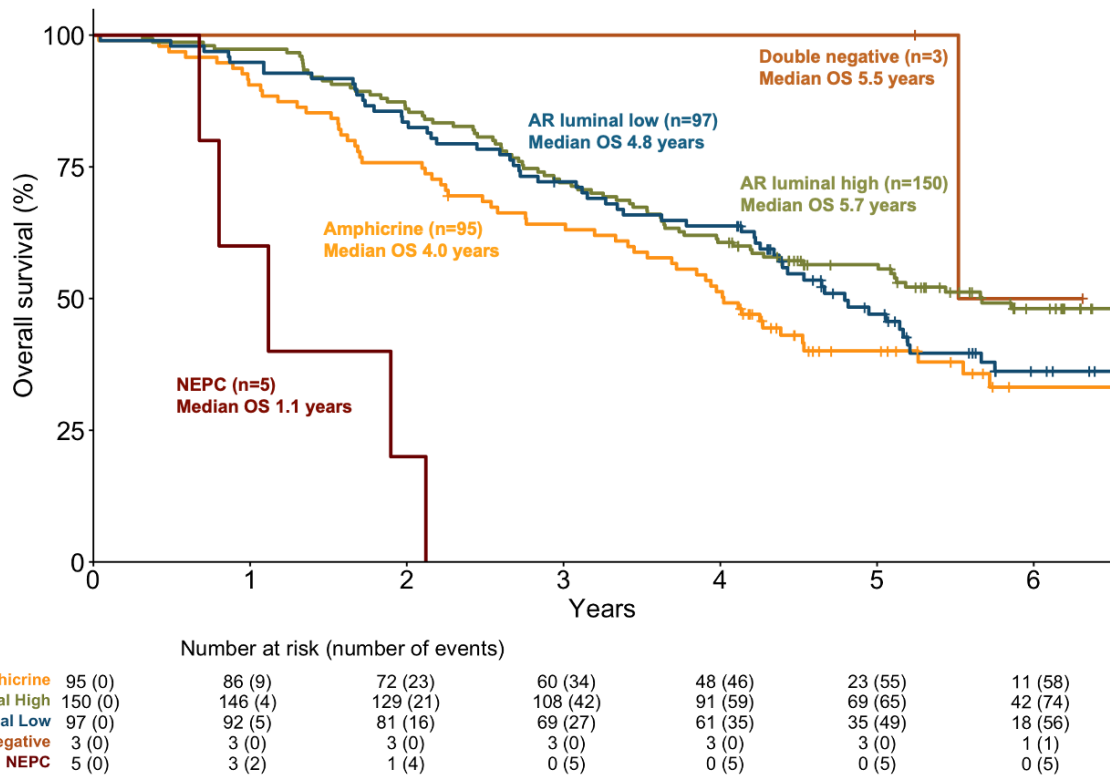


Figure 21: OS according to the 5 phenotypes.

Table 12: Unadjusted and adjusted rPFS according to phenotypes with AR luminal high as a reference. HR for NEPC phenotype and double negative were not assessable due to the low number of patients.

	Unadjusted rPFS			Adjusted rPFS*		
	HR	CI95%	p	HR	CI95%	p
<i>Amphotericin (n=98)</i>	1.56	1.16-2.10	0.003	1.41	1.04-1.91	0.028
<i>AR luminal high (n=170)</i>	-	-	-	-	-	-
<i>AR luminal low (n=116)</i>	1.26	0.94-1.69	0.120	1.17	0.87-1.57	0.300

*Cox PH models were computed and adjusted on age, ECOG, disease burden, Gleason, type of castration, and treatment received (radiotherapy, docetaxel and abiraterone).

Table 13: Unadjusted and adjusted OS according to phenotypes with AR luminal high as a reference. HR for NEPC phenotype and double negative were not assessable due to the low number of patients.

	Unadjusted OS			Adjusted OS*		
	HR	CI95%	p	HR	CI95%	p
<i>Amphicrine (n=98)</i>	1.60	1.15-2.23	0.006	1.52	1.08-2.13	0.015
<i>AR luminal high (n=170)</i>	-	-	-	-	-	-
<i>AR luminal low (n=116)</i>	1.18	0.85-1.64	0.300	1.13	0.81-1.58	0.500

*Cox PH models were computed and adjusted on age, ECOG, disease burden, Gleason, type of castration, and treatment received (radiotherapy, docetaxel and abiraterone).

Immunochemistry markers

In multivariate analyses with data imputation, NEmk patients had a shorter rPFS (HR=1.38, CI95%[1.06-1.81], p=0.017) and OS (HR=1.53, CI95%[1.14-2.06], p=0.005). Regarding each NEPC markers, synaptophysin and chromogranin A positive patients had a shorter rPFS (HR=1.45, CI95%[1.08-1.94], p=0.013 and HR=1.78, CI95%[1.16-2.75], p=0.009 respectively) and a shorter OS (HR=1.62, CI95%[1.17-2.24], p=0.004 and HR=1.90, CI95%[1.18-3.06], p=0.009). CD56 positivity alone had no significant effect but a trend for worse rPFS and OS (HR=1.24, CI95%[0.84-1.83], p=0.300 and HR=1.90, CI95%[1.18-3.06], p=0.009 respectively). Patients with ERG-positive tumor had a longer rPFS (HR=0.71, CI95%[0.53-0.94], p=0.019) and p53 abnormality (positive or NULL) was associated with a shorter rPFS (HR=1.30 CI95%[1.01-1.68], p=0.041). No other IHC biomarker was found to influence outcomes (table 14 to 17). Prognostic effects of each IHC markers are summarized in figure 22.

Table 14: Unadjusted and adjusted rPFS according to AR expression with AR nuclear as a reference.

	Unadjusted rPFS			Adjusted rPFS*		
	HR	CI95%	p	HR	CI95%	p
<i>AR negative (n=10)</i>	1.86	0.80-4.32	0.150	2.41	1.04-5.59	0.040
<i>AR nuclear only (n=225)</i>	-	-	-	-	-	-
<i>AR nuclear and cytoplasmic (n=116)</i>	1.19	0.91-1.56	0.200	1.09	0.83-1.45	0.500
<i>AR weak (n=43)</i>	1.28	0.86-1.91	0.200	1.28	0.86-1.92	0.200

*Cox PH models were computed and adjusted on age, ECOG, disease burden, Gleason, type of castration, and treatment received (radiotherapy, docetaxel and abiraterone).

Table 15: Unadjusted and adjusted rPFS for each IHC marker.

	Unadjusted rPFS			Adjusted rPFS*		
	HR	CI95%	p	HR	CI95%	p
<i>Synaptophysin positive (n=73 vs 321)</i>	1.52	1.14-2.03	0.005	1.45	1.08-1.94	0.013
<i>CD56 positive (n=43 vs 351)</i>	1.40	0.96-2.05	0.084	1.24	0.84-1.83	0.300
<i>Chromogranin A positive (n=36 vs 358)</i>	2.01	1.34, 3.02	<0.001	1.78	1.16-2.75	0.009
<i>NE marker positive i.e. at least one among synaptophysin, CD56 or chromogranin A (n=103 vs 291)</i>	1.51	1.17-1.97	0.002	1.38	1.06-1.81	0.017
<i>p53 positive or NULL (n=148 vs 246)</i>	1.28	1.01-1.64	0.044	1.30	1.01-1.68	0.041
<i>Rb1 negative (n=102 vs 292)</i>	1.01	0.76-1.35	0.900	0.89	0.66-1.21	0.500
<i>Log(Ki-67 + 1)</i>	1.12	0.99-1.26	0.072	1.14	1.00-1.30	0.120
<i>ERG positive (n=139 vs 255)</i>	0.68	0.52-0.89	0.005	0.71	0.53-0.94	0.019
<i>NKX3.1 loss of expression i.e. H-score <300 (n=219 vs 175)</i>	1.11	0.86-1.42	0.400	1.02	0.79-1.31	0.900

*Cox PH models were computed and adjusted on age, ECOG, disease burden, Gleason, type of castration, and treatment received (radiotherapy, docetaxel and abiraterone).

Table 16: Unadjusted and adjusted OS according to AR expression with AR nuclear as a reference.

	Unadjusted OS			Adjusted OS*		
	HR	CI95%	p	HR	CI95%	p
<i>AR negative (n=10)</i>	2.32	1.03-5.20	0.042	2.60	1.16-5.83	0.021
<i>AR nuclear only (n=225)</i>	-	-	-	-	-	-
<i>AR nuclear and cytoplasmic (n=116)</i>	1.16	0.85-1.57	0.300	1.08	0.79-1.48	0.600
<i>AR weak (n=43)</i>	1.30	0.84-2.01	0.200	1.29	0.83-2.00	0.300

*Cox PH models were computed and adjusted on age, ECOG, disease burden, Gleason, type of castration, and treatment received (radiotherapy, docetaxel and abiraterone).

Table 17: Unadjusted and adjusted OS for each IHC marker.

<i>IHC markers</i>	Unadjusted OS			Adjusted OS*		
	HR	CI95%	p	HR	CI95%	p
<i>Synaptophysin positive (n=73 vs 321)</i>	1.68	1.22-2.32	0.002	1.62	1.17-2.24	0.004
<i>CD56 positive (n=43 vs 351)</i>	1.35	0.89-2.05	0.200	1.29	0.85-1.97	0.200
<i>Chromogranin A positive (n=36 vs 358)</i>	1.93	1.25-3.00	0.004	1.90	1.18-3.06	0.009
<i>NE marker positive i.e. at least one among synaptophysin, CD56 or chromogranin A (n=103 vs 291)</i>	1.61	1.20-2.15	0.002	1.53	1.14-2.06	0.005
<i>p53 positive or NULL (n=148 vs 246)</i>	1.22	0.93-1.61	0.200	1.24	0.92-1.65	0.200
<i>Rb1 negative (n=102 vs 292)</i>	0.92	0.67-1.27	0.600	0.83	0.59-1.15	0.300
<i>Log(Ki-67 + 1)</i>	1.12	0.97-1.29	0.120	1.14	0.98-1.32	0.300
<i>ERG positive (n=139 vs 255)</i>	0.70	0.51-0.96	0.025	0.77	0.55-1.06	0.110
<i>NKX3.1 loss of expression i.e. H-score <300 (n=219 vs 175)</i>	1.08	0.81-1.43	0.600	1.03	0.78-1.37	0.800

*Cox PH models were computed and adjusted on age, ECOG, disease burden, Gleason, type of castration, and treatment received (radiotherapy, docetaxel and abiraterone).

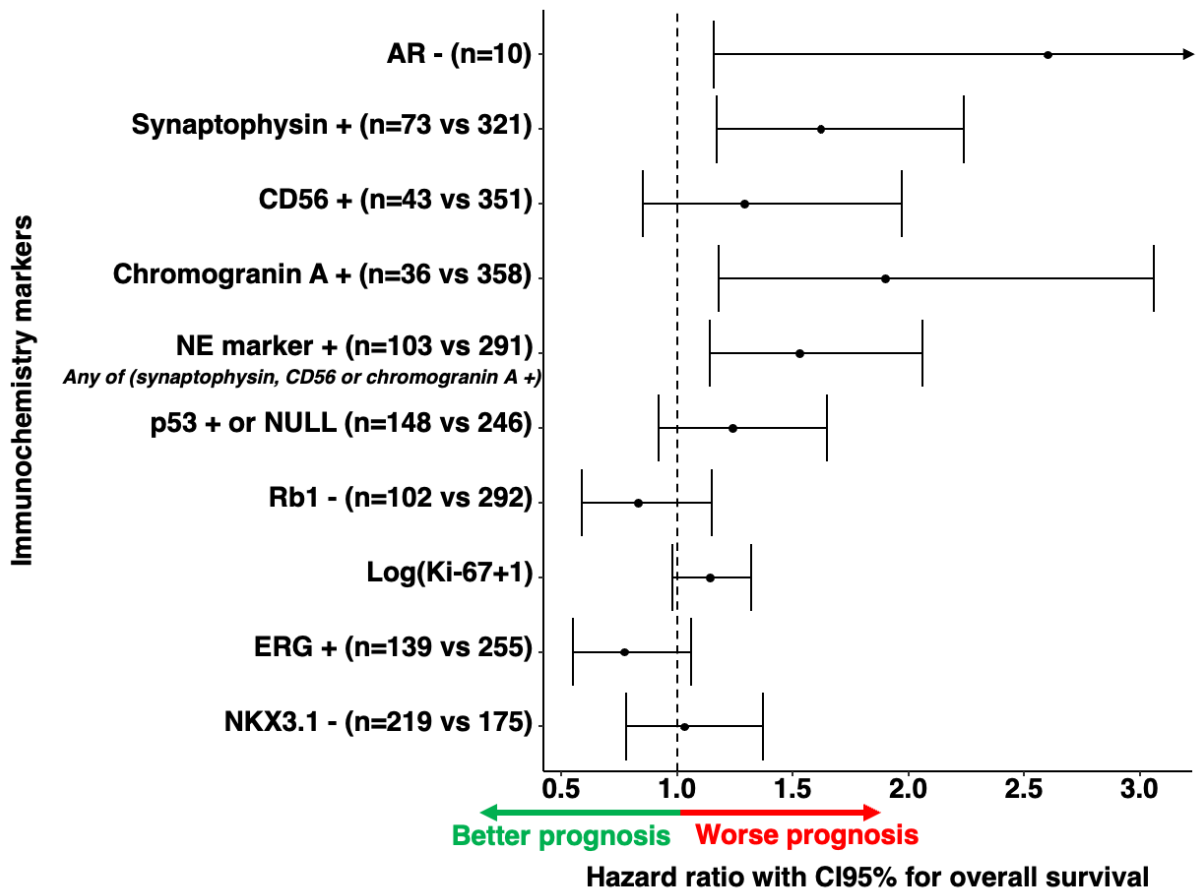


Figure 22: Forest plot of HR and their CI95% for each IHC markers computed and adjusted on age, ECOG, disease burden, Gleason, type of castration, and treatment received (radiotherapy, docetaxel and abiraterone).

ii. Genomic analysis cohort

Among the 119 patients with contributive NGS, median rPFS was 2.8 years CI95% [2.1-4.3] with 80 events and median OS 5.1 years CI95% [4.3-NA] with 64 events. TSalt patients (n=9) had a shorter rPFS with a median of 1.1 year vs 3.0 years (HR=3.10, CI95% [1.33-7.24], p=0.009 and a shorter OS with a median of 2.2 years vs 5.4 (HR=2.63, CI95% [1.10-6.30], p=0.03, figure 23). Patients with *BRCA1/2* alterations (n=11) had a tendency for shorter OS with a median of 3.1 years vs 5.4 (HR=2.10 CI95% [0.90-4.91], p=0.086, figure 24). A similar trend was found for patients with only a *BRCA2* alteration (n=9) with a median OS of 3.1 years vs 5.4 (HR=2.24, CI95% [0.91-5.50], p=0.078). No other alterations were found to influence rPFS or OS (table 18 & 19).

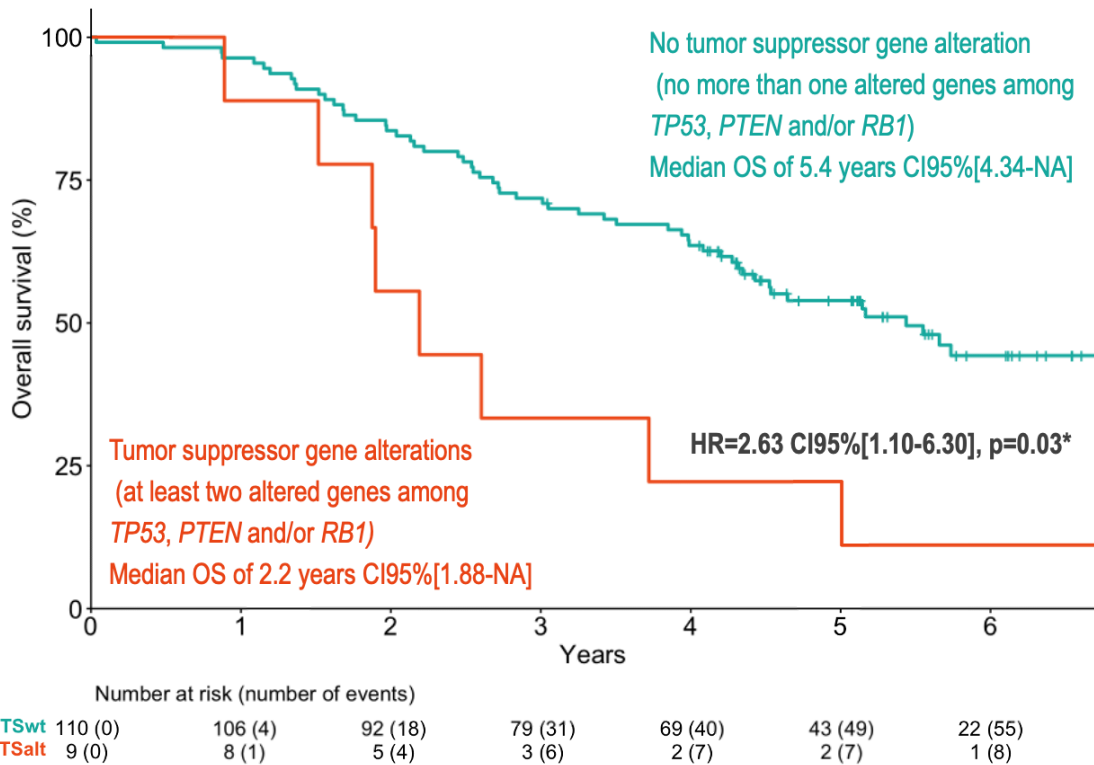


Figure 23: OS according to the alterations of two genes among the tumor suppressor *TP53*, *PTEN* or *RB1*.

*Adjusted on age, ECOG, disease burden, Gleason, type of castration, and treatment received (radiotherapy, docetaxel and abiraterone).

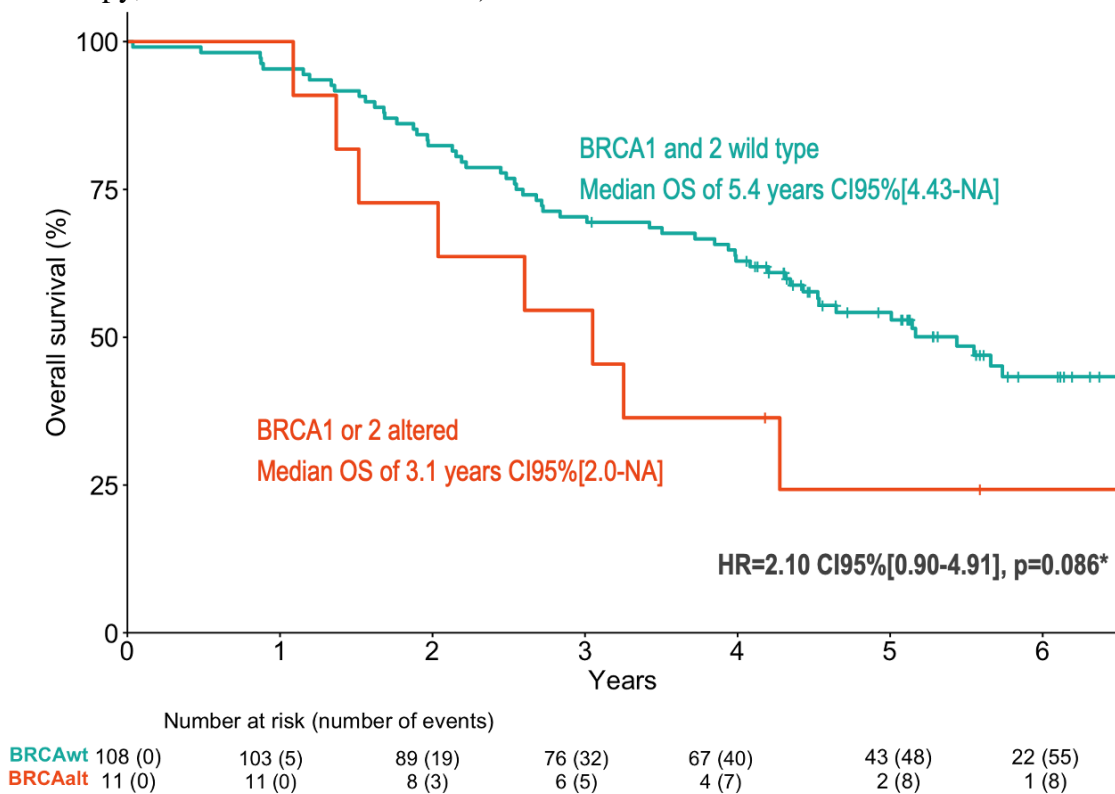


Figure 24: OS according to *BRCA* alterations.

*Adjusted on age, ECOG, disease burden, Gleason, type of castration, and treatment received (radiotherapy, docetaxel and abiraterone).

Table 18: Unadjusted and adjusted rPFS for the most frequent somatic gene alterations.

	Unadjusted rPFS			Adjusted rPFS*		
	HR	CI95%	p	HR	CI95%	p
<i>TP53</i> (n=35 vs 84)	0.91	0.56-1.49	0.700	0.79	0.46-1.35	0.392
<i>PTEN</i> (n=16 vs 103)	1.50	0.81-2.77	0.200	2.02	1.02-4.03	0.044
<i>CDK12</i> (n=11 vs 108)	0.82	0.38-1.78	0.600	0.77	0.34-1.76	0.536
<i>ATM</i> (n=10 vs 109)	0.97	0.42-2.22	0.900	1.51	0.57-4.02	0.409
<i>BRCA2</i> (n=9 vs 110)	2.08	0.96-4.54	0.060	2.59	1.10-6.12	0.030
<i>BRCA1 or 2</i> (n=11 vs 108)	1.71	0.82-3.55	0.100	2.37	1.04-5.42	0.040
<i>DNA repair genes</i> [°] (n=20 vs 60)	1.08	0.65-1.79	0.800	1.45	0.82-2.55	0.198
<i>TSalt</i> [†] (n=9 vs 110)	2.95	1.41-6.20	0.003	3.10	1.33-7.24	0.009

*Cox PH models were adjusted on age, ECOG, disease burden, Gleason, type of castration, and treatment received (radiotherapy, docetaxel and abiraterone).

[°] Alterations of *BRCA1*, *BRCA2*, *ATM*, *CDK12* or *CHEK2*.

[†] At least 2 genes altered among *TP53*, *PTEN* or *RBI*.

Table 19: Unadjusted and adjusted OS for the most frequent somatic gene alterations

	Unadjusted OS			Adjusted OS*		
	HR	CI95%	p	HR	CI95%	p
<i>TP53</i> (n=35 vs 84)	0.90	0.52-1.57	0.700	0.71	0.39-1.31	0.277
<i>PTEN</i> (n=16 vs 103)	1.33	0.67-2.61	0.400	1.49	0.70-3.17	0.299
<i>CDK12</i> (n=11 vs 108)	0.97	0.42-2.25	0.900	0.82	0.34-1.99	0.664
<i>ATM</i> (n=10 vs 109)	1.05	0.45-2.45	0.900	1.93	0.67-5.54	0.223
<i>BRCA2</i> (n=9 vs 110)	2.42	1.10-5.35	0.020	2.24	0.91-5.50	0.078
<i>BRCA1 or 2</i> (n=11 vs 108)	1.99	0.94-4.18	0.070	2.10	0.90-4.91	0.086
<i>DNA repair genes</i> [°] (n=20 vs 60)	1.33	0.78-2.28	0.300	1.65	0.92-2.96	0.095
<i>TSalt</i> [†] (n=9 vs 110)	2.87	1.36-6.06	0.004	2.63	1.10-6.29	0.030

*Cox PH models were adjusted on age, ECOG, disease burden, Gleason, type of castration, and treatment received (radiotherapy, docetaxel and abiraterone).

[°] Alterations of *BRCA1*, *BRCA2*, *ATM*, *CDK12* or *CHEK2*.

[†] At least 2 genes altered among *TP53*, *PTEN* or *RBI*.

iii. Transcriptomic analysis cohort

NEPC and AR signature

When adjusted on age, ECOG, disease burden, Gleason, type of castration, and treatment received (radiotherapy, docetaxel and abiraterone), patients with a higher NEPC z-score had a shorter OS (HR=1.63, CI95[1.02-2.63], p=0.042) and patients with a higher AR z-score a longer OS (HR=0.61, CI95[0.42-0.89], p<0.001). The mitochondrial metabolism z-score was not associated with rPFS or OS (table 20 & 21).

Table 20: Unadjusted and adjusted rPFS according to NEPC and AR z-score.

	Unadjusted rPFS			Adjusted rPFS*		
	HR	CI95%	p	HR	CI95%	p
<i>NEPC z-score (continuous)</i>	1.71	1.15-2.52	0.007	1.55	1.01-2.38	0.046
<i>AR z-score (continuous)</i>	0.54	0.40-0.73	<0.001	0.54	0.39-0.75	<0.001
<i>Mitochondrial metabolism z-score (continuous)</i>	1.04	0.66-1.63	0.900	1.29	0.80-2.10	0.298

*Adjusted on age, ECOG, disease burden, Gleason, type of castration, and treatment received (radiotherapy, docetaxel and abiraterone).

Table 21: Unadjusted and adjusted OS according to NEPC and AR z-score.

	Unadjusted OS			Adjusted OS*		
	HR	CI95%	p	HR	CI95%	p
<i>NEPC z-score (continuous)</i>	1.60	1.04-2.46	0.030	1.63	1.02-2.63	0.042
<i>AR z-score (continuous)</i>	0.61	0.44-0.86	0.005	0.61	0.42-0.89	<0.001
<i>Mitochondrial metabolism z-score (continuous)</i>	1.10	0.66-1.83	0.700	1.49	0.85-2.60	0.166

*Adjusted on age, ECOG, disease burden, Gleason, type of castration, and treatment received (radiotherapy, docetaxel and abiraterone).

Non-responder vs responder

The following genes, ordered by their p adjusted values, were significantly over-expressed in non-responder (rPFS < 1 year): *ARG1*, *HSD11B1*, *AURKB*, *PCLAF*, *S100A12*, *FOXM1*, *EZH2*, *MCM4*, *CCNB1*, *RFC2*, *UBE2T*, *E2F1* and *MCM2* (figure 25). Supervised clustering with Euclidean algorithm according to responder vs responder adjusted with size factor and tumoral percentage is shown in figure 26. Patients in cluster 1 had a shorter OS compared to cluster 2 (HR= 2.560 CI95%[1.681-3.898], p<0.001, figure 27). Regarding hallmarks, the androgen response was suppressed and E2F targets and G2M checkpoint pathways were activated in non-responders as well as the xenobiotic metabolism pathway. The custom AR signature was also suppressed (figure 28). In GSVA, our custom AR signature (with overexpressed genes only) was significantly less expressed in non-responder (p=0.001).

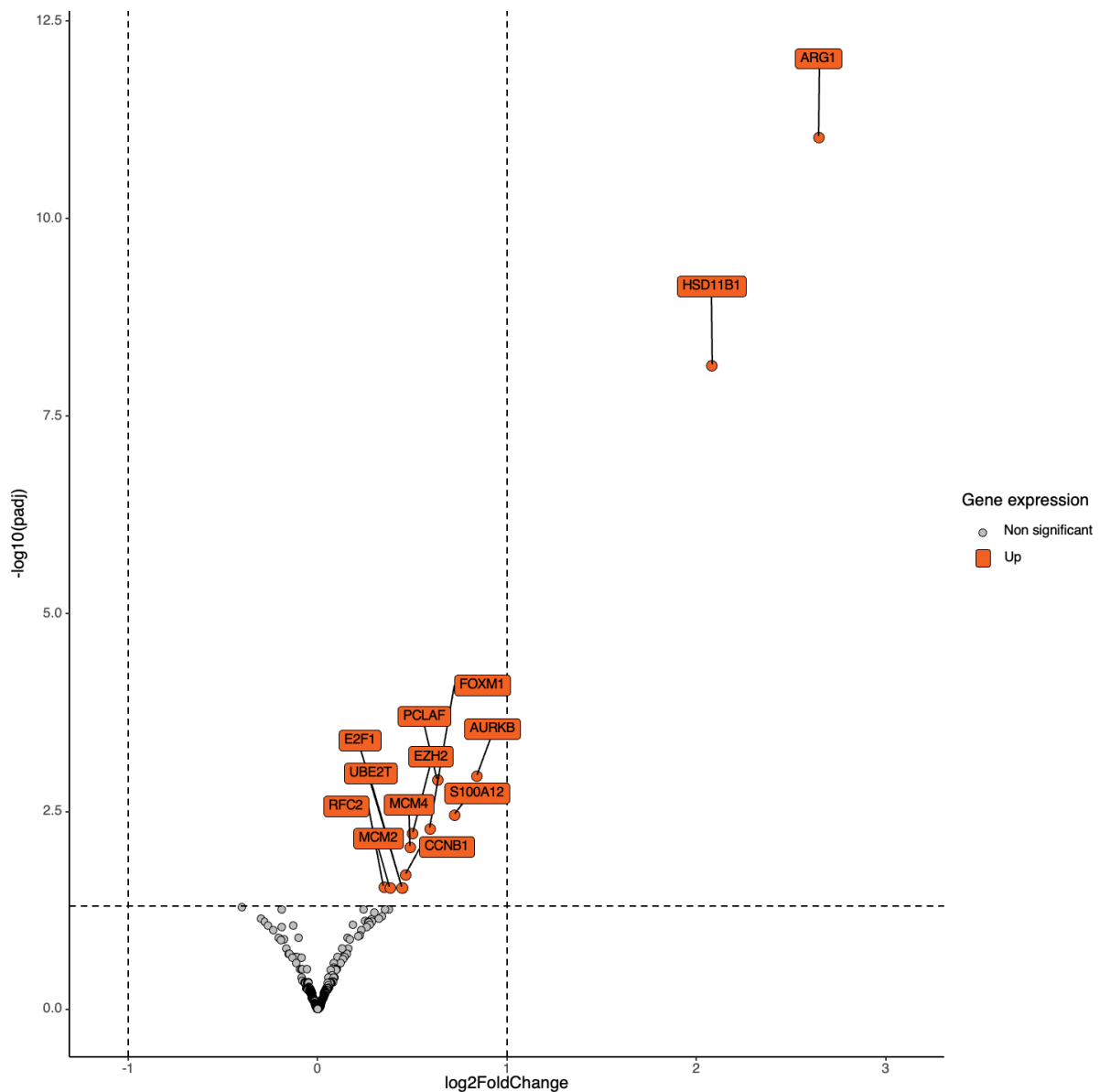


Figure 25: Volcano plot representing the differential gene expression of non-responder vs responder.

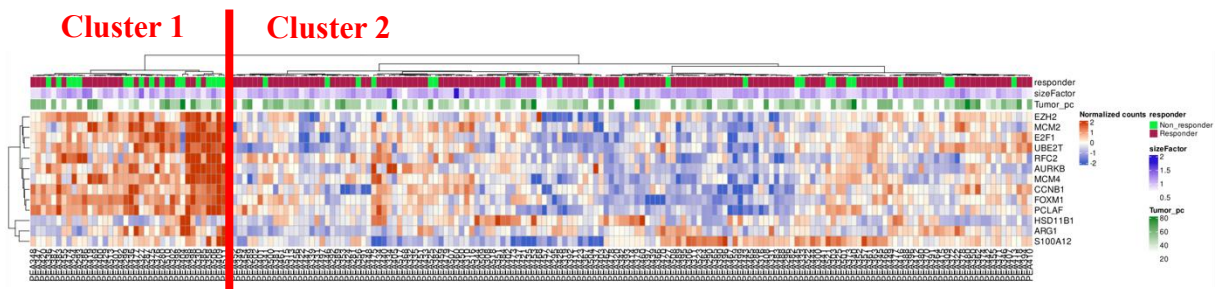


Figure 26: Supervised clustering according to response to treatment (Euclidean algorithm).

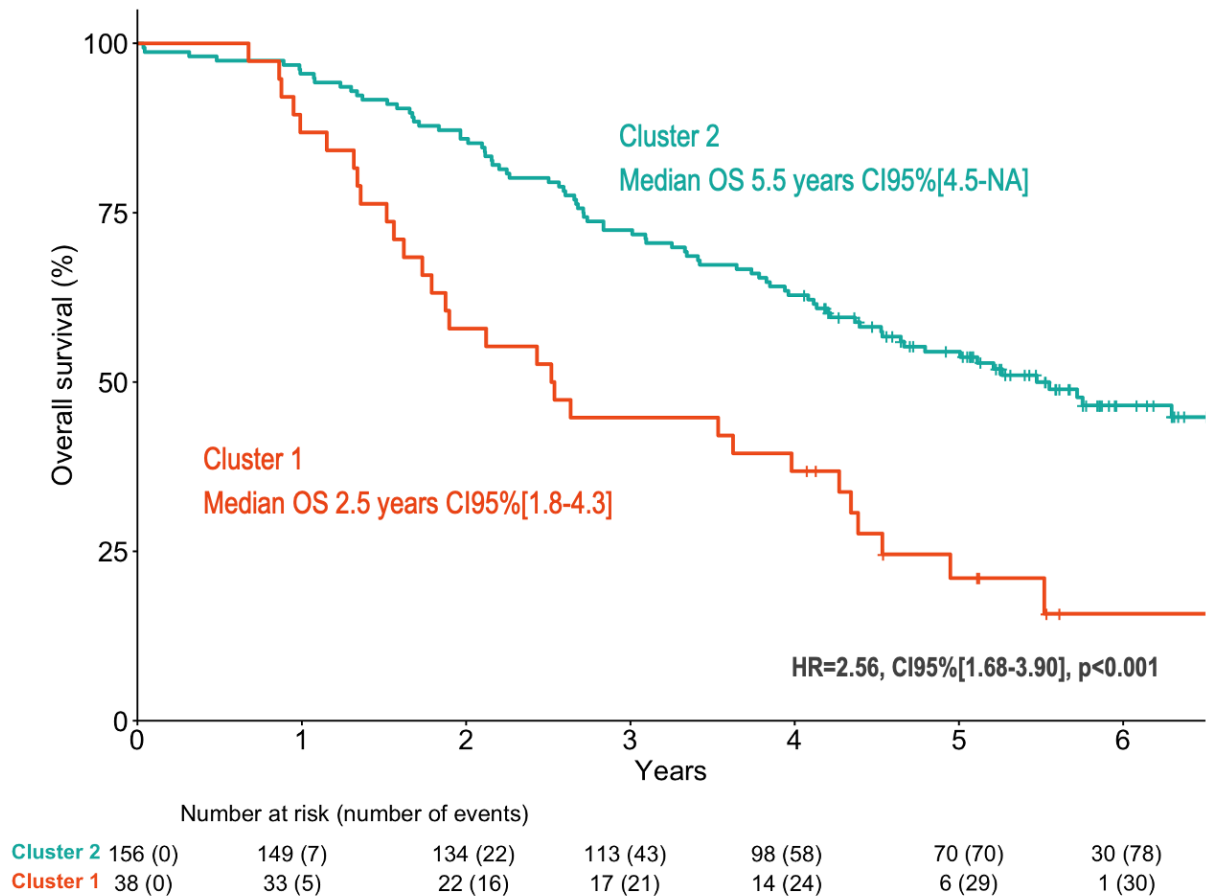


Figure 27: OS of cluster 1 and 2 from supervised clustering according to response to treatment.

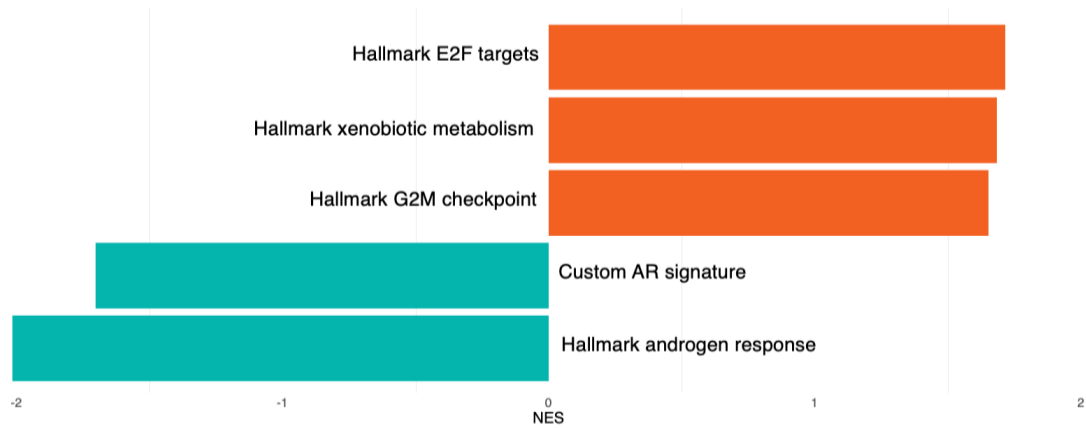


Figure 28: GSEA in non-responder vs responder patients.

NEPC markers in IHC

In NEmk patients, over-expressed genes were FOS, PROX1, DLL3, RAC3, SOCS3, CDK1, MMP9, NUF2, SERPINE1, DNMT1, KDM1A, SEZ6, PGK1, TPX2, TOP2A, SOGA3, *FANCI*, *UBE2T* and *TIMELESS* whereas under-expressed genes were *EGF*, *GRAP2* and *NBL1* (figure 29). Supervised clustering with Euclidean algorithm according to NEmk adjusted with size factor and tumoral percentage is shown in figure 30. Patients in cluster 1 had a shorter OS compared to cluster 2 (HR= 2.524, CI95% [1.618-3.937], p<0.001, figure 31). In patients with at least one NEPC marker positive in IHC, the androgen response, the custom AR signature and the KRAS signaling were suppressed whereas E2F targets, G2M checkpoint, hypoxia and MYC targets pathway were activated (figure 32). In GSVA, our custom AR signature (with overexpressed genes only) was significantly less expressed in NEmk patients (p=0.012).

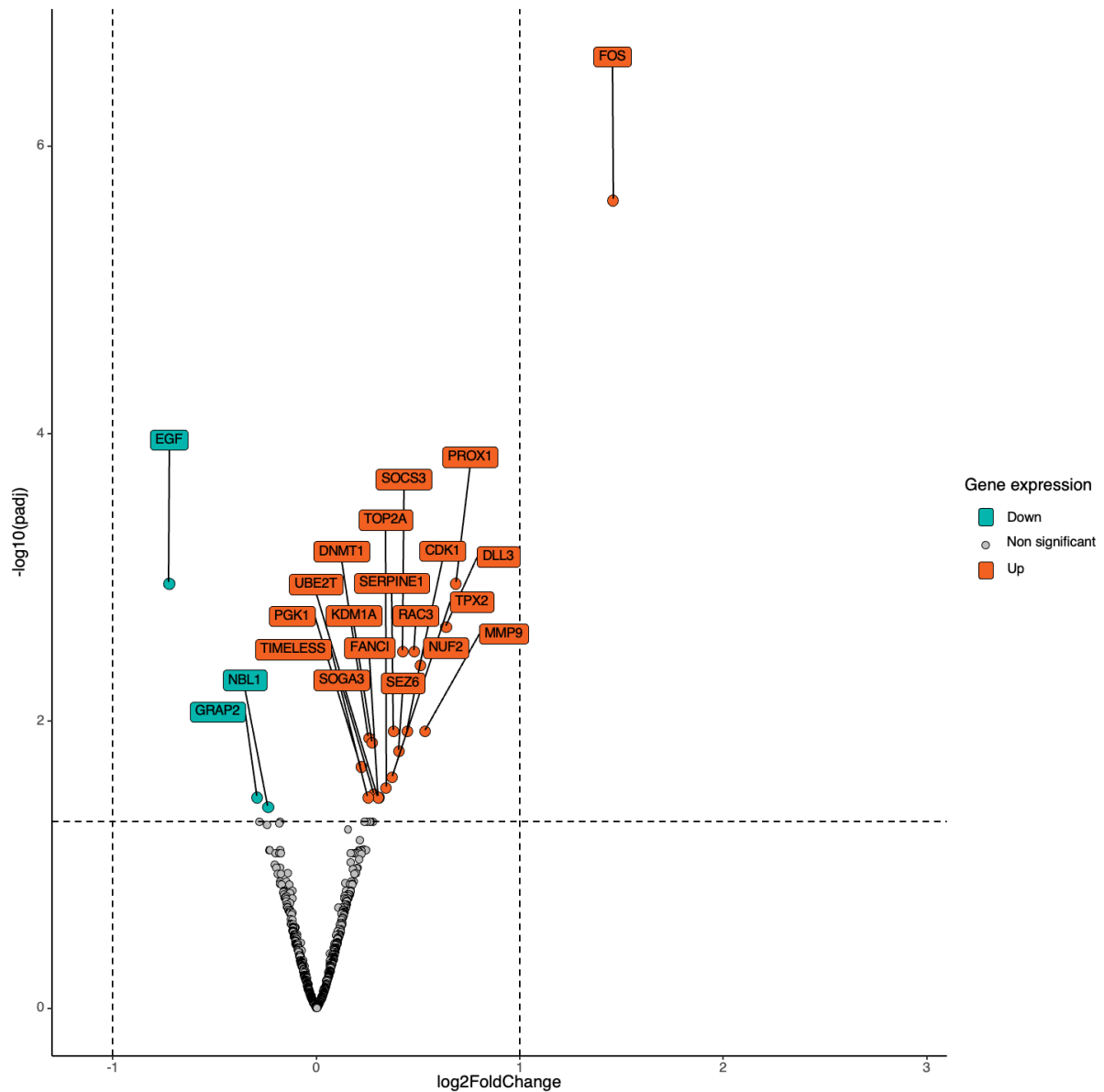


Figure 29: Volcano plot representing the differential gene expression of patients with NEmk positive vs others.

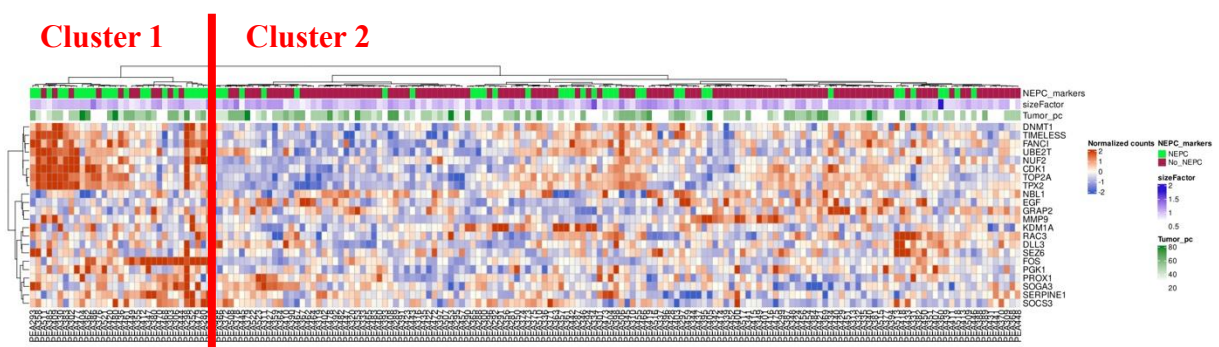


Figure 30: Supervised clustering according to NEmk expression (Euclidean algorithm).

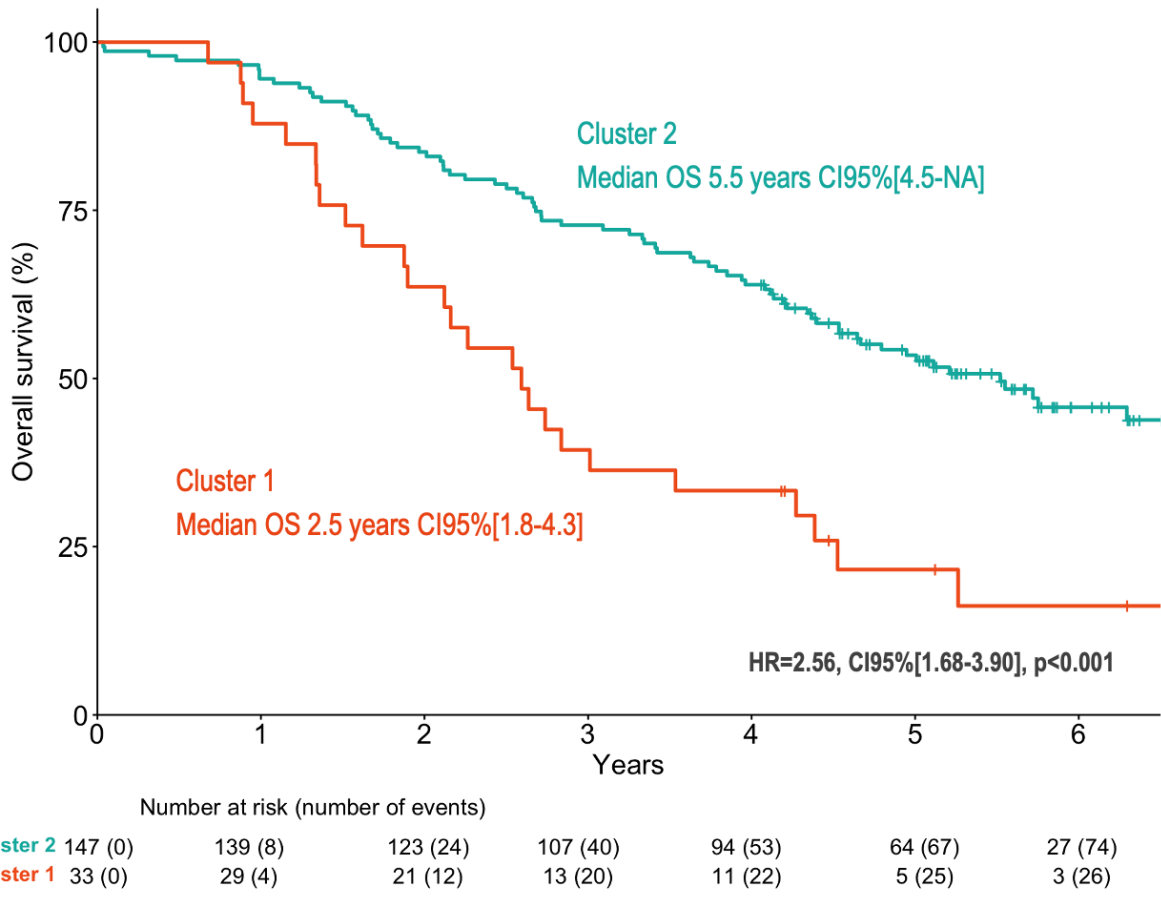


Figure 31: OS of cluster 1 and 2 from supervised clustering according to NEPC markers.

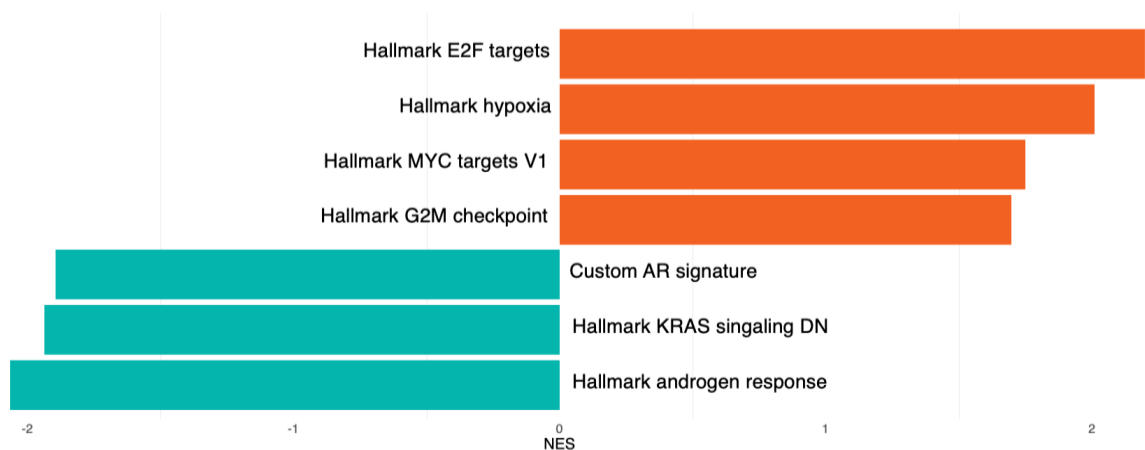


Figure 32: GSEA in NEmk positive vs other patients.

Tumor suppressor genes alterations in NGS

Patients with TSalt had an overexpression of *CALML3*, *TFRC*, *SOX2*, *RRM2*, *RFC4*, *DLL3*, *NUF2*, *PROX1*, *TOP2A*, *DNMT1*, and an under expression of *FMOD*, *IGF1R*, *PDGFRB* and *PDLIM5* (figure 33). Supervised clustering with Euclidean algorithm according to TSalt adjusted with size factor and tumoral percentage is shown in figure 34. Patients in cluster 2 had a shorter OS compared to cluster 1 (HR= 2.849, CI95% [1.229-6.603], p=0.020, figure 35). More pathways were over-expressed in TSalt patients including the E2F, G2M, MYC, MTOR and spermatogenesis pathways. Allograft rejection, TNF α signaling, the custom AR signature,

KRAS, EMT and UV response were under-expressed (figure 36). In GSVA, our custom AR signature (with overexpressed genes only) was significantly less expressed in TSalt ($p=0.025$).

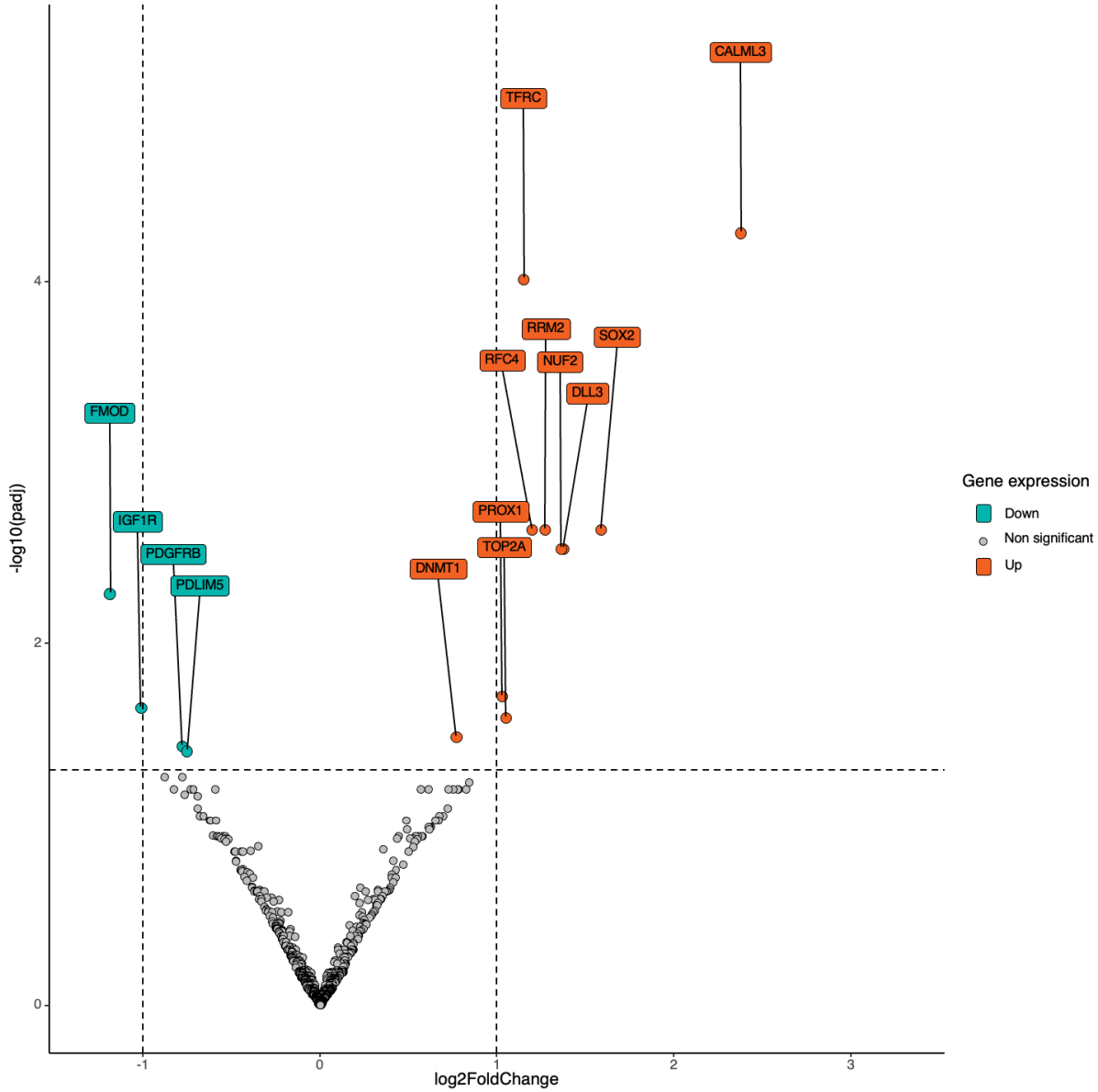


Figure 33: Volcano plot representing the differential gene expression of TSalt patients vs others.

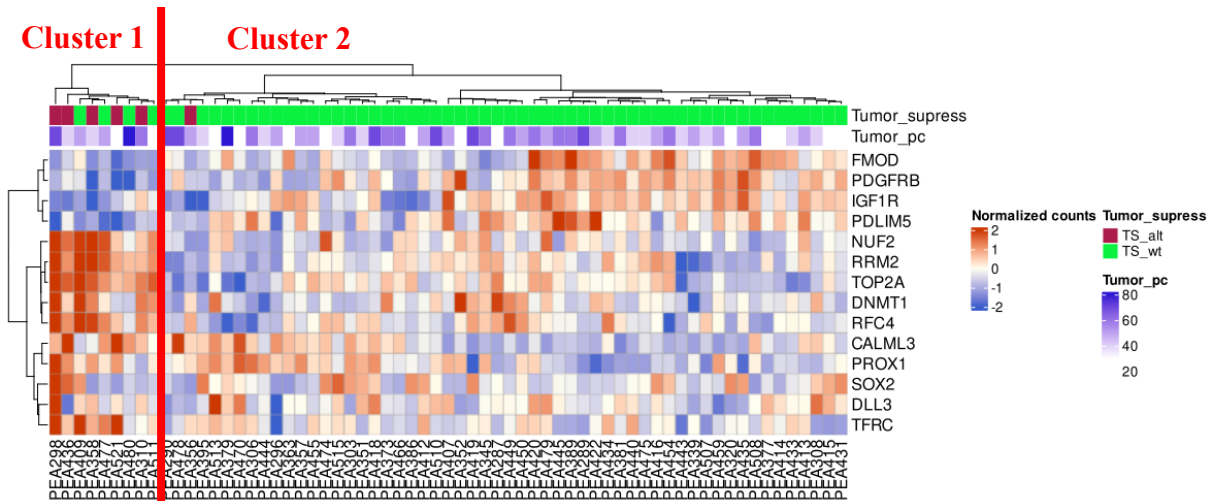


Figure 34: Supervised clustering according to TSalt (Euclidean algorithm).

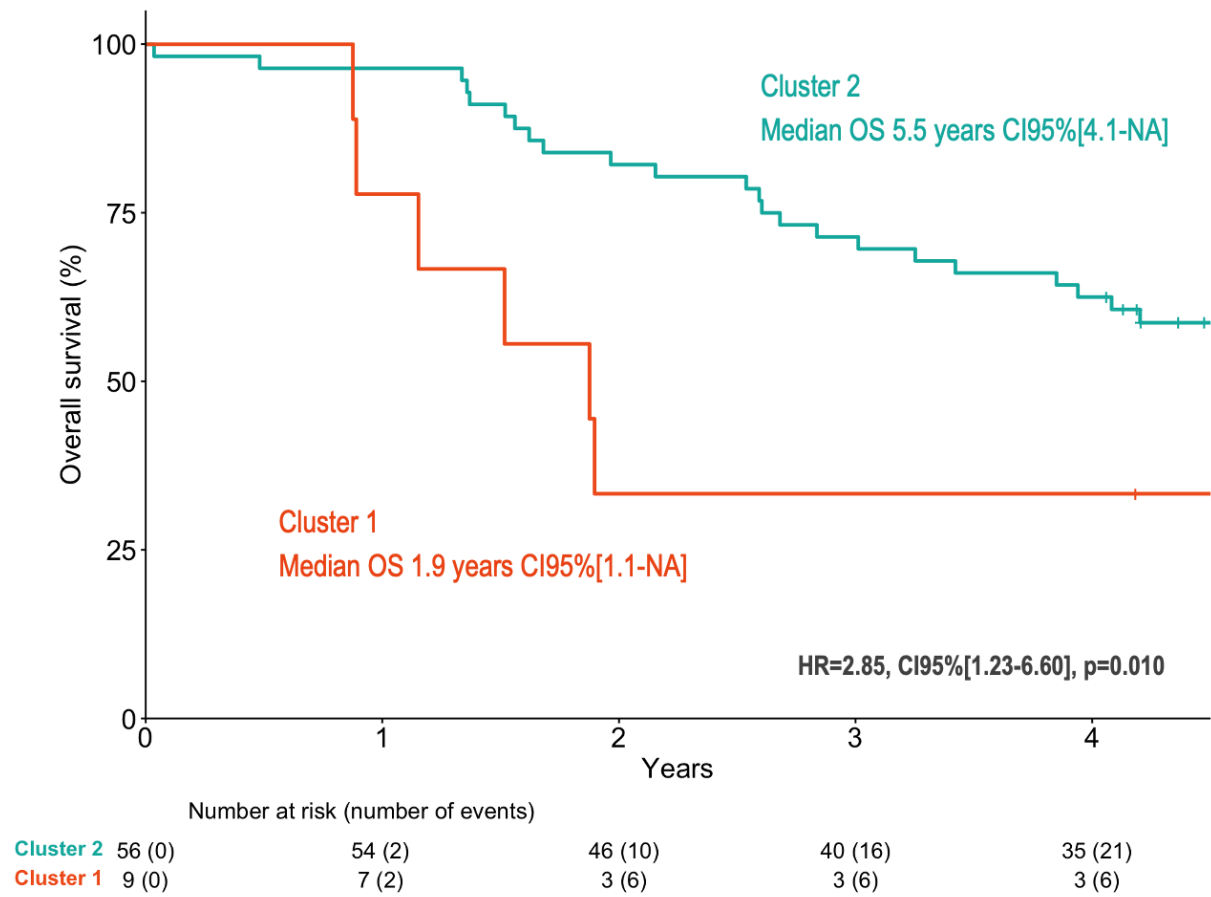


Figure 35: OS of cluster 1 and 2 from supervised clustering according to TSalt.

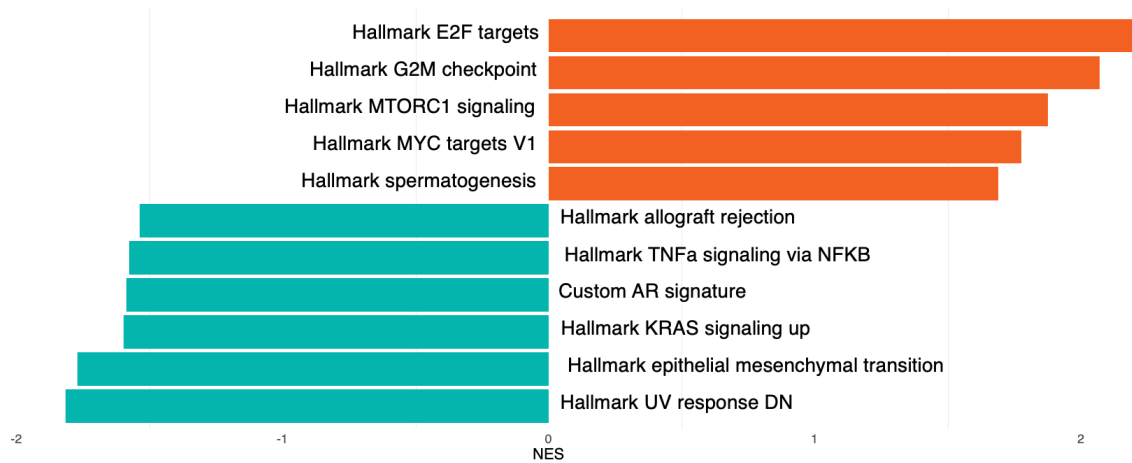


Figure 36: GSEA in TSalt vs other patients.

BRCA alterations in NGS

Patients with *BRCA* alterations had an over-expression of *SLPI* and under-expression of *HLA-C*, *GZMK*, *PTPRC* and *ITGB2* (figure 37). Supervised clustering with Euclidean algorithm according to *BRCA* alterations is shown in figure 38. No statistical difference and even a trend for shorter OS was found for patients in cluster 2 (with less *BRCA* alterations) vs cluster 1 (HR= 2.023, CI95% [0.914-4.478], p=0.080, figure 39). In *BRCA* alerted patients, only the E2F targets pathway was activated (figure 40). In GSVA, our custom AR signature (with overexpressed genes only) was significantly less expressed in high burden patients (p=0.017).

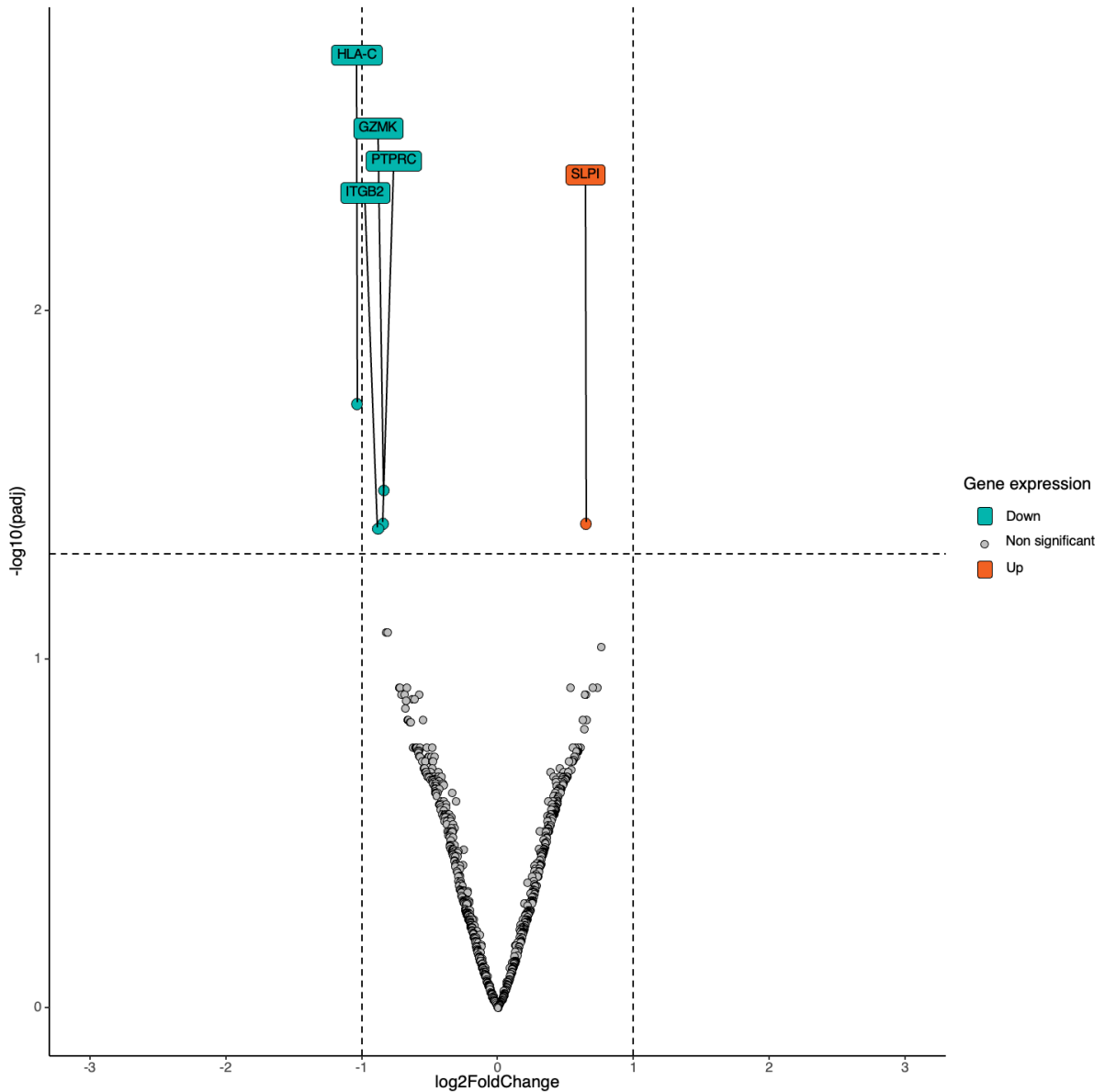


Figure 37: Volcano plot representing the differential gene expression of patients with *BRCA* alterations vs others.

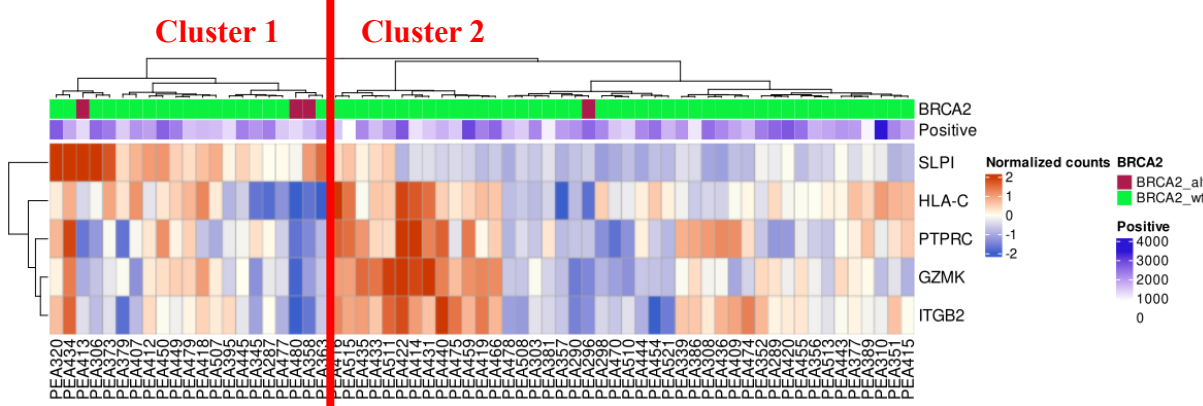
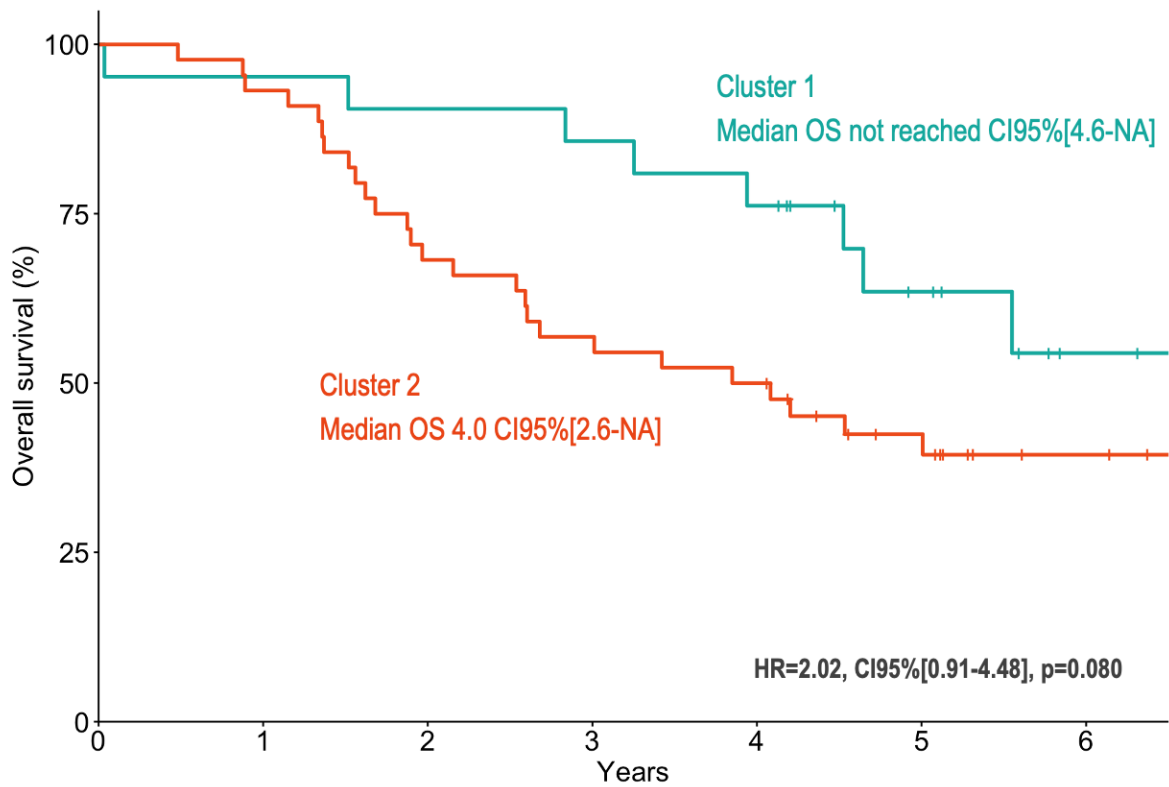


Figure 38: Supervised clustering according to *BRCA* alterations (Euclidean algorithm).



	Number at risk (number of events)						
Cluster 1	21 (0)	20 (1)	19 (2)	18 (3)	16 (5)	9 (7)	3 (8)
Cluster 2	44 (0)	41 (3)	30 (14)	25 (19)	22 (22)	14 (25)	6 (26)

Figure 39: OS of cluster 1 and 2 from supervised clustering according to BRCA alterations.

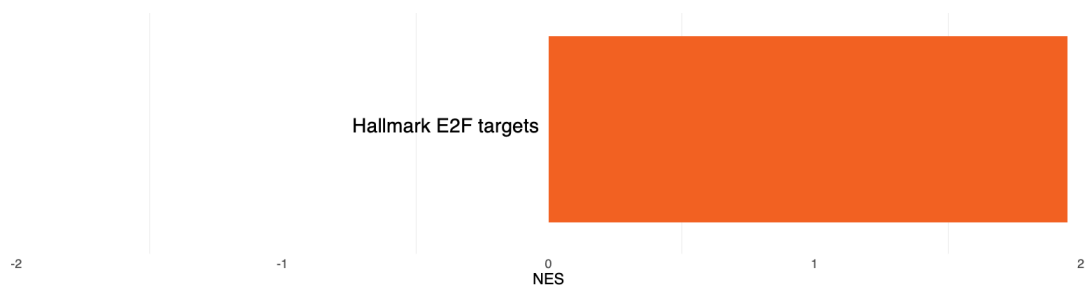


Figure 40: GSEA in BRCA altered vs other patients.

Unsupervised clustering

None of the clusters were significantly associated with rPFS or OS.

c. Predictive analysis

i. Phenotypic analysis cohort

No predictive value for abiraterone benefit was found when adjusted on age, ECOG, disease burden, Gleason, type of castration, and treatment received (radiotherapy, docetaxel and abiraterone) using an interaction test for rPFS and OS (table 22).

Table 22: Predictive value of each IHC biomarker assessed with an interaction test.

	Adjusted rPFS*			Adjusted OS*		
	HR	95%CI	p	HR	95%CI	p
<i>Abiraterone*AR</i>						
<i>AR cytoplasmic & nuclear</i>	1.00	0.57- 1.73	1.000	0.93	0.50- 1.73	0.800
<i>AR negative</i>	0.45	0.06- 3.69	0.500	0.46	0.06- 3.56	0.500
<i>AR nuclear</i>	-	-	-	-	-	-
<i>AR weak</i>	1.46	0.63- 3.37	0.400	1.73	0.69- 4.34	0.200
<i>Abiraterone*Synaptophysin</i>						
<i>Synaptophysin positive</i>	1.30	0.72-2.34	0.400	1.18	0.62-2.26	0.600
<i>abiraterone*CD56</i>						
<i>CD56 positive</i>	1.50	0.67- 3.37	0.300	1.62	0.67-3.91	0.300
<i>Abiraterone*Chromogranin A</i>						
<i>Chromogranin A positive</i>	0.93	0.38- 2.25	0.900	0.74	0.30-1.86	0.500
<i>Abiraterone*p53</i>						
<i>p53 positive or null</i>	0.89	0.52-1.50	0.600	0.99	0.54-1.81	1.000
<i>Abiraterone * Rb1</i>						
<i>Rb1 negative</i>	1.13	0.61- 2.10	0.700	1.09	0.55-2.16	0.800
<i>Abiraterone * ERG</i>						
<i>ERG positive</i>	0.59	0.34- 1.03	0.061	0.56	0.30-1.04	0.068
<i>Abiraterone * NKX3.1</i>						
<i>NKX3.1 negative (< 300)</i>	1.25	0.76- 2.07	0.400	1.18	0.67- 2.07	1.180
<i>Abiraterone * Ki67_log</i>						
<i>Log(Ki-67 + 1)</i>	0.87	0.67- 1.13	0.300	0.82	0.61- 1.10	0.200
<i>Abiraterone*NEmk</i>						
<i>NEmk</i>	1.60	0.93- 2.74	0.088	1.50	0.84- 2.71	0.200

*Cox PH models were adjusted on age, ECOG, disease burden, Gleason, type of castration, and treatment received (radiotherapy, docetaxel and abiraterone).

ii. Genomic analysis cohort

The number of patients for each alteration and TSalt was not sufficient to assess predictive value for abiraterone benefit.

iii. Transcriptomic analysis cohort

Regarding the NEPC and AR z-scores, no predictive value for abiraterone benefit was found when adjusted on age, ECOG, disease burden, Gleason, type of castration, and treatment received (radiotherapy, docetaxel and abiraterone) using an interaction test for rPFS and OS.

d. Correlation with PSA response at 8 months

i. Phenotypic analysis cohort

A higher Ki67 was associated with a PSA response at 8 months (i.e. < 0.2 ng/ml). The median in log scale [IQR] was 3.2 [2.5-3.6] for responder vs 2.7 [2.1-3.5] for non-responder, $p=0.025$. Regarding other IHC markers, no association was found with PSA response (table 23).

Table 23: Correlation between IHC markers and PSA response at 8 months.

n (%)	PSA response at 8 months (<0.2 ng/ml)	No PSA response at 8 months (≥0.2 ng/ml)	Unknown	p
AR				
AR cytoplasmic	33 (30.2)	58 (30.2)	19	0.747
AR negative	1 (9.7)	4 (2.1)	3	
AR nuclear	67 (65.0)	110 (57.3)	44	
AR weak	8 (7.8)	20 (10.4)	11	
Unknown	4	7	5	
Synaptophysin				
Synaptophysin negative	94 (86.2)	155 (80.3)	61	0.193
Synaptophysin positive	15 (13.7)	38 (19.7)	19	
Unknown	4	6	2	
CD56				
CD56 negative	98 (93.3)	159 (86.4)	68	0.071
CD56 positive	7 (6.7)	25 (13.6)	9	
Unknown	8	15	5	
Chromogranin A				
Chromogranin A negative	100 (93.5)	173 (91.5)	68	0.553
Chromogranin A positive	7 (6.5)	16 (8.5)	10	
Unknown	6	10	4	
PTEN				
PTEN > 10	4 (22.2)	7 (18.9)	1	1.000
PTEN ≤ 10	14 (77.8)	30 (81.1)	4	
Unknown	95	162	77	
p53				
p53 positive or null	46 (42.6)	66 (36.3)	25	0.284
p53 wild type	62 (57.4)	116 (63.7)	53	
Unknown	5	17	4	
Rb1				
Rb1 negative	25 (24.5)	50 (27.9)	10	0.533
Rb1 positive	77 (75.5)	129 (72.1)	63	
Unknown	11	20	9	
ERG				
ERG negative	63 (59.4)	111 (59.7)	47	0.245
ERG positive	39 (36.8)	59 (31.7)	28	
Non contributive	4 (3.8)	16 (8.6)	3	
Unknown	7	13	4	
NKX3.1				
NKX3.1 < 300	49 (49.0)	100 (55.6)	43	0.292
NKX3.1 = 300	51 (51.0)	80 (44.4)	31	
Unknown	13	19	8	
Ki67 in log scale				
Mean (IQR)	3.2 [2.5-3.6]	2.7 [2.1-3.5]	2.9 [2.3-3.6]	0.025
n (unknown)	108 (5)	179 (20)	77 (5)	
NEmk				
Negatives	83 (79.8)	122 (68.2)	53	0.087
Positives	21 (20.2)	57 (31.8)	24	
Unknown	9	20	5	
Phenotype				
Amphicrine	21 (20.6)	52 (29.9)	22	0.320
AR Luminal High	50 (49.0)	70 (40.2)	30	
AR Luminal low	30 (29.4)	48 (27.6)	19	
Double negative	1 (1.0)	1 (0.6)	1	
NEPC	0	3 (1.7)	2	
AR or NE markers missing	11	25	8	

ii. Genomic analysis cohort

None of the gene alterations were associated with the PSA response at 8 months < 0.2 ng/ml (table 24).

Table 24: Correlation between the most frequent gene alterations and the PSA response at 8 months.

n (%)	PSA response at 8 months (<0.2 ng/ml)	No PSA response at 8 months (≥0.2 ng/ml)	Unknown	p
TP53				
<i>TP53wt</i>	49 (67.1)	24 (32.9)	11	0.234
<i>TP53alt</i>	17 (54.8)	14 (45.2)	4	
<i>Unknown</i>	145	80	68	
PTEN				
<i>PTENwt</i>	56 (63.6)	32 (36.4)	15	0.931
<i>PTENalt</i>	10 (62.5)	6 (37.5)	0	
<i>Unknown</i>	145	80	68	
CDK12				
<i>CDK12wt</i>	61 (64.9)	33 (35.1)	14	0.491
<i>CDK12alt</i>	5 (50.0)	5 (50.0)	1	
<i>Unknown</i>	145	80	68	
ATM				
<i>ATMwt</i>	58 (61.7)	36 (38.3)	15	0.319
<i>ATMalt</i>	8 (80.0)	2 (20.0)	0	
<i>Unknown</i>	145	80	68	
BRCA2				
<i>BRCA2wt</i>	61 (63.5)	35 (36.5)	14	1.000
<i>BRCA2alt</i>	5 (62.5)	3 (37.5)	1	
<i>Unknown</i>	145	80	68	
BRCA1/2				
<i>BRCAwt</i>	60 (63.8)	34 (36.2)	14	1.000
<i>BRCAalt</i>	6 (60.0)	4 (40.0)	1	
<i>Unknown</i>	145	80	68	
Tumor suppressor				
<i>TSwt</i>	62 (64.6)	34 (35.4)	14	0.459
<i>TSalt</i>	4 (50.0)	4 (50.0)	1	
<i>Unknown</i>	145	80	68	
DNA repair				
<i>DNA repair wt</i>	48 (63.2)	28 (36.8)	13	0.916
<i>DNA repai alt</i>	18 (64.3)	10 (35.7)	2	
<i>Unknown</i>	145	80	68	

iii. Transcriptomic analysis cohort

Patients with no PSA response at 8 months (i.e > 0.2 ng/ml) had an overexpression of *ADH1A*, *CEACAM1* and *ACOT12* and an under expression of *MMP9*, *CD38* and *PSCA* (figure 41). Supervised clustering with Euclidean algorithm according to PSA response did not show any clear cluster (figure 42). No difference was found in OS for patients in cluster 2 vs cluster 1 (HR= 0.915, CI95% [0.587-1.426], p=0.700, figure 43). No pathway was found to be activated or suppressed according to PSA response in GSEA. In GSVA, for our custom AR signature (with overexpressed genes only) no significant difference was found (p=0.962).

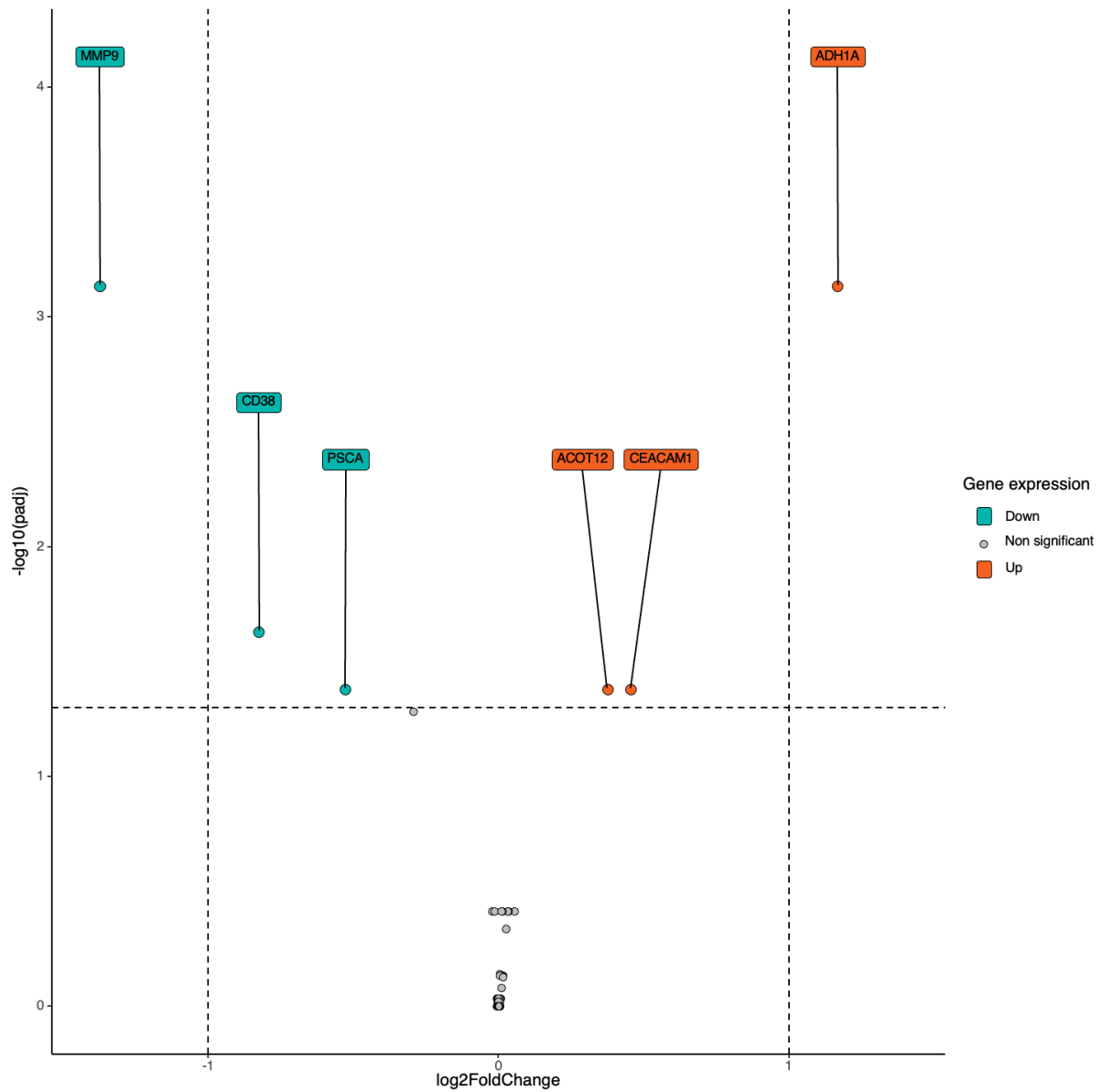


Figure 41: Volcano plot representing the differential gene expression of patients with or without PSA response at 8 months.

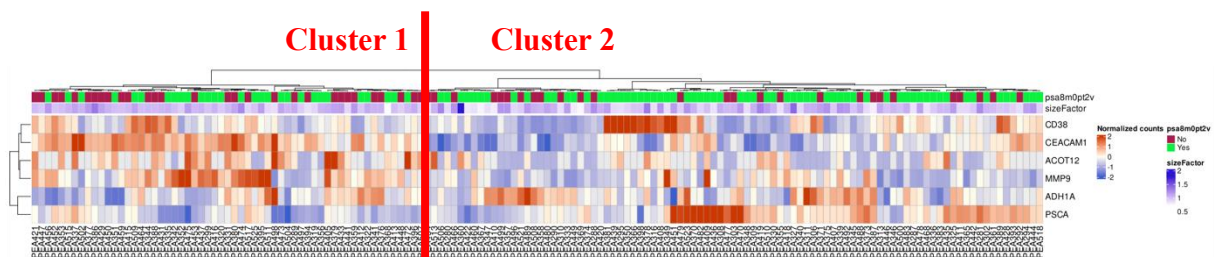


Figure 42: Supervised clustering according to tumor suppressor genes alterations (Euclidean algorithm).

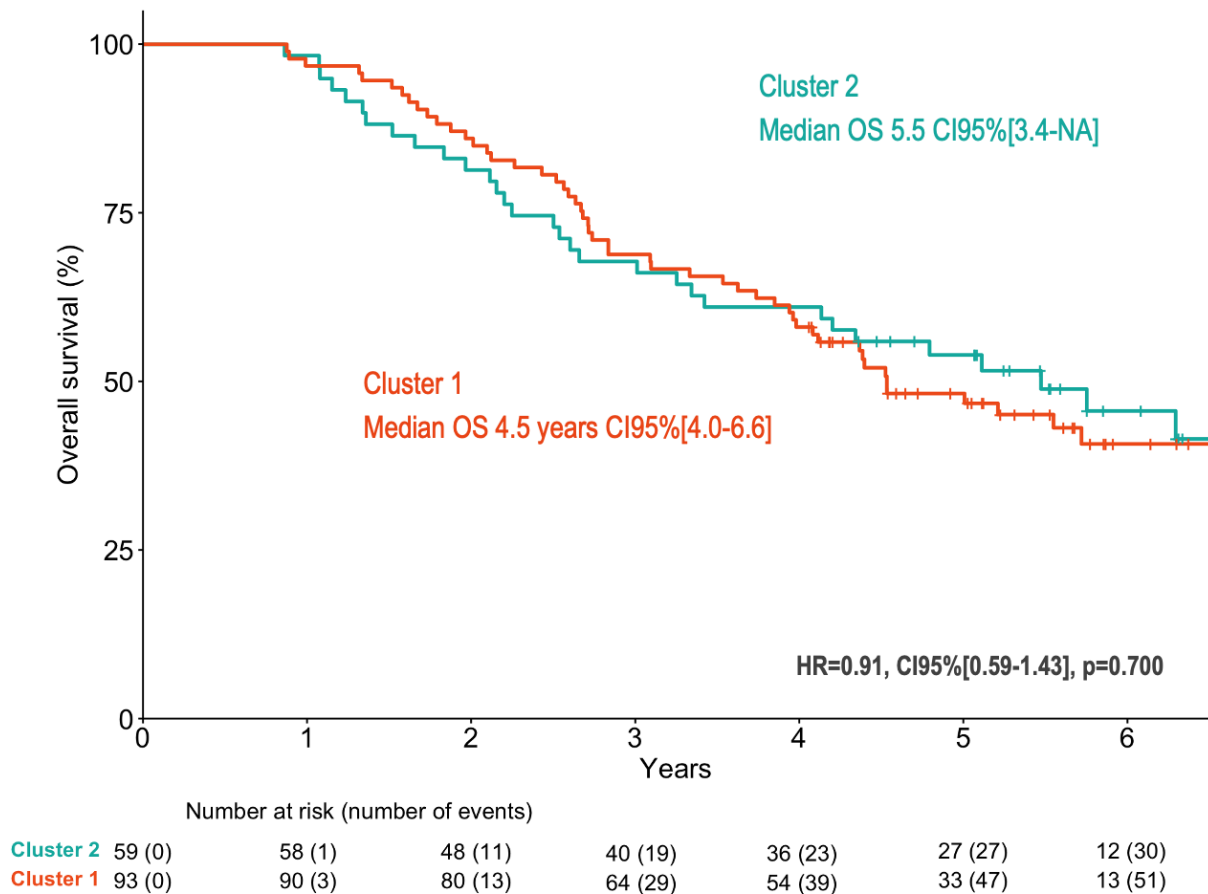


Figure 43: OS of cluster 1 and 2 from supervised clustering according to PSA response.

e. Correlation with tumoral burden

i. Phenotypic analysis cohort

Similarly, none of the IHC markers were associated with disease burden (table 25)

Table 25: Correlation between IHC markers and disease burden.

N (%)	High burden	Low burden	p
AR			
AR cytoplasmic	65 (30.5)	45 (27.3)	0.496
AR negative	6 (2.8)	2 (1.2)	
AR nuclear	123 (57.7)	98 (59.4)	
AR weak	19 (8.9)	20 (12.1)	
Unknown	8	8	
Synaptophysin			
Synaptophysin negative	172 (79.6)	138 (83.1)	0.385
Synaptophysin positive	44 (20.4)	28 (16.9)	
Unknown	5	7	
CD56			
CD56 negative	180 (87.8)	145 (90.1)	0.497
CD56 positive	25 (12.2)	16 (9.9)	
Unknown	16	12	
Chromogranin A			
Chromogranin A negative	189 (90.0)	152 (92.7)	0.364
Chromogranin A positive	21 (10.0)	12 (7.3)	
NA	11	9	
PTEN			
PTEN > 10	10 (27.0)	2 (8.7)	0.107
PTEN ≤ 10	27 (73.0)	21 (91.3)	
NA	184	150	
p53			
p53 positive or null	77 (37.4)	60 (37.0)	0.946
p53 wild type	129 (62.6)	102 (63.0)	
	15	11	
Rb1			
Rb1 negative	48 (24.1)	37 (23.9)	0.956
Rb1 positive	151 (75.9)	118 (63.0)	
NA	22	18	
ERG			
ERG negative	132 (63.8)	89 (54.6)	0.200
ERG positive	63 (30.4)	63 (38.7)	
Non contributory	12 (5.8)	11 (6.7)	
Unknown	14	10	
NKX3.1			
NKX3.1 < 300	106 (53.0)	86 (55.8)	0.594
NKX3.1 = 300	94 (47.0)	68 (44.2)	
Unknown	21	19	
Ki67 in log scale			
Mean (IQR)	2.9 [2.2;3.6]	2.8 [2.1;3.5]	0.236
n (unknown)	200 (21)	164 (9)	
NEmk			
Negatives	142 (69.6)	116 (74.4)	0.463
Positives	62 (30.4)	40 (25.6)	
Unknown	17	17	
Phenotype			
Amphicrine	55 (27.6)	40 (26.5)	0.317
AR Luminal High	81 (40.7)	69 (45.7)	
AR Luminal low	57 (28.6)	40 (26.5)	
Double negative	1 (0.5)	2 (1.3)	
NEPC	5 (2.5)	0	
AR or NE markers missing	22	22	

ii. Genomic analysis cohort

Patients with a low burden disease had more ATM mutations (80 vs 20%, p=0.023) but with a low number of patients. No other associations were found between alteration and disease burden (table 26).

Table 26: Correlation between the most frequent gene alterations and disease burden.

	High burden	Low burden	Unknown	p
TP53				
<i>TP53wt</i>	44 (52.4)	40 (47.6)	11	0.295
<i>TP53alt</i>	22 (62.9)	13 (37.1)	4	
<i>Unknown</i>	165	128	68	
PTEN				
<i>PTENwt</i>	56 (54.4)	47 (45.6)	15	0.543
<i>PTENalt</i>	10 (62.5)	6 (37.5)	0	
<i>Unknown</i>	165	128	68	
CDK12				
<i>CDK12wt</i>	59 (54.6)	49 (45.4)	14	0.753
<i>CDK12alt</i>	7 (63.6)	4 (36.4)	1	
<i>Unknown</i>	165	128	68	
ATM				
<i>ATMwt</i>	64 (58.7)	45 (41.3)	15	0.023
<i>ATMalt</i>	2 (20.0)	8 (80.0)	0	
<i>Unknown</i>	165	128	68	
BRCA2				
<i>BRCA2wt</i>	59 (53.6)	51 (46.4)	14	0.296
<i>BRCA2alt</i>	7 (77.8)	2 (22.2)	1	
<i>Unknown</i>	165	128	68	
BRCA1/2				
<i>BRCAwt</i>	58 (53.7)	50 (46.3)	14	0.342
<i>BRCAalt</i>	8 (72.7)	3 (27.3)	1	
<i>Unknown</i>	165	128	68	
Tumor suppressor				
<i>TSwt</i>	60 (54.5)	50 (45.5)	14	0.729
<i>TSalt</i>	6 (66.7)	3 (33.3)	1	
<i>Unknown</i>	165	128	68	
DNA repair				
<i>DNA repair wt</i>	51 (57.3)	38 (42.7)	13	0.486
<i>DNA repai alt</i>	15 (50.0)	15 (50.0)	2	
<i>Unknown</i>	165	128	68	

iii. Transcriptomic analysis cohort

Patients with high burden disease had an overexpression of *ADH1A*, *ARG1*, *ACOT12*, *HSD11B1*, *TTK*, *LAMC2*, *PDK1*, *MMP9*, *NUF2* and *AR*, and an under expression of *ADAM7* and *EGF* (figure 44). Supervised clustering according to disease burden did not show any clear cluster either (figure 45). No difference was found in OS for patients in cluster 2 vs cluster 1 (HR= 1.041, CI95%[0.717-1.510], p=0.800, figure 46). In high burden patients, only the xenobiotic metabolism pathway was activated (figure 47). In GSVAs, our custom AR signature (with overexpressed genes only) was significantly less expressed in high burden patients (p=0.017).

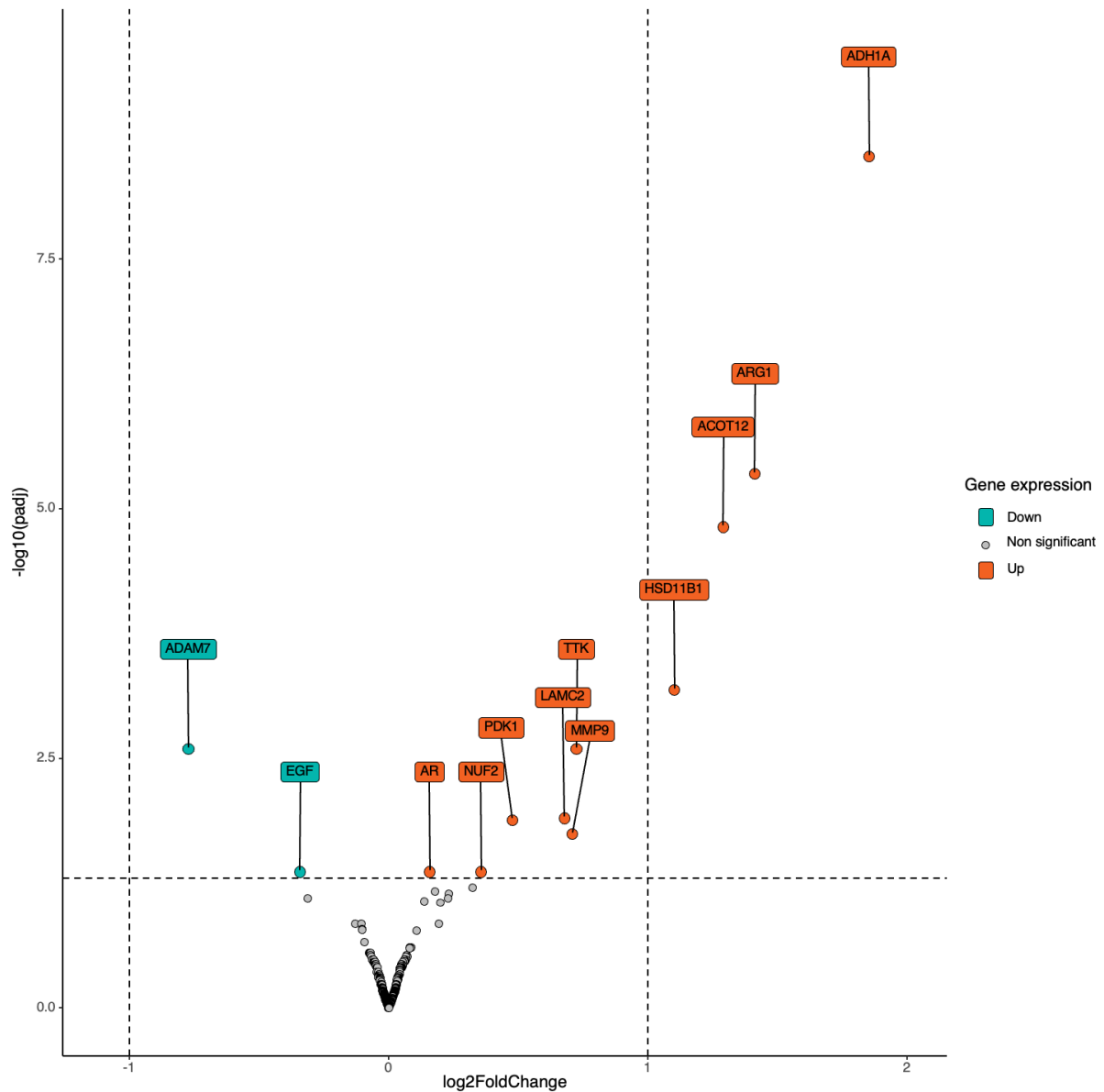


Figure 44: Volcano plot representing the differential gene expression of patients with high or low tumoral burden.

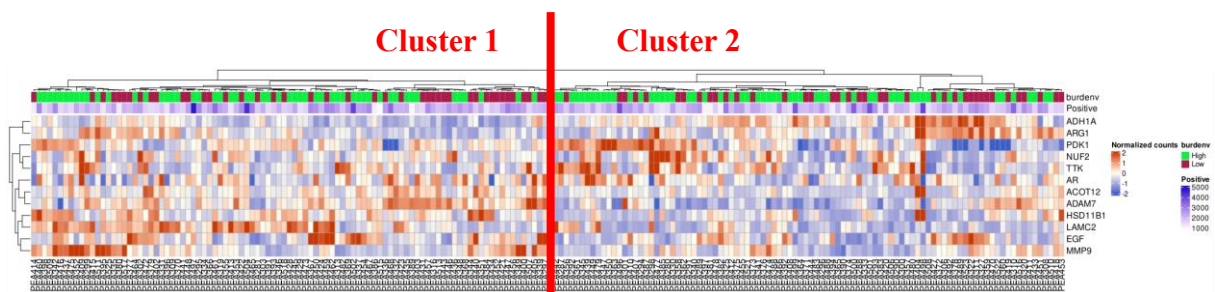


Figure 45: Supervised clustering according to tumoral burden (Euclidean algorithm).

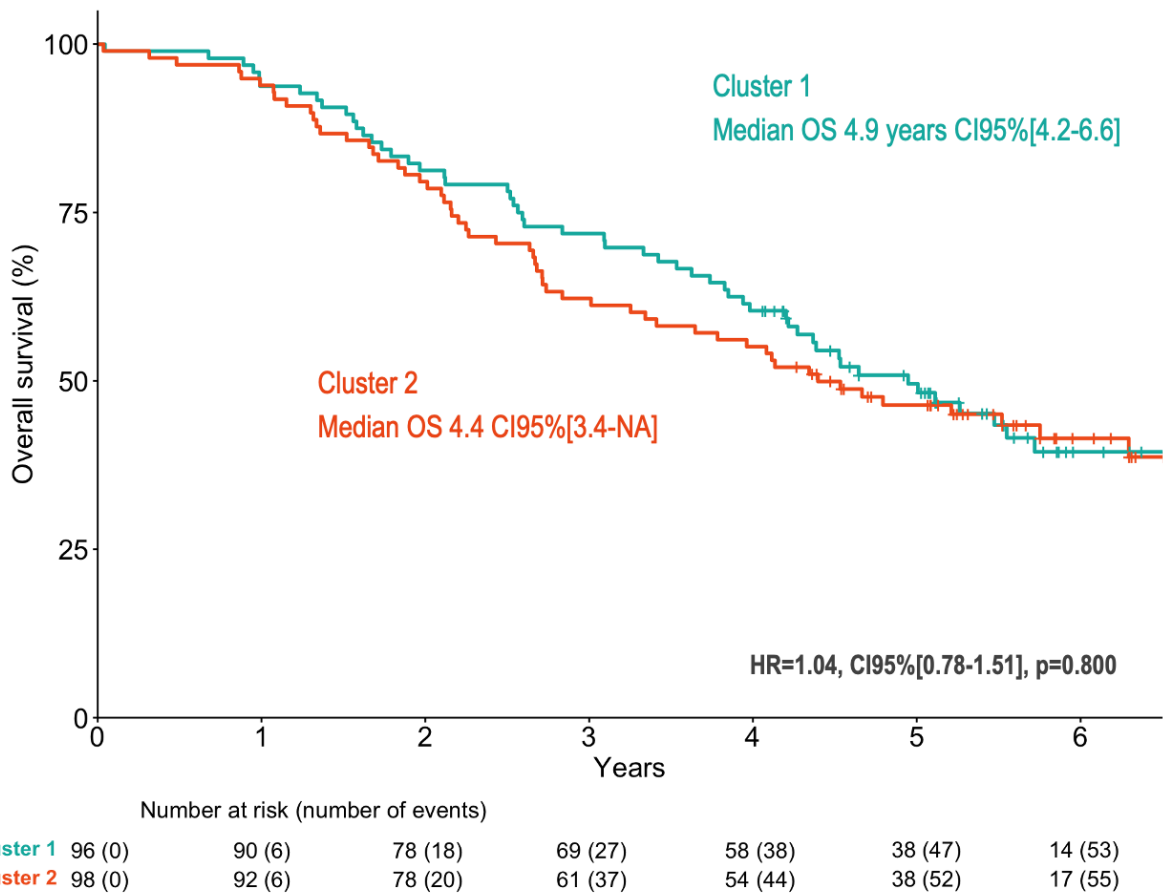


Figure 46: OS of cluster 1 and 2 from supervised clustering according to tumoral burden.

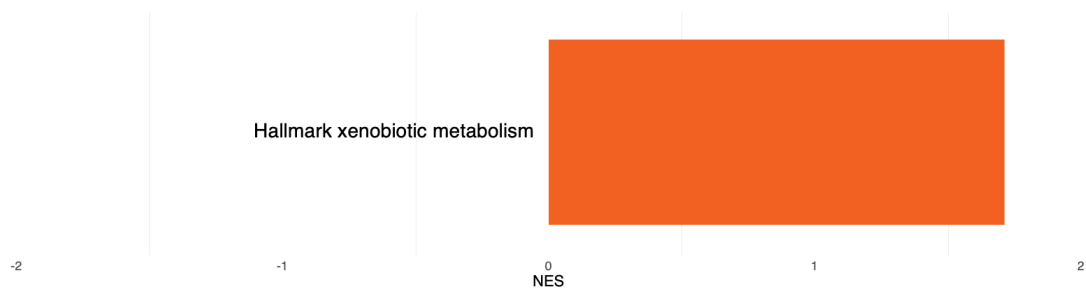


Figure 47: GSEA in high vs low burden patients.

f. Correlation between IHC and NGS

No correlation between TSwt and NEmk or NEPC phenotype in IHC was found (table 27). Among the 3 suppressor genes, only *TP53* was correlated with an abnormal p53 IHC expression (either positive or null) with 58.6% of samples abnormal in IHC harboring a *TP53* gene alteration (table 28). No correlation was found between *BRCA* alterations and NEPC markers expression in IHC nor TSwt (table 29). Other p values for correlation between IHC and NGS are displayed in table 30.

Table 27: Correlation between TSwt and NEmk or NEPC phenotypes in IHC.

	TSwt	TSalt	Unknown	p
<i>NEmk</i>				
<i>Negatives</i>	63 (94.0)	4 (6.0)	191	0.130
<i>Positives</i>	25 (83.3)	5 (16.7)	72	
<i>Unknown</i>	22	0	30	
<i>Phenotypes</i>				
<i>Amphicrine</i>	24 (85.7)	4 (14.3)	67	
<i>AR Luminal High</i>	31 (91.2)	3 (8.8)	116	
<i>AR Luminal Low</i>	29 (96.7)	1 (3.3)	67	0.100
<i>Double negative</i>	1 (100.0)	0 (0)	2	
<i>NEPC</i>	0 (0)	1 (100.0)	4	
<i>Unknown</i>	25	0	37	

TSwt: tumor suppressor wild type, TSalt: tumor suppressor altered.

Table 28: Correlation between each suppressor gene and IHC staining of the corresponding protein.

	NGS alterations			p
	<i>TP53wt</i>	<i>TP53alt</i>	<i>Unknown</i>	
<i>p53 positive or null</i>	12 (41.4)	17 (58.6)	108	<0.001
<i>p53 wild type</i>	51 (81.0)	12 (19.0)	168	
<i>Unknown</i>	21	6	17	
	<i>PTENwt</i>	<i>PTENalt</i>	<i>Unknown</i>	1.000
<i>PTEN > 10</i>	2 (100.0)	0 (0)	10	
<i>PTEN ≤ 10</i>	3 (75.0)	1 (25.0)	44	
<i>Unknown</i>	98	15	239	
	<i>RBIwt</i>	<i>RBIalt</i>	<i>Unknown</i>	0.075
<i>Rb1 negative</i>	24 (85.7)	4 (14.3)	57	
<i>Rb1 positive</i>	59 (96.7)	2 (3.3)	208	
<i>Unknown</i>	30	0	28	

Table 29: Correlation between *BRCA* alterations with NEPC markers expression and the tumor suppressor signature.

	<i>BRCAwt</i>	<i>BRCAalt</i>	<i>Unknown</i>	p
<i>NEPC IHC markers</i>				
<i>Negative</i>	60 (89.6)	7 (10.4)	191	0.720
<i>Positive</i>	28 (93.3)	2 (6.7)	72	
<i>Unknown</i>	20	2	30	
<i>Tumor suppressor (≥2/3 among TP53, PTEN and/or RBI)</i>				
<i>TSwt</i>	101 (91.8)	9 (8.2)	0	0.195
<i>TSalt</i>	7 (77.8)	2 (22.2)	0	
<i>Unknown</i>	0	0	293	

Table 30: Correlation between the most frequent alterations and IHC markers.

	<i>TP53</i>	<i>PTEN</i>	<i>CDK12</i>	<i>ATM</i>	<i>BRCA2</i>	<i>RBI</i>	Tumor suppressor genes	DNA repair alterations	<i>BRCA1 or 2</i>
<i>AR negative</i>	1	1	1	1	1	0.120	0.178	1	1
<i>Synaptophysin</i>	0.442	0.513	0.686	0.218	0.644	0.115	0.404	1	1
<i>CD56</i>	<0.001	0.418	0.686	0.129	0.236	0.182	0.017	1	0.346
<i>Chromogranin A</i>	0.755	1	0.351	0.123	1	0.029	0.094	1	1
<i>PTEN</i>	0.333	1	1	1	1	1	1	1	1
<i>p53</i>	<0.001	0.003	1	0.456	0.030	0.375	0.001	0.458	0.025
<i>Rb1</i>	0.630	1	0.703	0.454	0.374	0.075	0.703	0.454	0.703
<i>Ki67_log (Welch's t-test)</i>	0.463	0.259	0.105	0.238	0.360	0.823	0.194	0.437	0.582
<i>ERG</i>	0.498	0.550	0.715	0.309	0.691	1	0.710	0.348	1
<i>NKX3.1</i>	0.530	0.412	1	0.020	1	0.225	0.292	0.073	0.501

g. Phenotypic heterogeneity

AR and NE markers expression were heterogenous and non-exclusive. Therefore, it was difficult to distinguish a unique pattern. AR and NE markers could be either expressed on the same tumor cells area or in a different one of the same slides. When looking at survival data on few cases rPFS and OS did not seem to be linked to the staining intensity or to the proportion of tumor stained (figure 48).

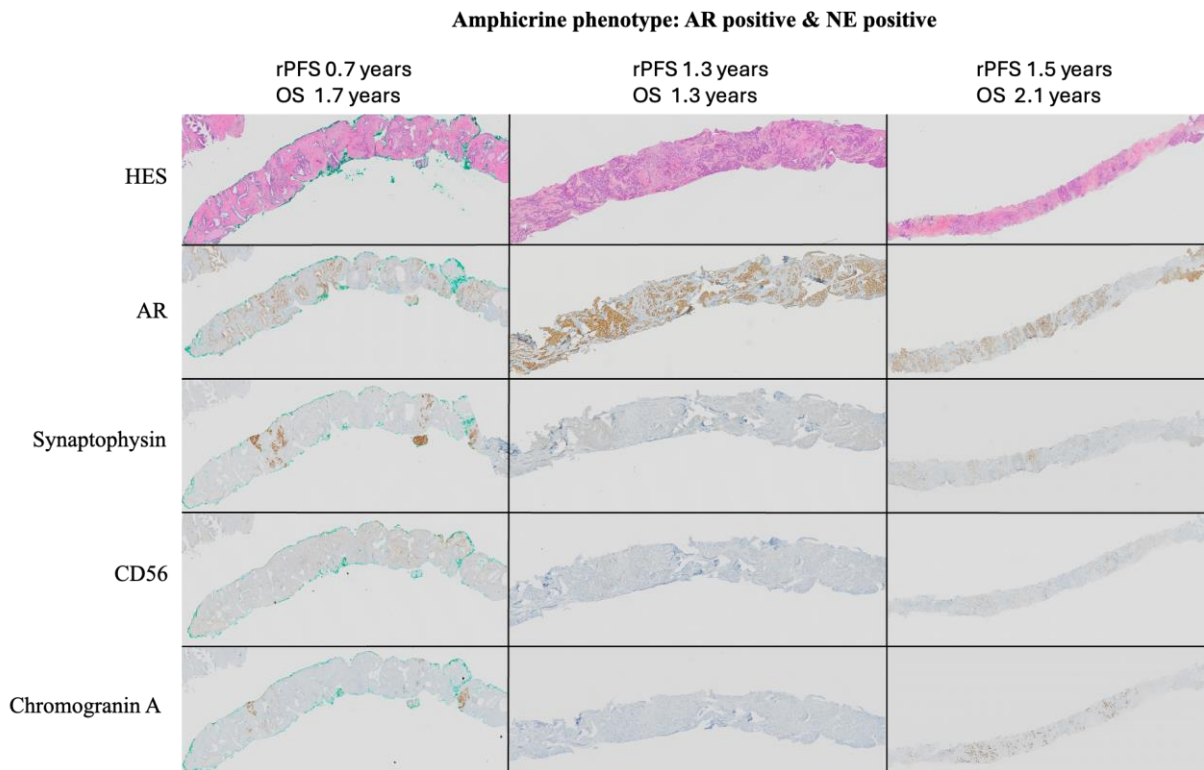
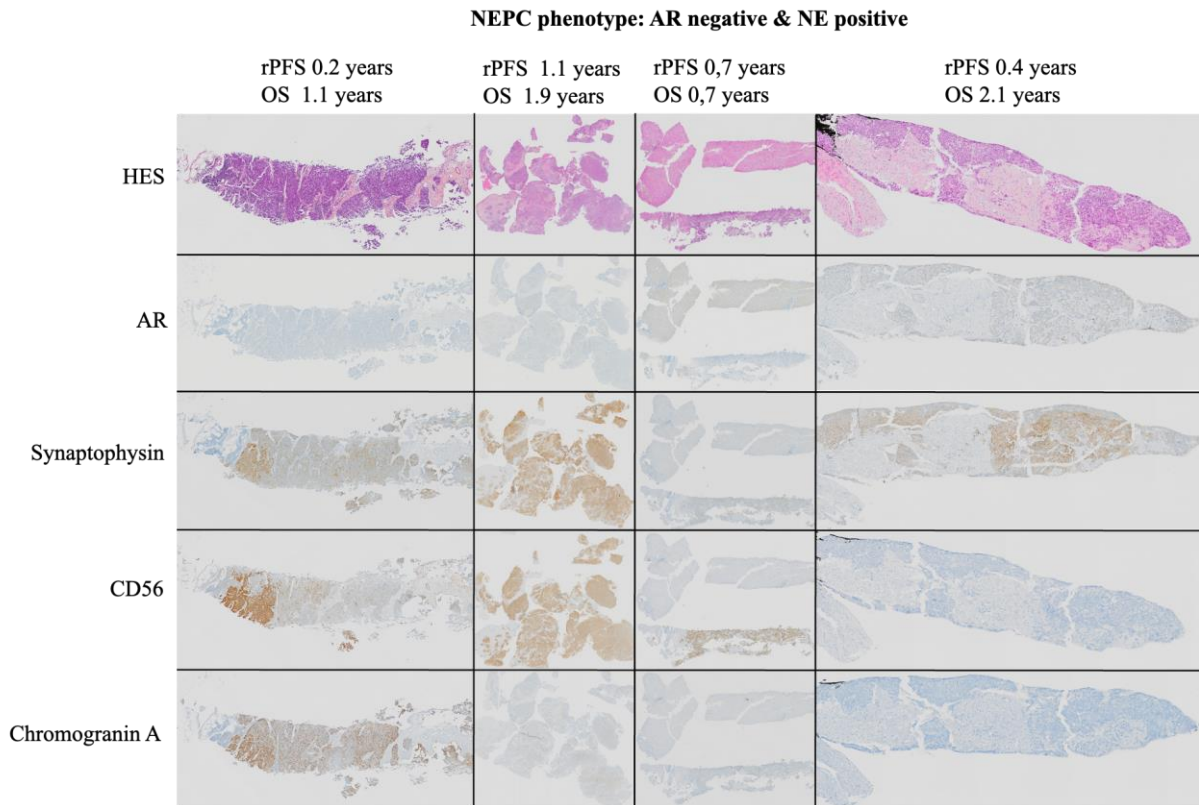


Figure 48: HES and IHC slides of NEPC and amphicrine phenotypes.

h. Comparison with local pathologist reports

Regarding our ancillary cohort, comparison of IHC on blocks centrally retrieved with local pathologist reports showed a correlation between NEMk and adenocarcinoma mixed with NE ($p < 0.001$). However, among the tumor classified as pure adenocarcinoma by local pathologist, a large number of patients ($n=90$, 23.4%) harbored at least one NE positive marker (table 31 and 32). No central pathologist histological assessment or grading for ISUP score was performed.

Table 31: Correlation between the 5 phenotypes centrally reviewed and histological subtypes from local pathologist reports.

	Amphicrine	AR Luminal High	AR Luminal Low	Double negative	NEPC	Unknown	p
<i>Adenocarcinoma</i>	87 (91.6)	144 (96.0)	90 (92.8)	3 (100)	1 (25.0)	59	
<i>Adenocarcinoma mixed with ductal</i>	0	6 (4.0)	5 (5.2)	0	0	2	
<i>Adenocarcinoma mixed with NE</i>	8 (8.4)	0	2 (2.1)	0	2 (50.0)	0	<0.001
<i>Undifferentiated</i>	0	0	0	0	1 (25.0)	0	
<i>Unknown</i>	0	0	0	0	1	1	

Table 32: Correlation between the NEPC markers centrally reviewed and histological subtypes from local pathologist reports.

	NEPC marker positive	NEPC markers negative	p
<i>Adenocarcinoma</i>	90 (23.4)	294 (76.6)	
<i>Adenocarcinoma mixed with ductal</i>	0	13 (100.0)	
<i>Adenocarcinoma mixed with NE</i>	10 (83.3)	2 (16.7)	<0.001
<i>Undifferentiated</i>	1 (100.0)	0	
<i>Unknown</i>	1	1	

4. Discussion

De novo mCSPC is poorly described and there is a need for biomarker predicting treatment response but also new prognosis markers for treatment intensification in poor responder patients.

Surprisingly, an important number of patients, about one-fourth of our IHC cohort, harbored at least one NE marker, with most of them having an amphicrine phenotype. A retrospective study on local pathologist reports from the PEACE1 full trial cohort showed a low number of patients with NE features assessed in daily practice. Among the 190 patients (17.5% of the 1172 full trial cohort) with NE features assessed, 14.0% had adenocarcinoma with NEPC differentiation and 0.5% a pure NEPC. All these 26 patients had worse outcomes compared to the other 1056 patients⁷⁹. This difference in terms of frequency highlights the underestimated number of patients with NE features at baseline in *de novo* mCSPC as common practice recommend NE staining for high Gleason grades or suspected NEPC on morphology. As there is a range of different prostate cancers from adenocarcinoma to pure small cell NE it is difficult to compare these results with previous data, but *de novo* morphological NEPC has been reported in 1 to 5% patients and IHC expression of NE markers alone is probably more frequent²⁸. A more recent retrospective study assessing initial biopsies at diagnosis in a mCRPC cohort found 9.8% of patients harboring either morphologic or IHC NE markers at baseline. This smaller proportion compared to our results could be explained by the lower number of patients having a *de novo* metastatic disease (46.8%)⁸⁰. Regarding other phenotypes, NEPC having an AR loss of expression associated were rare with only 1.3% of patients in our study. Pure NEPC were excluded from inclusion in the PEACE-1 trial explaining this low percentage. We only had 0.7% of patients with a double negative tumor probably reflecting the fact that this phenotype is mostly induced under hormone therapy. Albeit mostly defined by gene expression rather than IHC in other studies, double negative tumors were found at a higher frequency of 5.4% at mCRPC stage which was increased by ARPI introduction in 2011 at 23.3%⁸¹. The frequency of genes alterations were similar to previously published data³⁹, with less AR alterations compared to mCRPC but a close number of *BRCA* alterations (9.2% of patients in our NGS cohort vs 7.3% in MSK-IMPACT³⁹ and 9.3% in SU2-PCF³⁸). Regarding TSG, only 7.6% of patients harbored this signature. Previous analyses of the TCGA found that 9.9% mCRPC patients had the same signature⁸².

NE transdifferentiation at mCRPC stage has been extensively reported to be associated with worse outcomes and could be found in 20 to 30% of patients biopsied at this advanced stage³⁰. In our study, these NE features were also associated with a worse prognosis at an earlier mCSPC stage. If the morphological NEPC is well known for its worse prognosis, data for IHC marker independent prognosis value are controversial²⁸. NEPC are also associated with AR, ERG and NKX3.1 loss of expression²⁸. In our study we only found ERG expression among these proteins to be associated with a longer rPFS. The p53 protein abnormal expression was associated with worse rPFS, in line with data showing an association with worse outcomes for p53⁸³. A higher Ki67 was correlated to a better PSA response at 8 months, maybe reflecting the sensitivity of these tumors to docetaxel. A higher Ki67 has been reported to be of worse prognosis for localized prostate cancer only^{84,85}. NEPC found in prostatectomy have a similar Ki67 compared to adenocarcinoma⁸⁶. However, Ki67 level of expression has no effect on rPFS and OS in PEACE1 in which a large part of patients received docetaxel. A previous study reported a low Ki67 expression in foci of synaptophysin positive cells of mCRPC cancer. Perhaps proliferation of these NE cells could be activated later under treatment pressure by a “proliferative switch”⁸⁷. Growing evidence of alterations linked with NE-like or aggressive variant in these mCRPC

have been reported this last five years with the key role of the tumor suppressor genes *TP53*, *PTEN* and *RBI*⁸². In our study, the alteration of at least two of these genes was associated with a worse prognosis. Several studies have reported the combination of more or less *TP53*, *PTEN* and *RBI* genes to be associated with worse outcomes in both mCSPC and mCRPC patients^{88,89}. In our study, none of these genes were separately associated with prognosis. In the same STAMPEDE abi781 cohort, they found that *TP53* and *PTEN* assessed by transcriptomic is associated with prognosis, perhaps reflecting the same signature³⁶. Mechanistically, *TP53* and *RBI* are involved in cell cycle control and play a role in plasticity through NE differentiation. These mechanisms are initiated by *PTEN* loss of function leading ultimately to the over-expression of the epigenic regulator *EZH2* and the reprogramming transcription factor *SOX2*^{90,91}. Alterations in the DNA repair genes have previously been reported to be associated with worse prognosis mainly in mCRPC⁹² and with a slightly lower but almost similar frequency in mCSPC³⁹. Albeit, the prognosis value of *BRCA* genes is poorly reported for mCSPC⁹³ and a tendency was found in our study for worse OS of patients with *BRCA* alterations.

At a gene expression level, we adapted a 70-gene NEPC score previously reported in mCRPC NEPC but also elevated in 20% of adenocarcinomas³¹. In our cohort, a higher NEPC z-score and a lower AR z-score were associated with worse outcomes. *EZH2* involved in plasticity during NEPC transdifferentiation³⁰ was found over-expressed in non-responders patients. *DLL3*, a surface protein inhibiting the Notch signaling pathway, has been reported in mCRPC with NEPC transdifferentiation and several treatment targeting this surface protein are currently in clinical development⁹⁴. In our transcriptomic data, *DLL3* was over-expressed in both NEmk and TSalt patients. *PROX1*, a less known transcription factor inducing EMT⁹⁵, was also over-expressed in the same subgroups of patients. *SEZ6* is an emerging surface protein suspected to have neurosecretory functions expressed in SCLC and other neuroendocrine cancers⁹⁶. In our cohort it was overexpressed in NEmk patients. The transcription factor *SOX2* suspect to be involved in the differentiation process to a NE lineage³³ was found over-expressed in our study but only for TSalt patients. *AURKB* was over-expressed in non-responders and is one of the aurora kinases (A, B, and C) which regulate mitosis and meiosis, with some inhibitors of these kinase in development⁹⁷. *TOP2A* has been reported to be over-expressed concomitantly to *EZH2* in more aggressive primary and metastatic patients and overlapped with genes involved in mitotic regulation⁹⁸. In our dataset, *TOP2A* was upregulated in NEPC and TSalt patients but not *EZH2* in these subgroups. *DNMT1*, over-expressed here for these two patient subgroups, is an epigenetic regulator found to be expressed with *EZH2* as well, promoting proliferation and tumor migration. Mechanistically, *DNMT1* via cytosine methylation inhibits TRAF6 transcriptional expression and therefore the TRAF6-mediated *EZH2* ubiquitination⁹⁹. *KDM1A* also known as *LSD1* is a histone demethylase and was found over-expressed in NEPC as it was in our cohort for NEmk patients. Apart from these NE genes, some others related to metabolism were over-expressed such as *ADH1* and *ACOT12* in the more aggressive groups of patients with no PSA response at 8 months and high burden disease at diagnosis. Although, it is important to note that these proteins are expressed in normal livers, and that two patients with a worse prognosis had liver biopsy at diagnosis. *ARG1* is an enzyme involved in arginine metabolism linked to an immunosuppressive microenvironment in prostate cancer and its expression is induced by androgens^{100,101}. *HSD11B1* encode for the glucocorticoid-activating enzyme 11 β -hydroxysteroid dehydrogenase type 1 which catalyzes the 17 β -reduction of androstenedione to testosterone in peripheral tissue¹⁰². In our cohort both of them were over-expressed in non-responder and high burden patients as described in our previously reported cohort MATCH-R of mCRPC patients in non-responder¹⁰³. Although their role has been poorly

studied in prostate cancer, we could hypothesize that these enzymes would play a role in resistance to hormone therapy.

Accordingly, in GSEA, we found an AR pathway underexpression with an E2F pathway overexpression in non-responder, NEmk and TSalt patients. These findings were consistent with the NEPC transdifferentiation gene expression profile as previously described in mCRPC stages^{30,103}. Mechanistically, E2F binds to Rb1 which induce cell cycle dysregulation and tumoral proliferation¹⁰⁴. G2M checkpoint is another hallmark pathway involved in proliferation¹⁰⁵ and poorly reported in prostate cancer. It was also over-expressed in these patient's tumors, probably reflecting their proliferation potential. AR pathway independence has also been described in NEPC transdifferentiation with the loss of sensitivity for hormonal treatment as ARPIs, and *TP53/RB1* loss might an early event preceding this AR loss¹⁰⁶. A continuum has been described from AR dependent tumor to NEPC in Bluemn et al. work. However, NE features emergence did not seem to follow AR pathway loss of expression in double negative prostate cancer preclinical model⁸¹. Other studies supported that NE transdifferentiation in mCRPC arise from luminal cells⁸⁷. In our cohort of *de novo* mCSPC, almost all tumors with NEPC markers positivity restrained an AR expression in IHC but with a loss of AR pathway at a gene expression level. We can hypothesize that even before hormonal treatment some more aggressive tumors are already less dependent from the AR axis. Interestingly, this hallmark AR pathway was found under-expressed in the more aggressive *de novo* mCSPC compared to relapsing mCSPC¹⁰⁷. *MYC* drives the epigenetic reprogramming by interacting with *AR*, *EZH2* and other *PRC2* components. This pathway is associate with NEPC or worse prognosis in adenocarcinoma³³ and was found over-expressed in NEmk and TSalt patients. Other surprising pathways inactivated in TSalt patients were the immune score allograft rejection and TNFa via NFkB pathways¹⁰⁵ and could reflect an immunosuppressed environment in these tumors compared to pure adenocarcinoma, but needs further validation as it never been reported in prostate cancer.

However, none of these IHC markers or transcriptomic z-scores were predictive of abiraterone benefit, meaning that all patient benefit from this treatment. These findings are in line with previous work in the STAMPEDE abi781 cohort in which using several RNAseq signatures, no predictive biomarker for abiraterone benefit was found either³⁶.

Regarding correlation between IHC and NGS, only the p53 protein and the *TP53* gene abnormal expressions were statistically correlated but with a low number of matchings (58.0%). A previous study has found a positive predictive value of p53 nuclear accumulation to detect missense mutation of 84.0% (38/45) with a negative predictive value of 97.0% (56/58) in paraffin prostate cancer tissue¹⁰⁸. In our study, the detection of *TP53* alterations could have been limited due to the poor quality of samples available to perform NGS. A higher number of NEmk patients were TSalt as well as patients with ampicrine phenotype, and the one patient with a NEPC phenotype was TSalt. However, all the different phenotypes were found to harbor more or less this mutational signature. Even if the interpretation is limited by the low number of TSalt patients, we can hypothesize that tumor heterogeneity would lead to undetectable TS genes alterations if, for example only a low fraction of tumoral cells extracted for NGS are stained by NE markers. In our study, Rb1 protein loss of expression was not associated with *RB1* alterations. Aparicio et al. showed a moderate correlation for Rb1 between IHC and copy number with some low IHC samples having neutral Rb1 copy number, suggesting another mechanism for Rb1 protein loss. No correlation for other markers were found by the authors⁸². A more recent study on a cohort of 20 patients with mCRPC harboring treatment related NEPC show a concordance of 70.0% for RB1 and 80.0% for TP53 between IHC and NGS¹⁰⁹.

Regarding tumor heterogeneity but at a protein expression level, we had a wide range of different AR and NE staining combinations with some tumor area AR positive and NE positive. In the PEACE1 trial, only patients with adenocarcinoma and those with minor NE differentiation could be included. Pure NEPC were excluded, therefore they could not be encountered in our ancillary study. All these different situations reflect the complex tumor heterogeneity and all the transition states from adenocarcinoma to NE phenotype. It is important to note that even patients with tumor expressing a low NE H-score or with only a few tumor areas stained had a similar or even shorter rPFS and OS as tumor expressing NE markers more intensively. In a study looking at metastases biopsies in mCRPC patients, 17% of them had NE features but with heterogeneity on the same biopsy core⁸. Intra-tumoral heterogeneity in prostate cancer has been widely reported in the recent years. It has been shown with genomic clonal evolution that distant metastases originate from one clone. Moreover, heterogeneity seems to increase with disease burden, providing a rationale for earlier intensive treatment before resistance emerges. However, most of these results have been reported in mCRPC setting and data in *de novo* mCSPC and primitive tumor samples are lacking¹¹⁰.

One of the limitations of this study was the low sample quality reflecting the challenges for sequencing in daily practice. Only a few number of patients had contributive sequencing among the ones for whom DNA was extracted (43.7%). Therefore, the prognostic value of our TSalt signature is impaired giving the low number of positive patients. This could be due for some of them to the long-term storage of the samples. This low percentage is an argument in favor of performing genomic analyses at diagnosis before paraffined embedded tissue degradation happen, especially regarding the longest delay between biopsy and samples collection for patients without contributive NGS in our cohort. NE markers were more easily assessable for a larger number of samples and this assay is less costly. We chose to assess the older and therefore more published markers synaptophysin, CD56 and chromogranin A rather than the more sensitive IHC antibody INSM1 (insulinoma-associated protein 1)¹¹¹ which could be debatable. However, PTEN markers were not assessable in our study due the poor quality of antibodies available and RB1 staining was also of poor quality limiting its interpretation. In a lesser extent, CD56 was also difficult to read and could explain its non-significant association with prognosis. ERG fusion were not assessable with our NGS panels due to low RNA quantity and quality but we reported above the impact on survival of ERG expression in IHC, which was previously described as well correlated with genomic alterations¹¹². Nonetheless, both IHC and NGS could be complementary to detect NE tumoral subpopulation. Transcriptomic analysis finally required less tumoral material for analysis. However, in our cohort few patients had all of the 3-analysis performed which is another limitation.

The two theories of rather NE clones selection or adenocarcinoma transdifferentiation under treatment pressure as previously formulated are not necessarily contradictory³¹. Here we can hypothesize that our findings reflect the clonal evolution of the minor contingent of NE cells already present at diagnosis and selected later by treatments pressure, eventually evolving to resistance and a more lethal disease. A spatial transcriptomic analysis is ongoing to explore these results at a gene expression level. A longitudinal clonal evolution analysis using a NE methylation score from circulation free DNA¹¹³ at different timepoints could also help exploring this hypothesis. Other potential target for treatment, ARG1 and HSD11B1, were found but need to be confirmed in other cohorts. Regarding other phase 3 trial cohort of mCSPC patients, STAMPEDE³⁶ and CHARTEED¹¹⁴ ancillary studies had different types of transcriptomic analysis performed making them difficult to compare. If retrieving at least 2 white slides per patient from one of those cohorts to perform the same ncounter nanostring analysis seems delusional, pathomics based on more available HE(S) slides could be a

reasonable option. This analysis of our cohort for prognosis and predictive value is ongoing, in which we also aim to decipher potential NE features used for this pathomics model.

Altogether, these data confirmed at a multiple omics level our initial hypothesis that rare aggressive clones with NE features are already present at diagnosis in *de novo* mCSPC and are associated with worse prognosis. The underlying mechanisms could be a clonal selection of this tumoral subpopulation under treatment, leading to the emergence of aggressive tumor at a later stage. There is an opportunity to target these clones up front to enhance patient survival with combination therapies.

5. Perspectives

Consequently, tackle this NE differentiation up-front will probably require the combination of adenocarcinoma-targeting treatment (i.e. hormonal therapy) with a combination of innovative treatment. Platine based regimen could be an option despite low efficacy and a certain toxicity. Combination of cisplatin etoposide and doxorubicin showed an overall response rate of 61% and a PFS of 5.8 months among 36 patients with a small cell prostate cancer but 3 patients died from toxicity. In patients with aggressive variant of prostate cancer based on criteria such as visceral metastases or serum NE markers various based has been assessed in non-randomized trial with disappointing efficacy signals. Interestingly, patients with at least two alterations among *TP53*, *PTEN* and/or *RBI* had a longer PFS of 7.5 months vs 1.7 months and OS of 20.2 vs 8.5 months when treated with cabazitaxel-carboplatin vs cabazitaxel alone. Checkpoint inhibitors with or without chemotherapy are under investigation in this setting without proof of efficacy yet³³. Lurbinectedin is a new generation of chemotherapy inhibiting transcription and showed encouraging signal of activity in second line for SCLC. It is currently evaluated in randomized trial for SCLC¹¹⁵ but data are lacking to use this drug in NEPC¹¹⁶.

Apart from chemotherapy, DLL3 is a surface protein expressed in NEPC⁹⁴ with several drugs in development for these tumors but also for SCLC. Among them, the antibody drug conjugate rovalpituzumab tesirine (Rova-T) is the most advanced in terms of clinical development with a phase 2 trial showing important toxicity (63% of grade ≥ 3 mostly photosensitivity reaction and pericardial/pleural effusion) and moderate activity in SCLC even if DLL3 positive in IHC¹¹⁷. Accordingly, a first phase 3 TAHOE trial enrolling the same selected population in second line even showed a reduced OS for patients receiving Rova-T with 5 of the 64 drug related deaths, leading to the end of recruitment¹¹⁸. The MERU phase 3 trial assessed Rova-T in maintenance after first line platin-based regimen, was also stopped for futility without any benefit in OS with the same high rate of adverse events leading to discontinuation in 20% of patients¹¹⁹. Other phase 2 enrolled NEPC, with the same modest activity and profile of toxicity¹²⁰ compromising the further development of this drug even if lower doses of Rova-T combine with ICI are under investigation. More promising are the bispecific T-cell engagers such as AMG757 (Tarlatab) facilitating interactions between DLL3 on tumor cells with the activation of lymphocyte through CD3. It showed a much better tolerance profile with cytokine-release syndrome (mostly grade ≤ 2) and an interesting activity in solid tumor including NEPC in a phase 2 trial with an ORR up to 40%^{121,122}. A phase 1b for metastatic *de novo* or treatment-emergent NEPC is ongoing¹²³. BI-764532 is another bispecific T-cell engager under investigation in phase 2 trials¹²⁴. A more innovative and costly option is CAR-T-Cells, a genetically modified T-cell targeting specific antigens. AMG119 is one of them in development for DLL3¹²⁵.

CEACAM5, a member of the carcinoembryonic antigen family, is another emergent surface protein for which antibodies drug conjugate are in development. Among them SAR408701 is the most advanced with a phase 2 showing mostly corneal toxicity as adverse event and a prolonged response to treatment in SCLC with CEACAM5 expression in IHC¹²⁶. A phase 3 trial is ongoing in the same population¹²⁷. The most advanced of them is Tusamitamab ravtansine which showed in a phase 1 acceptable toxicity in various solid tumors but without any patients with a prostate cancer included in this study. In terms of efficacy, the ORR was 9.7% but 35.5% of patients had a stable disease¹²⁸. In NEPC, Labetuzumab govitecan induced DNA damage *in vitro* and antitumor response *in vivo*. However, CEACAM5 did not seem to be expressed on amphicrine mCRPC tumors, but with only 3 tumors harboring this phenotype¹²⁹. CAR-T cells against CEACAM5 are also in preclinical development¹³⁰. Another protein surface, SEZ6 was targeted by an ADC in a phase 1 showing manageable safety profile and an objective response rate of 21%¹³¹.

Inhibition of the histone methyltransferase EZH2 leads to AR expression restoration and therefore sensitivity to hormonotherapy *in vitro*⁹⁰. CPI-1205 is currently being evaluated in a phase 1/2 clinical trial for advanced solid tumors (NCT03525795) and a phase 1/2 clinical trial for metastatic castration-resistant prostate cancer (NCT03480646). As DNMT1 overexpression has been related to EZH2, the DNMT1 inhibitor Decitabine could be of interest by suppressing both DNMT1 DNA methylation and EZH2 histone methylation *in vitro*¹³². *AURKA* regulates mitosis and spindle assembly but also N-Myc by preventing its degradation³³. Alisertib is an *AURKA* inhibitor evaluated in a phase 2 trial including 75% of patients with NEPC features and showed acceptable toxicity. Two patients harboring *AURKA* and *MYC* overexpression had an interesting response with liver metastases disappearance. One of them had a *de novo* NEPC. These exceptional responders appeared to have tumoral homogeneity¹³³ meaning that other mixed tumor could benefit from combination treatment targeting adenocarcinoma.

More recent data showed that LSD1 (also known as KDM1A) a histone demethylase and therefore a gene expression regulator leading to NEPC could be a potential target³³. SP-2509 is a small molecule blocking demethylase-independent functions and suppressing mCRPC cell viability *in vitro*¹³⁴. BET proteins are gene expression regulators through the binding of acetylated histones. ZEN-3694 is a BET inhibitor leading to down-regulation of AR-signaling, AR splice variants, *MYC*, glucocorticoid receptor among other oncogenes in mCRPC *in vitro*. This inhibitor was assessed in combination with enzalutamide and showed acceptable toxicity with encouraging signals of efficacy in a phase 2 trial. The longer responses were seen in patients harboring a lower hallmark androgen response and 5 gene custom AR signature in transcriptomic¹³⁵. To note, the same under-expressed pathways were found in the non-responder, NEmk and TSalt patients of our study.

Apart from these NE targets, *BRCA 1/2* has been extensively targeted recently in practice changing trial for mCRPC with PARPi in monotherapy or combined with ARPIs¹³⁶. These drugs has yet to be approved in mCSPC setting with phase 3 randomized trial ongoing such as AMPLITUDE with niraparib or TALAPRO-3 with talazoparib¹³⁷. Nevertheless, these PARPi are compared against castration and ARPI as standard of care. Therefore, the question will remain of their benefit compared to now standard of care triplet therapy. Further mechanistic studies are needed to explore ARG1 inhibition and potentially restore the immune microenvironment antitumoral function¹³⁸. HSD11B1 is poorly described and would also need further pre-clinical investigations of its role in testosterone production and how to impair it¹³⁹.

In total, given all the upcoming therapies targeting NE differentiation in mCRPC there is a space to develop them up-front in *de novo* mCSPC patients in combination with already approved adenocarcinoma-targeting treatments. These patients should be selected based on NE features assessment at diagnostic. To that purpose, IHC seems to be the most cost-effective method. Genomic with the TSalt signature (≥ 2 genes altered among *TP53*, *PTEN* and/or *RB1*) could complement this phenotypic assay by catching up patients having NE features missed on the IHC slides, due to tumoral heterogeneity not seen on prostate biopsy for example. Transcriptomic data in our study were exploratory and need further investigation of the potential targets ARG1 and HSD11B1 in this *de novo* mCSPC population.

6. References

1. Bergengren O, Pekala KR, Matsoukas K, et al. 2022 Update on Prostate Cancer Epidemiology and Risk Factors-A Systematic Review. *Eur Urol.* 2023;84(2):191-206. doi:10.1016/j.eururo.2023.04.021
2. Prostate cancer burden in EU-27. July 1, 2021. Accessed April 8, 2024. <http://visitors-centre.jrc.ec.europa.eu/en/media/infographics/prostate-cancer-burden-eu-27>
3. Ploussard G, Fiard G, Barret E, et al. French AFU Cancer Committee Guidelines - Update 2022-2024: prostate cancer - Diagnosis and management of localised disease. *Prog Urol.* 2022;32(15):1275-1372. doi:10.1016/j.purol.2022.07.148
4. Piombino C, Oltrecolli M, Tonni E, et al. De Novo Metastatic Prostate Cancer: Are We Moving toward a Personalized Treatment? *Cancers (Basel).* 2023;15(20):4945. doi:10.3390/cancers15204945
5. Welch HG, Gorski DH, Albertsen PC. Trends in Metastatic Breast and Prostate Cancer — Lessons in Cancer Dynamics. *New England Journal of Medicine.* 2015;373(18):1685-1687. doi:10.1056/NEJMp1510443
6. Humphrey PA. Histopathology of Prostate Cancer. *Cold Spring Harb Perspect Med.* 2017;7(10):a030411. doi:10.1101/cshperspect.a030411
7. Labrecque MP, Coleman IM, Brown LG, et al. Molecular profiling stratifies diverse phenotypes of treatment-refractory metastatic castration-resistant prostate cancer. *J Clin Invest.* 2019;129(10):4492-4505. doi:10.1172/JCI128212
8. Aggarwal R, Huang J, Alumkal JJ, et al. Clinical and Genomic Characterization of Treatment-Emergent Small-Cell Neuroendocrine Prostate Cancer: A Multi-institutional Prospective Study. *J Clin Oncol.* 2018;36(24):2492-2503. doi:10.1200/JCO.2017.77.6880
9. Lonergan PE, Tindall DJ. Androgen receptor signaling in prostate cancer development and progression. *J Carcinog.* 2011;10:20. doi:10.4103/1477-3163.83937
10. Dong HY, Ding L, Zhou TR, Yan T, Li J, Liang C. FOXA1 in prostate cancer. *Asian J Androl.* 2022;25(3):287-295. doi:10.4103/aja202259
11. Wang Z, Song Y, Ye M, Dai X, Zhu X, Wei W. The diverse roles of SPOP in prostate cancer and kidney cancer. *Nat Rev Urol.* 2020;17(6):339-350. doi:10.1038/s41585-020-0314-z
12. Adamo P, Ladomery MR. The oncogene ERG: a key factor in prostate cancer. *Oncogene.* 2016;35(4):403-414. doi:10.1038/onc.2015.109
13. Tan PY, Chang CW, Chng KR, Wansa KDSA, Sung WK, Cheung E. Integration of Regulatory Networks by NKX3-1 Promotes Androgen-Dependent Prostate Cancer Survival. *Mol Cell Biol.* 2012;32(2):399-414. doi:10.1128/MCB.05958-11
14. Antao AM, Ramakrishna S, Kim KS. The Role of Nkx3.1 in Cancers and Stemness. *Int J Stem Cells.* 2021;14(2):168-179. doi:10.15283/ijsc20121
15. Morgan TM, Koreckij TD, Corey E. Targeted Therapy for Advanced Prostate Cancer: Inhibition of the PI3K/Akt/mTOR Pathway. *Curr Cancer Drug Targets.* 2009;9(2):237-249.
16. da Silva HB, Amaral EP, Nolasco EL, et al. Dissecting Major Signaling Pathways throughout the Development of Prostate Cancer. *Prostate Cancer.* 2013;2013:920612. doi:10.1155/2013/920612
17. Zhang W, van Gent DC, Incrocci L, van Weerden WM, Nonnekens J. Role of the DNA damage response in prostate cancer formation, progression and treatment. *Prostate Cancer Prostatic Dis.* 2020;23(1):24-37. doi:10.1038/s41391-019-0153-2
18. Wu YM, Cieřlik M, Lonigro RJ, et al. Inactivation of CDK12 Delineates a Distinct Immunogenic Class of Advanced Prostate Cancer. *Cell.* 2018;173(7):1770-1782.e14. doi:10.1016/j.cell.2018.04.034
19. Teroerde M, Nientiedt C, Duensing A, Hohenfellner M, Stenzinger A, Duensing S. Revisiting the Role of p53 in Prostate Cancer. In: Bott SR, Ng KL, eds. *Prostate Cancer.*

Exon Publications; 2021. Accessed April 27, 2024.

<http://www.ncbi.nlm.nih.gov/books/NBK571319/>

20. Sharma A, Yeow WS, Ertel A, et al. The retinoblastoma tumor suppressor controls androgen signaling and human prostate cancer progression. *J Clin Invest.* 2010;120(12):4478-4492. doi:10.1172/JCI44239
21. Kase AM, Iii JAC, Tan W. Novel Therapeutic Strategies for CDK4/6 Inhibitors in Metastatic Castrate-Resistant Prostate Cancer. *OncoTargets and therapy.* 2020;13:10499. doi:10.2147/OTT.S266085
22. Conteduca V, Hess J, Yamada Y, Ku SY, Beltran H. Epigenetics in prostate cancer: clinical implications. *Transl Androl Urol.* 2021;10(7):3104-3116. doi:10.21037/tau-20-1339
23. Vanacore D, Boccellino M, Rossetti S, et al. Micromas in prostate cancer: an overview. *Oncotarget.* 2017;8(30):50240-50251. doi:10.18632/oncotarget.16933
24. He Y, Xu W, Xiao YT, Huang H, Gu D, Ren S. Targeting signaling pathways in prostate cancer: mechanisms and clinical trials. *Signal Transduct Target Ther.* 2022;7(1):198. doi:10.1038/s41392-022-01042-7
25. Papanikolaou S, Vourda A, Syggelos S, Gyftopoulos K. Cell Plasticity and Prostate Cancer: The Role of Epithelial–Mesenchymal Transition in Tumor Progression, Invasion, Metastasis and Cancer Therapy Resistance. *Cancers.* 2021;13(11):2795. doi:10.3390/cancers13112795
26. Bahmad HF, Jalloul M, Azar J, et al. Tumor Microenvironment in Prostate Cancer: Toward Identification of Novel Molecular Biomarkers for Diagnosis, Prognosis, and Therapy Development. *Front Genet.* 2021;12. doi:10.3389/fgene.2021.652747
27. D’Amico AV, Whittington R, Malkowicz SB, et al. Biochemical outcome after radical prostatectomy, external beam radiation therapy, or interstitial radiation therapy for clinically localized prostate cancer. *JAMA.* 1998;280(11):969-974.
28. Abdulfatah E, Fine SW, Lotan TL, Mehra R. De novo neuroendocrine features in prostate cancer. *Hum Pathol.* 2022;127:112-122. doi:10.1016/j.humpath.2022.07.002
29. Jairath NK, Dal Pra A, Vince R, et al. A Systematic Review of the Evidence for the Decipher Genomic Classifier in Prostate Cancer. *Eur Urol.* 2021;79(3):374-383. doi:10.1016/j.eururo.2020.11.021
30. Kouroukli O, Bravou V, Giannitsas K, Tzelepi V. Tissue-Based Diagnostic Biomarkers of Aggressive Variant Prostate Cancer: A Narrative Review. *Cancers.* 2024;16(4):805. doi:10.3390/cancers16040805
31. Beltran H, Prandi D, Mosquera JM, et al. Divergent clonal evolution of castration-resistant neuroendocrine prostate cancer. *Nat Med.* 2016;22(3):298-305. doi:10.1038/nm.4045
32. Li H, Gigi L, Zhao D. CHD1, a multifaceted epigenetic remodeler in prostate cancer. *Front Oncol.* 2023;13:1123362. doi:10.3389/fonc.2023.1123362
33. Yamada Y, Beltran H. Clinical and Biological Features of Neuroendocrine Prostate Cancer. *Curr Oncol Rep.* 2021;23(2):15. doi:10.1007/s11912-020-01003-9
34. Seven-Month Prostate-Specific Antigen Is Prognostic in Metastatic Hormone-Sensitive Prostate Cancer Treated With Androgen Deprivation With or Without Docetaxel - PMC. Accessed October 23, 2024. <https://pmc.ncbi.nlm.nih.gov/articles/PMC5805480/>
35. G Gravis Mescam, Maldonado X, Roubaud G, et al. 1361MO - 8-month PSA strongly predicts outcomes of men with metastatic castration-sensitive prostate cancer in the PEACE-1 phase III trial. *Annals of Oncology (2022) 33 (suppl_7): S616-S652* 101016/annonc/annonc1070. Published online ESMO2022. <https://oncologypro.esmo.org/meeting-resources/esmo-congress-2022/8-month-psa-strongly-predicts-outcomes-of-men-with-metastatic-castration-sensitive-prostate-cancer-in-the-peace-1-phase-iii-trial>

36. Parry MA, Grist E, Mendes L, et al. Clinical testing of transcriptome-wide expression profiles in high-risk localized and metastatic prostate cancer starting androgen deprivation therapy: an ancillary study of the STAMPEDE abiraterone Phase 3 trial. *Res Sq*. Published online February 8, 2023:rs.3.rs-2488586. doi:10.21203/rs.3.rs-2488586/v1
37. Cancer Genome Atlas Research Network. The Molecular Taxonomy of Primary Prostate Cancer. *Cell*. 2015;163(4):1011-1025. doi:10.1016/j.cell.2015.10.025
38. Robinson D, Van Allen EM, Wu YM, et al. Integrative Clinical Genomics of Advanced Prostate Cancer. *Cell*. 2015;161(5):1215-1228. doi:10.1016/j.cell.2015.05.001
39. Abida W, Armenia J, Gopalan A, et al. Prospective Genomic Profiling of Prostate Cancer Across Disease States Reveals Germline and Somatic Alterations That May Affect Clinical Decision Making. *JCO Precis Oncol*. 2017;1:PO.17.00029. doi:10.1200/PO.17.00029
40. Gilson C, Ingleby F, Gilbert DC, et al. Genomic Profiles of De Novo High- and Low-Volume Metastatic Prostate Cancer: Results From a 2-Stage Feasibility and Prevalence Study in the STAMPEDE Trial. *JCO Precis Oncol*. 2020;4:882-897. doi:10.1200/PO.19.00388
41. HUGGINS C, STEVENS RE Jr, HODGES CV. STUDIES ON PROSTATIC CANCER: II. THE EFFECTS OF CASTRATION ON ADVANCED CARCINOMA OF THE PROSTATE GLAND. *Archives of Surgery*. 1941;43(2):209-223. doi:10.1001/archsurg.1941.01210140043004
42. Tannock IF, de Wit R, Berry WR, et al. Docetaxel plus prednisone or mitoxantrone plus prednisone for advanced prostate cancer. *N Engl J Med*. 2004;351(15):1502-1512. doi:10.1056/NEJMoa040720
43. Sweeney CJ, Chen YH, Carducci M, et al. Chemohormonal Therapy in Metastatic Hormone-Sensitive Prostate Cancer. *N Engl J Med*. 2015;373(8):737-746. doi:10.1056/NEJMoa1503747
44. de Bono JS, Oudard S, Ozguroglu M, et al. Prednisone plus cabazitaxel or mitoxantrone for metastatic castration-resistant prostate cancer progressing after docetaxel treatment: a randomised open-label trial. *Lancet*. 2010;376(9747):1147-1154. doi:10.1016/S0140-6736(10)61389-X
45. de Bono JS, Logothetis CJ, Molina A, et al. Abiraterone and increased survival in metastatic prostate cancer. *N Engl J Med*. 2011;364(21):1995-2005. doi:10.1056/NEJMoa1014618
46. Fizazi K, Tran N, Fein L, et al. Abiraterone plus Prednisone in Metastatic, Castration-Sensitive Prostate Cancer. *N Engl J Med*. 2017;377(4):352-360. doi:10.1056/NEJMoa1704174
47. Scher HI, Fizazi K, Saad F, et al. Increased survival with enzalutamide in prostate cancer after chemotherapy. *N Engl J Med*. 2012;367(13):1187-1197. doi:10.1056/NEJMoa1207506
48. Armstrong AJ, Szmulewitz RZ, Petrylak DP, et al. ARCHES: A Randomized, Phase III Study of Androgen Deprivation Therapy With Enzalutamide or Placebo in Men With Metastatic Hormone-Sensitive Prostate Cancer. *J Clin Oncol*. 2019;37(32):2974-2986. doi:10.1200/JCO.19.00799
49. Small EJ, Saad F, Chowdhury S, et al. Apalutamide and overall survival in non-metastatic castration-resistant prostate cancer. *Ann Oncol*. 2019;30(11):1813-1820. doi:10.1093/annonc/mdz397
50. Fizazi K, Shore N, Tammela TL, et al. Darolutamide in Nonmetastatic, Castration-Resistant Prostate Cancer. *N Engl J Med*. 2019;380(13):1235-1246. doi:10.1056/NEJMoa1815671

51. Hussain M, Fizazi K, Saad F, et al. Enzalutamide in Men with Nonmetastatic, Castration-Resistant Prostate Cancer. *N Engl J Med.* 2018;378(26):2465-2474. doi:10.1056/NEJMoa1800536
52. Chi KN, Agarwal N, Bjartell A, et al. Apalutamide for Metastatic, Castration-Sensitive Prostate Cancer. *N Engl J Med.* Published online May 31, 2019. doi:10.1056/NEJMoa1903307
53. Fizazi K, Foulon S, Carles J, et al. Abiraterone plus prednisone added to androgen deprivation therapy and docetaxel in de novo metastatic castration-sensitive prostate cancer (PEACE-1): a multicentre, open-label, randomised, phase 3 study with a 2 × 2 factorial design. *Lancet.* 2022;399(10336):1695-1707. doi:10.1016/S0140-6736(22)00367-1
54. Smith MR, Hussain M, Saad F, et al. Darolutamide and Survival in Metastatic, Hormone-Sensitive Prostate Cancer. *N Engl J Med.* 2022;386(12):1132-1142. doi:10.1056/NEJMoa2119115
55. de Bono J, Mateo J, Fizazi K, et al. Olaparib for Metastatic Castration-Resistant Prostate Cancer. *New England Journal of Medicine.* 2020;382(22):2091-2102. doi:10.1056/NEJMoa1911440
56. Chi KN, Sandhu S, Smith MR, et al. Niraparib plus abiraterone acetate with prednisone in patients with metastatic castration-resistant prostate cancer and homologous recombination repair gene alterations: second interim analysis of the randomized phase III MAGNITUDE trial☆. *Annals of Oncology.* 2023;34(9):772-782. doi:10.1016/j.annonc.2023.06.009
57. Saad F, Clarke NW, Oya M, et al. Olaparib plus abiraterone versus placebo plus abiraterone in metastatic castration-resistant prostate cancer (PROpel): final prespecified overall survival results of a randomised, double-blind, phase 3 trial. *The Lancet Oncology.* 2023;24(10):1094-1108. doi:10.1016/S1470-2045(23)00382-0
58. Agarwal N, Azad AA, Carles J, et al. Talazoparib plus enzalutamide in men with first-line metastatic castration-resistant prostate cancer (TALAPRO-2): a randomised, placebo-controlled, phase 3 trial. *The Lancet.* 2023;402(10398):291-303. doi:10.1016/S0140-6736(23)01055-3
59. Dias MP, Moser SC, Ganesan S, Jonkers J. Understanding and overcoming resistance to PARP inhibitors in cancer therapy. *Nat Rev Clin Oncol.* 2021;18(12):773-791. doi:10.1038/s41571-021-00532-x
60. Parker C., Nilsson S., Heinrich D., et al. Alpha Emitter Radium-223 and Survival in Metastatic Prostate Cancer. *New England Journal of Medicine.* 2013;369(3):213-223. doi:10.1056/NEJMoa1213755
61. Sartor Oliver, de Bono Johann, Chi Kim N., et al. Lutetium-177-PSMA-617 for Metastatic Castration-Resistant Prostate Cancer. *New England Journal of Medicine.* 2021;385(12):1091-1103. doi:10.1056/NEJMoa2107322
62. Fizazi K, Carducci M, Smith M, et al. Denosumab versus zoledronic acid for treatment of bone metastases in men with castration-resistant prostate cancer: a randomised, double-blind study. *Lancet.* 2011;377(9768):813-822. doi:10.1016/S0140-6736(10)62344-6
63. Fizazi K, Roubaud G, Bernard-Tessier A, et al. MK-5684 (ODM-208), a CYP11A1 inhibitor, in patients with metastatic castration-resistant prostate cancer (mCRPC) with and without AR-LBD mutations: CYPIDES phase 2 results. *JCO.* 2024;42(4_suppl):159-159. doi:10.1200/JCO.2024.42.4_suppl.159
64. Chandrasekar T, Yang JC, Gao AC, Evans CP. Mechanisms of resistance in castration-resistant prostate cancer (CRPC). *Transl Androl Urol.* 2015;4(3):365-380. doi:10.3978/j.issn.2223-4683.2015.05.02

65. Zang T, Taplin ME, Tamae D, et al. Testicular vs adrenal sources of hydroxy-androgens in prostate cancer. *Endocr Relat Cancer*. 2017;24(8):393-404. doi:10.1530/ERC-17-0107
66. Sekino Y, Teishima J. Molecular mechanisms of docetaxel resistance in prostate cancer. *Cancer Drug Resist*. 2020;3(4):676-685. doi:10.20517/cdr.2020.37
67. Schmidt KT, Huitema ADR, Chau CH, Figg WD. Resistance to second-generation androgen receptor antagonists in prostate cancer. *Nat Rev Urol*. 2021;18(4):209-226. doi:10.1038/s41585-021-00438-4
68. Duran GE, Wang YC, Francisco EB, et al. Mechanisms of resistance to cabazitaxel. *Mol Cancer Ther*. 2015;14(1):193-201. doi:10.1158/1535-7163.MCT-14-0155
69. Hongo H, Kosaka T, Oya M. Analysis of cabazitaxel-resistant mechanism in human castration-resistant prostate cancer. *Cancer Sci*. 2018;109(9):2937-2945. doi:10.1111/cas.13729
70. Stuparu AD, Capri JR, Meyer CAL, et al. Mechanisms of Resistance to Prostate-Specific Membrane Antigen-Targeted Radioligand Therapy in a Mouse Model of Prostate Cancer. *J Nucl Med*. 2021;62(7):989-995. doi:10.2967/jnumed.120.256263
71. Scher HI, Halabi S, Tannock I, et al. Design and End Points of Clinical Trials for Patients With Progressive Prostate Cancer and Castrate Levels of Testosterone: Recommendations of the Prostate Cancer Clinical Trials Working Group. *Journal of clinical oncology : official journal of the American Society of Clinical Oncology*. 2008;26(7):1148. doi:10.1200/JCO.2007.12.4487
72. Peterson B, George SL. Sample size requirements and length of study for testing interaction in a 2 x k factorial design when time-to-failure is the outcome [corrected]. *Control Clin Trials*. 1993;14(6):511-522. doi:10.1016/0197-2456(93)90031-8
73. Love MI, Huber W, Anders S. Moderated estimation of fold change and dispersion for RNA-seq data with DESeq2. *Genome Biol*. 2014;15(12):550. doi:10.1186/s13059-014-0550-8
74. Wu T, Hu E, Xu S, et al. clusterProfiler 4.0: A universal enrichment tool for interpreting omics data. *The Innovation*. 2021;2(3):100141. doi:10.1016/j.xinn.2021.100141
75. Yu G, Wang LG, Yan GR, He QY. DOSE: an R/Bioconductor package for disease ontology semantic and enrichment analysis. *Bioinformatics*. 2015;31(4):608-609. doi:10.1093/bioinformatics/btu684
76. Hänzelmann S, Castelo R, Guinney J. GSEA: gene set variation analysis for microarray and RNA-seq data. *BMC Bioinformatics*. 2013;14:7. doi:10.1186/1471-2105-14-7
77. Hornik K, Feinerer I, Kober M, Buchta C. Spherical k-Means Clustering. *Journal of Statistical Software*. 2012;50:1-22. doi:10.18637/jss.v050.i10
78. Benjamini Y, Hochberg Y. Controlling the False Discovery Rate: A Practical and Powerful Approach to Multiple Testing. *Journal of the Royal Statistical Society Series B (Methodological)*. 1995;57(1):289-300.
79. Bernard-Tessier A, Cancel M, Tombal B, et al. 1421P - Effect of abiraterone-prednisone in metastatic castration-sensitive prostate cancer (mCSPC) with neuroendocrine and very high-risk features in the PEACE-1 trial. *Annals of Oncology (2022) 33 (suppl_7): S616-S652 101016/annonc/annonc1070*. <https://oncologypro.esmo.org/meeting-resources/esmo-congress-2022/effect-of-abiraterone-prednisone-in-metastatic-castration-sensitive-prostate-cancer-mcspc-with-neuroendocrine-and-very-high-risk-features-in-the>
80. Farinea G, Calabrese M, Carfi F, et al. Impact of Neuroendocrine Differentiation (NED) on Enzalutamide and Abiraterone Efficacy in Metastatic Castration-Resistant Prostate Cancer (mCRPC): A Retrospective Analysis. *Cells*. 2024;13(16):1396. doi:10.3390/cells13161396

81. Bluemn EG, Coleman IM, Lucas JM, et al. Androgen Receptor Pathway-Independent Prostate Cancer Is Sustained through FGF Signaling. *Cancer Cell*. 2017;32(4):474-489.e6. doi:10.1016/j.ccell.2017.09.003
82. Aparicio AM, Shen L, Tapia ELN, et al. Combined Tumor Suppressor Defects Characterize Clinically Defined Aggressive Variant Prostate Cancers. *Clin Cancer Res*. 2016;22(6):1520-1530. doi:10.1158/1078-0432.CCR-15-1259
83. Gesztes W, Lap C, Dalivand M, et al. Evaluating p53 nuclear expression and prostate cancer progression in a predominantly African American cohort. *JCO*. 2023;41(6_suppl):217-217. doi:10.1200/JCO.2023.41.6_suppl.217
84. Berney DM, Gopalan A, Kudahetti S, et al. Ki-67 and outcome in clinically localised prostate cancer: analysis of conservatively treated prostate cancer patients from the Trans-Atlantic Prostate Group study. *Br J Cancer*. 2009;100(6):888-893. doi:10.1038/sj.bjc.6604951
85. Kammerer-Jacquet SF, Ahmad A, Møller H, et al. Ki-67 is an independent predictor of prostate cancer death in routine needle biopsy samples: proving utility for routine assessments. *Modern pathology : an official journal of the United States and Canadian Academy of Pathology, Inc*. 2019;32(9):1303. doi:10.1038/s41379-019-0268-y
86. Bubendorf L, Sauter G, Moch H, et al. Ki67 labelling index: an independent predictor of progression in prostate cancer treated by radical prostatectomy. *J Pathol*. 1996;178(4):437-441. doi:10.1002/(SICI)1096-9896(199604)178:4<437::AID-PATH484>3.0.CO;2-4
87. Zou M, Toivanen R, Mitrofanova A, et al. Transdifferentiation as a Mechanism of Treatment Resistance in a Mouse Model of Castration-Resistant Prostate Cancer. *Cancer Discov*. 2017;7(7):736-749. doi:10.1158/2159-8290.CD-16-1174
88. Hamid AA, Gray KP, Shaw G, et al. Compound Genomic Alterations of TP53, PTEN, and RB1 Tumor Suppressors in Localized and Metastatic Prostate Cancer. *Eur Urol*. 2019;76(1):89-97. doi:10.1016/j.eururo.2018.11.045
89. Velez MG, Kosiorek HE, Egan JB, et al. Differential impact of tumor suppressor gene (TP53, PTEN, RB1) alterations and treatment outcomes in metastatic, hormone-sensitive prostate cancer. *Prostate Cancer Prostatic Dis*. 2022;25(3):479-483. doi:10.1038/s41391-021-00430-4
90. Ku SY, Rosario S, Wang Y, et al. Rb1 and Trp53 cooperate to suppress prostate cancer lineage plasticity, metastasis, and antiandrogen resistance. *Science*. 2017;355(6320):78-83. doi:10.1126/science.aah4199
91. Mu P, Zhang Z, Benelli M, et al. SOX2 promotes lineage plasticity and antiandrogen resistance in TP53- and RB1-deficient prostate cancer. *Science*. 2017;355(6320):84-88. doi:10.1126/science.aah4307
92. Fettke H, Dai C, Kwan EM, et al. BRCA-deficient metastatic prostate cancer has an adverse prognosis and distinct genomic phenotype. *eBioMedicine*. 2023;95. doi:10.1016/j.ebiom.2023.104738
93. Blas L, Shiota M, Eto M. Current status and future perspective on the management of metastatic castration-sensitive prostate cancer. *Cancer Treatment and Research Communications*. 2022;32:100606. doi:10.1016/j.ctarc.2022.100606
94. Ajkunic A, Sayar E, Roudier MP, et al. Assessment of TROP2, CEACAM5 and DLL3 in metastatic prostate cancer: Expression landscape and molecular correlates. *npj Precis Onc*. 2024;8(1):1-9. doi:10.1038/s41698-024-00599-6
95. Papanikolaou S, Vourda A, Syggelos S, Gyftopoulos K. Cell Plasticity and Prostate Cancer: The Role of Epithelial–Mesenchymal Transition in Tumor Progression, Invasion, Metastasis and Cancer Therapy Resistance. *Cancers*. 2021;13(11):2795. doi:10.3390/cancers13112795

96. Marks JA, Sweeney K, Elliott A, et al. P3.13D.11 SEZ6 Expression in Neuroendocrine Tumors. *Journal of Thoracic Oncology*. 2024;19(10, Supplement):S364. doi:10.1016/j.jtho.2024.09.656
97. Kovacs AH, Zhao D, Hou J. Aurora B Inhibitors as Cancer Therapeutics. *Molecules*. 2023;28(8):3385. doi:10.3390/molecules28083385
98. Labbé DP, Sweeney CJ, Brown M, et al. TOP2A and EZH2 Provide Early Detection of an Aggressive Prostate Cancer Subgroup. *Clin Cancer Res*. 2017;23(22):7072-7083. doi:10.1158/1078-0432.CCR-17-0413
99. Li Z, Li B, Yu H, et al. DNMT1-mediated epigenetic silencing of TRAF6 promotes prostate cancer tumorigenesis and metastasis by enhancing EZH2 stability. *Oncogene*. 2022;41(33):3991-4002. doi:10.1038/s41388-022-02404-9
100. Gannon PO, Godin-Ethier J, Hassler M, et al. Androgen-Regulated Expression of Arginase 1, Arginase 2 and Interleukin-8 in Human Prostate Cancer. *PLoS ONE*. 2010;5(8):e12107. doi:10.1371/journal.pone.0012107
101. Matos A, Carvalho M, Bicho M, Ribeiro R. Arginine and Arginases Modulate Metabolism, Tumor Microenvironment and Prostate Cancer Progression. *Nutrients*. 2021;13(12):4503. doi:10.3390/nu13124503
102. Oestlund I, Snoep J, Schiffer L, Wabitsch M, Arlt W, Storbeck KH. The glucocorticoid-activating enzyme 11 β -hydroxysteroid dehydrogenase type 1 catalyzes the activation of testosterone. *The Journal of Steroid Biochemistry and Molecular Biology*. 2024;236:106436. doi:10.1016/j.jsbmb.2023.106436
103. Menssoury N, Poiraudau L, Helissey C, et al. Genomic profiling of metastatic castration-resistant prostate cancer samples resistant to androgen-receptor pathway inhibitors. *Clin Cancer Res*. Published online June 26, 2023:CCR-22-3736. doi:10.1158/1078-0432.CCR-22-3736
104. Müller H, Helin K. The E2F transcription factors: key regulators of cell proliferation. *Biochimica et Biophysica Acta (BBA) - Reviews on Cancer*. 2000;1470(1):M1-M12. doi:10.1016/S0304-419X(99)00030-X
105. Liberzon A, Birger C, Thorvaldsdóttir H, Ghandi M, Mesirov JP, Tamayo P. The Molecular Signatures Database (MSigDB) hallmark gene set collection. *Cell systems*. 2015;1(6):417. doi:10.1016/j.cels.2015.12.004
106. Formaggio N, Rubin MA, Theurillat JP. Loss and revival of androgen receptor signaling in advanced prostate cancer. *Oncogene*. 2021;40(7):1205-1216. doi:10.1038/s41388-020-01598-0
107. Sutura PA, Shetty AC, Hakansson A, et al. Transcriptomic and clinical heterogeneity of metastatic disease timing within metastatic castration-sensitive prostate cancer. *Annals of Oncology*. 2023;34(7):605-614. doi:10.1016/j.annonc.2023.04.515
108. Guedes LB, Almutairi F, Haffner MC, et al. Analytic, Preanalytic, and Clinical Validation of p53 IHC for Detection of TP53 Missense Mutation in Prostate Cancer. *Clin Cancer Res*. 2017;23(16):4693-4703. doi:10.1158/1078-0432.CCR-17-0257
109. Ueki H, Jimbo N, Terakawa T, et al. Evaluating RB1 and p53 as diagnostic markers in treatment-related neuroendocrine prostate cancer through immunohistochemistry and genomic analysis of RB1 and TP53. *Prostate*. Published online September 15, 2024. doi:10.1002/pros.24791
110. Haffner MC, Zwart W, Roudier MP, et al. Genomic and phenotypic heterogeneity in prostate cancer. *Nat Rev Urol*. 2021;18(2):79-92. doi:10.1038/s41585-020-00400-w
111. Xin Z, Zhang Y, Jiang Z, et al. Insulinoma-associated protein 1 is a novel sensitive and specific marker for small cell carcinoma of the prostate. *Hum Pathol*. 2018;79:151-159. doi:10.1016/j.humphath.2018.05.014

112. Park K, Tomlins SA, Mudaliar KM, et al. Antibody-based detection of ERG rearrangement-positive prostate cancer. *Neoplasia*. 2010;12(7):590-598. doi:10.1593/neo.10726
113. Franceschini GM, Quaini O, Mizuno K, et al. Noninvasive Detection of Neuroendocrine Prostate Cancer through Targeted Cell-free DNA Methylation. *Cancer Discov*. 2024;14(3):424-445. doi:10.1158/2159-8290.CD-23-0754
114. Hamid AA, Huang HC, Wang V, et al. Transcriptional profiling of primary prostate tumor in metastatic hormone-sensitive prostate cancer and association with clinical outcomes: correlative analysis of the E3805 CHARTED trial. *Ann Oncol*. 2021;32(9):1157-1166. doi:10.1016/j.annonc.2021.06.003
115. Besse B, Paz-Ares LG, Peters S, et al. A phase III study of lurbinectedin alone or in combination with irinotecan vs investigator's choice (topotecan or irinotecan) in patients with relapsed small cell lung cancer (SCLC; LAGOON trial). *JCO*. 2023;41(16_suppl):TPS8613-TPS8613. doi:10.1200/JCO.2023.41.16_suppl.TPS8613
116. Meyer H, Sunkara R, Rothmann E, et al. The Use of Lurbinectedin for the Treatment of Small Cell and Neuroendocrine Carcinoma of the Prostate. *Clin Genitourin Cancer*. 2024;22(5):102172. doi:10.1016/j.clgc.2024.102172
117. Morgensztern D, Besse B, Greillier L, et al. Efficacy and Safety of Rovalpituzumab Tesirine in Third-Line and Beyond Patients with DLL3-Expressing, Relapsed/Refractory Small-Cell Lung Cancer: Results From the Phase II TRINITY Study. *Clinical Cancer Research*. 2019;25(23):6958-6966. doi:10.1158/1078-0432.CCR-19-1133
118. Blackhall F, Jao K, Greillier L, et al. Efficacy and Safety of Rovalpituzumab Tesirine Compared With Topotecan as Second-Line Therapy in DLL3-High SCLC: Results From the Phase 3 TAHOE Study. *J Thorac Oncol*. 2021;16(9):1547-1558. doi:10.1016/j.jtho.2021.02.009
119. Johnson ML, Zvirbule Z, Laktionov K, et al. Rovalpituzumab Tesirine as a Maintenance Therapy After First-Line Platinum-Based Chemotherapy in Patients With Extensive-Stage-SCLC: Results From the Phase 3 MERU Study. *J Thorac Oncol*. 2021;16(9):1570-1581. doi:10.1016/j.jtho.2021.03.012
120. Mansfield AS, Hong DS, Hann CL, et al. A phase I/II study of rovalpituzumab tesirine in delta-like 3—expressing advanced solid tumors. *NPJ Precision Oncology*. 2021;5:74. doi:10.1038/s41698-021-00214-y
121. Ahn MJ, Cho BC, Felip E, et al. Tarlatamab for Patients with Previously Treated Small-Cell Lung Cancer. *New England Journal of Medicine*. 2023;389(22):2063-2075. doi:10.1056/NEJMoa2307980
122. Malhotra J, Nikolinakos P, Leal T, et al. A Phase 1–2 Study of Rovalpituzumab Tesirine in Combination With Nivolumab Plus or Minus Ipilimumab in Patients With Previously Treated Extensive-Stage SCLC. *Journal of Thoracic Oncology*. 2021;16(9):1559-1569. doi:10.1016/j.jtho.2021.02.022
123. Aggarwal RR, Aparicio A, Heidenreich A, et al. Phase 1b study of AMG 757, a half-life extended bispecific T-cell engager (HLE BiTE immune-oncology therapy) targeting DLL3, in de novo or treatment emergent neuroendocrine prostate cancer (NEPC). *JCO*. 2021;39(15_suppl):TPS5100-TPS5100. doi:10.1200/JCO.2021.39.15_suppl.TPS5100
124. First-in-human dose-escalation trial of BI 764532, a delta-like ligand 3 (DLL3)/CD3 IgG-like T-cell engager in patients (pts) with DLL3-positive (DLL3+) small-cell lung cancer (SCLC) and neuroendocrine carcinoma (NEC). | *Journal of Clinical Oncology*. Accessed October 24, 2024. https://ascopubs.org/doi/10.1200/JCO.2023.41.16_suppl.8502
125. Byers LA, Chiappori A, Smit MAD. Phase 1 study of AMG 119, a chimeric antigen receptor (CAR) T cell therapy targeting DLL3, in patients with relapsed/refractory small cell

- lung cancer (SCLC). *JCO*. 2019;37(15_suppl):TPS8576-TPS8576. doi:10.1200/JCO.2019.37.15_suppl.TPS8576
126. Ricordel C, Barlesi F, Cousin S, et al. Safety and efficacy of tusamitamab ravtansine (SAR408701) in long-term treated patients with nonsquamous non–small cell lung cancer (NSQ NSCLC) expressing carcinoembryonic antigen-related cell adhesion molecule 5 (CEACAM5). *JCO*. 2022;40(16_suppl):9039-9039. doi:10.1200/JCO.2022.40.16_suppl.9039
127. Johnson ML, Chadjaa M, Yoruk S, Besse B. Phase III trial comparing antibody-drug conjugate (ADC) SAR408701 with docetaxel in patients with metastatic non-squamous non-small cell lung cancer (NSQ NSCLC) failing chemotherapy and immunotherapy. *JCO*. 2020;38(15_suppl):TPS9625-TPS9625. doi:10.1200/JCO.2020.38.15_suppl.TPS9625
128. Gazzah A, Bedard PL, Hierro C, et al. Safety, pharmacokinetics, and antitumor activity of the anti-CEACAM5-DM4 antibody–drug conjugate tusamitamab ravtansine (SAR408701) in patients with advanced solid tumors: first-in-human dose-escalation study. *Annals of Oncology*. 2022;33(4):416-425. doi:10.1016/j.annonc.2021.12.012
129. DeLucia DC, Cardillo TM, Ang L, et al. Regulation of CEACAM5 and Therapeutic Efficacy of an Anti-CEACAM5-SN38 Antibody-drug Conjugate in Neuroendocrine Prostate Cancer. *Clin Cancer Res*. 2021;27(3):759-774. doi:10.1158/1078-0432.CCR-20-3396
130. Baek DS, Kim YJ, Vergara S, et al. A highly-specific fully-human antibody and CAR-T cells targeting CD66e/CEACAM5 are cytotoxic for CD66e-expressing cancer cells in vitro and in vivo. *Cancer Lett*. 2022;525:97-107. doi:10.1016/j.canlet.2021.10.041
131. Chandana SR, Choudhury NJ, Dowlati A, et al. First-in-human study of ABBV-706, a seizure-related homolog protein 6 (SEZ6)–targeting antibody-drug conjugate (ADC), in patients (pts) with advanced solid tumors. *JCO*. 2024;42(16_suppl):3001-3001. doi:10.1200/JCO.2024.42.16_suppl.3001
132. Li Z, Li B, Yu H, et al. DNMT1-mediated epigenetic silencing of TRAF6 promotes prostate cancer tumorigenesis and metastasis by enhancing EZH2 stability. *Oncogene*. 2022;41(33):3991-4002. doi:10.1038/s41388-022-02404-9
133. Beltran H, Oromendia C, Danila DC, et al. A Phase II Trial of the Aurora Kinase A Inhibitor Alisertib for Patients with Castration-resistant and Neuroendocrine Prostate Cancer: Efficacy and Biomarkers. *Clin Cancer Res*. 2019;25(1):43-51. doi:10.1158/1078-0432.CCR-18-1912
134. Sehrawat A, Gao L, Wang Y, et al. LSD1 activates a lethal prostate cancer gene network independently of its demethylase function. *Proceedings of the National Academy of Sciences of the United States of America*. 2018;115(18):E4179. doi:10.1073/pnas.1719168115
135. Aggarwal R, Schweizer MT, Nanus DM, et al. A Phase 1b/2a Study of the Pan-BET Bromodomain Inhibitor ZEN-3694 in Combination with Enzalutamide in Patients with Metastatic Castration Resistant Prostate Cancer. *Clinical cancer research : an official journal of the American Association for Cancer Research*. 2020;26(20):5338. doi:10.1158/1078-0432.CCR-20-1707
136. Taylor AK, Kosoff D, Enamekhoo H, Lang JM, Kyriakopoulos CE. PARP inhibitors in metastatic prostate cancer. *Front Oncol*. 2023;13. doi:10.3389/fonc.2023.1159557
137. Mittal A, Sridhar SS, Ong M, Jiang DM. Triplet Therapy in Metastatic Castrate Sensitive Prostate Cancer (mCSPC)—A Potential New Standard of Care. *Current Oncology*. 2023;30(4):4365. doi:10.3390/curroncol30040332
138. Matos A, Carvalho M, Bicho M, Ribeiro R. Arginine and Arginases Modulate Metabolism, Tumor Microenvironment and Prostate Cancer Progression. *Nutrients*. 2021;13(12):4503. doi:10.3390/nu13124503
139. Oestlund I, Snoep J, Schiffer L, Wabitsch M, Arlt W, Storbeck KH. The glucocorticoid-activating enzyme 11 β -hydroxysteroid dehydrogenase type 1 catalyzes the

activation of testosterone. *J Steroid Biochem Mol Biol.* 2024;236:106436.
doi:10.1016/j.jsbmb.2023.106436

Annex 1: Proteomics and mitochondrial metabolism in mCRPC MATCH-R cohort

Apart from the PEACE1 cohort, we performed exploratory retrospective proteomics analysis on the MATCH-R cohort. Our aim was to use a training set for further analysis on the PEACE1 blood samples.

1. Materials and methods

a. Patients and samples

We retrieved baseline serum from 54 patients of the MATCH-R cohort treated with androgen receptor pathway inhibitors (ARPI, i.e. abiraterone acetate or enzalutamide) with previous immunochemistry, whole exom sequencing and RNA sequencing performed¹. Among them, 14 patients had serum samples at progression for secondary resistance characterization (progression had to occur at least 4 months after starting the treatment to avoid primary resistance samples).

b. Olink assay

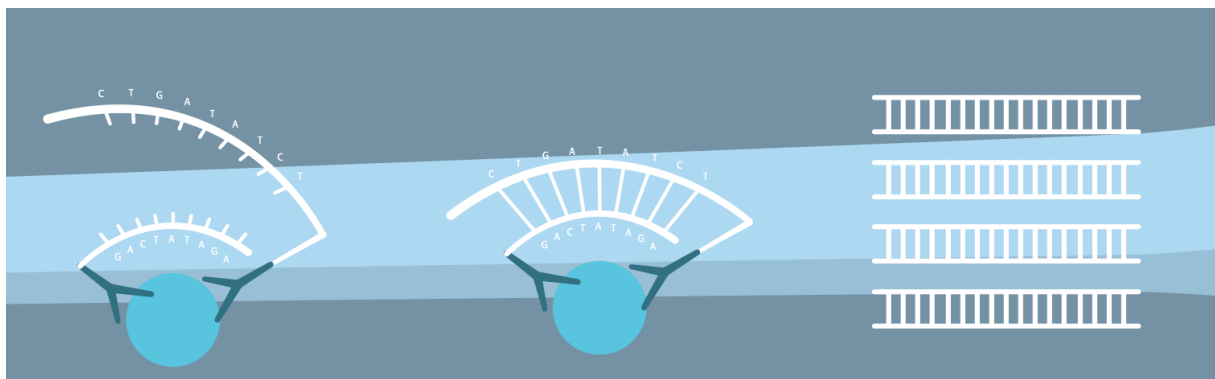
i. Samples preparation

I added 40µL of each sample in temperature-resistant, non-protein binding plastics in a PCR-clean 96-well PCR-plate. Their position on the plate were randomized using the Olink Plate Randomizer from the OlinkAnalyze R package in the order ready to be run. Each well was separately sealed using an adhesive film or individual seals. The 12th was left empty for controls.

ii. Olink platform analyses

The plate was then shipped on dry ice to olink platform for protein measurement using a High-throughput protein biomarker discovery platform based on Olink's Proximity Extension Assay (PEA) technology coupled with NGS readout on Illumina instruments. I selected the Olink® Explore 3072 library consisting of ~3000 protein assays including:

- Low-abundant inflammation proteins
- Proteins actively secreted into blood circulation
- Approved and ongoing drug target proteins
- Organ-specific proteins that have leaked into blood circulation
- Proteins representing more exploratory potential biomarkers



c. Elisa assay

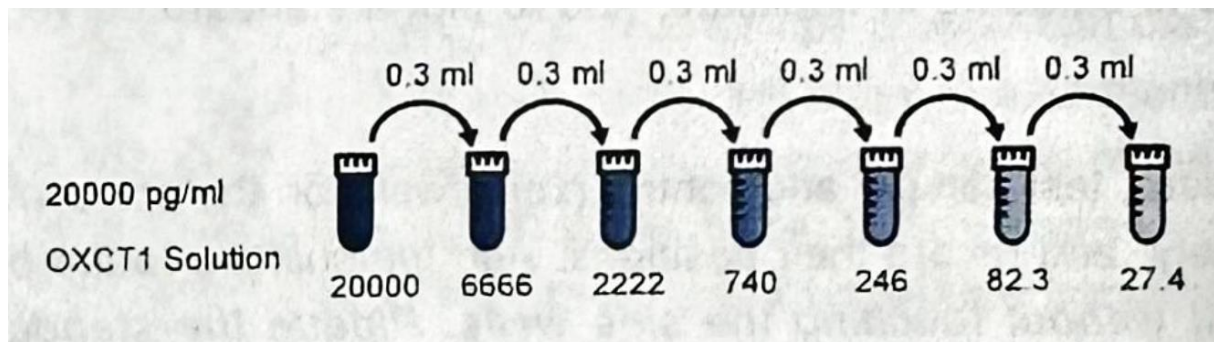
To confirm proteomics results I performed an ELISA assay with the Human 3-Oxoacid Coenzyme A Transferase 1 (OXCT1) CLIA Kit from abbexa®.

- Sample Preparation

Serum samples were centrifugated at approximately 1000 x g for 20 mins to remove precipitate and aliquoted at -80°C.

- Reagent Preparation

Standard reagents were prepared with 1.0 ml of Standard Diluent buffer to make the 20000 pg/ml Standard Solution (highest standard). Serial dilutions were made by adding aliquots of 0.6 ml of the Standard Diluent Buffer into each tube (apart from the highest standard tube). I added 0.3 ml of the highest standard solution into the 1st tube and mixed thoroughly. I transferred 0.3 ml from the 1st to the 2nd tube and so on.



Wash Buffer were prepared by dilatation of the concentrated Wash Buffer 30-fold (1/30) with distilled water.

Detection Reagent A Working Solution Preparation was prepared no more than 15 minutes before the experiment. First, I calculated the total volume of working solution required. Then I diluted Detection Reagent A 100-fold with Diluent A, and mixed thoroughly.

Detection Reagent B Working Solution Preparation was prepared no more than 15 minutes before the experiment. First, I calculated the total volume of working solution required. Then I diluted Detection Reagent B 100-fold with Diluent B, and mixed thoroughly.

Preparation of Substrate Working Solution was made by calculating the total volume of working solution required and in a separate tube, I added Substrate A and Substrate B in a 99:1 ratio, respectively (e.g. add 990 pl Substrate A to 10 pl Substrate B).

- Assay Protocol

After preparing all standards, samples and reagents as described above, I equilibrated the kit components and samples to room temperature prior to use. All measurement were performed in duplicates and the mean protein concentration was retained. I set standard, test sample and control (zero) wells on the pre-coated plate respectively and recorded their positions. I added the solution to the bottom of each well without touching the side walls. I aliquoted 100 ul of the diluted standards into the standard wells. I aliquoted 100 ul of Standard Diluent buffer into the control (zero) well.

I aliquoted 10 ul of appropriately diluted sample into the test sample wells. I covered the plate with a plate sealer and incubated it for 1 hour at 37°C. Then I removed the cover and discarded the liquid. I aliquoted 10 ul of Detection Reagent A working solution into each well. I covered

the plate with a plate sealer and incubated for 1 hour at 37°C. I removed the cover and discarded the solution. I washed the plate 3 times with the Wash Buffer. I aliquoted 100 ul of Detection Reagent B working solution to each well. I sealed the plate and incubated it for 30 minutes at 37°C. I removed the cover, discarded the solution and repeated the washing process as described above, 5 times. I aliquoted 100 ul of Substrate working solution into each well. I covered the plate with a plate sealer and incubated for 10 minutes at 37°C. After all these steps, I measured the chemiluminescence signal in a microplate luminometer immediately. For calculation, I averaged the duplicate readings for each set of reference standard, control and samples and subtract the average zero standard RLU (Relative Light Unit).

d. Data analyses

The threshold for statistical significance was set at $p < 0.05$. R® software version 4.2.2 was used for the statistical analyses.

i. Normalization

Data were presented as NPX values by Olink platform. NPX is Olink's relative protein quantification unit on log₂ scale. NPX values are calculated from the number of matched counts, using NGS (Next Generation Sequencing) as readout.

ii. Samples quality control

Three internal controls were added to each sample, the Incubation control, the Extension Control and the Amplification control. The Extension Control was used for the generation of the NPX values. The Incubation Control and the Amplification Control are used to monitor the quality of assay performance, as well as the quality of individual samples.

Three external controls were included in each run, the Plate Control (healthy pooled plasma), Sample Control (healthy pooled plasma) and Negative Control. The Plate Control was used for data normalization, the Sample Control was used to assess potential variation between runs and plates, and the Negative Control was used to calculate Limit of Detection for each assay and to assess potential contamination of assays.

The following parameters were evaluated in the Quality Control (QC):

1. The average matched counts for each sample. To pass QC, there should be at least 500 counts, otherwise the sample receives a QC warning status.
2. The deviation of the median value of the Negative Controls from a predefined value set for each assay. To pass QC, the deviation of the median of the Negative Controls must be less or equal to 5 standard deviations from the set predefined value, otherwise the assay will receive a warning status.

All samples with a QC_warning were excluded for further analyses.

iii. Differential of expression

I used `Olink_test` function of the `OlinkAnalyze` R package to perform a Welch 2-sample t-test or paired t-test at confidence level 0.95 for every protein (by OlinkID) for a given grouping variable using the function `t.test` from the R library `stats` and correct for multiple testing using the Benjamini-Hochberg method (“`fdr`”) using the function `p.adjust` from the R library `stats`. Adjusted p-values are logically evaluated towards adjusted p-value < 0.05. The resulting t-test table was arranged by ascending p-values.

iv. Immune signature

I explored outcomes according to a previously published suppression of tumor immunity score². Our signature included the following proteins: IL4, IL5, CCL13, CCL17, CXCL1, CXCL5, CXCL11, PDCD1LG2, IL6, CXCL8, CCL19, GAL, TGFB1, CXCL13, CCL20, IL10, MMP12, LAMP3, IL18, CXCL8, CSF1, CD274, PDCD1, CD5, CD4, MICA, MICAB. GAL9 and MMP7 were not included because of low quality measurement for these proteins. Then I calculated the suppression of tumor immunity score for each patient as the mean *z*-score value for the proteins belonging to the respective biological process. For analysis, we grouped suppression of tumor immunity scores into low (\leq median) and high ($>$ median).

v. Survival analyses

Survival data were calculated using the Kaplan-Meier method and compared using a log-rank test. Hazard ratios (HRs) were calculated using the Cox model.

vi. GSEA

We performed enrichment analysis with the clusterProfiler R package based on statistical test results and full data using clusterProfiler's GSEA and enrich functions of MSigDB. Ontology argument used in this package are KEGG, GO and Reactome. ClusterProfiler was originally developed by Guangchuang Yu at the School of Basic Medical Sciences at Southern Medical University³. Clustering with Hallmarks was not included in the package due to gene nomenclature incompatibility.

vii. In vivo experiment:

All animal procedures and studies were conducted in accordance with the approved guidelines for animal experimentation by the ethics committee at University Paris-Saclay (CEEA 26, Project 2020_074_27871) and followed the regulations set by the European Union. The animals were housed in pathogen-free conditions and provided with unlimited access to food and water. PDX MR-0009 were subcutaneously grafted (one graft per mouse) into male NSG micewhich were supplemented with a pellet of 10 mg of testosterone. The grafts were allowed to grow until the tumor volume reached 80-200 mm³. Subsequently, the mice were randomly assigned to either the treatment group (n=6), receiving arecolin hydrobromide vetranal via oral gavage at 50 mg/kg, or the vehicle group (n=6). Tumor progression was monitored by measuring their volume twice weekly using calipers throughout the treatment period.

2. Results

a. Serum proteins dosage

i. Proteins level comparison between no responder vs responder on baseline serum (n=54)

Among the 54 patients, comparison between baseline samples showed OXCT1 was the only protein to be significantly overexpressed in non-responder i.e. patients showing progression within the first 4 months of ARPI treatment (figure 1 & table 1).

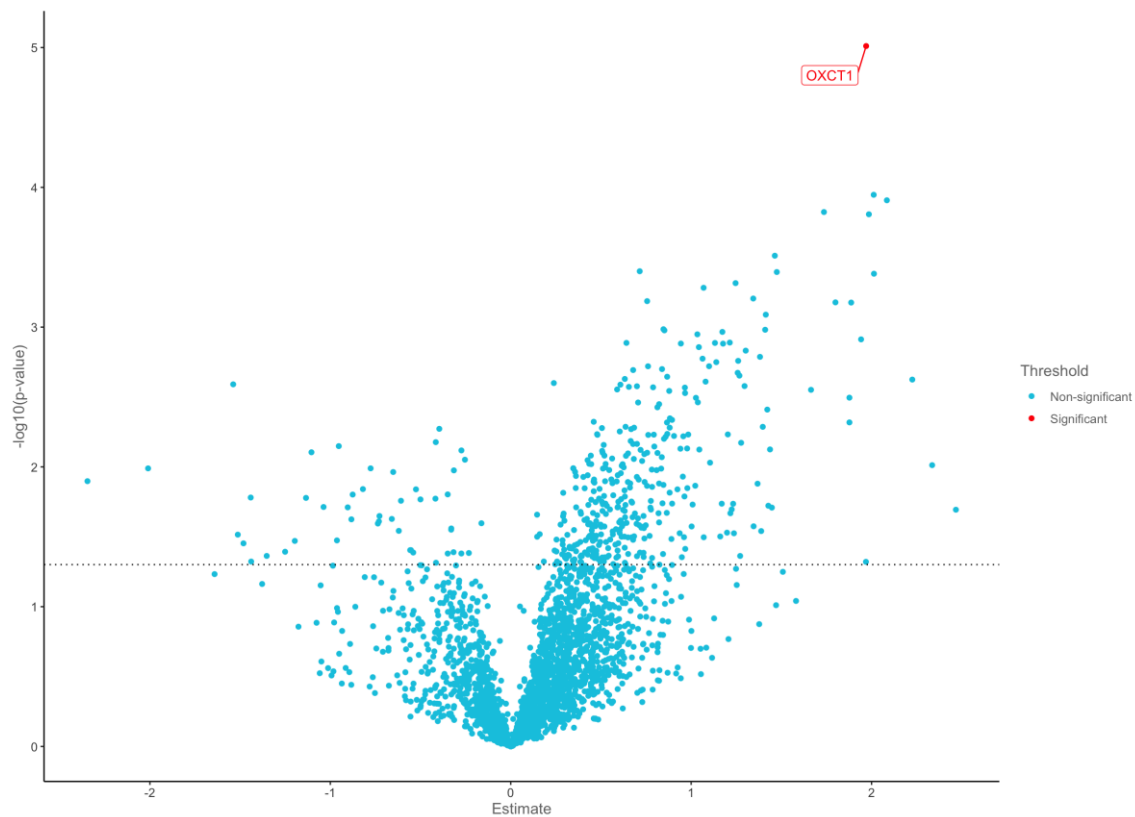


Figure 1: Proteins differential expression between non-responder vs responder in baseline samples (overexpressed proteins in non-responder are on the right with a positive estimate).

Table 1: Proteins differential expression between non-responder vs responder in baseline samples (overexpressed proteins in non-responder have a positive estimate).

Assay	Estimate	Non-responders	Reponders	Adjusted_pval	Thresho ld
OXCT1	1.9699575	4.66117083333333	2.69121333333333	0.0282550680647346	Significant
TCOF1	2.01192833333333	2.958825	0.946896666666667	0.0903244584754631	Non-significant
GRPEL1	2.0849425	3.36642916666667	1.28148666666667	0.0903244584754631	Non-significant
LETM1	1.73608166666667	2.21195833333333	0.475876666666667	0.0903244584754631	Non-significant
DPY30	1.985235	2.37749166666667	0.392256666666667	0.0903244584754631	Non-significant
EVPL	1.46375416666667	0.911904166666667	-0.55185	0.128908127273774	Non-significant
FOXJ3	0.714968333333333	1.89664166666667	1.18167333333333	0.128908127273774	Non-significant

MAD1 L1	1.47476083333 333	2.16922083333 333	0.69446	0.12890812727 3774	Non- signific ant
RCOR 1	2.01333333333 333	2.84401666666 667	0.83068333333 3333	0.12890812727 3774	Non- signific ant
PRDX3	1.24623	1.55788333333 333	0.31165333333 3333	0.12890812727 3774	Non- signific ant
BRK1	1.069095	2.44154166666 667	1.37244666666 667	0.12890812727 3774	Non- signific ant
GATD 3	1.34417083333 333	1.0434875	- 0.30068333333 3333	0.12890812727 3774	Non- signific ant
SIRT1	0.7560375	1.74487083333 333	0.98883333333 3333	0.12890812727 3774	Non- signific ant
RRM2	1.7998375	3.9505875	2.15075	0.12890812727 3774	Non- signific ant
LEO1	1.8870075	1.7610875	-0.12592	0.12890812727 3774	Non- signific ant
RBFO X3	1.41375166666 667	2.60729166666 667	1.19354	0.14089421987 0756	Non- signific ant
ENO1	0.84649916666 6667	1.99449583333 333	1.14799666666 667	0.14089421987 0756	Non- signific ant
PMS1	1.41027083333 333	3.67937083333 333	2.2691	0.14089421987 0756	Non- signific ant
TOMM 20	0.8517775	1.82775416666 667	0.97597666666 6667	0.14089421987 0756	Non- signific ant
ZBTB1 7	1.17300166666 667	2.88920833333 333	1.71620666666 667	0.14089421987 0756	Non- signific ant

ii. Proteins level comparison between no responder vs long responder on baseline serum (n=31)

Among 31 patients, no responders (PFS less than 4 months) vs long responder (PFS more than 25 months) had a significant overexpression of OXCT1, LRIG1, TCOF1, DPY30, C9, ZNRD2, SNRPB2 and PRDX3 (figure 2 & table 2).

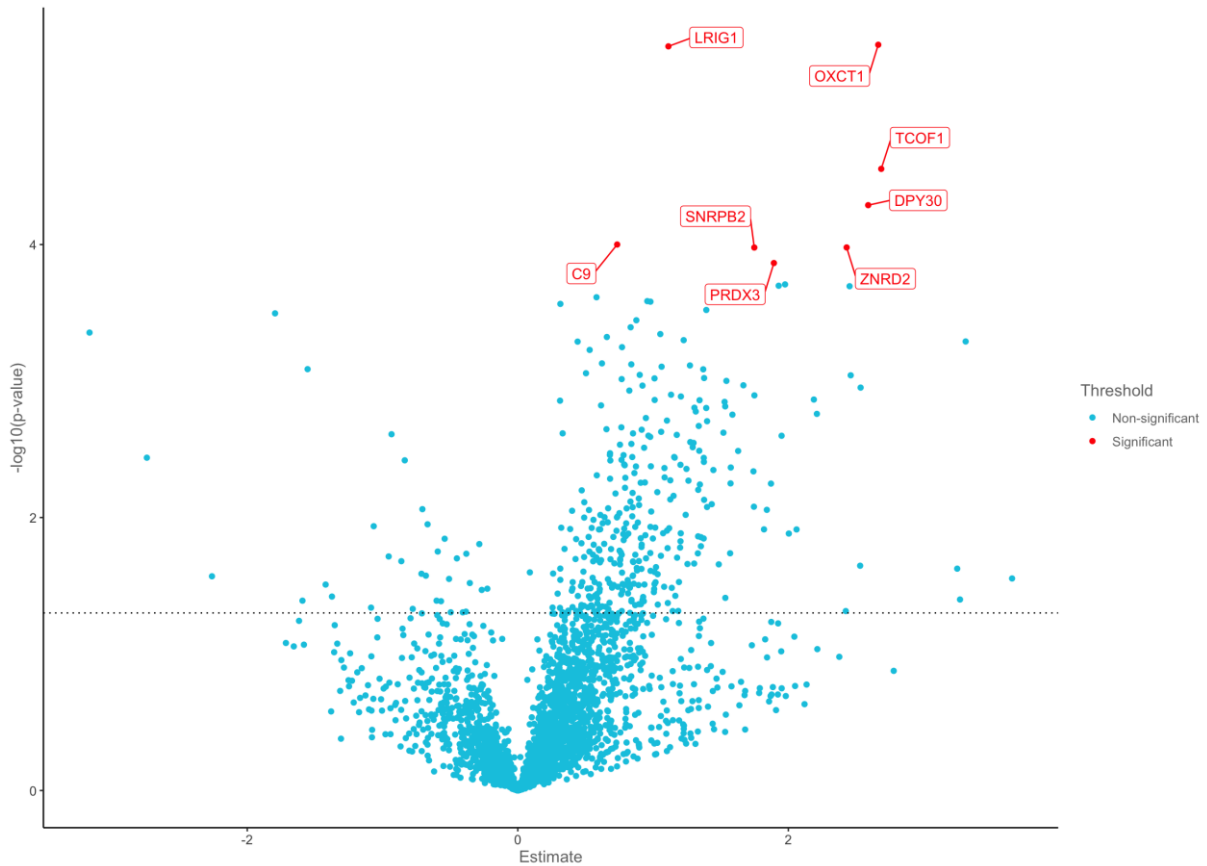


Figure 2: Proteins differential expression between no responder vs long responder in baseline samples (overexpressed proteins in no responder are on the right with a positive estimate).

Table 2: Proteins differential expression between no responder vs long responder in baseline samples (overexpressed proteins in no responder have a positive estimate).

Assay	Estimate	No responder	Long responder	Adjusted_pval	Threshold
OXCT1	2.66478	4.741855	2.077075	0.0051143727949308	Significant
LRIG1	1.1134375	1.316575	0.2031375	0.0051143727949308	Significant
TCOF1	2.6868725	3.19456	0.5076875	0.0269366517032754	Significant
DPY30	2.59046	2.65961	0.06915	0.0372724253685072	Significant
C9	0.7346225	1.225885	0.4912625	0.0435300672842602	Significant

ZNRD2	2.4311	5.734625	3.303525	0.0435300672842602	Significant
SNRPB2	1.748385	2.672485	0.9241	0.0435300672842602	Significant
PRDX3	1.893335	1.74386	-0.149475	0.0494741849918689	Significant
MAD1L1	1.97589	2.30354	0.32765	0.0525722825085994	Non-significant
RBFOX3	1.928735	2.77666	0.847925	0.0525722825085994	Non-significant
LETM1	2.4529075	2.475995	0.0230875	0.0525722825085994	Non-significant
ITIH4	0.5818875	0.120925	-0.4609625	0.0525722825085994	Non-significant
RNF43	0.957465	0.008639999999999997	-0.948825	0.0525722825085994	Non-significant
C4BPB	0.9806675	1.267505	0.2868375	0.0525722825085994	Non-significant
ROBO4	0.314705	0.62858	0.313875	0.0525722825085994	Non-significant
BRK1	1.393605	2.574055	1.18045	0.054410100901639	Non-significant
LEP	-1.7945	-2.065175	-0.270675	0.054410100901639	Non-significant
GADD45GIP1	0.8764225	1.21096	0.3345375	0.0577281743544528	Non-significant
GPKOW	0.83423	1.06928	0.23505	0.0596178655679146	Non-significant
LELP1	-3.16609	-2.79834	0.36775	0.0596178655679146	Non-significant

- iii. Proteins level comparison between short survivors (patients deceased before 24 months) vs long survivor (≥ 24 months) on baseline serum (n=33)

Comparison between short survivors (patients deceased before 24 months) vs long survivor (≥ 24 months) on baseline serum found no significant different level of protein expression (figure 3 & table 3).

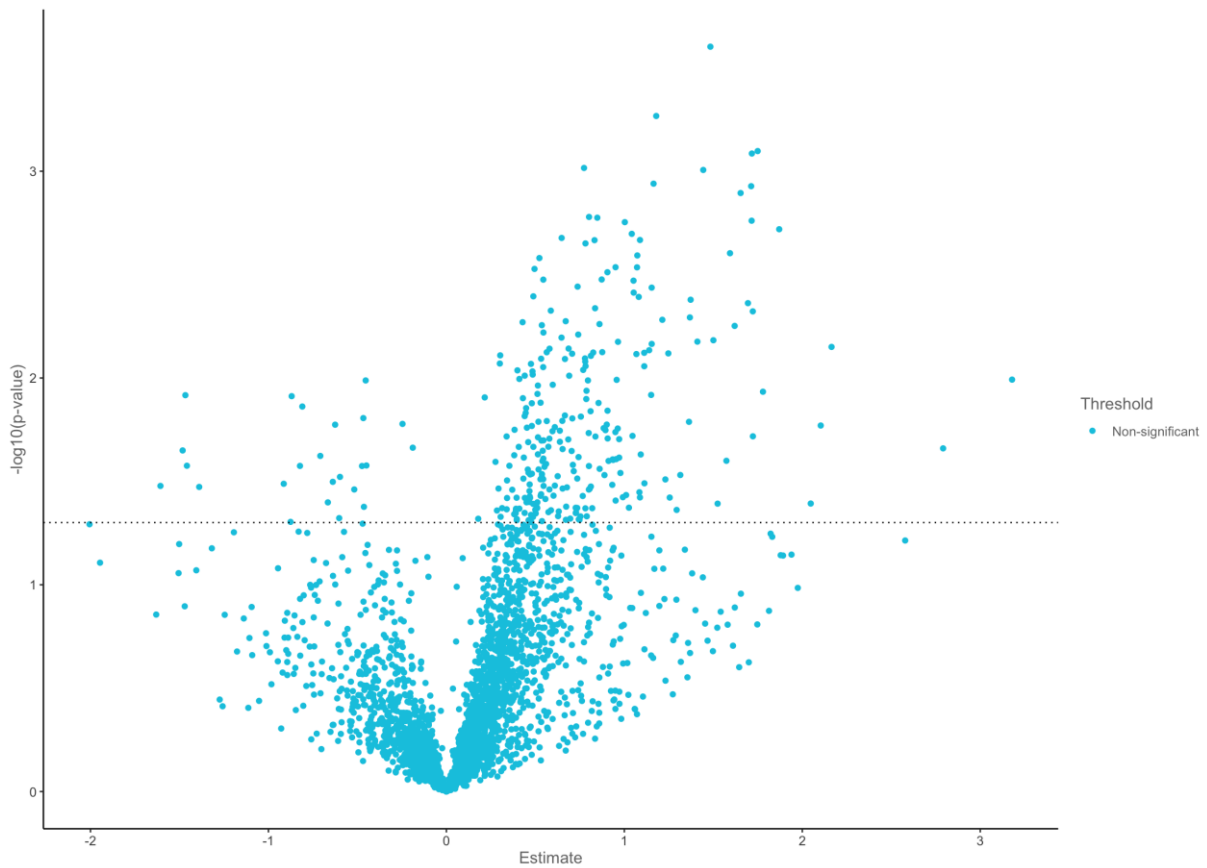


Figure 3: Proteins differential expression between short survivors (patients dead before 24 months) vs long survivor (≥ 24 months) in baseline samples (overexpressed proteins in short survivors are on the right with a positive estimate).

Table 3: Proteins differential expression between short survivors (patients dead before 24 months) vs long survivor (≥ 24 months) in baseline samples (overexpressed proteins in short survivors have a positive estimate).

Assay	Estimate	Adjusted_pval	Threshold
PLA2G2A	1.48352142857143	0.337976302579605	Non-significant
EDA2R	1.17917023809524	0.337976302579605	Non-significant

LETM1	1.74925714285714	0.337976302579605	Non-significant
AGR2	1.71660238095238	0.337976302579605	Non-significant
RNF43	0.773453571428572	0.337976302579605	Non-significant
ECI2	1.4434119047619	0.337976302579605	Non-significant
FGL1	1.16424642857143	0.337976302579605	Non-significant
TCOF1	1.71270357142857	0.337976302579605	Non-significant
OXCT1	1.6533369047619	0.337976302579605	Non-significant
STC1	0.801653571428572	0.337976302579605	Non-significant
LRIG1	0.848077380952381	0.337976302579605	Non-significant
PTGES2	1.71537142857143	0.337976302579605	Non-significant
CHCHD6	1.00269642857143	0.337976302579605	Non-significant
GRPEL1	1.87032261904762	0.337976302579605	Non-significant
CKAP4	1.04179404761905	0.337976302579605	Non-significant
AREG	0.647663095238095	0.337976302579605	Non-significant
HMOX2	1.08792619047619	0.337976302579605	Non-significant
LRG1	0.832395238095238	0.337976302579605	Non-significant
C4BPB	0.781471428571429	0.337976302579605	Non-significant
KRT19	1.59376785714286	0.337976302579605	Non-significant

iv. Proteins level comparison between progression (only if ≥ 4 months) vs baseline serum (n=28, 14 patients)

Comparison between serum at progression (only if ≥ 4 months) vs baseline did not find any difference in protein expression (figure 4 and table 4).

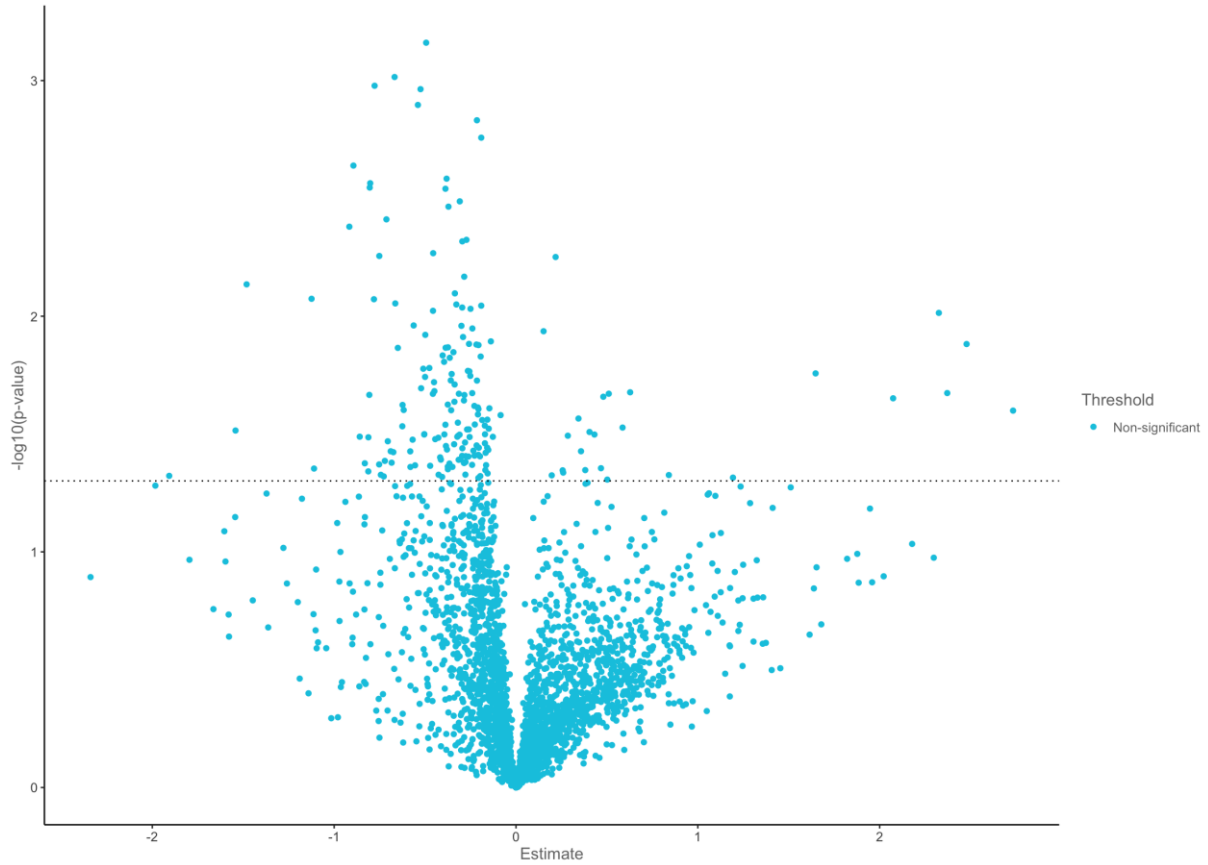


Figure 4: Proteins differential expression between serum at progression (only if ≥ 4 months) vs baseline (overexpressed proteins in serum at progression are on the right with a positive estimate).

Table 4: Proteins differential expression between serum at progression (only if ≥ 4 months) vs baseline (overexpressed proteins in serum at progression have a positive estimate).

Assay	estimate	Method	Alternative	Adjusted_pval	Threshold
HS3ST3B1	-0.49405	Paired t-test	two.sided	0.695045914865213	Non-significant
CDHR2	-0.667685714285714	Paired t-test	two.sided	0.695045914865213	Non-significant
FOLH1	-0.77755	Paired t-test	two.sided	0.695045914865213	Non-significant

PLXDC1	- 0.52498571428571 4	Paired t-test	two.sided	0.69504591486521 3	Non- significan t
XPNPEP2	- 0.53949285714285 7	Paired t-test	two.sided	0.69504591486521 3	Non- significan t
ATRAID	- 0.21487857142857 1	Paired t-test	two.sided	0.69504591486521 3	Non- significan t
RNF149	- 0.19105714285714 3	Paired t-test	two.sided	0.69504591486521 3	Non- significan t
CDKL5	- 0.89405714285714 3	Paired t-test	two.sided	0.69504591486521 3	Non- significan t
FUT3_FUT 5	- 0.38158571428571 4	Paired t-test	two.sided	0.69504591486521 3	Non- significan t
C19orf12	- 0.80176428571428 6	Paired t-test	two.sided	0.69504591486521 3	Non- significan t
ADH4	- 0.80434285714285 7	Paired t-test	two.sided	0.69504591486521 3	Non- significan t
CD38	- 0.38801428571428 6	Paired t-test	two.sided	0.69504591486521 3	Non- significan t
CD1C	- 0.30922142857142 9	Paired t-test	two.sided	0.70973067663428 3	Non- significan t
CALCA	- 0.37130714285714 3	Paired t-test	two.sided	0.70973067663428 3	Non- significan t
CCL21	- 0.71261428571428 6	Paired t-test	two.sided	0.74989303420331 5	Non- significan t
THSD1	- 0.91648571428571 4	Paired t-test	two.sided	0.75523547120634 3	Non- significan t
EDN1	- 0.27245714285714 3	Paired t-test	two.sided	0.77381621184021 2	Non- significan t
KAZALD1	- 0.29527142857142 9	Paired t-test	two.sided	0.77381621184021 2	Non- significan t
COL24A1	- 0.45552857142857 1	Paired t-test	two.sided	0.77381621184021 2	Non- significan t

MDK	- 0.75172142857142 9	Paired t-test	two.sided	0.77381621184021 2	Non- significan t
-----	----------------------------	------------------	-----------	-----------------------	-------------------------

v. Correlation analyses with baseline proteins assay

No strong correlation was found between OXCT1 level of expression and clinical variables, immunochemistry (IHC) markers and whole exome sequencing (figure 5).

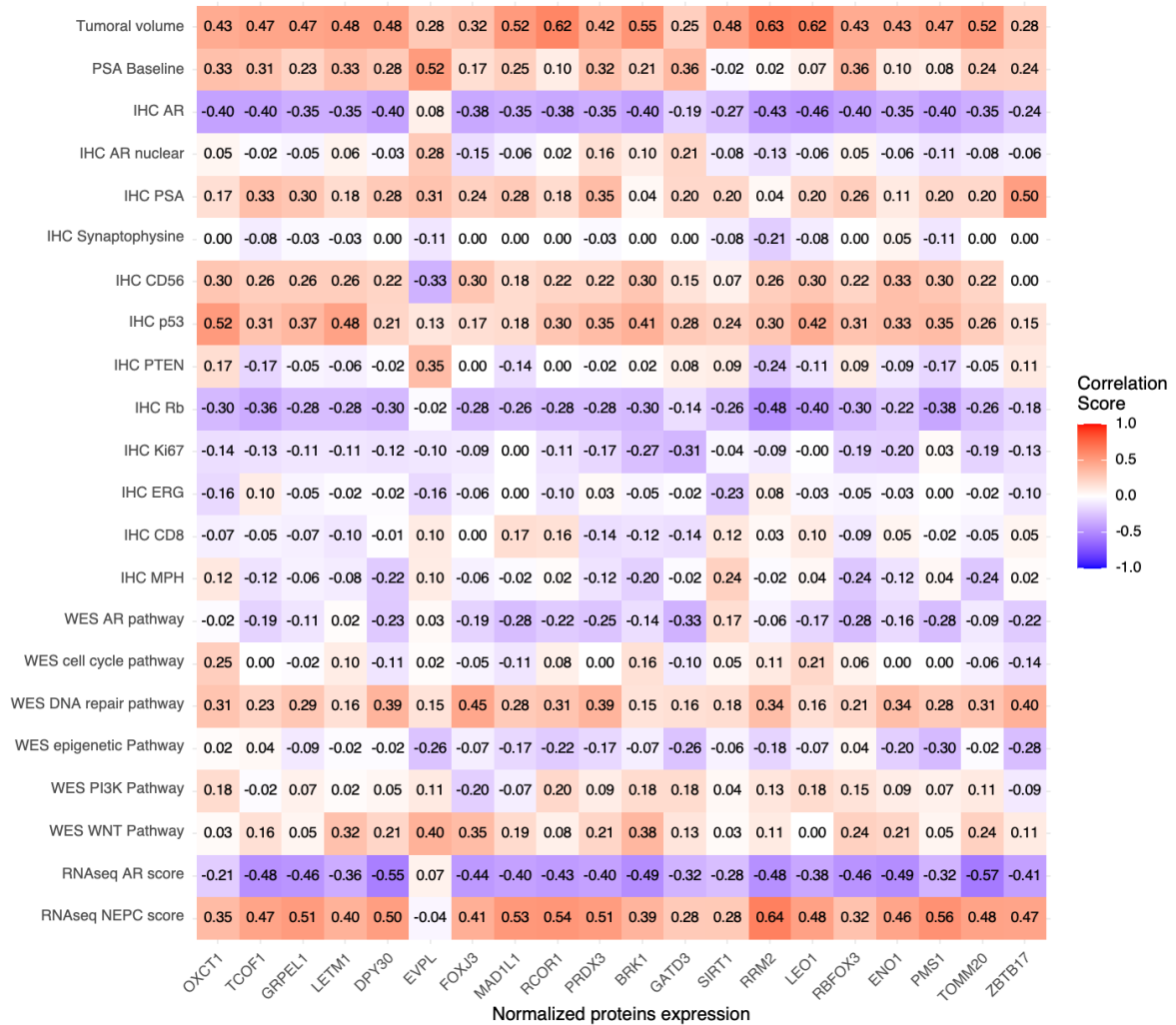


Figure 5: Correlation between normalized proteins expression and clinical, IHC, whole exome sequencing or RNAseq variable using a Pearson, Spearman or point-biserial correlation depending on the type of data, at baseline.

b. OXCT1 as a biomarker

i. PFS

Median normalized protein expression (NPX) of OXCT1 was 2.867. We classified patients as high (n=27) or low (n=27) expression based on this median and removed patients with missing data for survival. Patients with OXCT1 High expression (n=22) vs Low (n=25) had a shorter median PFS of 2.9 vs 10.0 months (HR= 3.245 CI95%[1.646-6.399], p<0.001, figure 6).

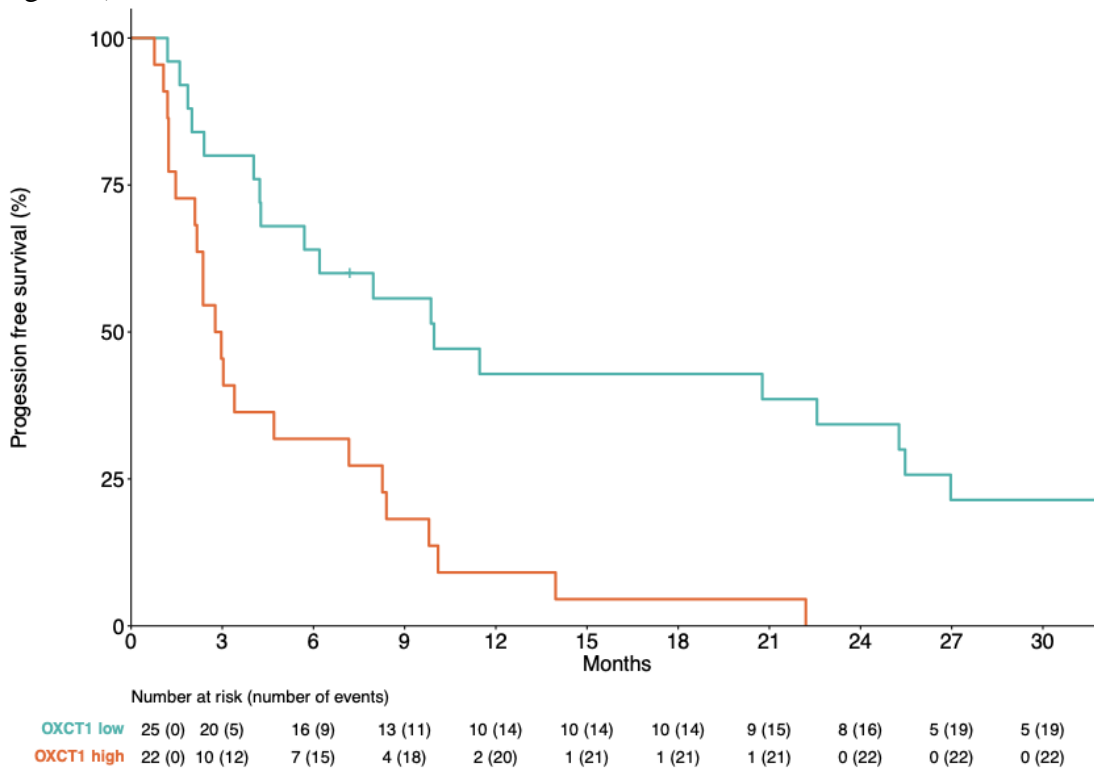


Figure 6: PFS according to OXCT1 expression (high vs low).

ii. OS

Patient with OXCT1 High expression level (n=22) had a shorter OS compare to low expression level (n=25) with a median of 16.1 months vs not reached (HR= 4.577 CI95%[1.882-11.130], p<0.001, figure 7).

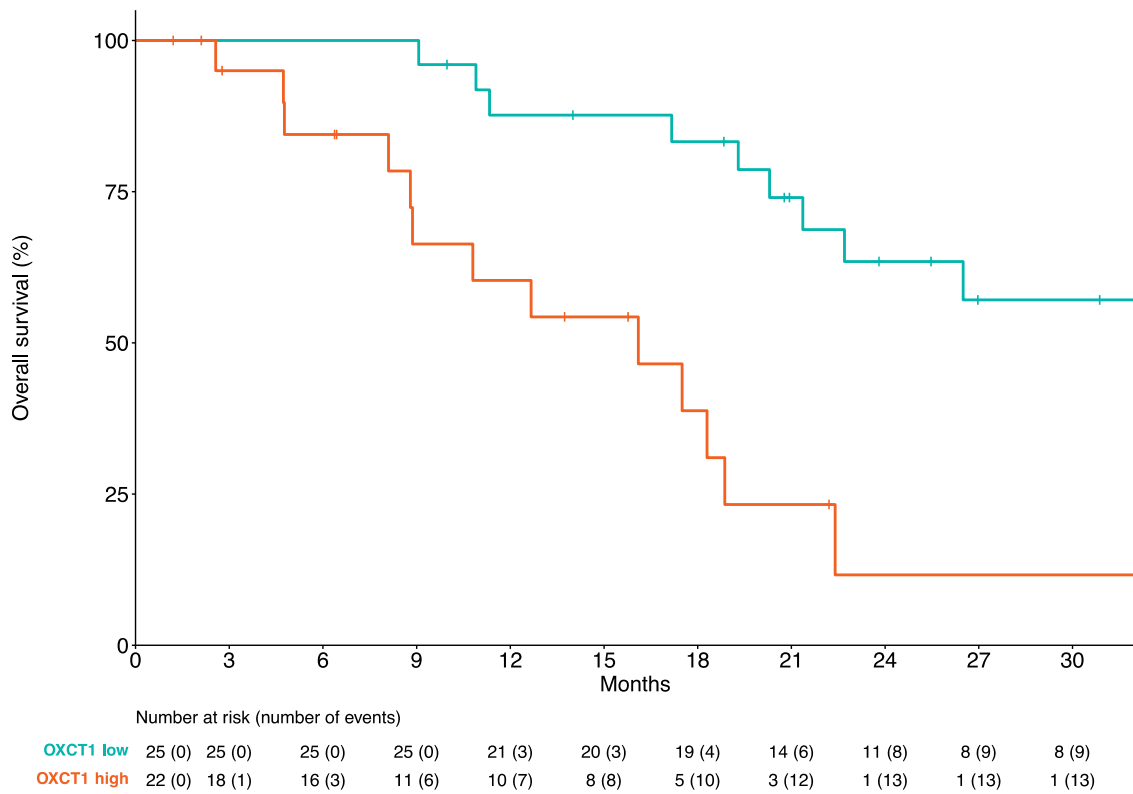


Figure 7: OS according to OXCT1 expression (high vs low).

c. Suppression of tumor immunity score

i. Number of responders to ARPI according to suppression of tumor immune signature

Among the 30 patients responders to ARPI, 14 (51.8) had a positive suppression of tumor immune signature and 13 (48.1) among the 24 patients without response to ARPI ($p=0.584$).

ii. PFS

Patients with a positive suppression of tumor immune signature ($n=25$) had a tendency for shorter median PFS compared to patients with a negative one ($n=22$) with 4.0 vs 9.9 months without statistical significance ($HR=1.308$ $CI_{95\%}[0.704-2.431]$, $p=0.400$, figure 8).

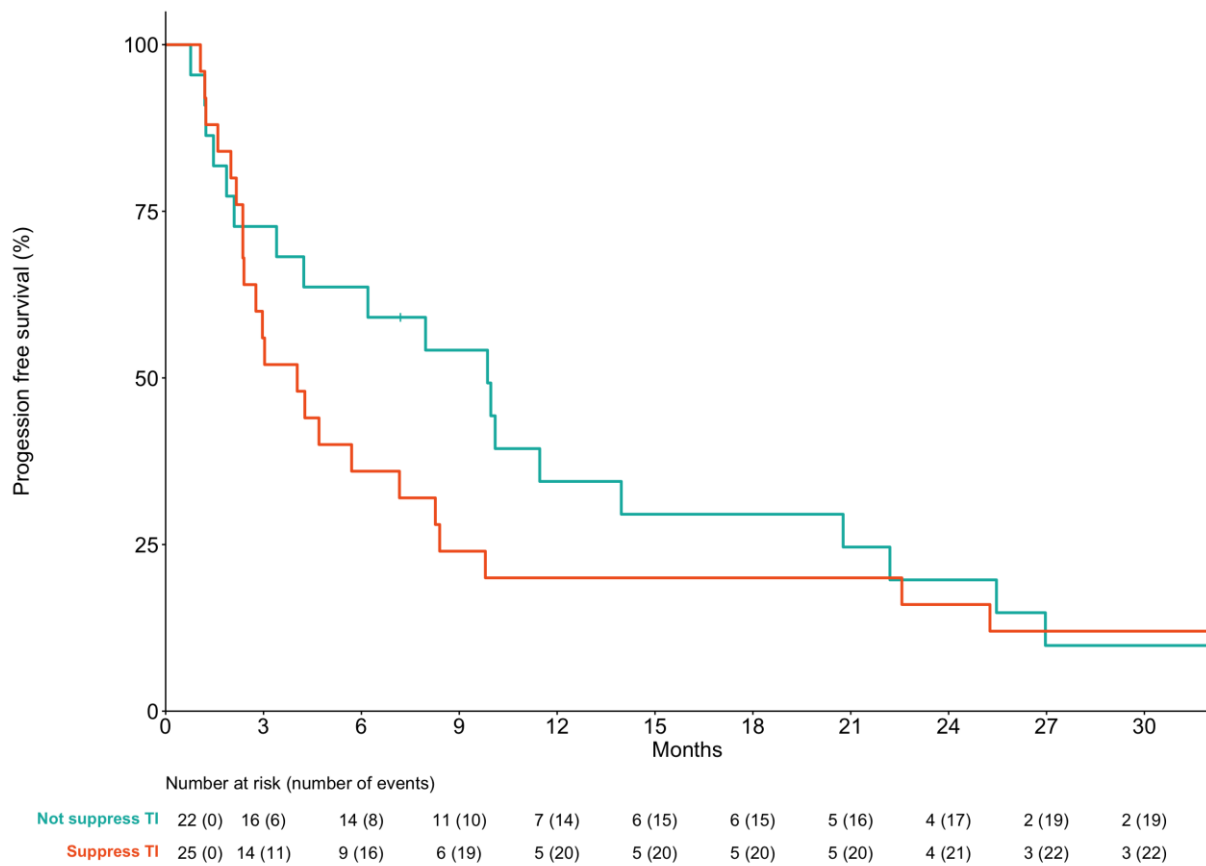


Figure 8: PFS according to suppression of tumor immune signature (positive vs negative).

iii. OS

Similarly, median OS was 18.3 months for positive signature vs not reached in case of a negative signature (HR=2.319 CI95% [0.944-5.695], p=0.060, figure 9).

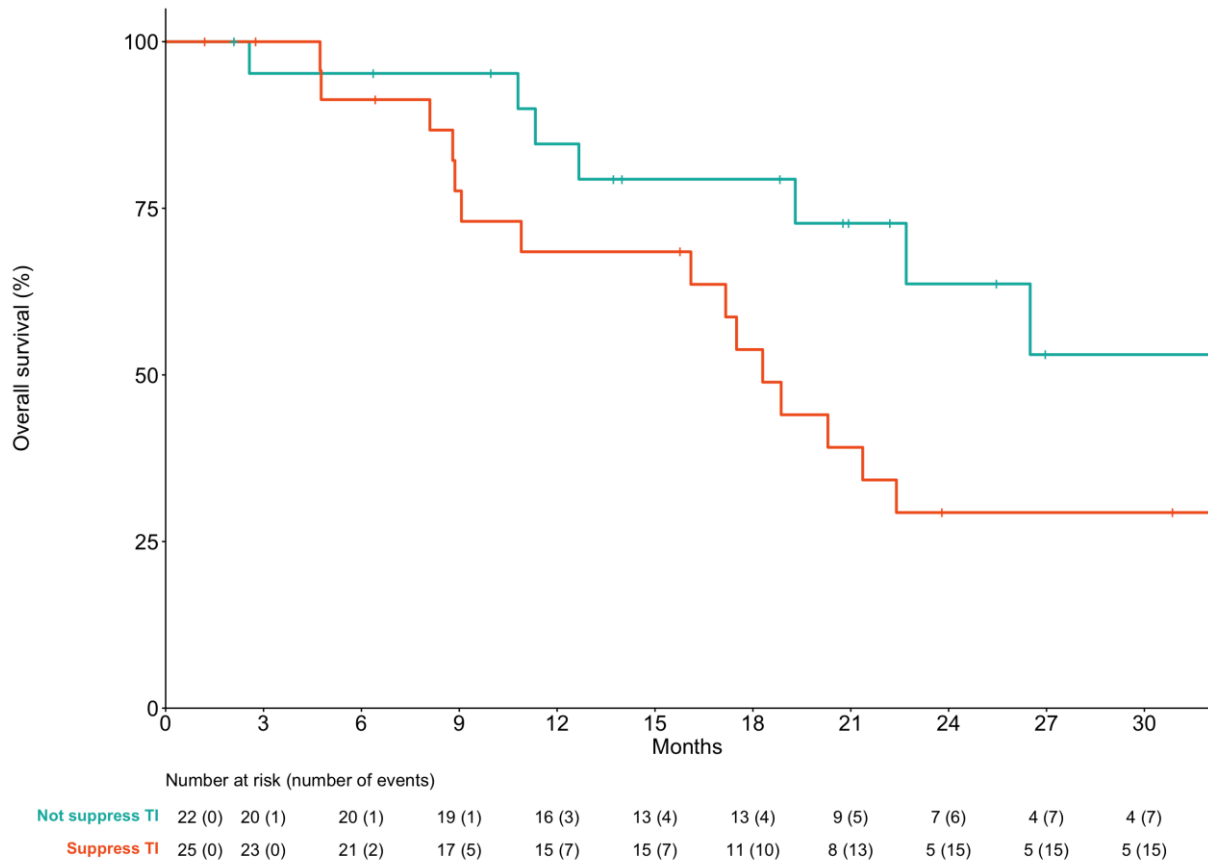


Figure 9: OS according to suppression of tumor immune signature (positive vs negative).

d. Heatmap for unsupervised clustering (baseline samples)

When performing unsupervised clustering, no cluster seems to be associated with response to ARPI, AR or NEPC RNAseq scores (figure 10).

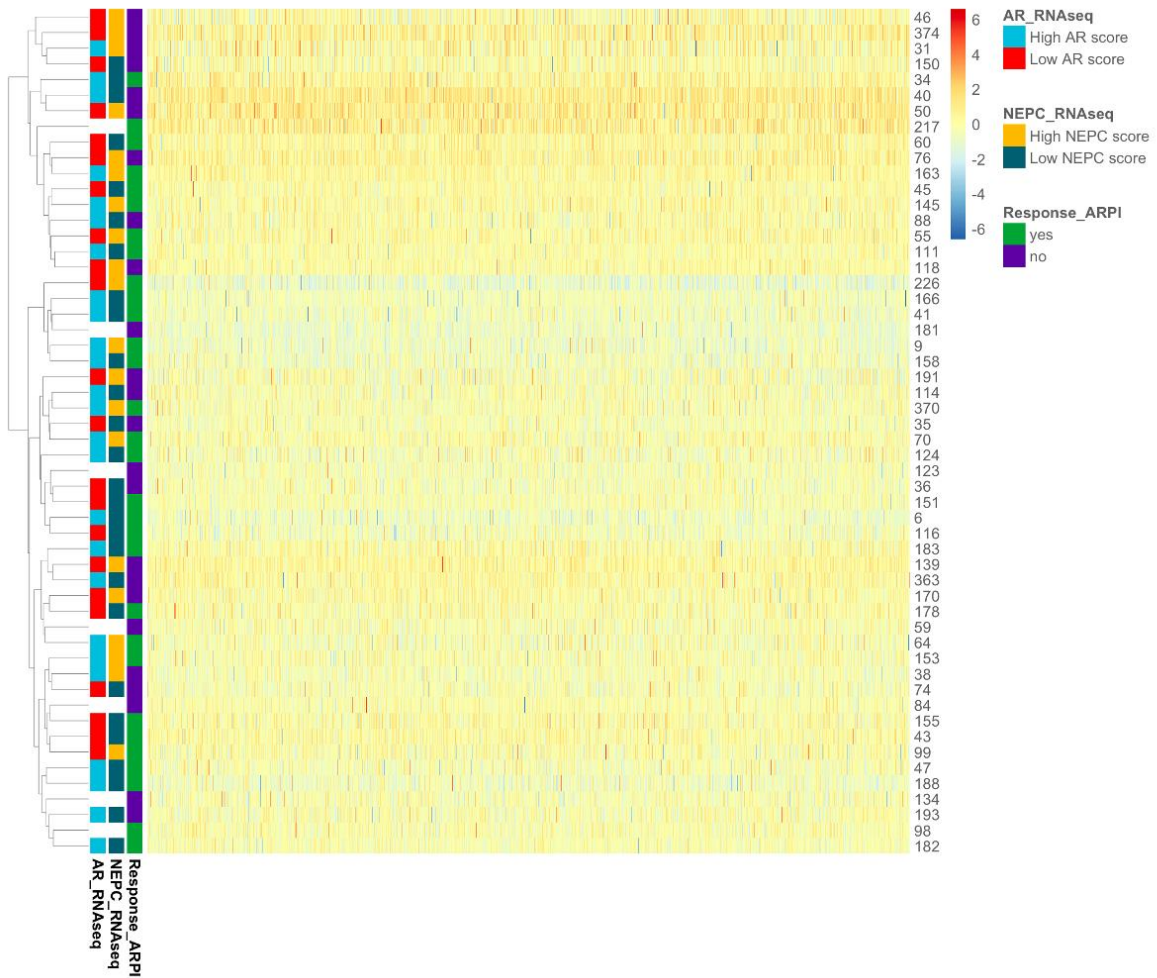


Figure 10: Heatmap for unsupervised clustering with ARPI, AR and NEPC RNAseq scores

e. Survival according to baseline samples clustering (k=2)

We first analyzed outcomes according to cluster 1 vs cluster 2 (k=2, figure 11)

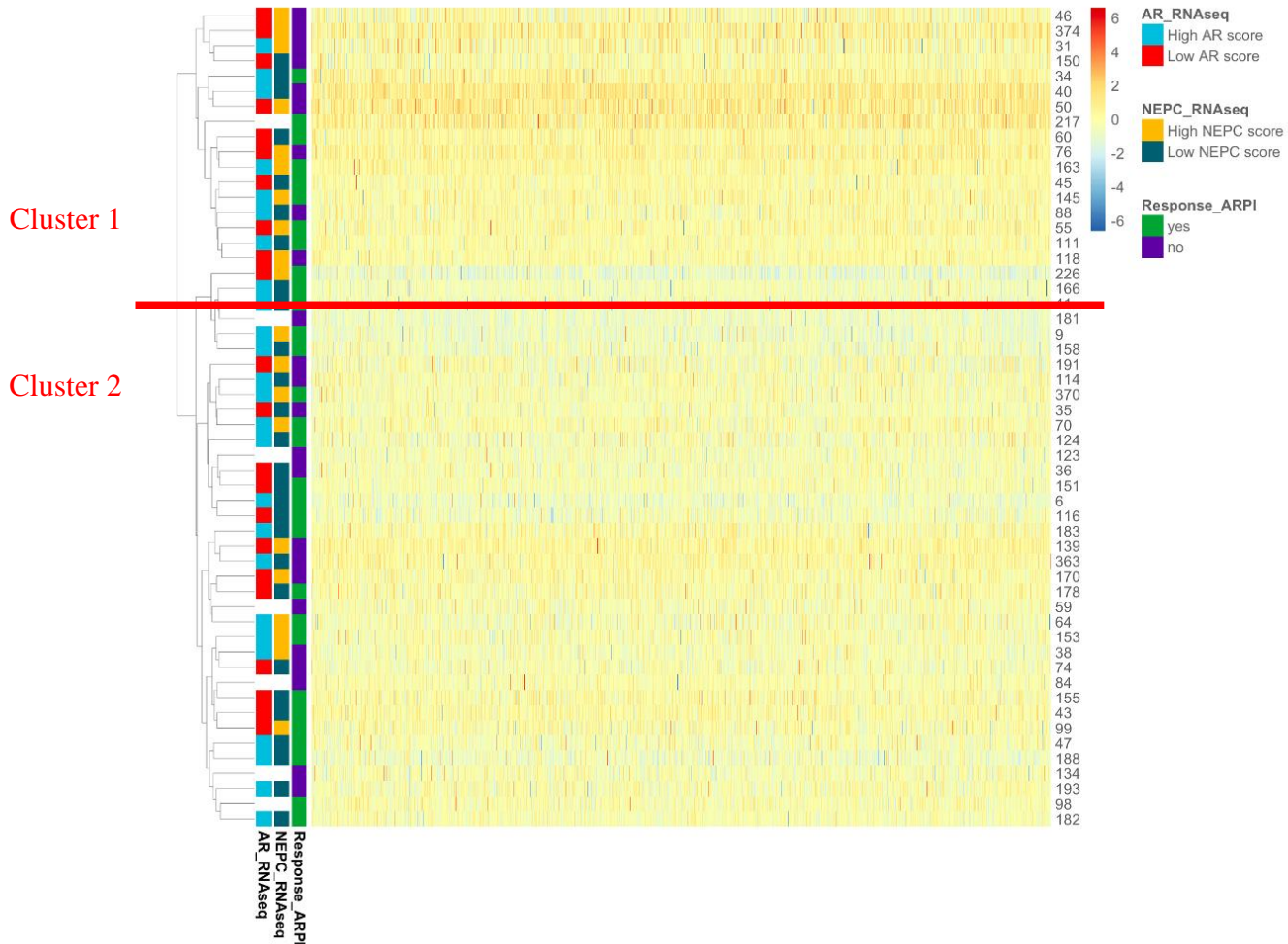


Figure 11: Heatmap for unsupervised clustering with ARPI, AR and NEPC RNAseq scores with 2 clusters (k=2).

i. PFS

Patients in cluster 1 (n=16) had a tendency for shorter PFS compared to patients in cluster 2 (n=28) with 2.7 months vs 8.3 months (HR=1.129 CI95%[0.579-2.201], p=0.700, figure 12)

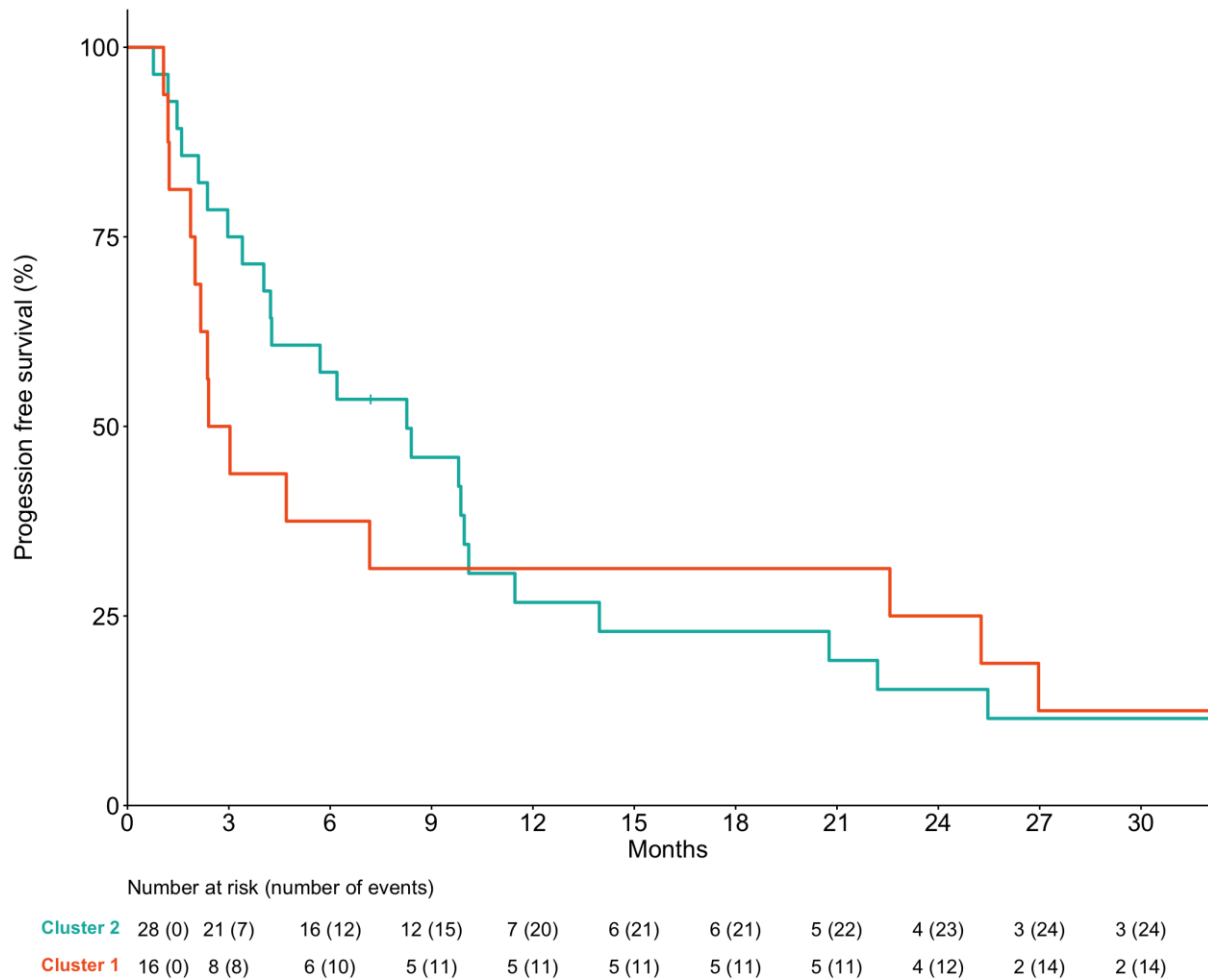


Figure 12: PFS according to clusters (k=2).

ii. OS

No difference was found for median OS between the two clusters with 19.3 vs 22.4 months (HR=1.153 CI95%[0.482-2.761], p=0.700, figure 13).

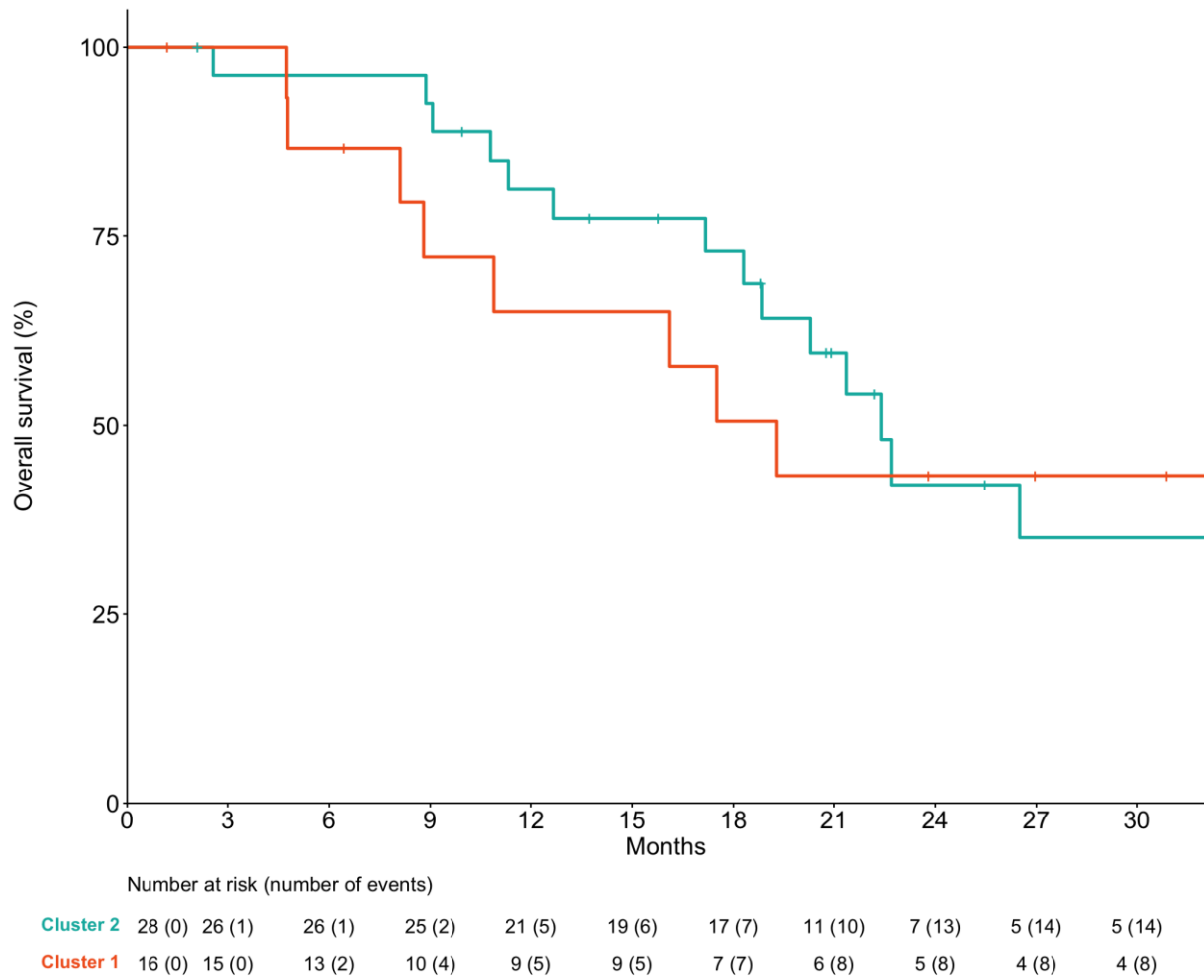


Figure 13: OS according to clusters (k=2).

f. Survival according to baseline samples clustering (k=6)

We then analyzed outcomes according to a more restricted cluster 1 with less responder patients compared to cluster 2-6 (k=6, figure 14).

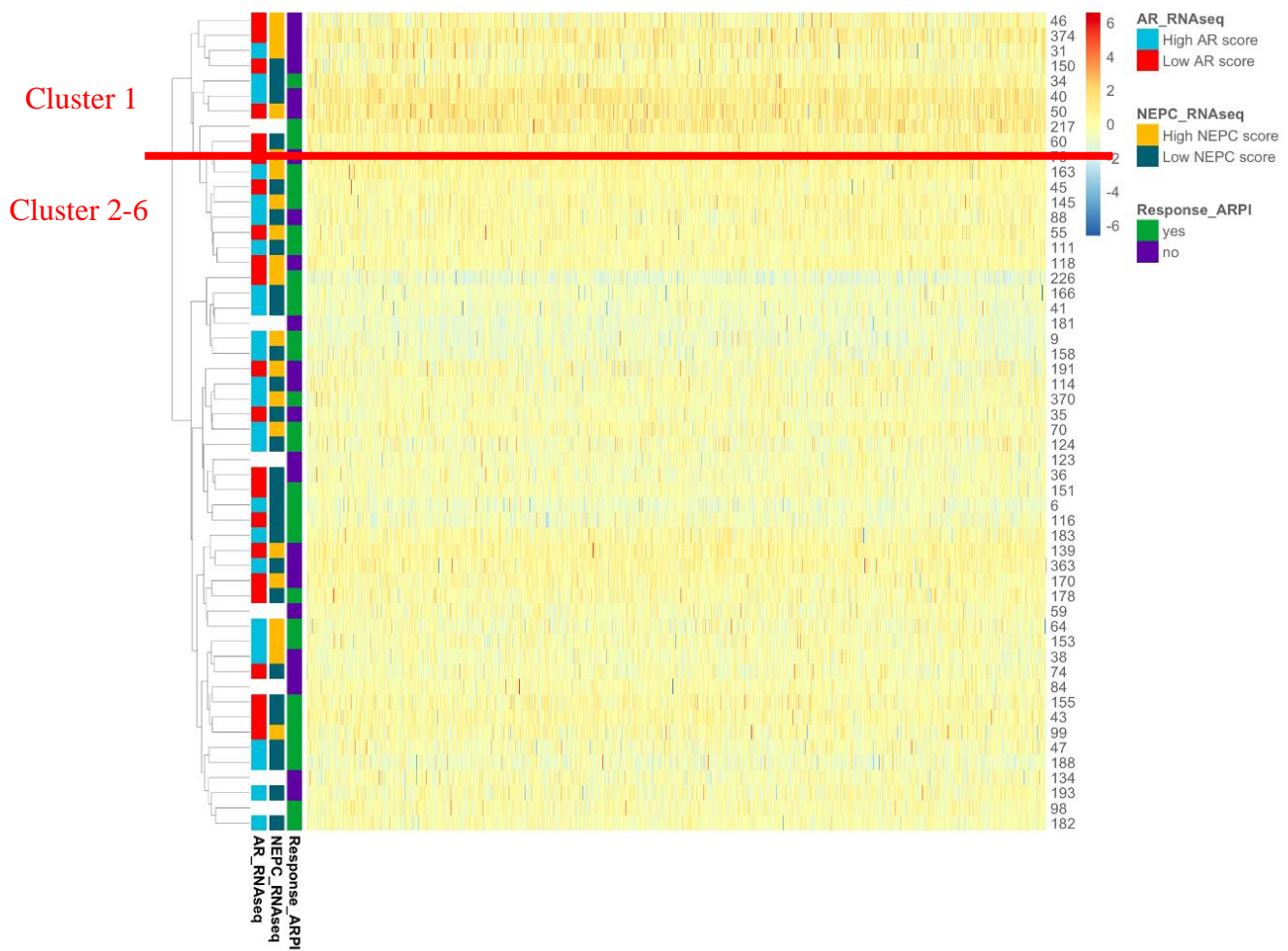


Figure 14: Heatmap for unsupervised clustering with ARPI, AR and NEPC RNAseq scores with 6 clusters (k=6).

i. PFS (cluster 1 vs 5 others)

Cluster 1 (n=7) showed a shorter median PFS of 2.2 months vs 8.4 for other patients (HR=5.197 CI95%[2.044-13.210], p<0.001, figure 15).

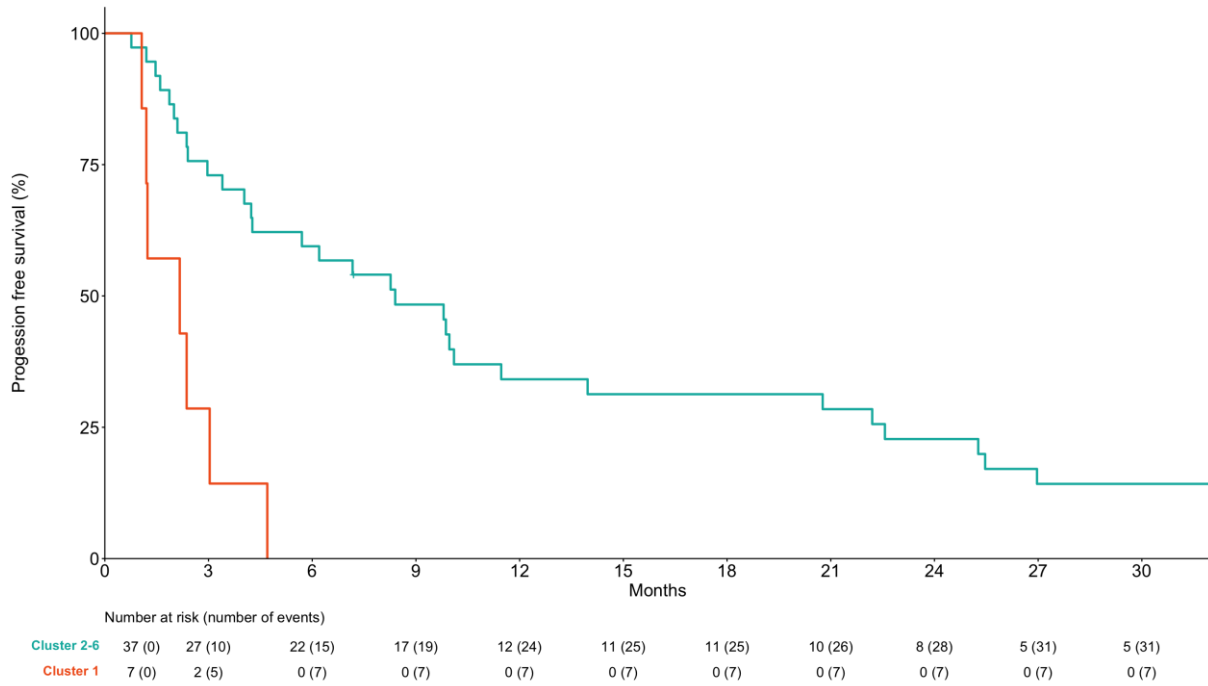


Figure 15: PFS according to clusters (k=6, Cluster 1 vs others).

ii. OS (cluster 1 vs 5 others)

Similar results were found for median OS with 8.1 months vs 22.7 (HR=10.12, CI95% [3.203-31.970], p<0.001, figure 16).

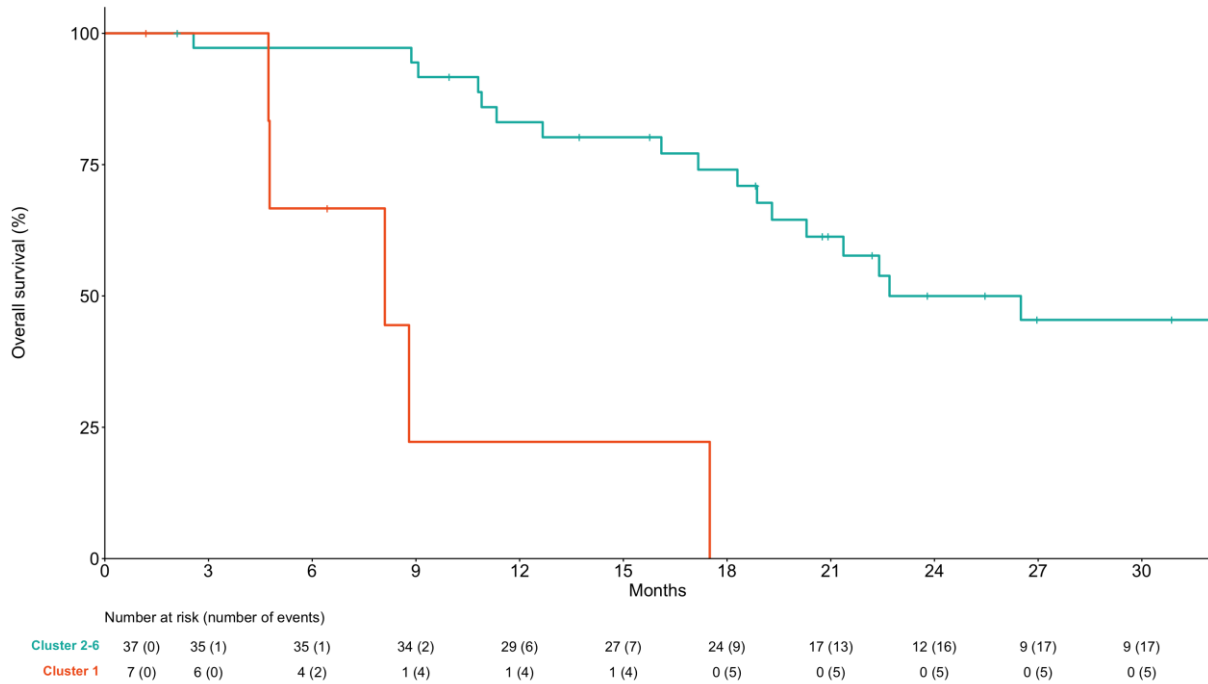


Figure 16: OS according to clusters (k=6, Cluster 1 vs others).

g. Differential expression baseline samples clustering cluster 1 vs 5 others (k=6)

Differential expression analyses on baseline samples in cluster 1 vs 5 others showed several overexpressed genes including OXCT1 (figure 17 & table 5)

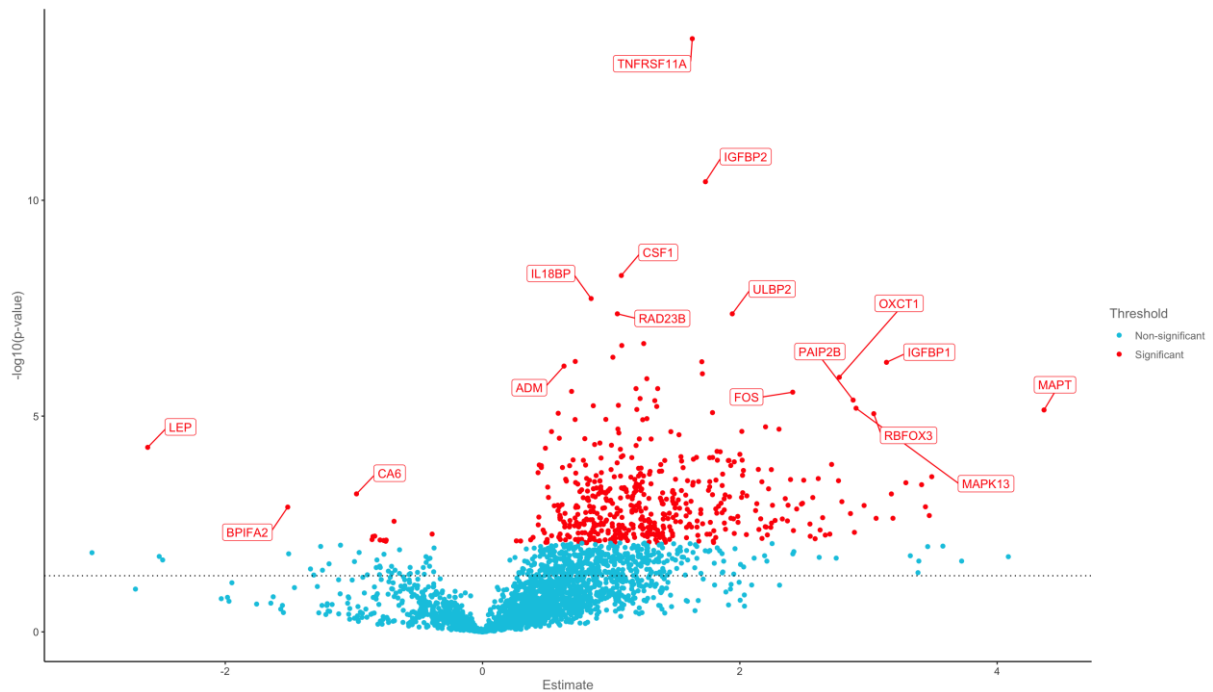


Figure 17: Proteins differential expression between samples in cluster 1 vs 5 others (overexpressed proteins in cluster 1 are on the right with a positive estimate).

Table 5: Proteins differential expression between samples in cluster 1 vs 5 others (overexpressed proteins in cluster 1 are on the right with a positive estimate).

Assay	Panel	Estimate	Cluster 1k6	Cluster 2plusk6	Adjusted_pval	Threshold
TNFRSF11A	Inflammation	1.63031558441558	2.65504285714286	1.02472727272727	5.21897056593715e-11	Significant
IGFBP2	Cardiometabolic	1.73265779220779	2.33787142857143	0.605213636363636	5.38130255520758e-08	Significant
CSF1	Inflammation	1.07896623376623	1.29985714285714	0.220890909090909	5.33874697591815e-06	Significant
IL18BP	Cardiometabolic	0.844107467532468	1.83831428571429	0.994206818181818	1.36966296629806e-05	Significant
RAD23B	Oncology	1.04786785714286	3.00184285714286	1.953975	2.06265193372049e-05	Significant
ULBP2	Neurology	1.94130649350649	2.73824285714286	0.796936363636364	2.06265193372049e-05	Significant
FKBP4	Neurology	1.25275454545455	3.4665	2.21374545454545	8.38267071625509e-05	Significant
PCDH17	Cardiometabolic	1.08222207792208	2.46458571428571	1.38236363636364	8.38267071625509e-05	Significant
PAG1	Cardiometabolic	1.01311623376623	3.35365714285714	2.34054090909091	0.00013717051625849	Significant
CLECSA	Cardiometabolic	0.720655844155844	1.55422857142857	0.833572727272727	0.00013717051625849	Significant
LRG1	Inflammation_II	1.70451655844156	2.00491428571429	0.300397727272727	0.00013717051625849	Significant
IGFBP1	Cardiometabolic	3.14003668831169	2.72715714285714	-0.412879545454545	0.00013717051625849	Significant
ADM	Oncology	0.633158441558441	3.54368571428571	2.91052727272727	0.000154650358266157	Significant
COX6B1	Cardiometabolic_II	1.70905324675325	1.77957142857143	0.0705181818181819	0.000216300453952731	Significant
OXCT1	Cardiometabolic_II	2.77334253246753	5.94508571428571	3.17174318181818	0.000243917488513278	Significant
FBLN2	Cardiometabolic_II	1.27690649350649	2.07124285714286	0.794336363636364	0.000246456212809082	Significant
FDX1	Cardiometabolic_II	1.36150422077922	2.03354285714286	0.672038636363636	0.000371831647919983	Significant
ORM1	Inflammation_II	1.19291525974026	1.63068571428571	0.437770454545455	0.000371831647919983	Significant
PHOSPHO1	Neurology	0.692057142857143	1.28525714285714	0.5932	0.000404608595433766	Significant
FOS	Oncology_II	2.41108376623377	3.96574285714286	1.55465909090909	0.000404608595433766	Significant

h. Gene set enrichment analyses (GSEA)

i. Non-responder vs responder

Figure 18 shows the pathways significantly enriched in no responder patients compared to responder.

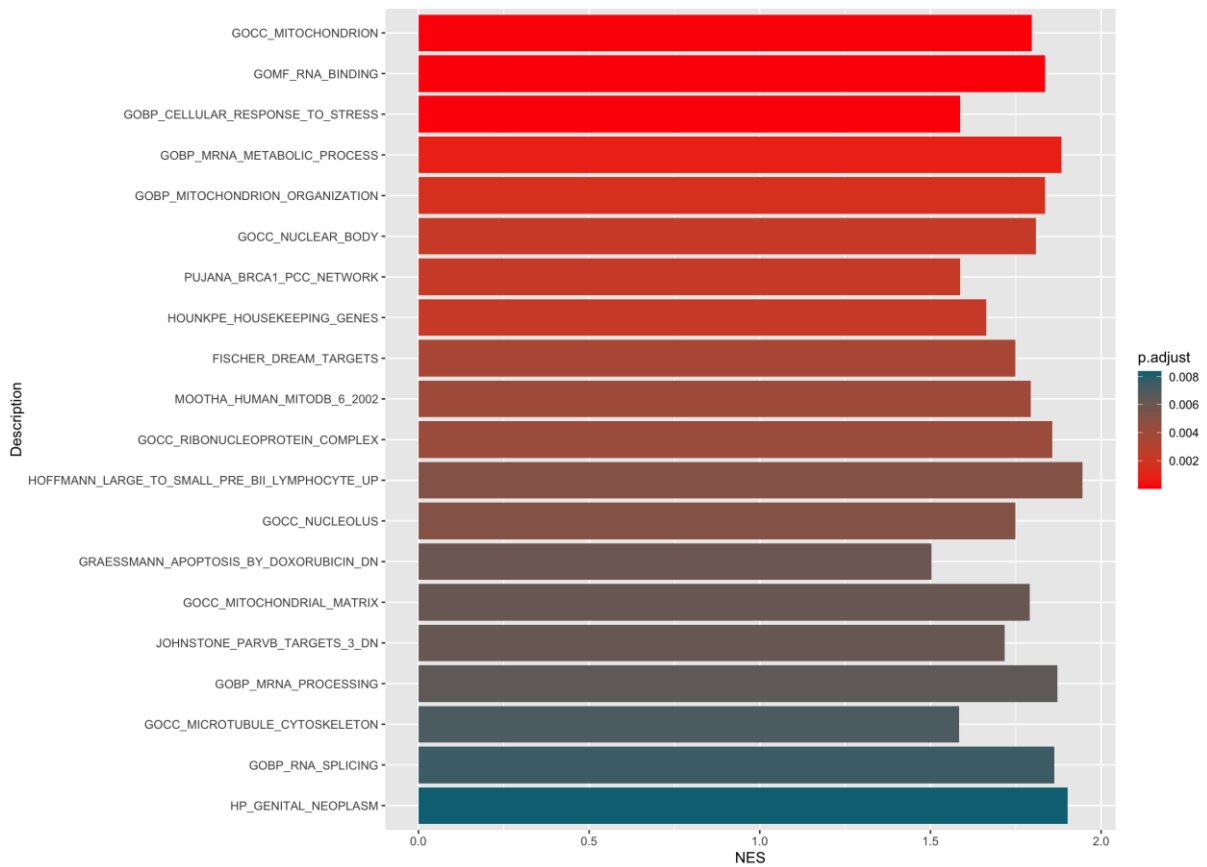


Figure 18: GSEA analyses in no responder patients compared to responder using KEGG, GO and Reactome.

ii. Progression vs baseline samples

Figure 19 shows the pathway enriched in samples at progression on right and the pathways enriched in baseline sample on the left.

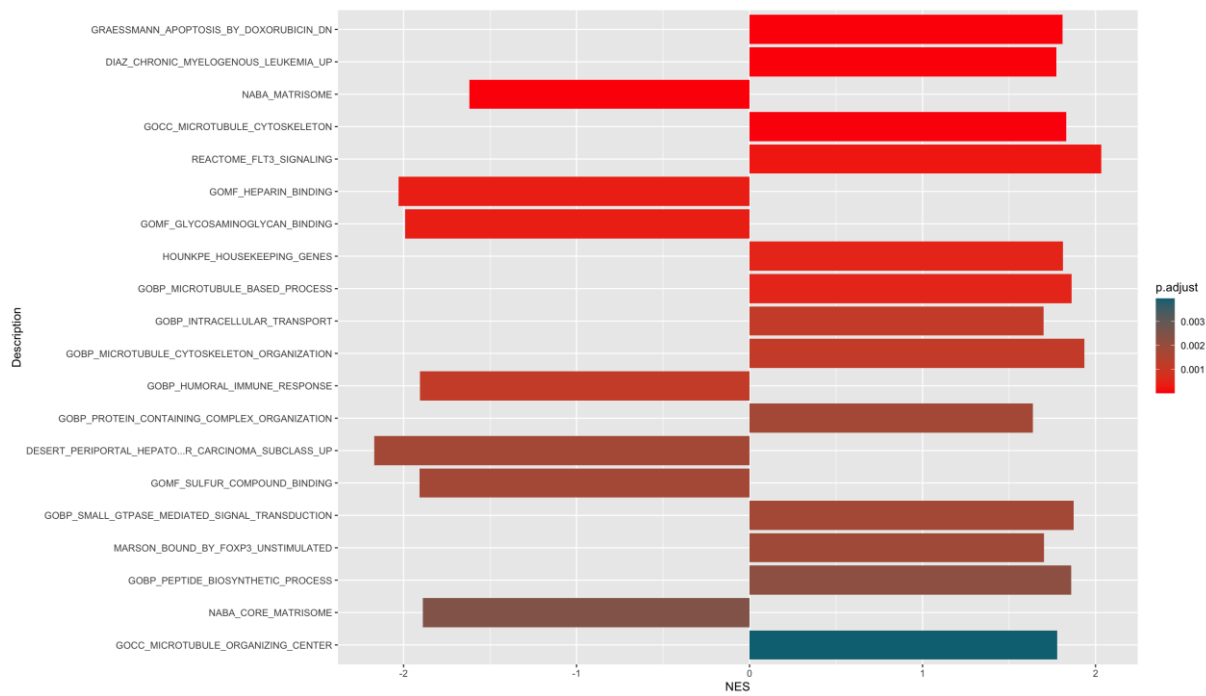


Figure 19: GSEA analyses samples at progression compared to baseline using KEGG, GO and Reactome.

iii. Cluster 1 vs 5 others

Figure 20 shows the pathways enriched in cluster 1 vs the 5 other clusters.

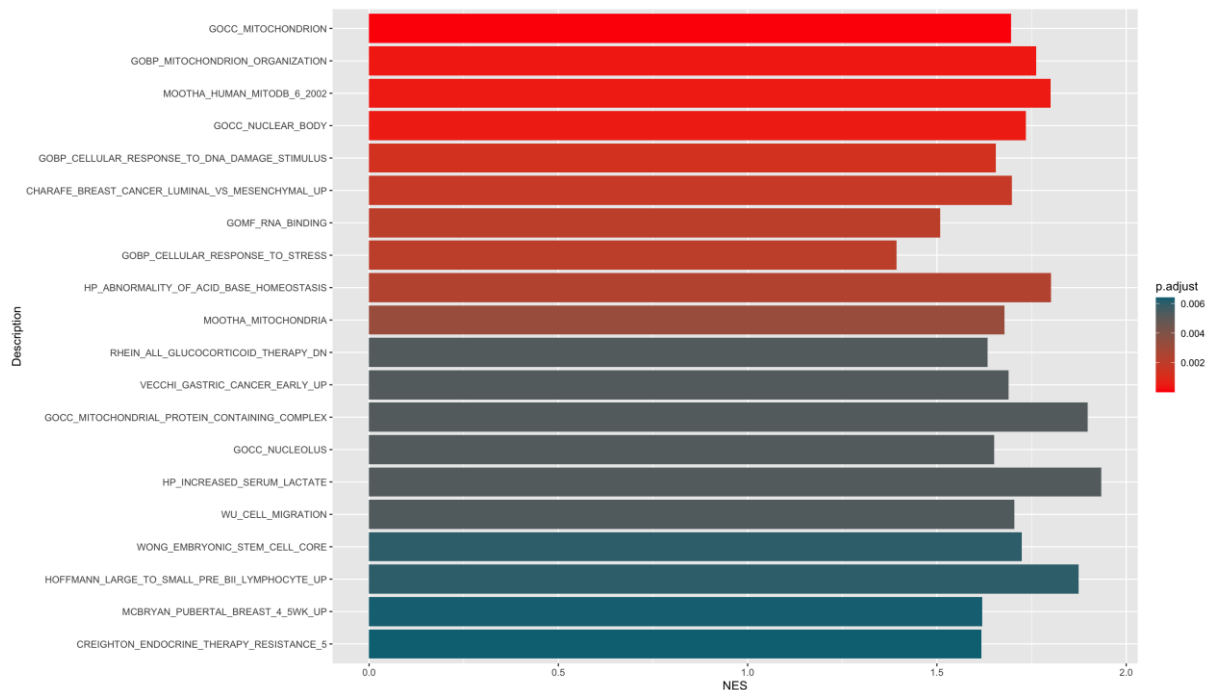


Figure 20: GSEA analyses samples of cluster 1 compared to cluster 2-6 using KEGG, GO and Reactome.

i. ELISA assay

i. Protein dosage compared between non-responder and responder in pg/ml

In the non-responder group, median OXCT1 concentration was 51.9 pg/ml (range: 12.3 – 830.4) vs 43.6 (range: 28.94-131.5) in the responder group without statistical difference $p=0.26$ using t-test (figure 21).

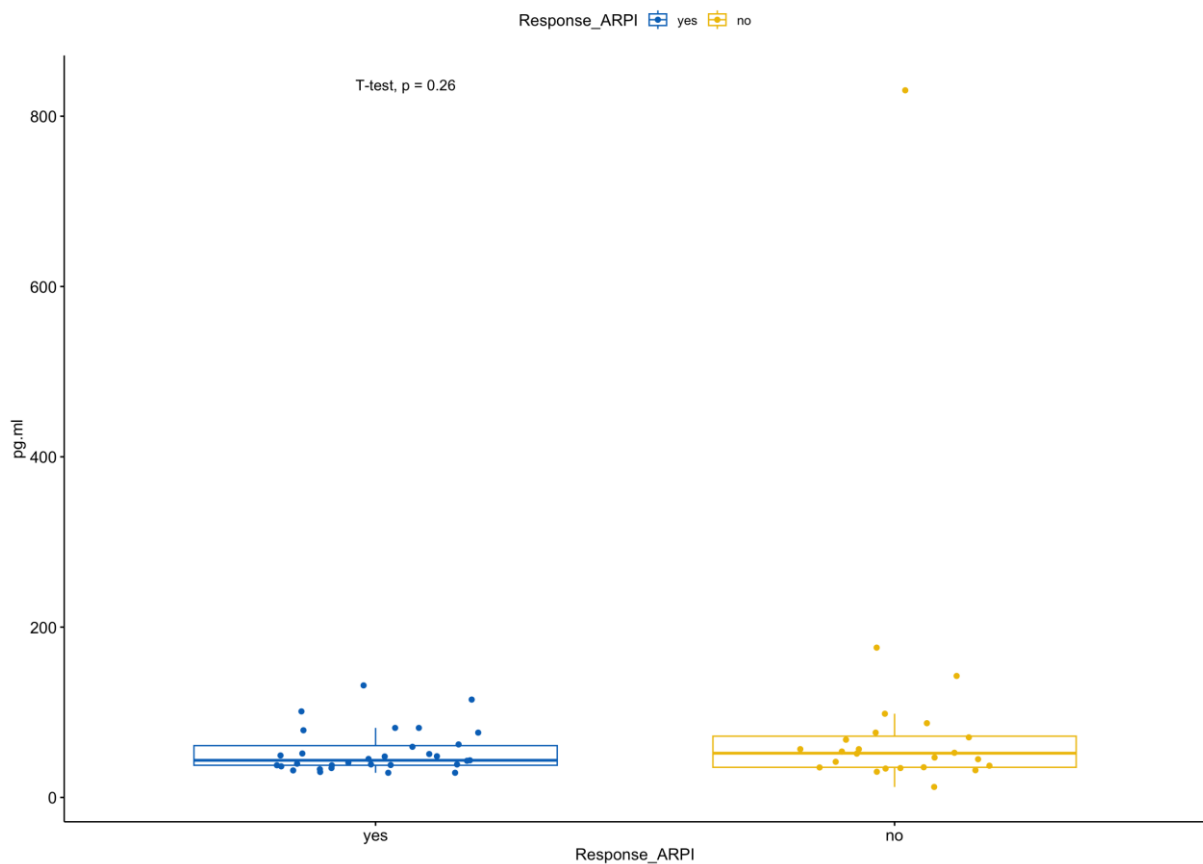


Figure 21: Boxplot of OXCT1 dosage using ELISA assay in pg/ml with median and interquartile range.

ii. Survival analyses according to OXCT1 expression level

1. PFS

Patients with high OXCT1 level had a shorter PFS of 4.13 vs 8.4 for patients with low level of OXCT1 without statistical significance (HR= 1.490, CI95[0.801-2.772], $p=0.205$, figure 22)

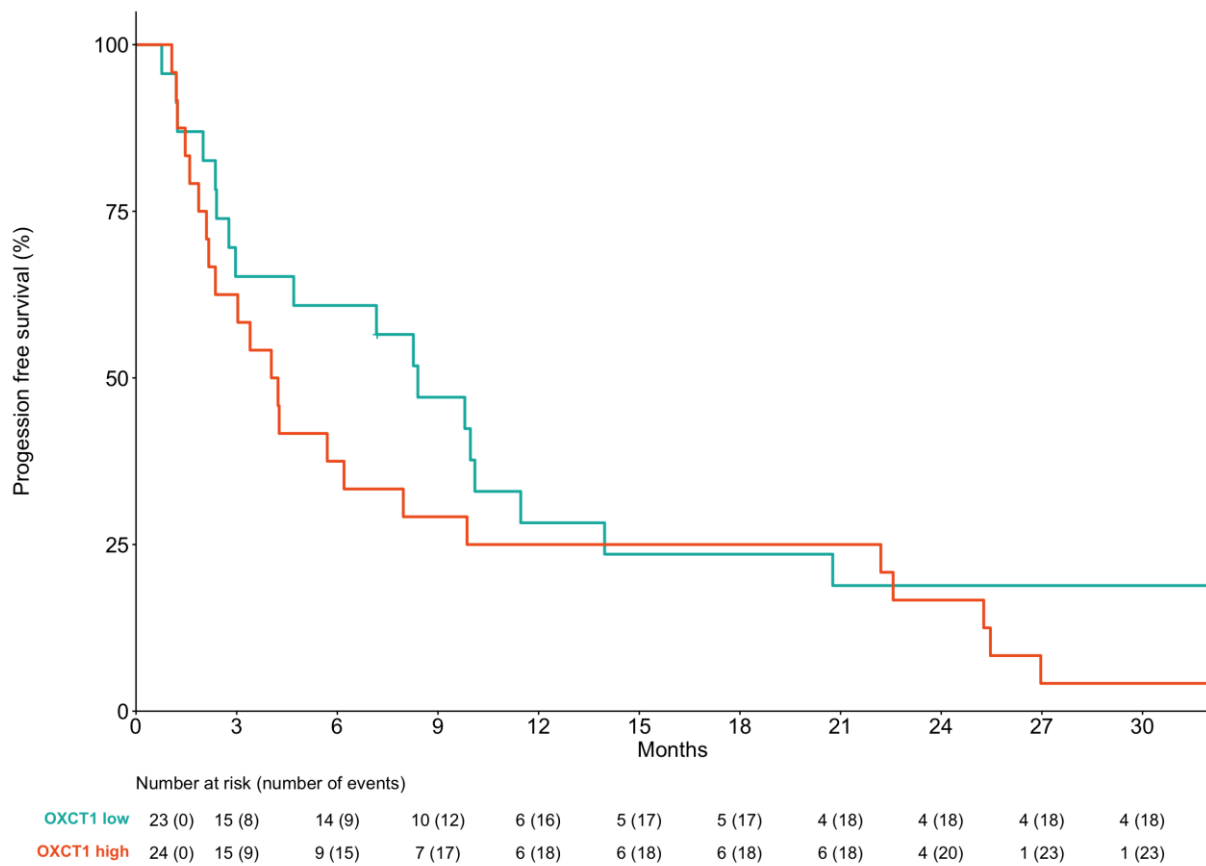


Figure 22: PFS according to OXCT1 expression (high vs low) with ELISA assay measurement.

2. OS

Median overall survival was shorter in patients with low OXCT1 expression with 20.3 vs 26.5 months without statistical significance difference (HR= 1.560, CI95[0.665-3.678], p=0.302, figure 23).

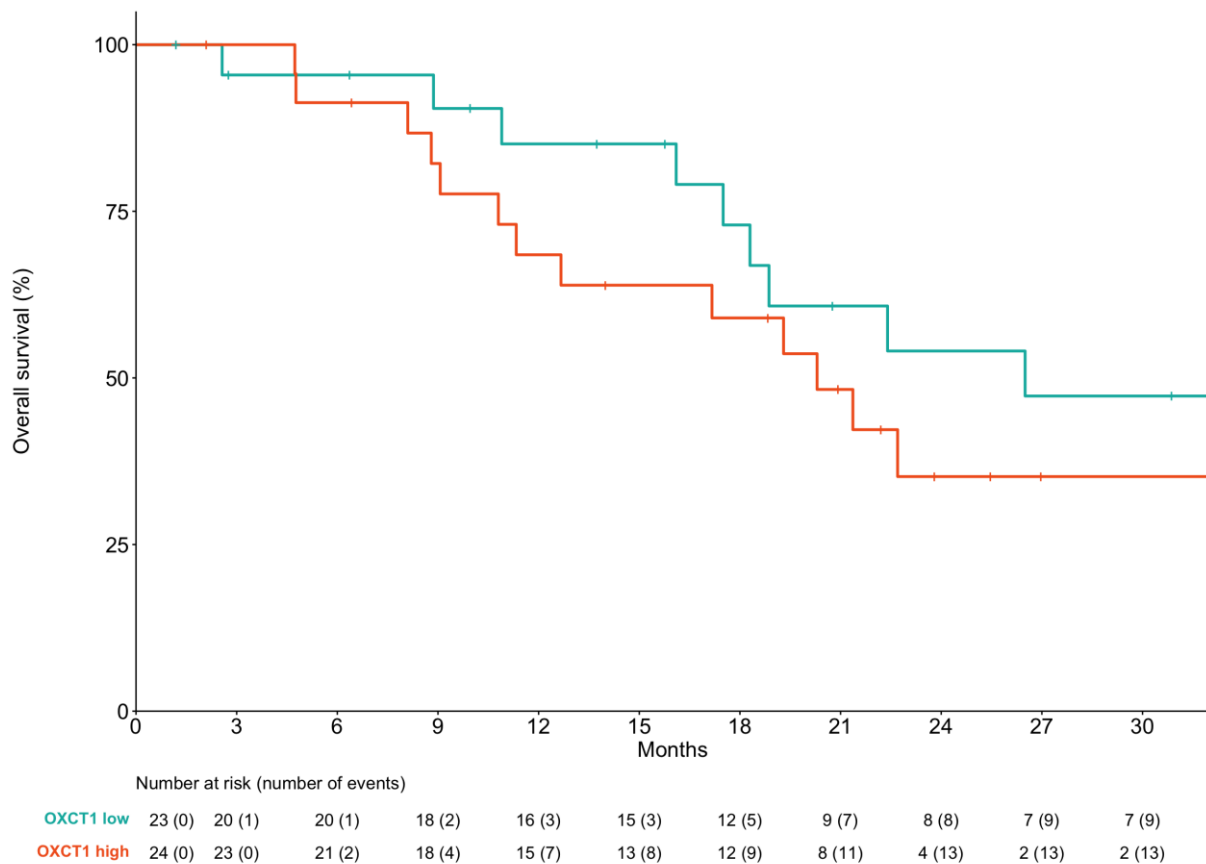


Figure 23: OS according to OXCT1 expression (high vs low) with ELISA assay measurement.

j. PDX selection

OXCT1 (or SCOT) is involved in ketogenic metabolism for ketolysis of ketones body in extrahepatic mitochondria. OXCT1 is upregulated by starvation and its activity may play a role in tumor growth and metastasis. ACAT1 also play a role in further steps of ketolysis by converting AcAc-CoA produced by SCOT in acetyl-CoA. ACAT1 and OXCT1 increased expression has both been reported in mCRPC (figure 24)⁴.

Figure 26: ACAT1 (on the left) and OXCT1 (on the right) expression in IHC found for MR-0009.

k. PDX treatment

Because no OXCT1 is available, we selected an ACAT1 inhibitor, arecoline hydrobromide, which disrupts ACAT1 tetramers by binding (figure 27)⁵.

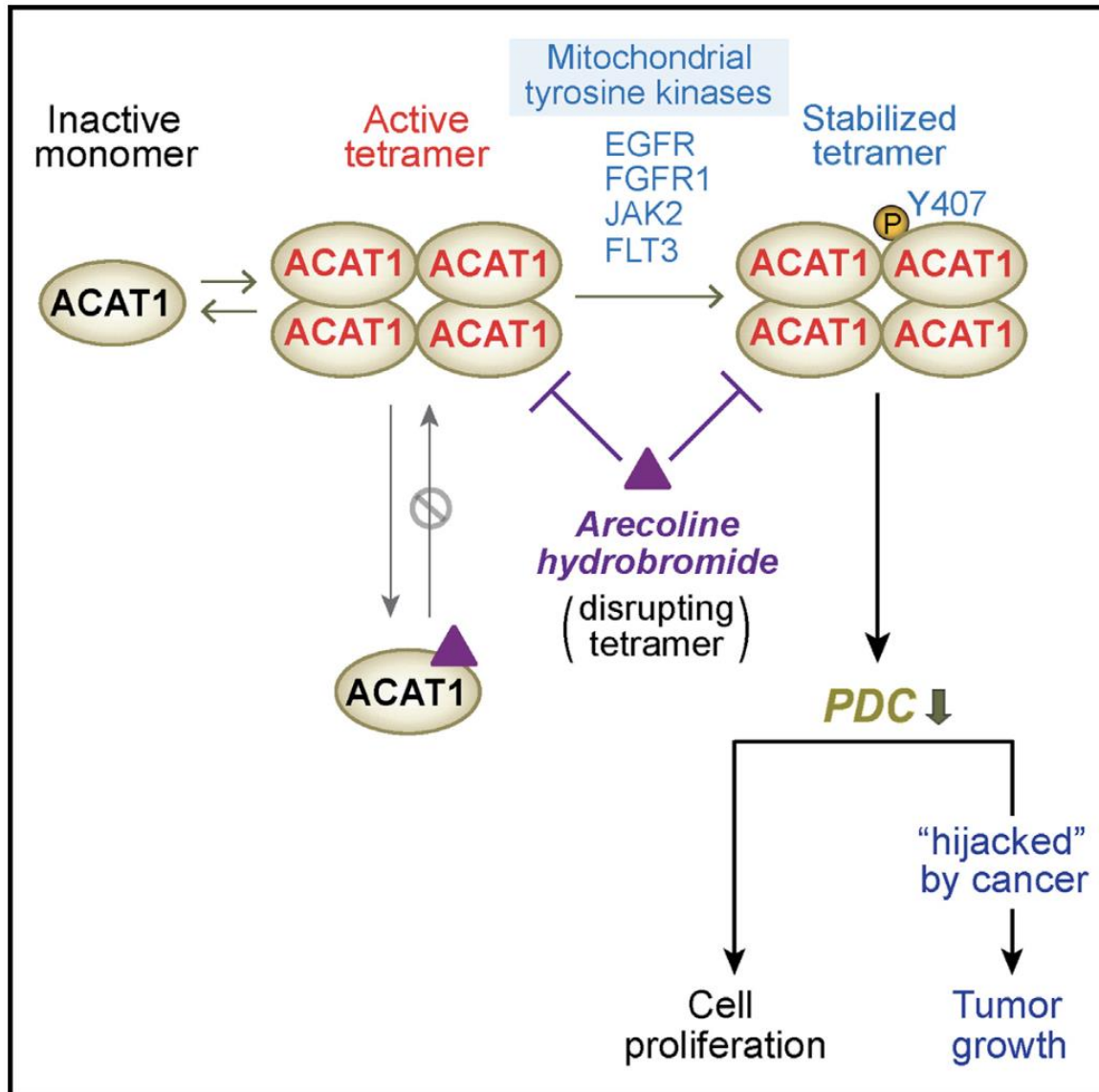


Figure 27: Arecoline hydrobromide mechanisms of action⁵.

Drugging of the MR-0009 nude mice model did not show any effect on PDX growth (figure 28).

MR-0009 ACAT1+ and OXCT1+

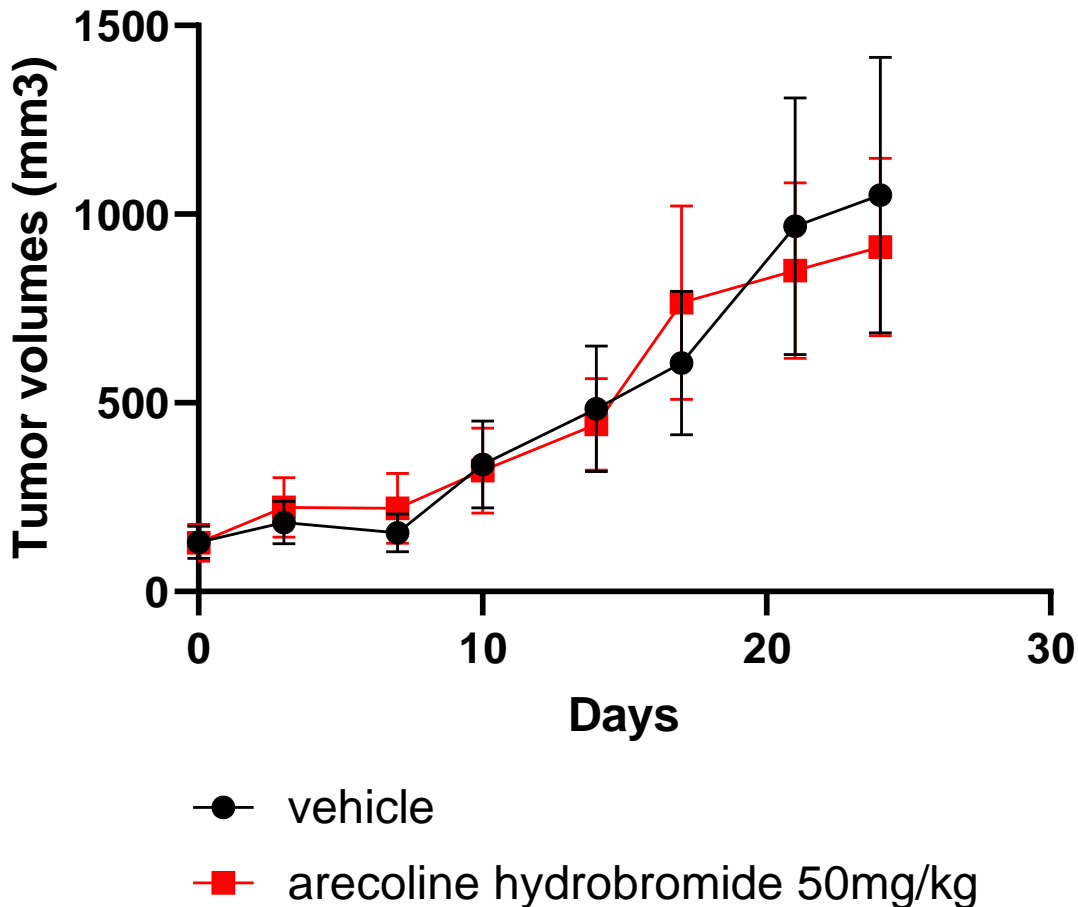


Figure 28: Effect of arecoline hydrobromide on tumor growth in MR-0009 PDX.

1. Menssouri N, Poiraudau L, Helissey C, et al. Genomic profiling of metastatic castration-resistant prostate cancer samples resistant to androgen-receptor pathway inhibitors. *Clin Cancer Res*. Published online June 26, 2023:CCR-22-3736. doi:10.1158/1078-0432.CCR-22-3736
2. Minas TZ, Candia J, Dorsey TH, et al. Serum proteomics links suppression of tumor immunity to ancestry and lethal prostate cancer. *Nat Commun*. 2022;13(1):1759. doi:10.1038/s41467-022-29235-2
3. Wu T, Hu E, Xu S, et al. clusterProfiler 4.0: A universal enrichment tool for interpreting omics data. *Innovation (Camb)*. 2021;2(3):100141. doi:10.1016/j.xinn.2021.100141
4. Hwang CY, Choe W, Yoon KS, et al. Molecular Mechanisms for Ketone Body Metabolism, Signaling Functions, and Therapeutic Potential in Cancer. *Nutrients*. 2022;14(22):4932. doi:10.3390/nu14224932

5. Fan J, Lin R, Xia S, et al. Tetrameric Acetyl-CoA Acetyltransferase 1 Is Important for Tumor Growth. *Mol Cell*. 2016;64(5):859-874. doi:10.1016/j.molcel.2016.10.014

Annex 2: first draft article

Characterization of de novo metastatic prostate cancer: an ancillary study of the PEACE-1 phase 3 clinical trial

Authors:

Cedric Pobel¹, Charlotte Bargain², Etienne Rouleau³, Bastien Job⁴, Jean-Yves Scoazec⁵, David Gentien⁶, Elodie Edmond⁷, Guilhem Roubaud⁸, Philippe Ronchin⁹, Stéphane Supiot¹⁰, Ali Hasbini¹¹, Marlon Silva¹², Aude Fléchon¹³, Brigitte Laguerre¹⁴, Sophie Abadie-Lacourtoisie¹⁵, Claude El Kouri¹⁶, Loïc Mourey¹⁷, Tristan Maurina¹⁸, Etienne Martin¹⁹, Loic Poiraudou¹, Ludovic Bigot¹, Patrick Saulnier⁶, Hélène Ribault²⁰, Alice Bernard-Tessier²¹, Fabrice Andre²¹, Stéphanie Foulon², Karim Fizazi²¹, Yohann Lorient²¹

Affiliations:

¹INSERM U981, Institut Gustave Roussy, Villejuif, France.

²Biostatistics and Epidemiology Office, Gustave Roussy - Cancer Campus, Villejuif, France.

³Tumor Genetics Dept., Gustave Roussy- Cancer Campus, Villejuif, France.

⁴Inserm US23, Plateforme de Bioinformatique, Gustave Roussy, 94805, Villejuif, France.

⁵Pathology Dept., Institut Gustave Roussy, Villejuif, France.

⁶AMMICA Platform, INSERM US23, CNRS UAR 3655, AMMICA, Villejuif, France.

⁷Experimental and Translational Pathology Platform (PETRA), AMMICA Inserm US23/UAR CNRS 3655, Gustave Roussy Institute, Villejuif, France.

⁸Medical Oncology, Institute Bergonié, Bordeaux, France.

⁹Radiotherapy, Centre Azuréen de Cancérologie, Mougins, France.

¹⁰Radiotherapy, ICO Institut de Cancérologie de l'Ouest René Gauducheau, Saint-Herblain, France.

¹¹Radioterapy, Clinique Pasteur, Brest, France.

¹²Radiotherapy, Centre Francois Baclesse, Caen, Cedex, France.

¹³Medical Oncology Department, Centre Leon Berard, Lyon, France.

¹⁴Medical oncology, Centre Eugene - Marquis, Rennes, France.

¹⁵Medical oncology, Centre Paul Papin, Angers, France.

¹⁶Medical oncology, Centre Catherine de Sienne, Nantes, France.

¹⁷Medical Oncology, IUCT - Institut Universitaire du Cancer de Toulouse - Oncopole, Toulouse, France.

¹⁸Medical oncology, CHRU Besancon-Hopital Jean Minjoz, Besancon, France.

¹⁹Radiotherapy, Centre Georges-François Leclerc, Dijon, France.

²⁰R&D, Unicancer, Paris, France.

²¹Cancer Medicine Department, Institut Gustave Roussy, Villejuif, Cedex, France

Abstract

Introduction

De novo metastatic castration sensitive prostate cancer (*dnmCSPC*) represents 5–10% of PC diagnoses but causes 50% of PC-related deaths. In this ancillary study of the PEACE1 trial, we hypothesized that aggressive or neuroendocrine-like variants could be detected at diagnosis.

Materials and methods

We centrally retrieved paraffin-embedded biopsies at diagnosis for immunochemistry (IHC), next generation sequencing (NGS) and transcriptomic analyses.

Results

The expression in IHC of neuroendocrine markers was independently associated with a shorter overall survival (OS) for 26.2% of patients (HR=1.53, CI95%[1.14-2.06], p=0.005). The alteration of at least 2 genes among *TP53*, *PTEN* and/or *RBI* in NGS and a higher NEPC z-score in transcriptomic were independently associated with a shorter OS (HR=2.63, CI95%[1.10-6.30], p=0.03 and HR=1.63, CI95[1.02-2.63], p=0.042 respectively).

Conclusion

Altogether, we showed at a multiple omics level that neuroendocrine features are present at diagnosis in *dnmCSPC* and are associated with worse prognosis.

Keywords: prostatic neoplasms, prognosis, biomarkers, translational medicine, multiomics, neuroendocrine cell

1. Introduction

Prostate cancer is known to be the most frequently occurring cancer in men but only the third cause of cancer death after lung and colorectal cancers¹, due to its relatively better outcomes. However, *de novo* metastatic prostate represents 5–10% of total prostate cancer diagnoses but are causing almost 50% of prostate cancer-related deaths. This epidemiologic characteristic probably reflects their higher aggressiveness compared to localized prostate cancer secondarily evolving to metastatic relapse². The incidence of *de novo* metastatic castration-sensitive prostate cancer (mCSPC) has dramatically declined since the 1990's thanks to prostate-specific antigen (PSA) screening. Nevertheless, this trend has come to halt, which is potentially related to a reduction in prostate-specific antigen (PSA) screening³. This stagnation could be linked to the fact that some of these mCSPC exhibit aggressive features leading to a rapid metastatic evolution, even before any prostate-related urinary symptoms emerge.

Historically, affected men were managed with systemic androgen deprivation therapy (ADT) alone. Recent phase 3 data support treatment combination with taxane chemotherapy or androgen receptor (AR) targeted therapies such as abiraterone acetate or enzalutamide⁴⁻⁶. Both strategies (combining ADT and docetaxel or combining ADT + abiraterone acetate) are now standard of care for these patients. More recently, the PEACE-1 clinical trial found a beneficence from treatment with ADT + AA + docetaxel vs ADT + docetaxel⁷. However, all patients eventually progress regardless of initial therapy with variable response to treatment between individuals.

A part from the classic and more frequent adenocarcinoma, neuroendocrine prostate cancer (NEPC) are of worse prognosis and their diagnosis is based on morphology helped if needed by NE markers (i.e. synaptophysin, chromogranin and/or CD56)⁸. Even if pure NEPC are rare at diagnostic, NE transdifferentiation happen in up to 20-30% of mCRPC. Another form of non-NE but more aggressive prostate cancer with poorer response to treatment could be found. This type of cancer is clinically defined by younger age at diagnosis, visceral rather than only bone metastasis, lytic rather than osteoblastic bone lesions and relatively low PSA. In immunohistochemistry (IHC), these NE or aggressive forms of prostate cancer are characterized by at least one NE marker positivity and a certain level of AR expression loss. At a molecular level, lineage plasticity linked to *TP53*, *PTEN* and/or *RBI* alterations with other epigenetic mechanisms have been reported in this more aggressive subtype⁹.

All these biological mechanisms and biomarkers have been widely assessed in mCRPC but less in *de novo* mCSPC. In this presentation of prostate cancer with a worse prognostic, mechanisms of aggressivity linked to AR bypass or NEPC differentiation could probably be detected at an early event from diagnosis. For these reasons, we aimed to perform multiomic analysis on baseline samples of patients treated in this setting who were included in the PEACE1 trial. Our objectives were to identify biomarkers present in prostate cancer cells pre-treatment to predict patient outcomes and decipher the genomic landscape of *de novo* mCSPC.

2. Results

i. Descriptive analysis

Overall cohort

Of the 1172 patients full trial population randomized in PEACE-1 (NCT01957436), 745 patients from France consented to this ancillary study. Paraffin-embedded samples were

collected for 595 pts (80%) and centrally reviewed. Phenotypic analyses were performed on 394 patients, genomic on 180 and transcriptomic on 243 (figure 1).

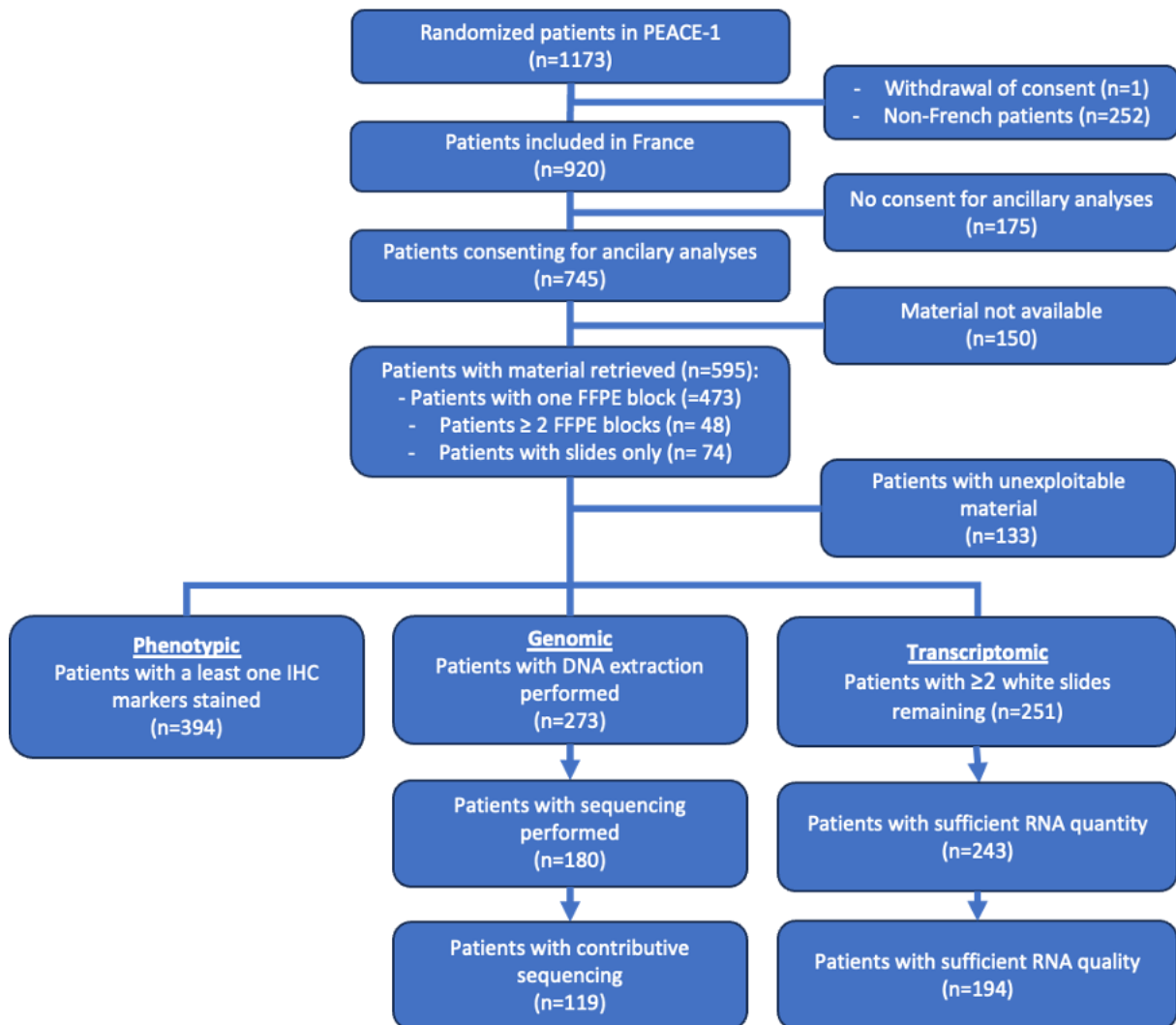


Figure 1: flowchart. HES: Hematoxylin eosine safran, IHC: immunochemistry.

The distribution of clinical variables was similar between the full trial, phenotypic, genomic, transcriptomic and pathomic populations (Supplementary data table 1).

Most of the biopsies at baseline were prostate cores for 185 patients (86.9%), transurethral resection of the prostate for 51 (8.6%), bone metastases for 10 (1.7%), lymph nodes for 8 (1.3%), prostatectomies for 2 (0.3%), liver metastases for 2 (0.3%) and lung metastases for 1 (0.2%). Other biopsies were less frequent (supplementary table 2).

Phenotypic analysis

Among the 394 patients with a contributive IHC, only 60 (10.1%) had an interpretable PTEN marker due to technical difficulties. Therefore, PTEN was excluded from analyses. AR negative tumor was found for 8 patients (2.1%), synaptophysin positive for 72 (18.8%), CD56 for 41 (11.2%), chromogranin A for 102 (73.8%). At least one NEPC markers (NEPCmk) among these 3 was positive in 102 patients (26.2%). IHC marker expressions are illustrated in figure 2 and

other markers detailed results are summarized in supplementary data table 3 and figure 1. Phenotypes were AR luminal high for 150 patients (38.1%), AR luminal weak for 97 (24.6%), amphicrine for 95 (24.1%), double negative for 3 (0.8%) and NEPC for 5 (1.3%).

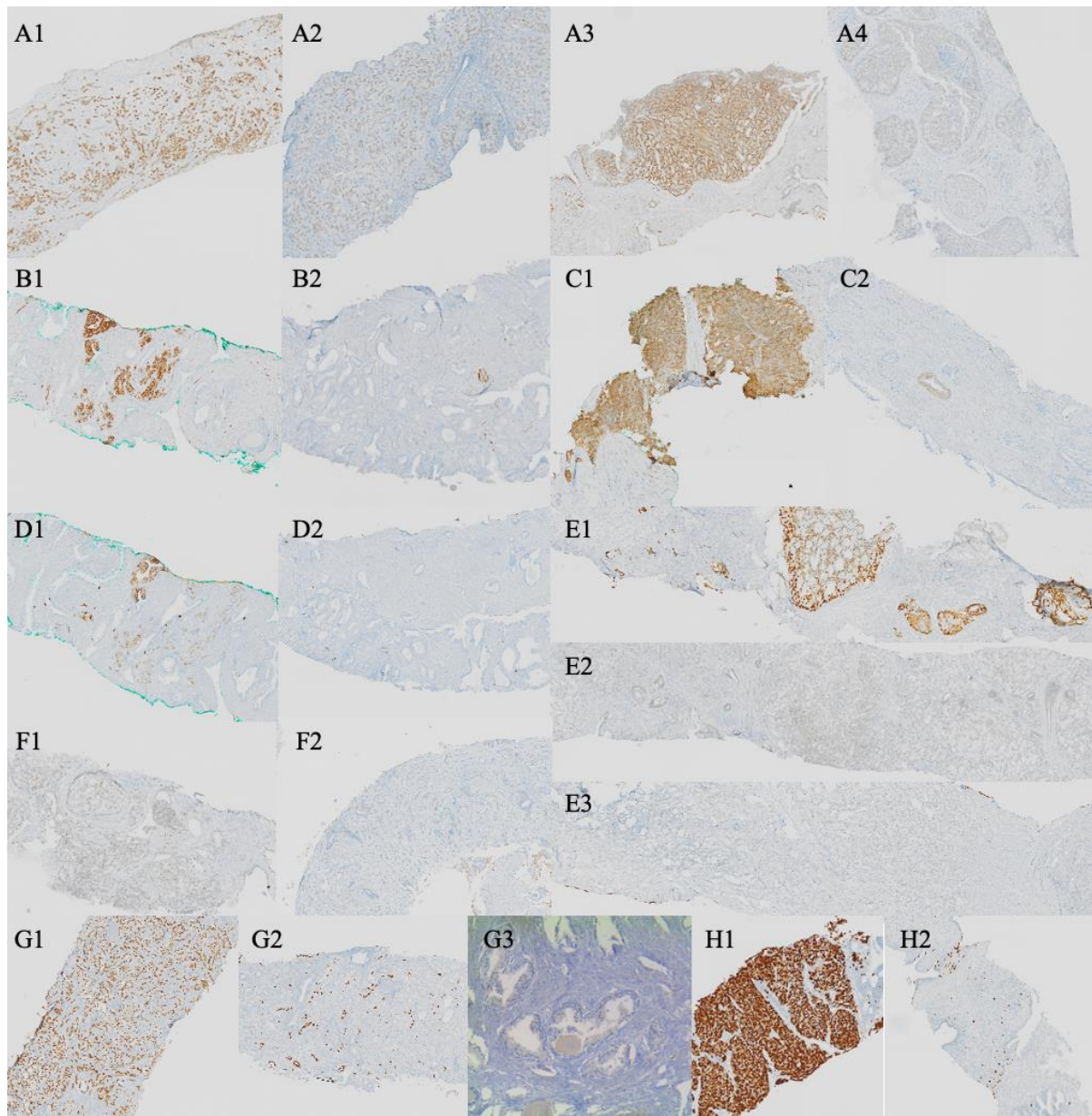


Figure 2: IHC expression.

A1: AR positive, A2: AR weak, A3: AR positive cytoplasmic and nuclear, A4: AR negative

B1: Synaptophysin positive, B2: Synaptophysin negative,

C1: CD56 positive, C2: CD56 negative,

D1: Chromogranin positive, D2: Chromogranin negative,

E1: p53 positive, E2: p53 normal, E3: p53 null,

F1: Rb1 positive, F2: Rb1 negative,

G1: ERG positive, G2: ERG negative with border cell positive (positive control), G3: ERG negative with border cell negative (positive control negative),

H1: Ki67 high at 95%, H2: Ki67 low at 2%.

Genomic analysis

In total, 273 patients had material extraction for sequencing. Among them, 180 had a sufficient quantity of DNA for sequencing. Twenty patients were sequenced by oncodeep panel with 9 contributive and 160 patients were sequenced by the Cancer core Europe panel with 110 contributive. At the end, sequencing was interpretable for 119 patients (i.e 43.6% of 272 extracted and 66.1% of 180 sequenced, figure 1 flowchart). We found 183 single nucleotide variants (SNVs), 17 copy number variation (CNVs) with 15 deletion and 3 amplifications among these patients (supplementary data table 4). All patients had a microsatellite stability (MSS) status. Most frequent alterations involved *TP53*, *PTEN*, *CDK12*, *ATM*, *BRCA2*, *APC*, *SPOP*, *CREBBP*, *PIK3CA*, *MUTYH* and *RBI*. Only one patient had an *AR* mutation. (supplementary data figure 4, table 5 & 6). When looking at alterations per patients, no cluster was found to be visually associated with tumor burden (supplementary data figure 5) nor PSA response at 8 months ≥ 0.2 ng/ml (supplementary data figure 6).

No correlation was found between each of the most frequent alterations even when compared with the tumor suppressor genes signature i.e. 2 genes altered among *TP53*, *PTEN* or *RBI* (TSalt) and DNA repair alterations (*BRCA1*, *BRCA2*, *ATM*, *CDK12* or *CHEK2*) as shown in supplementary table 7 & 8.

j. Prognostic values

Phenotypic analysis

AR luminal high and AR luminal low had a median OS of 5.7 and 4.8 years respectively. Amphicrine patients had a median OS of 4.0 years which is slightly shorter compared to other patients. NEPC phenotype had also the worse OS with a median of 1.1 years and double negative patients seemed to have a longer OS with a median of 5.5 but again limited by the number of patients (figure 3A). Adjusted cox model with imputation for rPFS and OS analyses for the phenotypes with enough patients are summarized in supplementary data figure 7, table 9 & 10.

When looking at the same data but focusing on each protein expression in multivariate analyses with data imputation, NEPCmk patients had a shorter OS (HR=1.53, CI95%[1.14-2.06], p=0.005). Regarding each NE markers, synaptophysin and chromogranin A positive patients had a OS (HR=1.62, CI95%[1.17-2.24], p=0.004 and HR=1.90, CI95%[1.18-3.06], p=0.009). CD56 positivity alone had no significant effect but a trend for worse OS (HR=1.90, CI95%[1.18-3.06], p=0.009). Patients with ERG-positive tumor had a longer rPFS (HR=0.71, CI95%[0.53-0.94], p=0.019) and p53 abnormality (positive or NULL) was associated with a shorter rPFS (HR=1.30 CI95%[1.01-1.68], p=0.041). No other IHC biomarker was found to influence outcomes (supplementary data table 11 to 14). Prognostic effects of each IHC markers are summarized in figure 3B.

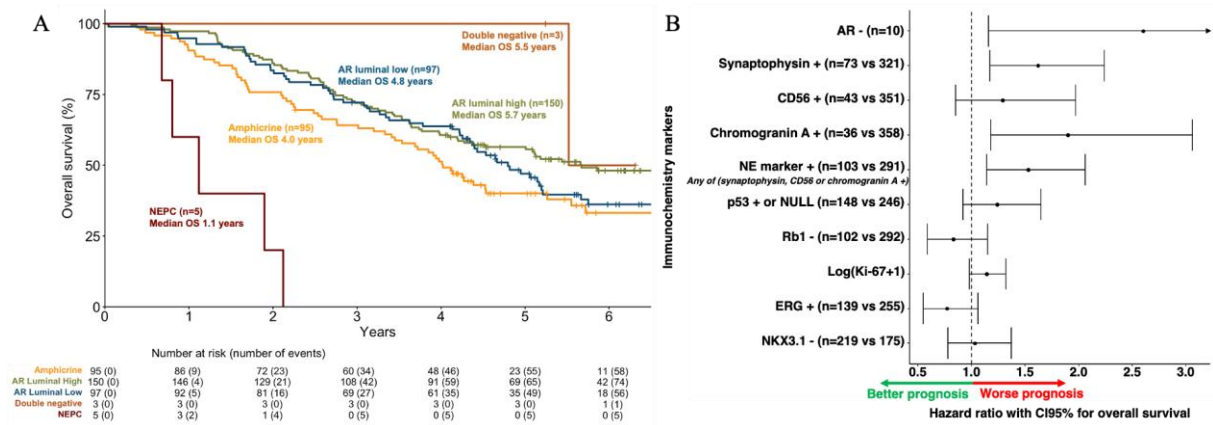


Figure 3: A: OS according to the 5 phenotypes with AR-high luminal (AR+ nuclear/NE-), AR-low luminal (AR+ nuclear weak or cytoplasmic/NE-), amphicrine (AR+/NE+), double-negative tumors (AR-/NE-) and NEPC (AR-/NE+). B: Forest plot of HR and their CI95% for each IHC markers with imputation and adjusted on age, ECOG, disease burden, Gleason, type of castration, and treatment received (radiotherapy, docetaxel and abiraterone).

Genomic analysis

The 9 TSalt patients had a shorter OS with a median of 2.2 years vs 5.4 (HR=2.63, CI95% [1.10-6.30], p=0.03, figure 4A). Patients with *BRCA1* or 2 alterations (n=11) had a tendency for shorter OS with a median of 3.1 years vs 5.4 (HR=2.10 CI95% [0.90-4.91], p=0.086, figure 4B). No other frequent alterations were found to influence rPFS or OS (supplementary table 15 & 16).

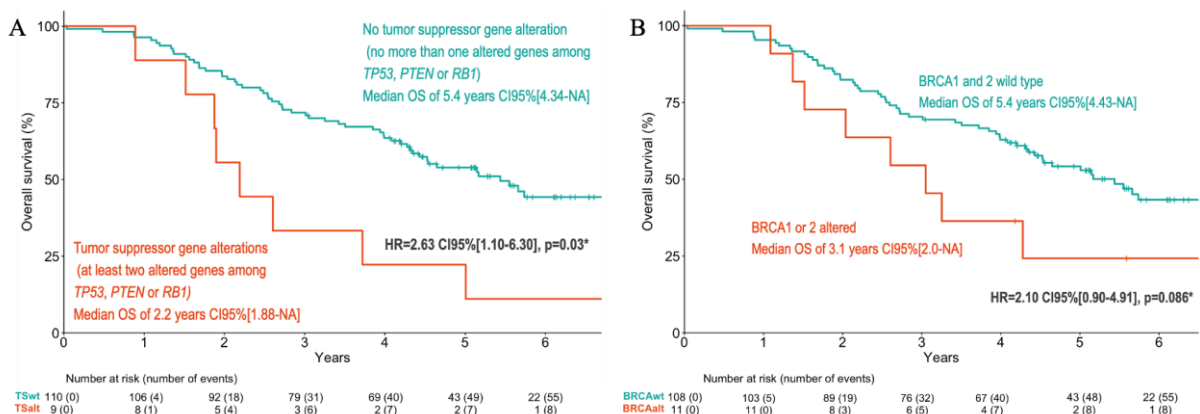


Figure 4: A: OS according to the alterations of two genes among the tumor suppressor *TP53*, *PTEN* or *RB1*. B: OS according to *BRCA* alterations (either *BRCA1* or 2).

*Adjusted on age, ECOG, disease burden, Gleason, type of castration, and treatment received (radiotherapy, docetaxel and abiraterone).

Transcriptomic analysis

When adjusted on age, ECOG, disease burden, Gleason, type of castration, and treatment received (radiotherapy, docetaxel and abiraterone), patients with a higher NEPC z-score had a shorter OS (HR=1.63, CI95[1.02-2.63], p=0.042) and patients with a higher AR z-score a longer OS (HR=0.61, CI95[0.42-0.89], p<0.001). The mitochondrial metabolism z-score was not associated with rPFS or OS (supplementary data table 17 & 18).

In non-responder (patients with a rPFS < 1 year) genes related to NEPC were overexpressed such as *AURKB*, *EZH2* and *E2F1* with an androgen response and a custom AR signature suppressed while E2F targets and G2M checkpoint pathways were activated. *ARG1*, and *HSD11B1* were the most overexpressed genes among others. In GSVA, our custom AR signature (with overexpressed genes only) was significantly less expressed in non-responder (p=0.001). In NEPCmk and TSalt patients, other NEPC genes were overexpressed with *SOX2*, *DLL3*, *TOP2A*, *DNMT1* and *KDM1A*. The same pathways in GSEA were found with the addition MYC targets V1 overexpression (figure 5). BRCA altered patients had only an overexpression of E2F pathway in GSEA (Supplementary data figure 8).

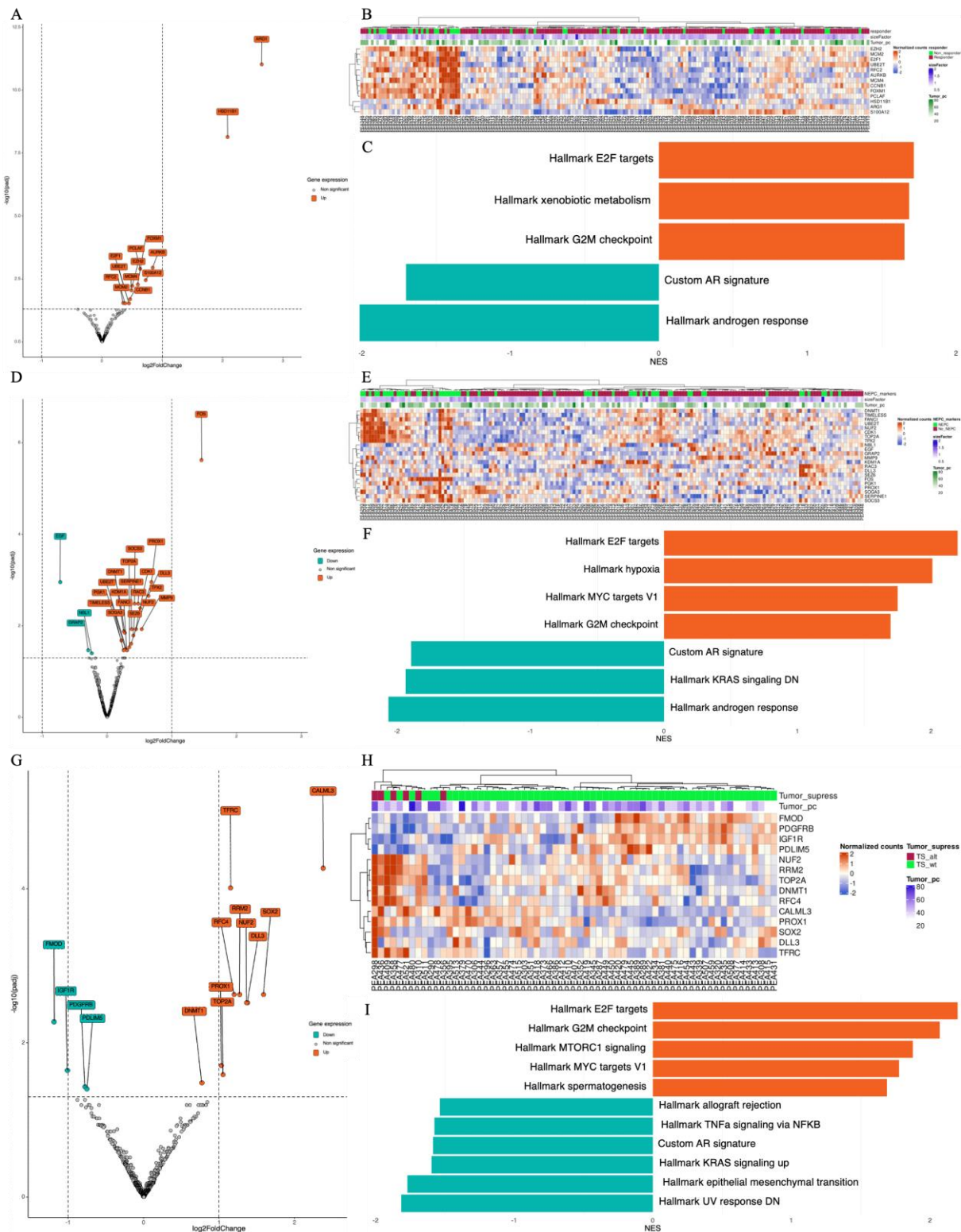


Figure 5: Transcriptomic analyses for non-responder, NEPCmk and TSalt patients. A: Volcano plot representing the differential gene expression of non-responder vs responder. B: Supervised clustering according to response to treatment (Euclidean algorithm). C: GSEA in non-responder vs responder patients. D: Volcano plot representing the differential gene expression of patients with NEPCmk positive vs others. E: Supervised clustering according to NEPCmk expression (Euclidean algorithm). F: GSEA in NEPCmk positive vs other patients. G: Volcano plot representing the differential gene expression of TSalt patients vs others. H: Supervised clustering according to TSalt (Euclidean algorithm). I: GSEA in TSalt vs other patients.

k. Predictive value

The predictive analyses were only planned for IHC biomarkers because of the larger number of patients expected to have contributive IHC. No predictive value to abiraterone response was found when adjusted using an interaction test for rPFS and OS (supplementary data table 19). The number of patients for each alteration and TSalt was not sufficient to assess predictive value for abiraterone benefit. Regarding the NEPC and AR z-scores, no predictive value for abiraterone benefit was found when adjusted on age, ECOG, disease burden, Gleason, type of castration, and treatment received (radiotherapy, docetaxel and abiraterone) using an interaction test for rPFS and OS.

l. Correlation with PSA response at 8 months and tumoral burden

Phenotypic analysis

A higher Ki67 was associated with a PSA response at 8 months (i.e. ≤ 0.2 ng/ml). The median in log scale [IQR] was 3.2 [2.5-3.6] for responder vs 2.7 [2.1-3.5] for non-responders, $p=0.025$. Regarding other IHC markers, no association was found with PSA response (supplementary data table 20). Similarly, none of the IHC marker was associated with disease burden (supplementary data table 21).

Genomic analysis

None of the gene alteration was associated with the PSA response at 8 months ≤ 0.2 ng/ml (supplementary data table 22). Patients with a low burden disease had more ATM mutations (80 vs 20%, $p=0.023$) but with a low number of patients. No other associations were found between alteration and disease burden (supplementary data table 23).

Transcriptomic analysis

ADH1A was the most overexpressed gene in patients without PSA response and high tumoral burden (Supplementary data figure 8 & supplementary excel).

m. Correlation between IHC and NGS

No correlation between TSalt and NEPCmk or NEPC phenotype was found (supplementary data table 24). Among the 3 suppressor genes, only *TP53* was correlated with an abnormal p53 IHC expression (either positive or null) with 58.6% of samples abnormal in IHC harboring a *TP53* gene alteration (supplementary data table 25). No correlation was found between *BRCA* alterations and NE markers expression in IHC nor tumor suppressor signature (supplementary data table 26). Other p values for correlation between IHC and NGS are displayed in supplementary data table 27.

n. Tumor heterogeneity regarding neuroendocrine features

AR and NE markers expression were heterogenous and non-exclusive. Therefore, it was difficult to distinguish a unique pattern. AR and NE markers could be either express on the same tumor cells area or in a different one of the same slide. When looking at survival data on a few cases, rPFS and OS did not seem to be linked to the staining intensity or to the proportion of tumor stained (figure 6).

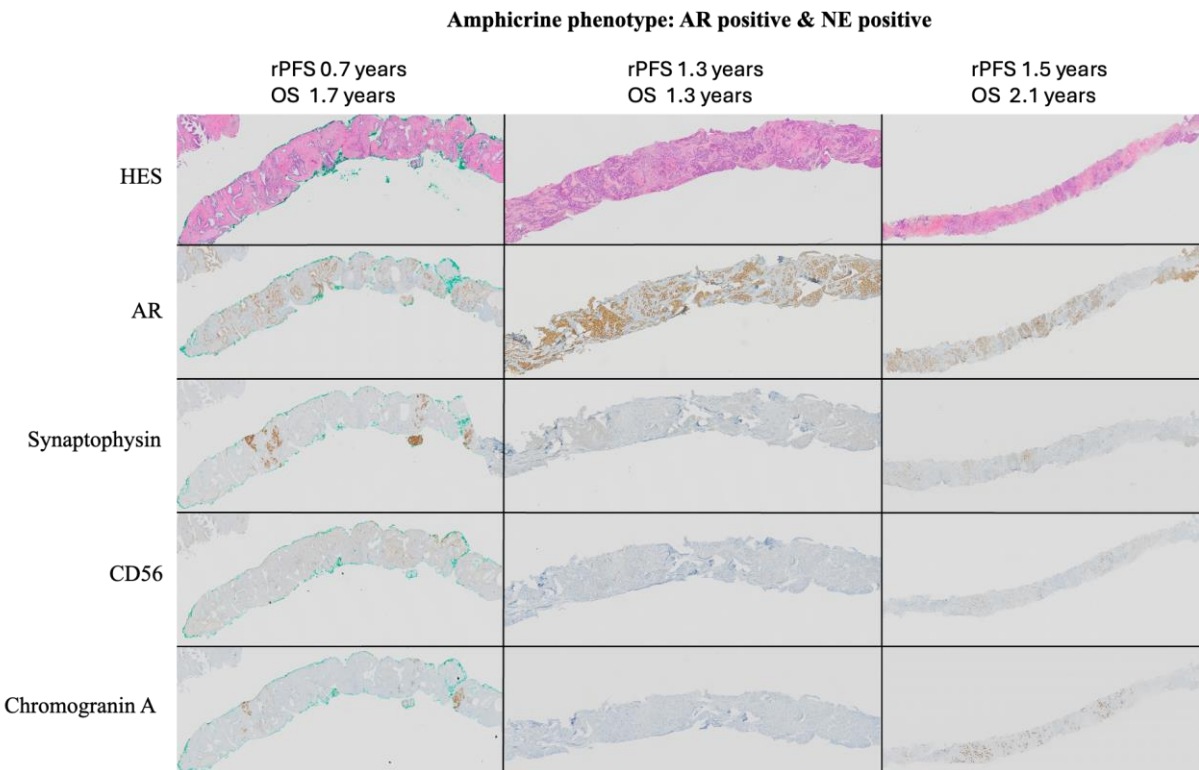
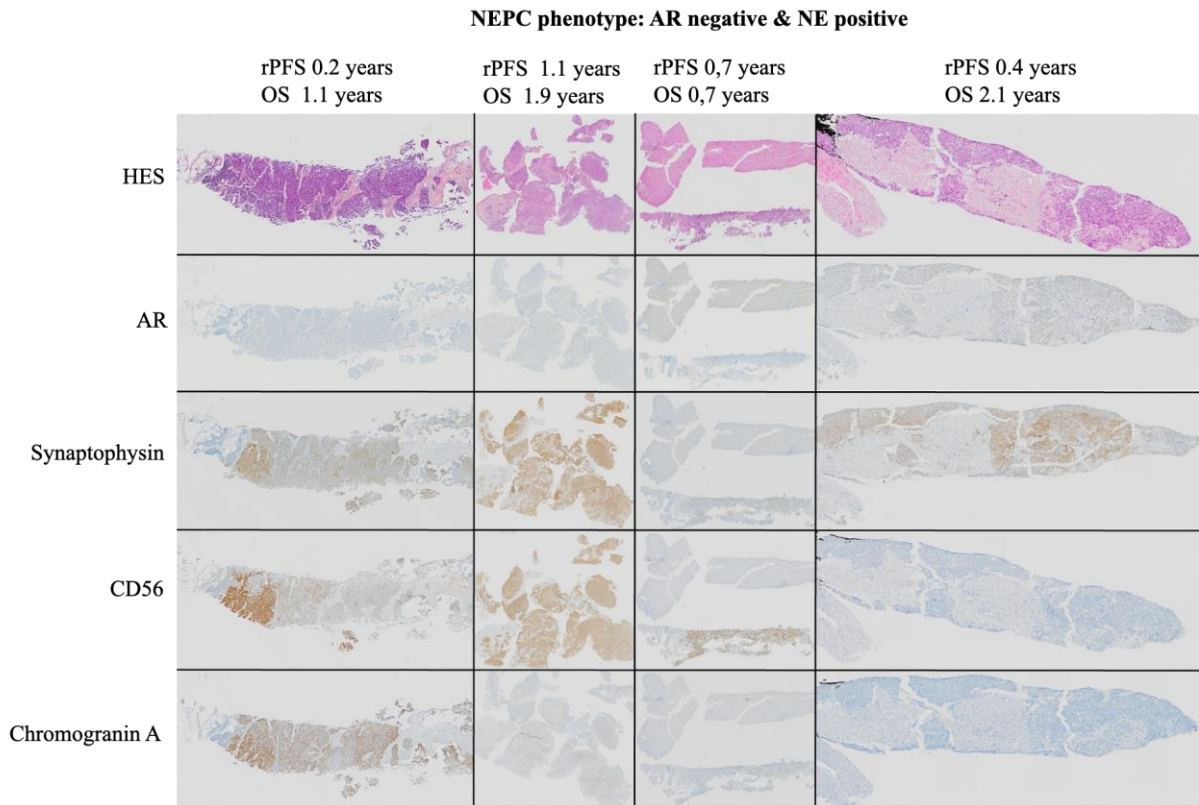


Figure 6: HES and IHC slides of NE and amphicrine phenotypes.

o. Comparison with local pathologist report

Regarding our ancillary cohort, comparison of IHC on blocks centrally retrieved with local pathologist reports showed a correlation between NEPCmk and adenocarcinoma mixed with NE ($p < 0.001$). However, among the pure adenocarcinoma reported by a local pathologist, a large number of patients ($n=90$, 23.4%) were NEPCmk positive (supplementary data table 28 & 29). No central pathologist histological assessment or grading for ISUP score was performed.

3. Discussion

De novo mCSPC is poorly described and there is a need for biomarker predicting treatment response but also new prognosis markers for treatment intensification in poor responder patients.

Surprisingly, an important number of patients, about one-fourth of our IHC cohort, harbored at least one NE marker, with most of them having amphicrine phenotype. A retrospective study on local pathologist reports from the PEACE1 full trial cohort showed a low number of patients with NE features assessed in daily practice. Among the 190 patients (17.5% of the 1172 full trial cohort) with NE features assessed, 14.0% had adenocarcinoma with NEPC differentiation and 0.5% a pure NEPC. All these 26 patients had worse outcomes compared to the other 1056 patients¹⁰. This difference in terms of frequency highlights the underestimated number of patients with NE features at baseline in *de novo* mCSPC as common practice recommend NE staining for high Gleason grades or suspected NEPC on morphology. As there is a range of different prostate cancers from adenocarcinoma to pure small cell NE it is difficult to compare these results with previous data, but *de novo* morphological NEPC has been reported in 1 to 5% patients and IHC expression of NE markers alone is probably more frequent¹¹. A more recent retrospective study assessing initial biopsies at diagnosis in a mCRPC cohort found 9.8% of patients harboring either morphologic or IHC NE markers at baseline. This smaller proportion compared to our results could be explained by the lower number of patients having a *de novo* metastatic disease (46.8%)¹². Regarding other phenotypes, NEPC having an AR loss of expression associated were rare with only 1.3% of patients in our study. Pure NEPC were excluded from inclusion in PEACE-1 trial explaining this low percentage. We only had 0.7% of patients with a double negative tumor probably reflecting the fact that this phenotype is mostly induced by hormonotherapy. Albeit mostly defined by gene expression rather than IHC in other studies, double negative tumor were found at a higher frequency of 5.4% at mCRPC stage which was increased by ARPI introduction in 2011 at 23.3%¹³. The frequency of genes alterations were similar to previously published data¹⁴, with less AR alterations compared to mCRPC but a close number of *BRCA* alterations (9.2% of patients in our NGS cohort vs 7.3% in MSK-IMPACT¹⁴ and 9.3% in SU2-PCF¹⁵). Regarding TSalt, only 7.6% of patients harbored this signature. Previous analyses of the TCGA found that 9.9% mCRPC patients had the same signature¹⁶.

NE transdifferentiation at mCRPC stage has been extensively reported to be associated with worse outcomes and could be found in 20 to 30% of patients biopsied at this advanced stage¹⁷. In our study, these NE features were also associated with a worse prognosis at an earlier mCSPC stage. If morphological NEPC are well known for their worse prognosis, data for IHC marker independent prognosis value are controversial¹¹. NEPC are also associated with AR, ERG and NKX3.1 loss of expression¹¹. In our study we only found ERG expression among these proteins to be associated with a longer rPFS. The p53 protein abnormal expression was associated with worse rPFS, in line with data showing an association with worse outcomes for p53¹⁸. A higher

Ki67 was correlated to a better PSA response at 8 months, maybe reflecting the sensitivity of these tumors to docetaxel. A higher Ki67 has been reported to be of worse prognosis for localized prostate cancer only^{19,20}. NEPC found in prostatectomy have a similar Ki67 level compared to adenocarcinoma²¹. However, Ki67 level of expression has no effect on rPFS and OS in PEACE1 in which a large part of patients received docetaxel. A previous study reported a low Ki67 expression in foci of synaptophysin positive cells of mCPRC cancer. Perhaps proliferation of these NE cells could be activated later under treatment pressure by a “proliferative switch”²². Growing evidence of alterations linked with NE-like or aggressive variant in these mCRPC have been reported this last five years with the key role of the tumor suppressor genes *TP53*, *PTEN* and *RBI*¹⁶. In our study, the alteration of at least two of these genes was associated with a worse prognosis but with only 7.6% of patients harboring this signature. Previous analyses of the TCGA found that 9.9% mCRPC patients had the same signature¹⁶. Several studies have reported the combination of more or less *TP53*, *PTEN* and *RBI* genes to be associated with worse outcomes in both mCSPC and mCRPC patients^{23,24}. In our study, none of these genes were separately associated with prognosis. Mechanistically, *TP53* and *RBI* are involved in cell cycle control and play a role in plasticity through NE differentiation. These mechanisms are initiated by *PTEN* loss of function leading ultimately to the over-expression of the epigenic regulator *EZH2* and the reprogramming transcription factor *SOX2*^{25,26}. Alterations in the DNA repair genes have previously been reported to be associated with worse prognosis mainly in mCRPC²⁷ and with a slightly lower but almost similar frequency in mCSPC¹⁴. Albeit, the prognosis value of *BRCA* genes is poorly reported for mCSPC²⁸ and a tendency was found in our study for worse OS of patients with *BRCA* alterations.

However, none of these IHC markers or transcriptomic z-scores were predictive of abiraterone benefit, meaning that all patient benefit from this treatment. These findings are in line with previous work in the STAMPEDE abi781 cohort in which using several RNAseq signatures, no predictive biomarker for abiraterone benefit was found either²⁹.

At a gene expression level, we adapted a 70-gene NEPC score previously reported in mCRPC NEPC but also elevated in 20% of adenocarcinomas³⁰. In our cohort, a higher NEPC z-score and a lower AR z-score were associated with worse outcomes. We also found previously reported genes in mCRPC involved in NE lineage differentiation³¹ such as *EZH2*, *DLL3*, *SOX2*, *KDM1A* (also known as *LSD1*) and one of the aurora kinase (*AURKB*) over-expressed in worse prognostic subgroups reinforcing our phenotypic and genomic findings. Other less described genes, *TOP2* linked to *EZH2*³² and *DNMT1* inhibiting *EZH2* ubiquitination³³, were also over-expressed in aggressive subgroups. Accordingly, in GSEA, we found an over-expression of E2F, G2M and MYC pathways in more aggressive subgroups of patients, as previously described in NEPC at mCRPC stages^{17,34}, also reflecting their proliferation potential. We had an AR pathway under-expression, in line with the AR pathway independence described in NEPC transdifferentiation with the loss of sensitivity for hormone therapy³⁵. A continuum has been described from AR dependent tumor to NEPC in Bluemn et al. work. However, NE features emergence did not seem to follow AR pathway loss of expression in double negative prostate cancer preclinical model¹³. Other studies supported that NE transdifferentiation in mCRPC arise from luminal cells²². In our cohort of *de novo* mCSPC, almost all tumors with NEPC markers positivity restrained an AR expression in IHC but with a loss of AR pathway at a gene expression level. We can hypothesize that even before hormonal treatment some more aggressive tumors are already less dependent from the AR axis. Interestingly, this hallmark AR pathway was found under-expressed in the more aggressive *de novo* mCSPC compared to relapsing mCSPC³⁶.

A part from these NEPC related genes, ARG1 is an enzyme involved in arginine metabolism linked to an immunosuppressive microenvironment in prostate cancer and its expression is induced by androgens^{37,38}. *HSD11B1* encode for the glucocorticoid-activating enzyme 11 β -hydroxysteroid dehydrogenase type 1 which catalyzes the 17 β -reduction of androstenedione to testosterone in peripheral tissue³⁹. In our cohort both of them were over-expressed in non-responder and high burden patients as described in our previously reported cohort MATCH-R of mCRPC patients in non-responder³⁴. Although their role has been poorly studied in prostate cancer, we could hypothesize that these enzymes would play a role in resistance to hormone therapy. Other surprising pathways inactivated in TSalt patients were the immune score allograft rejection and TNF α via NF κ B pathways⁴⁰ and could reflect an immunosuppressed environment in these tumors compared to pure adenocarcinoma, but needs further validation as it never been reported in prostate cancer.

Regarding tumor heterogeneity but at a protein expression level, we had a wide range of different AR and NE staining combinations with some tumor area AR positive and NE positive. In the PEACE1 trial, only patients with adenocarcinoma and those with minor NE differentiation could be included. Pure NEPC were excluded, therefore they could not be encountered in our ancillary study. All these different situations reflect the complex tumor heterogeneity and all the transition states from adenocarcinoma to NE phenotype. It is important to note that even patients with tumor expressing a low NE H-score or with only a few tumor areas stained had a similar or even shorter rPFS and OS as tumor expressing NE markers more intensively. In a study looking at metastases biopsies in mCRPC patients, 17% of them had NE features but with heterogeneity on the same biopsy core⁴¹. Intra-tumoral heterogeneity in prostate cancer has been widely reported in the recent years. It has been shown with genomic clonal evolution that distant metastases originate from one clone. Moreover, heterogeneity seems to increase with disease burden, providing a rationale for earlier intensive treatment before resistance emerge. However, most of these results have been reported in mCRPC setting and data in *de novo* mCSPC and primitive tumor samples are lacking⁴².

One of the limitations of this study was the low sample quality reflecting the challenges for sequencing in daily practice. Only a few number of patients had contributive sequencing among the ones for whom DNA was extracted (43.7%). This could be due for some of them to the long-term storage of the samples. NE markers were more easily assessable for a larger number of samples and this assay is less costly. However, PTEN markers were not assessable in our study due the poor quality of antibodies available and RB1 staining was also of poor quality limiting its interpretation. ERG fusion were not assessable with our NGS panels due to low RNA quantity and quality but we reported above the impact on survival of ERG expression in IHC, which was previously described as well correlated with genomic alterations⁴³. Nonetheless, both IHC and NGS could be complementary to detect NE tumoral subpopulation.

The two theories of rather NE clones selection or adenocarcinoma transdifferentiation under treatment pressure as previously formulated are not necessarily contradictory³⁰. Here we can hypothesize that our findings reflect the clonal evolution of the minor contingent of NE cells already present at diagnosis and selected later by treatments pressure, eventually evolving to resistance and a more lethal disease. A spatial transcriptomic analysis is ongoing to explore these results at a gene expression level.

Altogether, these data confirmed at a multiple omics level our initial hypothesis that rare aggressive clones with NE features are already present at diagnosis in *de novo* mCSPC and are

associated with worse prognosis. The underlying mechanisms could be a clonal selection of this tumoral subpopulation under treatment, leading to the emergence of aggressive tumor at a later stage. There is an opportunity to target these clones up front to enhance patient survival with combination therapies.

4. Online methods

a. Study design

PEACE-1 (Eudract 2012-00142-35; NCT 01957436) is a European academic randomized factorial design phase III trial. Since the PRTK-K translational research program was nationally funded, only French patients in the "PEACE-1" study were eligible. Archival tumor tissue from diagnosis have been centrally retrieved and stored at Unicancer tumor biobank Centre Léon BERARD to conduct analysis of tumor blocks. We retrieved baseline characteristics of patients from the clinical data record of PEACE1 at the frozen date of 14th April 2023. A sample size calculation was performed as described in supplementary methods. The initial protocol was reviewed and first approved on July 10, 2013, by the French Independent Ethics Committee (Comité de Protection des Personnes Ile de France VII). The protocol complied with the ethical principles of the Declaration of Helsinki and was approved by Institutional Review Boards at each study site. A pre-specified statistical analysis plan was approved by the PEACE-1 steering committee.

b. Endpoints

The co-primary endpoints for each studied biomarker, were the association between the biomarker and the outcomes (*prognostic value*) and the existence of an interaction between the biomarker and the treatment (AA) on the outcomes (*predictive value*). The outcomes assessed were the co-primary endpoints of the PEACE1 study, i.e. the radiographic Progression-Free Survival (rPFS) and the Overall Survival (OS) as previously reported⁷. The secondary endpoint was to decipher the landscape of DNA alterations and pathways dysregulations in *de novo* mCNPC from PEACE-1. For each study biomarker (molecular genetic mutations or phenotypes from immunohistochemistry data), we studied the association between the biomarker and the PSA response at 8 months defined as a PSA level ≤ 0.2 ng/ml or a PSA level > 0.2 ng/ml and disease burden according to CHARTED criteria⁴⁴.

c. Samples preparation

WP1: DNA analysis of tumor blocks

A semiquantitative analysis of the quality of the tumor tissue block was performed on a hematoxylin and eosin (H&E)-stained serial section of the tumor. Samples were excluded when the total tissue quality score is 2 or less, or when the tumor percentage $< 10\%$ for targeted exome sequencing. At least 2 mm³ of FFPE tissue was needed to obtain sufficient nucleic acid material by a microdissection. We avoided whole exome sequencing and rather used the oncodeep and CCE cancer genes panels to give much better coverage and increase the robustness of the data.

WP2: Phenotype analysis of tumor blocks

Pathology quality control processes were the same than those used for WP1. For IHC assays, 10x 4 μm -thick slides were prepared. Ten markers were used: AR, NKX3.1, ERG, synaptophysin, Chromogranin A, CD56, p53, Rb1, Ki67 and PTEN.

WP3: transcriptomic analyses

After completion of WP1 and WP2, we used remaining white slides with a tumor percentage \geq 30% and a minimum of two slides for gene expression assessment. We used the Nanostring nCounter® tumor signaling 360™ panel and an additional nCounter flex panel for AR activation and NEPC differentiation signature as decipher in supplementary data table 30.

d. Statistical analyses

Generalities

All analyses were performed following the intention-to-treat principle, i.e. analyzed as randomized. Quantitative variables were described in terms of median, interquartile range, minimum, and maximum or mean and standard deviation. Qualitative variables were described in terms of number and proportion. Univariate association between clinical factors and categorical biomarkers from IHC analyses were evaluated using Chi-squared tests or Fisher tests, if necessary. Survival curves were estimated using Kaplan-Meier methods and compared with the log-rank test. The type-I error rate α was fixed to 0.05 (two-sided). The statistical analyses were carried out using R software at Gustave Roussy (Biostatistics and Epidemiology Office).

Data interpretation

For WP1, only alterations classified as pathogenic or likely pathogenic were considered for analyses. For WP2, a semi-quantitative score (H-score) considered the staining intensity, and two independent pathologists established the percentage of stained cells for each marker. Percentage values of ki67 was normalized using a log transformation. NE markers (Synaptophysin, CD56 and Chromogranin A) were considered as negatives if the H-scores were all equal to 0, or positives if at least one H-score is strictly positive. Five different categories of phenotypes according to current phenotypes classification were investigated grouping NE markers and AR markers: AR-high luminal (AR+ nuclear/NE-), AR-low luminal (AR+ nuclear weak or cytoplasmic/NE-), amphicrine (AR+/NE+), double-negative tumors (AR-/NE-) and NEPC (AR-/NE+). For WP3, we performed differential expression analyses GSEA (Gene Set Enrichment Analysis), ORA (Over-Representation Analysis), GSVA scores as described in supplementary data. NEPC, AR and metabolism scores were calculated for each study participant as z-score value for the genes under- or over-expressed (table 2).

Co-primary endpoints: prognostic and predictive analyses

For IHC biomarkers missing values handling, multiple imputation was planned to compute regression models on a complete data set. To evaluate the prognostic effect of a biomarker, multivariable Cox proportional hazard regression models were used. To evaluate the predictive effect of a biomarker, an interaction between the biomarker and the abiraterone was added. We adjusted the Cox regression analysis for radiotherapy, docetaxel, the randomization stratification criteria (ECOG 0 vs 1-2, type of castration and disease burden high vs low), as well as two known prognostic factors: the Gleason score <7 vs ≥ 7 and the age in categories (<60 years; $\geq 60-69$ years; ≥ 70 years).

Secondary endpoints

The frequency of DNA alterations was deciphered. The frequency of DNA alterations was compared between patients depending of PSA at 8 months ≥ 0.02 ng/ml or not, high volume vs low volume, and with corresponding protein expression in IHC.

References

1. Prostate cancer burden in EU-27. <http://visitors-centre.jrc.ec.europa.eu/en/media/infographics/prostate-cancer-burden-eu-27> (2021).
2. Piombino, C. *et al.* De Novo Metastatic Prostate Cancer: Are We Moving toward a Personalized Treatment? *Cancers (Basel)* **15**, 4945 (2023).
3. Welch, H. G., Gorski, D. H. & Albertsen, P. C. Trends in Metastatic Breast and Prostate Cancer — Lessons in Cancer Dynamics. *New England Journal of Medicine* **373**, 1685–1687 (2015).
4. James, N. D. *et al.* Addition of docetaxel, zoledronic acid, or both to first-line long-term hormone therapy in prostate cancer (STAMPEDE): survival results from an adaptive, multiarm, multistage, platform randomised controlled trial. *Lancet* **387**, 1163–1177 (2016).
5. Fizazi, K. *et al.* Abiraterone acetate plus prednisone in patients with newly diagnosed high-risk metastatic castration-sensitive prostate cancer (LATITUDE): final overall survival analysis of a randomised, double-blind, phase 3 trial. *Lancet Oncol* **20**, 686–700 (2019).
6. Armstrong, A. J. *et al.* ARCHES: A Randomized, Phase III Study of Androgen Deprivation Therapy With Enzalutamide or Placebo in Men With Metastatic Hormone-Sensitive Prostate Cancer. *J Clin Oncol* **37**, 2974–2986 (2019).
7. Fizazi, K. *et al.* Abiraterone plus prednisone added to androgen deprivation therapy and docetaxel in de novo metastatic castration-sensitive prostate cancer (PEACE-1): a multicentre, open-label, randomised, phase 3 study with a 2×2 factorial design. *Lancet* **399**, 1695–1707 (2022).
8. Humphrey, P. A. Histopathology of Prostate Cancer. *Cold Spring Harb Perspect Med* **7**, a030411 (2017).
9. Yamada, Y. & Beltran, H. Clinical and Biological Features of Neuroendocrine Prostate Cancer. *Current oncology reports* **23**, 15 (2021).
10. Bernard-Tessier, A. *et al.* 1421P - Effect of abiraterone-prednisone in metastatic castration-sensitive prostate cancer (mCSPC) with neuroendocrine and very high-risk features in the PEACE-1 trial. *Annals of Oncology (2022) 33 (suppl_7): S616-S652*. [10.1016/annonc/annonc1070](https://doi.org/10.1016/annonc/annonc1070).
11. Abdulfatah, E., Fine, S. W., Lotan, T. L. & Mehra, R. De novo neuroendocrine features in prostate cancer. *Hum Pathol* **127**, 112–122 (2022).
12. Farinea, G. *et al.* Impact of Neuroendocrine Differentiation (NED) on Enzalutamide and Abiraterone Efficacy in Metastatic Castration-Resistant Prostate Cancer (mCRPC): A Retrospective Analysis. *Cells* **13**, 1396 (2024).
13. Bluemn, E. G. *et al.* Androgen Receptor Pathway-Independent Prostate Cancer Is Sustained through FGF Signaling. *Cancer Cell* **32**, 474-489.e6 (2017).
14. Abida, W. *et al.* Prospective Genomic Profiling of Prostate Cancer Across Disease States Reveals Germline and Somatic Alterations That May Affect Clinical Decision Making. *JCO Precis Oncol* **1**, PO.17.00029 (2017).
15. Robinson, D. *et al.* Integrative Clinical Genomics of Advanced Prostate Cancer. *Cell* **161**, 1215–1228 (2015).

16. Aparicio, A. M. *et al.* Combined Tumor Suppressor Defects Characterize Clinically Defined Aggressive Variant Prostate Cancers. *Clin Cancer Res* **22**, 1520–1530 (2016).
17. Kouroukli, O., Bravou, V., Giannitsas, K. & Tzelepi, V. Tissue-Based Diagnostic Biomarkers of Aggressive Variant Prostate Cancer: A Narrative Review. *Cancers* **16**, 805 (2024).
18. Gesztes, W. *et al.* Evaluating p53 nuclear expression and prostate cancer progression in a predominantly African American cohort. *JCO* **41**, 217–217 (2023).
19. Berney, D. M. *et al.* Ki-67 and outcome in clinically localised prostate cancer: analysis of conservatively treated prostate cancer patients from the Trans-Atlantic Prostate Group study. *Br J Cancer* **100**, 888–893 (2009).
20. Kammerer-Jacquet, S.-F. *et al.* Ki-67 is an independent predictor of prostate cancer death in routine needle biopsy samples: proving utility for routine assessments. *Modern pathology : an official journal of the United States and Canadian Academy of Pathology, Inc* **32**, 1303 (2019).
21. Bubendorf, L. *et al.* Ki67 labelling index: an independent predictor of progression in prostate cancer treated by radical prostatectomy. *J Pathol* **178**, 437–441 (1996).
22. Zou, M. *et al.* Transdifferentiation as a Mechanism of Treatment Resistance in a Mouse Model of Castration-Resistant Prostate Cancer. *Cancer Discov* **7**, 736–749 (2017).
23. Hamid, A. A. *et al.* Compound Genomic Alterations of TP53, PTEN, and RB1 Tumor Suppressors in Localized and Metastatic Prostate Cancer. *Eur Urol* **76**, 89–97 (2019).
24. Velez, M. G. *et al.* Differential impact of tumor suppressor gene (TP53, PTEN, RB1) alterations and treatment outcomes in metastatic, hormone-sensitive prostate cancer. *Prostate Cancer Prostatic Dis* **25**, 479–483 (2022).
25. Ku, S. Y. *et al.* Rb1 and Trp53 cooperate to suppress prostate cancer lineage plasticity, metastasis, and antiandrogen resistance. *Science* **355**, 78–83 (2017).
26. Mu, P. *et al.* SOX2 promotes lineage plasticity and antiandrogen resistance in TP53- and RB1-deficient prostate cancer. *Science* **355**, 84–88 (2017).
27. Fettke, H. *et al.* BRCA-deficient metastatic prostate cancer has an adverse prognosis and distinct genomic phenotype. *eBioMedicine* **95**, (2023).
28. Blas, L., Shiota, M. & Eto, M. Current status and future perspective on the management of metastatic castration-sensitive prostate cancer. *Cancer Treatment and Research Communications* **32**, 100606 (2022).
29. Parry, M. A. *et al.* Clinical testing of transcriptome-wide expression profiles in high-risk localized and metastatic prostate cancer starting androgen deprivation therapy: an ancillary study of the STAMPEDE abiraterone Phase 3 trial. *Res Sq* rs.3.rs-2488586 (2023) doi:10.21203/rs.3.rs-2488586/v1.
30. Beltran, H. *et al.* Divergent clonal evolution of castration-resistant neuroendocrine prostate cancer. *Nat Med* **22**, 298–305 (2016).
31. Yamada, Y. & Beltran, H. Clinical and Biological Features of Neuroendocrine Prostate Cancer. *Curr Oncol Rep* **23**, 15 (2021).
32. Labbé, D. P. *et al.* TOP2A and EZH2 Provide Early Detection of an Aggressive Prostate Cancer Subgroup. *Clin Cancer Res* **23**, 7072–7083 (2017).
33. Li, Z. *et al.* DNMT1-mediated epigenetic silencing of TRAF6 promotes prostate cancer tumorigenesis and metastasis by enhancing EZH2 stability. *Oncogene* **41**, 3991–4002 (2022).
34. Menssouri, N. *et al.* Genomic profiling of metastatic castration-resistant prostate cancer samples resistant to androgen-receptor pathway inhibitors. *Clin Cancer Res* CCR-22-3736 (2023) doi:10.1158/1078-0432.CCR-22-3736.
35. Formaggio, N., Rubin, M. A. & Theurillat, J.-P. Loss and revival of androgen receptor signaling in advanced prostate cancer. *Oncogene* **40**, 1205–1216 (2021).

36. Suter, P. A. *et al.* Transcriptomic and clinical heterogeneity of metastatic disease timing within metastatic castration-sensitive prostate cancer. *Annals of Oncology* **34**, 605–614 (2023).
37. Gannon, P. O. *et al.* Androgen-Regulated Expression of Arginase 1, Arginase 2 and Interleukin-8 in Human Prostate Cancer. *PLoS ONE* **5**, e12107 (2010).
38. Matos, A., Carvalho, M., Bicho, M. & Ribeiro, R. Arginine and Arginases Modulate Metabolism, Tumor Microenvironment and Prostate Cancer Progression. *Nutrients* **13**, 4503 (2021).
39. Oestlund, I. *et al.* The glucocorticoid-activating enzyme 11 β -hydroxysteroid dehydrogenase type 1 catalyzes the activation of testosterone. *The Journal of Steroid Biochemistry and Molecular Biology* **236**, 106436 (2024).
40. Liberzon, A. *et al.* The Molecular Signatures Database (MSigDB) hallmark gene set collection. *Cell systems* **1**, 417 (2015).
41. Aggarwal, R. *et al.* Clinical and Genomic Characterization of Treatment-Emergent Small-Cell Neuroendocrine Prostate Cancer: A Multi-institutional Prospective Study. *J. Clin. Oncol.* **36**, 2492–2503 (2018).
42. Haffner, M. C. *et al.* Genomic and phenotypic heterogeneity in prostate cancer. *Nat Rev Urol* **18**, 79–92 (2021).
43. Park, K. *et al.* Antibody-based detection of ERG rearrangement-positive prostate cancer. *Neoplasia* **12**, 590–598 (2010).
44. Sweeney, C. J. *et al.* Chemohormonal Therapy in Metastatic Hormone-Sensitive Prostate Cancer. *N Engl J Med* **373**, 737–746 (2015).

Remerciements

Merci au Pr Yohann Lorient pour son encadrement, au Pr Christophe Massard pour son orientation et au Pr Karim Fizazi pour ses conseils et l'essai PEACE1. Merci également à Alice Bernard-Tessier pour ses conseils.

Merci au Pr Jean-Yves Scoazec pour la relecture anatomopathologique, à Elodie Edmond pour son énorme travail sur les blocs et lames, à Olivia Bawa pour le projet annexe sur le métabolisme, à Nicolas Signolle pour la plateforme de scanner des lames et à toute l'équipe de la plateforme PETRA.

Merci à Etienne Rouleau pour les analyses NGS, à Patrick Saulnier et David Gentien pour les analyses de transcriptomique, à Maeva Moreau et toute l'équipe de la plateforme AMMICA.

Merci à Stéphanie Foulon, Charlotte Bargain et Bastien Job pour l'énorme travail d'analyse statistique.

Merci à toute l'équipe prostate et PDX pour leur contribution Loic Poiraudé, Naoual Menssouri, Ludovic Bigot, Catline Nobre, Alice Moreau-Da Silva, Anne Chauchereau, Luce Dreno et Fares Ousalem.

Merci à l'équipe de CentraleSupélec Maria Vakalopoulou, Stergios Christodoulidis et Imane Chraki pour leur collaboration sur le projet de pathomic.

Merci à Zahira Merabet, Virginie Marty et Valerie Camara pour le projet de transcriptomique spatiale.